

The author(s) shown below used Federal funds provided by the U.S. Department of Justice and prepared the following final report:

Document Title: Ignitable Liquid Fuel Fires in Buildings – A Study of Fire Dynamics

Author(s): Christopher L. Mealy, Daniel T. Gottuk

Document No.: 241442

Date Received: March 2013

Award Number: 2009-DN-BX-K232

This report has not been published by the U.S. Department of Justice. To provide better customer service, NCJRS has made this Federally-funded grant report available electronically.

Opinions or points of view expressed are those of the author(s) and do not necessarily reflect the official position or policies of the U.S. Department of Justice.

HAI Project #1DTG00001.002

Ignitable Liquid Fuel Fires in Buildings – A Study of Fire Dynamics

FINAL

Grant No. 2009-DN-BX-K232

Prepared by:

Christopher L. Mealy and Daniel T. Gottuk
Hughes Associates, Inc.
3610 Commerce Drive, Suite 817
Baltimore, MD 21227
Ph. 410-737-8677 FAX 410-737-8688
www.haifire.com

January 31, 2013

ABSTRACT

Fires occurring within an enclosed space represent the majority of fire scenarios. Understanding the impact of this confinement on the burning dynamics of the fuels within is essential to accurately predicting fire development. Traditionally, heat release rate measurements are measured under open burning conditions. This data is often used to represent materials burning within an enclosure without fully understanding the impact the enclosure might have on the burning dynamics of the fuel. Depending on the geometry of the space and the ventilation conditions present, the enclosure may have a negative effect (i.e., reduce heat release), no effect, or have an enhancing effect on the burning rate of the fuels (i.e., increase heat release). The purpose of this research was to further develop the understanding of enclosure fire effects by conducting full-scale fire tests in both open and enclosed scenarios with both Class A and liquid fuels present. Identical fuel packages in the form of confined area liquid fuel fires (i.e., pan fires), unconfined liquid fuel fires (i.e., spill fires), and Class A fire scenarios were conducted in both the open and within an enclosure. Comparisons between the burning dynamics of the liquid and Class A fuels under these conditions were made. The results of this work provide insight into the varying effects that an enclosure can have on the burning dynamics of a fuel and identifies the impact of certain variables including fuel type, fuel location, and ventilation condition. It should be noted that a forensic research program was conducted in parallel with the testing described in this report and that a companion report was written describing the findings of this forensic work.

TABLE OF CONTENTS

	Page
ABSTRACT.....	ii
ACKNOWLEDGEMENTS.....	xiii
LIST OF ACRONYMS	xiv
EXECUTIVE SUMMARY	E-1
1.0 INTRODUCTION	1
2.0 OBJECTIVES AND APPROACH.....	2
3.0 LITERATURE REVIEW	2
3.1 Compartment Effects	2
3.2 Flashover.....	6
4.0 EXPERIMENTAL APPROACH.....	6
4.1 Test Floor	6
4.2 Test Enclosure.....	7
4.3 Spill Substrates.....	10
4.4 Class A Fuels	11
4.5 Enclosure Instrumentation	13
4.5.1 Temperature Measurements.....	13
4.5.2 Heat Flux Measurements	13
4.5.3 Gas Species Measurements.....	14
4.5.4 Mass Loss.....	15
4.5.5 Hood Calorimeters	15
4.5.6 Data Acquisition System.....	16
4.6 Video and Thermal Imaging.....	16
4.7 Qualitative Indicators.....	16
4.8 Liquid Fuels	18
5.0 EXPERIMENTAL PROCEDURES & RESULTS	19
5.1 Test Series 1 – Unconfined Liquid Fuel Fires in the Open.....	19
5.2 Test Series 2 – Pan Fires in the Open	24
5.3 Test Series 3 – Class A Fires in the Open.....	28
5.3.1 Class A Ignition Scenario	28
5.3.2 Upholstered Sofa.....	29
5.3.3 Upholstered Chair	30
5.3.4 Coffee Table.....	32
5.3.5 Car Seat.....	32
5.3.6 Flooring Material	34
5.4 Test Series 4 – Unconfined Liquid Fuel Fires in Enclosure	36
5.4.1 Gasoline Spill Fire on Vinyl	37
5.4.2 Gasoline Spill Fire on Carpet.....	41
5.5 Test Series 5 – Pan Fires in Enclosure.....	45

5.5.1	Rear Corner – Full Door Scenario	47
5.5.2	Rear Corner – Slit Vent Scenario.....	52
5.5.3	Center of Compartment – Full Door Scenario	57
5.5.4	Center of Compartment – Slit Vent Scenario	61
5.6	Test Series 6 – Class A Fires in an Enclosure	65
5.6.1	Class A Ignition Scenario	69
5.6.2	Gasoline on Carpet Floor with Full Door Opening	75
5.6.3	Gasoline on Carpet Floor with Slit Vent Opening.....	81
5.6.4	Gasoline on Upholstered Chair with Full Door Opening (w/Carpet).....	87
5.6.5	Gasoline on Upholstered Chair with Slit Vent Opening (w/Carpet)	94
5.6.6	Gasoline on Vinyl Floor with Full Door Opening	101
5.6.7	Gasoline on Vinyl Floor with Slit Vent Opening	107
5.6.8	Gasoline on Upholstered Chair with Full Door Opening (w/Vinyl).....	113
5.6.9	Gasoline on Upholstered Chair with Slit Vent Opening (w/Vinyl).....	121
6.0	ANALYSIS.....	127
6.1	Enclosure Fire Dynamics – Flashover	127
6.2	Enclosure Effects	132
6.2.1	Spill Fires.....	132
6.2.2	Pan Fires.....	136
6.2.3	Class A Fuel Fires.....	141
6.2.4	Ventilation Effects	144
6.2.5	First Item Ignited.....	148
6.3	Effect of Gasoline Spill on Fire Development.....	151
7.0	CONCLUSIONS.....	151
8.0	REFERENCES	155
	APPENDIX A – HOOD CALORIMETERS & CALIBRATION	A-1

TABLE OF FIGURES

	Page
Figure 1. Illustrative plot showing general enclosure fire progression.....	2
Figure 2. Plot of historical heptane burning rate data and curve fit using Babrauskas [1983] correlation parameters (thin red line) and curve fit based on historical data (thick blue line).	4
Figure 3. Vinyl floor constructed for open burn testing.	7
Figure 4. Test enclosure with full door vent used in Test Series 4–6.	8
Figure 5. Test enclosure with slit vent used in Test Series 4–6.....	9
Figure 6. Class A fuels.....	11
Figure 7. Typical Class A fuel layout in test enclosure.	12
Figure 8. Thermocouple locations within test enclosure.	14
Figure 9. External view camera locations for enclosure fires.....	17
Figure 10. Illustration of internal view camera locations for enclosure fires.	18
Figure 11. 2.0 L gasoline spill fire (Test SF1) on vinyl (left) and consequent burn pattern (right).	21
Figure 12. Heat release rates from triplicate testing of 2.0 L gasoline spills on vinyl flooring ignited 10s after release.	22
Figure 13. 2.0 L gasoline spill fire on carpet (Test SF4) (left), gasoline burning on carpet (center), burning carpet after gasoline is largely consumed (top right), and resulting burn pattern (lower right).	23
Figure 14. Heat release rates from triplicate testing of 2.0 L gasoline spills on carpet/pad flooring.....	23
Figure 15. Gasoline, heptane, and denatured alcohol pan fires shown left to right, respectively. 25	25
Figure 16. Heat release rate from 0.23 m ² (2.5 ft ²) gasoline pan fires burning in the open.	25
Figure 17. Heat release rate from 0.23 m ² (2.5 ft ²) heptane pan fires burning in the open.	26
Figure 18. Heat release rate from 1.0 m ² (10.8 ft ²) denatured alcohol pan fires burning in the open.....	27
Figure 19. Average heat release rate for Class B or hydrocarbon fuels burning in the open.	27
Figure 20. Photograph of Class A ignition scenario.	29
Figure 21. Upholstered sofa fire progression.....	29
Figure 22. Heat release rate of upholstered sofa.....	30
Figure 23. Photographs of upholstered chair fire progression.....	31
Figure 24. Heat release rate of upholstered chair.	31
Figure 25. Coffee table fire progression.	32

Figure 26. Heat release rate of coffee table.	33
Figure 27. Photographs of car seat fire progression.	33
Figure 28. Heat release rate of car seat.	34
Figure 29. Average transient heat release rates for vinyl flooring at different exposure fluxes. ...	36
Figure 30. Average transient heat release rates for carpet flooring at different exposure fluxes. ...	36
Figure 31. 2.0 L gasoline spill fire conducted in test enclosure.	38
Figure 32. Thermal degradation to vinyl sub-flooring occurring less than 10 seconds after ignition of the spill fire.	38
Figure 33. Heat release rate for 2.0 L gasoline spill on vinyl flooring within an enclosure.	39
Figure 34. Average enclosure temperatures measured during 2.0 L gasoline spill fire on vinyl. ...	39
Figure 35. Enclosure heat fluxes measured during 2.0 L gasoline spill fire on vinyl.	40
Figure 36. Gas species measurements collected high in the enclosure during 2.0 L gasoline spill fire on vinyl.	40
Figure 37. Gas species measurements collected low in the enclosure during 2.0 L gasoline spill fire on vinyl.	41
Figure 38. Heat release rate for 2.0 L gasoline spill on carpet flooring within an enclosure.	42
Figure 39. Enclosure temperatures measured during 2.0 L gasoline spill fire on carpet.	43
Figure 40. Enclosure heat fluxes measured during 2.0 L gasoline spill fire on carpet.	43
Figure 41. Gas species measurements collected high in the enclosure during 2.0 L gasoline spill fire on carpet.	44
Figure 42. Gas species measurements collected low in the enclosure during 2.0 L gasoline spill fire on carpet.	44
Figure 43. Pan locations within test enclosure.	45
Figure 44. Measured heat release rate from heptane pan fire burning in corner of enclosure with full-open doorway compared to open burning fire.	47
Figure 45. Enclosure temperatures during heptane pan fire burning in corner of enclosure with full-open doorway.	48
Figure 46. Thermal gradients at 1-minute intervals for heptane pan fire burning in corner of enclosure with full-open doorway.	48
Figure 47. Steady-state 0.23 m ² (2.5 ft ²) heptane pan fire burning in the corner of the enclosure.	49
Figure 48. Measured heat release rate from denatured alcohol pan fire burning in corner of enclosure with full-open doorway compared to open burning fire.	50
Figure 49. Compartment temperatures measured during denatured alcohol pan fire burning in corner of enclosure with full-open doorway.	50

Figure 50. Vent opening thermal gradients at 1-minute intervals for denatured alcohol pan fire burning in corner of enclosure with full-open doorway.	51
Figure 51. Steady-state 1.0 m ² (10.4 ft ²) denatured alcohol pan fire burning in the corner of the enclosure.	51
Figure 52. Measured heat release rate from heptane pan fire burning in corner of enclosure with slit vent compared to open burning fire.	52
Figure 53. Enclosure temperatures during heptane pan fire burning in corner of enclosure with slit vent.	53
Figure 54. Thermal gradients at 1-minute intervals for heptane pan fire burning in corner of enclosure with slit vent.	53
Figure 55. Steady-state 0.23 m ² (2.5 ft ²) heptane pan fire burning in the corner of the enclosure with a slit vent scenario.	54
Figure 56. Measured heat release rate from denatured alcohol pan fire burning in corner of enclosure with slit vent compared to open burning fire.	55
Figure 57. Enclosure temperatures during denatured alcohol pan fire burning in corner of enclosure with slit vent.	55
Figure 58. Thermal gradients at 1-minute intervals for heptane pan fire burning in corner of enclosure with slit vent.	56
Figure 59. Steady-state 1.0 m ² (10.8 ft ²) denatured alcohol pan fire burning in the corner of the enclosure with a slit vent scenario.	56
Figure 60. Measured heat release rate from heptane pan fire burning in center of enclosure with full open door compared to open burning fire.	57
Figure 61. Enclosure temperatures during heptane pan fire burning in center of enclosure with full-open doorway.	58
Figure 62. Thermal gradients at 1-minute intervals for heptane pan fire burning in center of enclosure with full-open doorway.	58
Figure 63. Flame tilt (towards the rear of the enclosure – away from vent) observed during heptane pan fire in center of enclosure with full-open doorway.	59
Figure 64. Measured heat release rate from denatured alcohol pan fire burning in center of enclosure with full open door compared to open burning fire.	60
Figure 65. Enclosure temperatures during denatured alcohol pan fire burning in center of enclosure with full open door.	60
Figure 66. Thermal gradients at 1-minute intervals for denatured alcohol pan fire burning in corner of enclosure with full open door.	61
Figure 67. Measured heat release rate from heptane pan fire burning in center of enclosure with slit vent compared to open burning fire.	62
Figure 68. Enclosure temperatures during heptane pan fire burning in center of enclosure with slit vent compared to open burning fire.	62

Figure 69. Thermal gradients at 1-minute intervals for heptane pan fire burning in center of enclosure with slit vent compared to open burning fire.....	63
Figure 70. Gradual migration of the heptane pan fire to the rear of the test enclosure. The dashed line indicates the corner of the pan	63
Figure 71. Measured heat release rate from denatured alcohol pan fire burning in center of enclosure with slit vent compared to open burning fire.....	64
Figure 72. Enclosure temperatures during denatured alcohol pan fire burning in center of enclosure with slit vent.	64
Figure 73. Thermal gradients at 1-minute intervals for denatured alcohol pan fire burning in corner of enclosure with slit vent.....	65
Figure 74. (a) Class A fire test layout and (b) photograph of Class A fuels from the doorway of the enclosure.	67
Figure 75. Class A ignition source on upholstered sofa.	67
Figure 76. Target spill area and Class A material locations within test enclosure (left) and representative photograph of the spill fire when initially ignited (right).....	68
Figure 77. Gasoline spill on seat of upholstered chair (left) and trailer leading from front of chair to doorway (right).	69
Figure 78. Fire progression observed in Test 6-0 for fully furnished, carpeted room with a full-open doorway. Sofa ignited by Class A source on top of seat.....	70
Figure 79. Heat release rate from Test 6-0.	71
Figure 80. Average temperature measured at four elevations in Test 6-0.	72
Figure 81. Temperature gradients measured in Test 6-0.	72
Figure 82. Heat flux on rear wall of enclosure opposite doorway in Test 6-0.	73
Figure 83. Average heat flux measured at floor in Test 6-0.	73
Figure 84. Gas concentrations measured 0.45 m (18 in.) above the floor in Test 6-0.....	74
Figure 85. Gas concentrations measured 0.45 m (18 in.) below the ceiling in Test 6-0.	74
Figure 86. Test 6-1 2.0 L (0.53 gal) gasoline spill fire ignition scenario.	75
Figure 87. Fire progression observed in Test 6-1.	76
Figure 88. Heat release rate from Test 6-1.	77
Figure 89. Average temperature measured at four elevations in Test 6-1.	78
Figure 90. Average temperature gradients measured during Test 6-1.....	78
Figure 91. Heat flux on rear wall of enclosure opposite doorway.....	79
Figure 92. Average heat flux measured at floor in Test 6-1.	80
Figure 93. Gas concentrations measured 0.45 m (18 in.) above the floor in Test 6-1.....	81
Figure 94. Gas concentrations measured 0.45 m (18 in.) below the ceiling in Test 6-1.	81

Figure 95. Fire progression observed in Test 6-2 (view from doorway).....	82
Figure 96. Heat release rate from Test 6-2.	83
Figure 97. Average temperature measured at four elevations in Test 6-2.....	84
Figure 98. Average temperature gradients measured during Test 6-2.....	84
Figure 99. Heat flux on rear wall of enclosure opposite doorway in Test 6-2.	85
Figure 100. Heat flux on sidewall of enclosure perpendicular to vent in Test 6-2.....	85
Figure 101. Heat fluxes measured at floor in Test 6-2.	86
Figure 102. Gas concentrations measured 0.45 m (18 in.) above the floor in Test 6-2.....	87
Figure 103. Gas concentrations measured 0.45 m (18 in.) below the ceiling in Test 6-2.	87
Figure 104. Fire progression in Test 6-3.....	88
Figure 105. Heat release rate from Test 6-3.	89
Figure 106. Average temperature measured at four elevations in Test 6-3.....	90
Figure 107. Average temperature gradients measured during Test 6-3.....	90
Figure 108. Heat flux on rear wall of enclosure opposite doorway in Test 6-3.	91
Figure 109. Heat flux on sidewall of enclosure perpendicular to vent in Test 6-3.....	92
Figure 110. Average heat flux measured at floor in Test 6-3.	92
Figure 111. Gas concentrations measured 0.45 m (18 in.) above the floor in Test 6-3.....	93
Figure 112. Gas concentrations measured 0.45 m (18 in.) below the ceiling in Test 6-3.	94
Figure 113. Fire progression observed in Test 6-4.	95
Figure 114. Heat release rate from Test 6-4.	96
Figure 115. Average temperature measured at four elevations in Test 6-4.....	97
Figure 116. Average temperature gradients measured during Test 6-4.....	97
Figure 117. Heat flux on rear wall of enclosure opposite doorway in Test 6-4.	98
Figure 118. Heat flux on sidewall of enclosure perpendicular to vent in Test 6-4.....	99
Figure 119. Average heat flux measured at floor in Test 6-4.	99
Figure 120. Gas concentrations measured 0.45 m (18 in.) above the floor in Test 6-4.....	100
Figure 121. Gas concentrations measured 0.45 m (18 in.) below the ceiling in Test 6-4.	100
Figure 122. Fire progression observed in Test 6-5.	101
Figure 123. Heat release rate from Test 6-5.	102
Figure 124. Average temperature measured at four elevations in Test 6-5.....	103
Figure 125. Temperature gradients measured during Test 6-5.....	103
Figure 126. Heat flux on rear wall of enclosure opposite doorway in Test 6-5.	104
Figure 127. Heat flux on sidewall of enclosure perpendicular to vent in Test 6-5.....	105

Figure 128. Average heat flux measured at floor in Test 6-5.	105
Figure 129. Gas concentrations measured 0.45 m (18 in.) above the floor in Test 6-5.....	106
Figure 130. Gas concentrations measured 0.45 m (18 in.) below the ceiling in Test 6-5.	106
Figure 131. Fire progression observed in Test 6-6.	107
Figure 132. Heat release rate from Test 6-6.	108
Figure 133. Average temperature measured at four elevations in Test 6-6.....	109
Figure 134. Average temperature gradients measured during Test 6-6.....	110
Figure 135. Heat flux on rear wall of enclosure opposite doorway in Test 6-6.	111
Figure 136. Heat flux on sidewall of enclosure perpendicular to vent in Test 6-6.....	111
Figure 137. Average heat flux measured at floor in Test 6-6.	112
Figure 138. Gas concentrations measured 0.45 m (18 in.) above the floor in Test 6-6.....	113
Figure 139. Gas concentrations measured 0.45 m (18 in.) below the ceiling in Test 6-6.	113
Figure 140. Fire progression observed in Test 6-7.	114
Figure 141. Heat release rate from Test 6-7.	115
Figure 142. Average temperature measured at four elevations in Test 6-7.....	116
Figure 143. Temperature gradients measured during Test 6-7.	117
Figure 144. Heat flux on rear wall of enclosure opposite doorway in Test 6-7.	118
Figure 145. Heat flux on sidewall of enclosure perpendicular to vent in Test 6-7.....	118
Figure 146. Average heat flux measured at floor in Test 6-7.	119
Figure 147. Gas concentrations measured 0.45 m (18 in.) above the floor in Test 6-7.....	120
Figure 148. Gas concentrations measured 0.45 m (18 in.) below the ceiling in Test 6-7.	120
Figure 149. Fire progression observed in Test 6-8.	122
Figure 150. Heat release rate from Test 6-8.	123
Figure 151. Average temperature measured at four elevations in Test 6-8.....	124
Figure 152. Temperature gradients measured during Test 6-8.	124
Figure 153. Heat flux on rear wall of enclosure opposite doorway in Test 6-8.	125
Figure 154. Heat flux on sidewall of enclosure perpendicular to vent in Test 6-8.....	125
Figure 155. Average heat flux measured at floor in Test 6-8.	126
Figure 156. Gas concentrations measured 0.45 m (18 in.) above the floor in Test 6-8.....	127
Figure 157. Gas concentrations measured 0.45 m (18 in.) below the ceiling in Test 6-8. Note that in this test the CO concentrations were not measured due to instrumentation error.	127
Figure 158. Comparison of gasoline spill fire heat release rate per unit area on vinyl floor between open burning and within enclosure with full-open doorway.....	133

Figure 159. Photographs of the condition of the vinyl flooring material after open burning (left) and enclosed (right) gasoline spill fire scenarios.....	133
Figure 160. Comparison of average heat release rates per unit area for open burning carpet spill fire and spill fire conducted within enclosure with full-open doorway.....	135
Figure 161. Thermal profile within enclosure during gasoline spill fire on carpet.....	136
Figure 162. Heat release rates for heptane pan fires in enclosures.....	137
Figure 163. Heat release rates for denatured alcohol pan fires in enclosures and in the open. ..	139
Figure 164. Comparison of floor heat fluxes for denatured alcohol pan fires in the enclosure with full door and slit vent ventilation conditions.....	140
Figure 165. Comparison of low-level oxygen concentrations in denatured alcohol pan fires located in corner of enclosure.....	140
Figure 166. Comparison of upper layer development during 1.0 m ² (10.8 ft ²) denatured alcohol pan fire in rear corner of enclosure with slit vent condition.....	141
Figure 167. Normalized mass loss of the upholstered sofa burning in the open.....	142
Figure 168. Comparison of normalized mass loss curves for open-burning and enclosed sofa fire scenarios with full door ventilation.....	143
Figure 169. Comparison of normalized mass loss curves for open burning and enclosed sofa fire scenarios with slit ventilation.....	143
Figure 170. Comparison of enclosure fire heat release rates from open door and slit vent scenarios with (a) carpet flooring and the upholstered sofa being the first item ignited, (b) vinyl flooring and the upholstered sofa being the first item ignited, (c) carpet flooring and the upholstered chair being the first item ignited, and (d) vinyl flooring and the upholstered chair being the first item ignited.....	146
Figure 171. Comparison of enclosure fire heat release rates from full-open door testing with carpet flooring where the upholstered sofa was the first item ignited (6-1) and where the upholstered chair was the first item ignited (6-3).....	148
Figure 172. Comparison of enclosure fire heat release rates from slit vent testing with carpet flooring where the upholstered sofa was the first item ignited (6-2) and where the upholstered chair was the first item ignited (6-4).....	149
Figure 173. Comparison of enclosure fire heat release rates from full-open door testing with vinyl flooring where the gasoline spill fire involved all combustibles simultaneously (6-5) and where the upholstered chair was the first item ignited (6-7).....	150
Figure 174. Comparison of enclosure fire heat release rates from slit vent testing with vinyl flooring where the gasoline spill fire involved all combustibles simultaneously (6-6) and where the upholstered chair was the first item ignited (6-8).....	150
Figure 175. Comparison of enclosure heat release rates from full open door testing with Class A ignition scenario on the sofa (Test 6-0) and with a gasoline spill in front of the sofa (Test 6-1).....	151

TABLE OF TABLES

	Page
Table E.1. Summary of experimental testing.....	E-1
Table 1. Summary of factors affecting enclosure fire dynamics.	1
Table 2. Summary of single pan experiments conducted by Parkes [2009] with mass loss rate per unit area (MLRPUA) results compared to open burning MLRPUA.	5
Table 3. Summary of testing conducted.	6
Table 4. Summary of fuel properties [Mealy et al. 2011].....	19
Table 5. Summary of unconfined gasoline spill fires.	20
Table 6. Summary of results from pan fires in the open.....	24
Table 7. Summary of Test Series 3 results.	28
Table 8. Summary of heat release rate data for flooring materials.	35
Table 9. Summary of 2.0 L gasoline spill fires in an enclosure.....	37
Table 10. Summary of pan fire testing in enclosure.	46
Table 11. Summary of Class A enclosure fire tests.	66
Table 12. Summary of mass loss of combustibles within Test 6-0.	71
Table 13. Summary of mass loss of combustibles within Test 6-1.	77
Table 14. Summary of mass loss of combustibles within Test 6-2.	83
Table 15. Summary of mass loss of combustibles within Test 6-3.	89
Table 16. Summary of mass loss of combustibles within Test 6-4.	96
Table 17. Summary of mass loss of combustibles within Test 6-5.	102
Table 18. Summary of mass loss of combustibles within Test 6-6.	108
Table 19. Summary of mass loss of combustibles within Test 6-7.	115
Table 20. Summary of mass loss of combustibles within Test 6-8.	123
Table 21. Summary of Flashover Indicators.....	129
Table 22. Comparison of heat release rates required to produce flashover conditions to average values measured in enclosure tests.	131
Table 23. Summary of enclosure effects on 0.23 m ² (2.5 ft ²) heptane pan fires.	137
Table 24. Comparison of enhanced burning phenomena for heptane pan fires in enclosures....	138
Table 25. Summary of enclosure effects on denatured alcohol pan fires.	139
Table 26. Summary of average mass loss rate (MLR) of upholstered sofas measured during open burning and enclosed fire scenarios.....	145
Table 27. Summary of Oxygen Concentrations at time when fire reached 500kW.	147

ACKNOWLEDGEMENTS

This project was supported by Award No. 2009-DN-BX-K232 awarded by the National Institute of Justice, Office of Justice Programs, U.S. Department of Justice. The opinions, findings, and conclusions or recommendations expressed in this publication/program/exhibition are those of the author(s) and do not necessarily reflect those of the Department of Justice.

LIST OF ACRONYMS

ATF	Bureau of Alcohol, Tobacco, Firearms and Explosives
FRL	Fire Research Laboratory
GWB	Gypsum Wallboard
OSB	Oriented Strand Board
CO	Carbon Monoxide
CO ₂	Carbon Dioxide
O ₂	Oxygen
THR	Total Heat Release
NPT	National Pipe Thread
SS	Steady-state
MBR	Mass Burning Rate
HRR	Heat Release Rate
HRRPUA	Heat Release Rate per Unit Area

EXECUTIVE SUMMARY

The development of a fire within an enclosure and the corresponding impact of the enclosure on the combustion process are dependent on numerous factors. These factors can be grouped into three different categories: enclosure geometry, ventilation, and fuel. The first category that needs to be considered is the geometry of the enclosure, which can include the volume of the space, the aspect ratio, and the ceiling height. When considering ventilation, both the area of the vent as well as the location/elevation of the vent must be considered. The third category is fuel, which includes the type of fuel, the total fuel surface area, the quantity of fuel, and the combustion characteristics of the fuel. As a fire develops within an enclosure, the factors listed in each of these categories begin to play a role in either the growth/decay of the fire depending on the combination of applicable factors. The extent to which the burning dynamics of a fuel change when burning in an enclosure compared to the open is dependent upon increased thermal effects, which result in increased burning rates, and reduced ventilation effects, resulting in reduced burning rates.

The purpose of this research was to characterize the changes in burning dynamics of fuels burning in enclosures as opposed to in the open and in doing so provide an experimental data set for both Class A and liquid fuels. To date, relatively little full-scale fire testing has been conducted to characterize these changes. This objective was achieved by way of full-scale fire testing and empirical-based analyses. A summary of the testing conducted and the rationale for their execution is provided in Table E.1.

Table E.1. Summary of experimental testing.

Test Series #	Test Series Name	Rationale for Testing
1	Unconfined Liquid Fuel Fires in the Open	Characterize the fire dynamics of the spill, pan, and Class A fire scenarios burning in the open
2	Pan Fires in the Open	
3	Class A Fires in the Open	
4	Enclosure Unconfined Liquid Fuel Fires	Characterize the fire dynamics of the spill, pan, and Class A fire scenarios burning within an enclosure
5	Enclosure Pan Fires	
6	Enclosure Class A Fire	

In this work, the burning dynamics of both confined and unconfined liquid fuel fires as well as Class A fuel packages were characterized. The liquid fuels used in this work were gasoline, heptane, and denatured alcohol. These fuels were selected for various reasons, including their prevalence in real-world forensic fire scenarios (gasoline), their historical presence in experimental fire research (heptane), and their differences in combustion chemistry (denatured alcohol). More specifically the denatured alcohol fuel was selected because of its negligible soot yield, which differs from both gasoline and heptane. The Class A materials (furniture and flooring) used in these tests were all selected because of their relevance to residential fires and their use in previous research efforts [Wolfe et al. 2009, Mealy et al. 2010] conducted which

allows for the comparison new data to existing data sets. The enclosure used in this work was designed to be representative of typical building spaces (i.e., height to width ratio of less than one).

These tests allowed for direct comparisons between full-scale open burning and enclosure fire scenarios. This work provides an improved understanding of the impact of the enclosure on fuel burning dynamics for three different fuel scenarios and identifies some of the key factors that govern this impact.

For unconfined liquid fuel fires (i.e., a spill), the impact of the enclosure was evaluated for both vinyl and carpet flooring systems. For both open (Test Series 1) and enclosed (Test Series 4) burning conditions, a 2.0 L (0.53 gal) gasoline spill was used as the spill fire scenario. For both flooring types, the enclosure fires behaved differently than the open burning scenarios. However, the difference was not due to enhanced burning of the liquid fuel; instead, the primary difference was the involvement of additional combustible material (i.e., adjacent flooring material outside the initial spill area). For the period of time in which the liquid fuel was the primary material burning, the fires grew in a similar manner and reached peak values that were comparable. For the vinyl substrate, the fire in the enclosure burned at peak values for an extended period of time as opposed to immediately transitioning to the decay phase as was observed in the open. Due to the involvement of additional flooring material, the carpet enclosure fire resulted in a larger fire than was observed in the open. Considering the short period of time in which the liquid fuel was the primary material burning (1 to 2 minutes), the enclosures did not have an effect on the spill fire, but did contribute to the fires growing larger and involving more material. There will be a certain critical room volume to fire size that will dictate whether an enclosure will lead to fires growing beyond the initial spill areas. Additional work is needed to identify this critical parameter.

The impact of an enclosure on confined area liquid fuel fires (i.e., pan fires) was determined to be dependent on fuel type, fuel location, and ventilation condition. Open (Test Series 2) and enclosed (Test Series 5) tests were conducted using 0.23 m² (2.5 ft²) and 1.0 m² (10.8 ft²) pans containing heptane and denatured alcohol, respectively. Pan fires in the enclosure were evaluated in two locations, center and corner, with full door ($AH^{0.5} = 2.6$) and slit vent ($AH^{0.5} = 0.6$) conditions. The quasi-steady-state heat release rates from these tests were compared.

In summary for the liquid fuel pan fires burning both in the open and within an enclosure (i.e., confined pool with sufficient depth to burn to steady-state), the results clearly show that enhanced burning occurs relative to open burning when a radiating upper layer is created in the compartment fire. During the initial 60–90 seconds of the heptane fire tests, both open burning and enclosed heat release rates were generally similar. After this initial period of burning, the enclosure fires continued to grow surpassing the steady-state value achieved in the open. The extent of this growth was dependent upon both the pan location and ventilation condition. In three of the four scenarios, the enclosed fires eventually reached a quasi-steady-state burning rate that was on average 60 percent higher than that measured in the open. However, an increase of only 19 percent over open burning conditions was measured for the slit vent corner fire scenario. The minimal enhancement observed in this test was attributed to the vitiation of the combustion air being entrained into the fire plume resulting in less efficient combustion of the heptane.

The second fuel evaluated was denatured alcohol. With the exception of the slit vent scenario with the fuel pan located in the corner, the denatured alcohol fires conducted within the enclosure were within three percent of that measured during tests conducted in the open and within one percent of other tests conducted within the enclosure. Open burning and enclosed denatured alcohol fires were comparable with respect to both fire growth and steady-state burning conditions. The enhanced burning observed for the denatured alcohol pan fire located in the corner of the enclosure with the slit vent condition was attributed again to the vitiation of the combustion air being entrained into the fire plume. However, in this case, the less efficient combustion produced a sootier, and thus a more radiative upper layer, which in turn enhanced the burning rate of the denatured alcohol. These tests illustrate the varying effect that an enclosure can have depending on the fuel that is burning within. For a non-sooting fuel (denatured alcohol), the enclosure/ventilation condition had only a minimal effect on the maximum heat release rate achieved, while for a sooty fuel (heptane) under the same conditions, the enclosure enhanced the burning of the fuel due to enhanced radiation to the floor and fuel surface.

In summary for liquid fuels in compartments:

- The fire size of a spill fire generally will not be affected by the compartment due to the relatively quick duration of the fire.
- If the fuel is contained in a pool so that it is deep enough (5 mm or more) to burn to a steady-state condition, a radiating upper smoke layer will increase the burning rate. An average 60 percent increase was observed for heptane pan fires with a full door vent. This increase can be moderated by restricted ventilation to the compartment.

For the Class A fuels, the impact of the enclosure on the burning dynamics of the fuel was evaluated based on analysis of the mass loss rates of the upholstered sofa which was the primary fuel item within the enclosure. In these tests, the Class A materials were evaluated using either a Class A ignition source or liquid fuel spill on either the floor of the enclosure or on an upholstered chair opposite the upholstered sofa. These fire scenarios were evaluated using both full door ($AH^{0.5} = 2.6$) and slit vent ($AH^{0.5} = 0.6$) ventilation conditions.

The mass burning rates associated with each of the enclosure fires with full door ventilation and the use of the liquid fuel ignition source were generally consistent with one another. The enhanced burning of the upholstered sofa within the enclosure was observed in all four, full door ventilation scenarios. In these scenarios, the average burning rate was 19 percent higher than that measured in the open with individual tests ranging from 15–24 percent increases. The greatest enhancement was observed in a test where the ignition scenario did not result in the direct ignition of the upholstered sofa and consequently the sofa became involved late in the fire. At the stage in which the sofa became involved, a hot upper layer had already developed and most likely pre-heated the sofa such that once involved it rapidly transitioned to fully-involved burning. In general, the degree of enhancement observed in these Class A fire tests was relatively minimal when compared to the values reported for the pan fire scenarios. Given the uncertainties in upholstered furniture calorimetry, the enhancement in burning for the scenarios evaluated are minor. However, as the room size to fire size ratio decreases, the effect may increase, assuming that vitiated conditions do not suppress the fire, as seen in the limited ventilation slit vent tests. Reduced mass loss rates compared to open air burning were measured for all slit ventilation

scenarios. The extent of the reduction was found to vary depending on the ignition scenario, which is indirectly related to the type of flooring material present. For tests in which vinyl was the flooring system installed, the average mass loss rates were 36–54 percent (31 and 47 g/s) that measured during open burning. For the carpeted scenarios, a reduction of 64 percent compared to open air burning was observed. These reduced mass loss rates were most likely due to the limited involvement of the sofa during the initial ignition fire and the vitiation of the enclosure later in the test when the upholstered sofa became involved. At this point in time in these tests, it was determined that lower level oxygen concentrations were on average 18 ± 1 percent which are considered to be in the range of the limiting oxygen index for combustion to occur.

In addition to evaluating the impact of the enclosure on Class A fuels, the upholstered sofa specifically, these full-scale Class A enclosure fires were also used to characterize the development of flashover conditions under varying ventilation and ignition scenarios. Flashover was evaluated relative to the ignition of paper indicators and flooring materials as well as to two established thermal criteria: the average upper layer temperature exceeding 600°C (1112°F) or the average floor level heat flux exceeding 20 kW/m^2 . In all of the full door ventilation tests conducted, the upper layer temperature threshold was reached first, followed by the floor level heat flux threshold, followed by flame extension from the vent. The occurrence of all three of these indicators typically occurred within 60 seconds. On average, the upper layer temperature threshold was reached less than ten seconds prior to the floor level flux threshold being reached. The occurrence of flashover was quite clear and indisputable for the full open door fires. Visual observations of the ignition of paper indicators and the flooring material were clearly definable. The ignition of floor level combustibles always occurred after both the 600°C (1112°F) and 20 kW/m^2 criteria were achieved, but before ignition of the door plume. The time differences between the two criteria and floor level ignition ranged from 5 to 43 seconds. In general, the layer temperature and floor heat flux criteria appear to be reasonably representative and conservative in that they predict flashover (ignition of all combustibles in the space) slightly earlier than may occur in actuality. The occurrence of external flames lagged behind the occurrence of flashover.

For the slit vent condition, the occurrence of flashover was not as clearly defined (visually) or consistent as was observed for full door ventilation. Only three of the four tests with the slit vent reached the thermal thresholds and the radiant ignition of visual indicators was only observed in one of the tests. Although the thermal criteria for flashover were achieved in these three fires, it is expected that flashover did not actually occur. In these tests, fire growth was inhibited by the limited ventilation condition. The vent condition created a vitiated upper layer that extended almost to the floor of the enclosure causing the fire to bank down and burn primarily at low levels. Over time, fire spread to adjacent combustibles and involved the whole room as evidenced post-test by fire damage across the whole space. The instantaneous involvement of all combustibles within the enclosure was not visually observed as the deep smoke layer prevented a clear view of the flooring and paper indicators. Although the average floor level heat flux reached a value of 20 kW/m^2 , this was due to a high reading above the criterion in only one of the two measurement locations. Consequently, this non-uniformity indicates that the thermal conditions throughout the space were not sufficient to cause a rapid transition from localized burning to wide spread ignition of combustibles throughout the room. In other words, flashover did not actually occur. The upper layer temperature measurements were generally consistent with this conclusion in that upper layer values were only slightly above

600°C (1112°F) and usually for only short periods of time. Despite this assessment, to a general observer after the fire, visual observations of the damage may lead to an interpretation that the space did flash over.

This work demonstrated that ventilation conditions must be considered when evaluating the fire dynamics of a fire event relative to the post-fire damage. A limited ventilation compartment may become fully involved and result in widespread fire damage across all flooring and furniture. In addition, a generic correlation for flashover may yield a required heat release rate that is well within reason given the fuel loads in the room. For example, in the testing in this program, correlations in the literature predicted heat release rates for flashover in the slit-vent fires of approximately 400 to 600 kW. These heat release rates are in the range of the upholstered chair and coffee table, respectively. Based on this calculation and the post-fire damage, one may conclude that the fire flashed over early in the fire development and reached temperatures well in excess of 600°C (1112°F). However, similar fire damage (i.e., wide spread with all surfaces burned) can occur without flashover due to limited ventilation that can actually limit fire growth so that it progresses over a longer timeframe with temperatures below 600°C (1112°F).

1.0 INTRODUCTION

Fires occurring within an enclosed space represent the vast majority of fire scenarios in both residential and commercial settings. Understanding the impact that an enclosure can have on the burning dynamics of fuels is essential to accurately predict fire development within a given space for fire protection system design or for fire hazard and forensic analysis. Traditionally, heat release rate measurements for a given fuel item are measured under open burning conditions. However, this data is often used to represent materials burning within an enclosure without fully understanding the impact the enclosure might have on the burning dynamics of the fuel. Depending on the geometry of the space and the ventilation conditions present, the enclosure may have no effect or it may either enhance or reduce fuel-burning rates. A summary of some of the factors that impact fuel burning dynamics within an enclosure is provided in Table 1.

Table 1. Summary of factors affecting enclosure fire dynamics.

Enclosure Geometry	Ventilation	Fuel
- Volume	- Area of Vents	- Fuel Surface Area
- Aspect Ratio	- Location of Vents	- Quantity of Fuel
- Ceiling Height		- Combustibility of Fuel

There are several competing factors that can affect the fuel-burning rate within a compartment. As a fire develops within a compartment, the boundaries of the space are heated both convectively and radiatively from the flame plume and hot gases. Once heated, these boundaries re-radiate energy back to the fuel surface, thus enhancing the burning rate of the fuel. Further enhancement of the fuel-burning rate results from the radiative energy being emitted by the developing hot gas layer. The extent of this enhancement is dependent upon both the fire size as well as the enclosure geometry (i.e., compartment aspect ratio and volume).

For ventilation-controlled fires, as the fire compartment volume decreases relative to the fire size, the initial amount of available air decreases, which will reduce the fuel-burning rate. In addition, if the enclosure geometry allows hot fire gases to descend down to the base of the fire (i.e., a table or elevated cabinets), the fuel burning rate can decrease because the layer of fire gases limits the amount of oxygen available to the fire. The extent of vitiation (i.e., reduced oxygen) can also depend on the area, configuration, and location of vents relative to the burning fuel surface. For single vent compartments, as the vent area is reduced or elevated relative to the burning fuel surface, mixing will increase between the vitiated upper layer exiting the vent and the fresh air entering [Quintiere 2006]. Consequently, the oxygen concentration in the air being entrained into the fire is reduced and the fuel-burning rate will correspondingly be reduced. In summary, the extent to which the burning dynamics of a fuel change when burning in an enclosure compared to the open is dependent upon increased thermal effects, which result in increased burning rates, and reduced ventilation effects, resulting in reduced burning rates.

This research compares the burning dynamics of liquid and Class A fuels burned in both an enclosure and in the open. The work builds on previous research programs investigating the burning dynamics of both liquid fuels and Class A fuel packages [Tewarson 1972, Bullen 1979, Fleischmann 1997].

2.0 OBJECTIVES AND APPROACH

The purpose of this research was to characterize the changes in dynamics of fuels burning in enclosures as opposed to in the open. In doing so, an experimental data set for both Class A and liquid fuels was developed. To date, relatively little full-scale fire testing has been conducted to characterize the change in burning dynamics of a fuel when burning within an enclosure compared to burning in the open. To achieve this objective, a series of tests were conducted where identical fuel packages were burned in both open and enclosed conditions with varying ventilation schemes. The comparisons of the heat release rate and thermal environment data from open burning fires and enclosure fires provide insights into the effects that the enclosure has on the burning dynamics of the various fuel packages.

3.0 LITERATURE REVIEW

3.1 Compartment Effects

Fires occurring within an enclosed space can typically be described in three phases; a growth phase, a fully-developed phase, and a decay phase. An illustration of the traditional enclosure fire heat release rate curve is provided in Figure 1. During the growth phase, fires are generally assumed to be burning under natural conditions; the burning dynamics of the fuel are not affected by the presence of the enclosure. With sufficient time, the fire will eventually grow to a maximum size (fully-developed), and the burning rate will be dictated by the amount and characteristics of the fuel (fuel-limited) or by the characteristics of the enclosure (ventilation limited). In general, ventilation controlled fires are the most prevalent fire scenario evaluated. The transition between the growth and fully developed phases of an enclosure fire can be marked by the occurrence of flashover. Although defined in numerous ways, a general definition of flashover is the relatively fast transition from a localized fire to the widespread involvement of combustible material within the compartment. A further discussion of flashover and the various indicators associated with this phenomenon is provided in Section 3.2. The decay phase can be described by the reduction in fire size as a result of either the consumption of all available fuel or depletion of oxygen in the vicinity of the burning material.

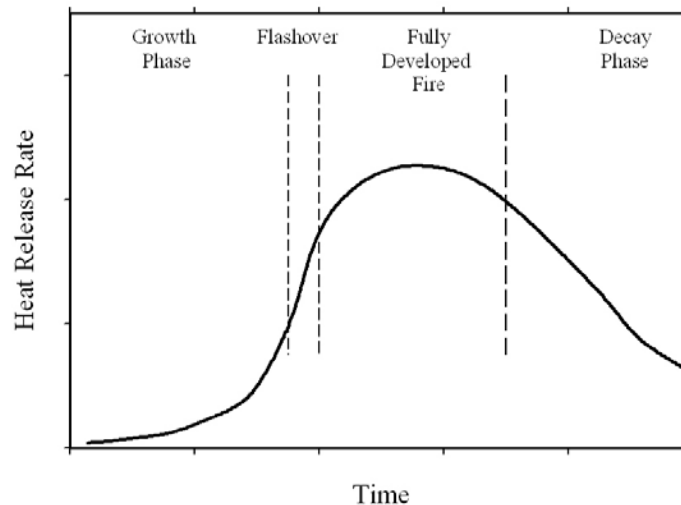


Figure 1. Illustrative plot showing general enclosure fire progression.

Some of the earliest experimental work on the effect of confinement on fire dynamics was conducted by Kawagoe [1963]. Fire tests were conducted in both model and full-scale rooms and houses. From this work, a correlation between the burning rate of cellulosic fuels and the ventilation opening of the enclosure was developed. The correlation showed that the burning rate of a fuel was not only a function of ventilation area, but also the height of the ventilation opening. Based upon this work, the ‘ventilation parameter’ was developed to describe ventilation conditions relative to the geometry of the ventilation opening. As shown in Equation 1, the ventilation parameter is calculated using the area of a vent (A_o) and the height of the vent (H_o).

$$\text{Ventilation Parameter} = A_o \sqrt{H_o} \quad (\text{m}^{5/2}) \quad (1)$$

Using first principles, Drysdale [2011] provided a summary of the derivation of this relationship thus further substantiating the findings of Kawagoe [1963]. Based upon this work, Tsuchiya et al. [1971] developed an early hydrocarbon burning model to predict fuel mass burning rates within an enclosure. The model provided both ventilation-limited and fuel-limited burning scenarios with the ventilation-limited scenarios being modeled after the findings of Kawagoe [1963].

Tewarson [1972] examined the effect of an enclosure on the burning rates of ethyl alcohol. In this work, 0.2 m (7.9 in.) diameter pan fires were conducted within a 0.2 m³ (7.0 ft³) enclosure. The enclosure was 0.4 x 1.0 x 0.5 m (1.3 x 3.3 x 1.6 ft) with dual full-width windows on opposing walls. The heights of the windows were modified to provide different degrees of ventilation. The mass burning rate for all fires was measured for the duration of the test, and in doing so the authors were able to characterize fuel mass burning rates prior to and after the fuel began to boil. Pre-boiling burning rates for the ethyl alcohol fires were on average sixty percent of that measured during the boiling liquid phases of the fires. In these tests, the burning rates for ethyl alcohol fires within an enclosure were as much as 1.8 times greater than those measured in open burning conditions, when burning in well-ventilated enclosure conditions. It was also found that under limited ventilation conditions, the mass burning rate of the fuel within the compartment was reduced to approximately 20 percent of that measured in the open burning state. These comparisons were made during the boiling stage of these fires.

Bullen et al. [1979] evaluated the differences in burning rates for ethanol in open conditions and within a compartment. The authors developed a model for liquid pool compartment fires. Their experimental work evaluated 0.19 and 0.37 m² (2 and 4 ft²) pan fires conducted within a 2 m x 1 m x 1 m high (6.6 ft x 3.3 ft x 3.3 ft high) compartment. Three different ventilation conditions were considered, and all enclosure fire burning rate data were compared to that collected for fires in the open. During the growth phase, most ethanol pool fires burned at a rate similar to that measured in the open. During the post-flashover phase, ethanol-burning rates were increased by as much as six times when compared to the open.

Fleischmann et al. [1997] investigated the impact of ventilation on liquid fuel fires burning within a 1.0 x 1.5 x 1.0 m (3.3 x 5.0 x 3.3 ft) enclosure. A total of ten different ventilation scenarios with ventilation parameters ranging from 0.004–0.07 m^{5/2} were evaluated, and the mass burning rate of a 0.2 m (7.9 in.) diameter, continuously-fed heptane fire was measured. The mass burning rates for all fires conducted within the enclosure were then compared to a mass burning rate for the pan in the open. The mass burning rate measured in the open ($\dot{m} = 35 \text{ g/s-m}^2$) was

approximately 1.8 times larger than that predicted ($\dot{m} = 20 \text{ g/s-m}^2$) using Equation 2 at a diameter, D , of 0.2 m and the constants provided for heptane by Babrauskas [1983].

$$\dot{m}'' = \dot{m}''_{\infty} * (1 - e^{-k\beta D}) \quad (2)$$

where \dot{m}''_{∞} is the maximum mass burning rate per unit area (g/s-m^2) for a given fuel, $k\beta$ is the product of the absorption coefficient and the mean-beam length corrector, and D is the equivalent diameter of the fire. However, analysis of the individual burning rate data sets used by Babrauskas [1983] to develop the aforementioned values for heptane (i.e., Kung 1982, Tarifa 1967) revealed that the average values presented by Babrauskas (i.e., \dot{m}''_{∞} of 101 g/s-m^2 and $k\beta$ of 1.1) are not representative of the experimental values reported in the Kung and Tarifa studies. A presentation of this difference along with the data on which correlation parameters were developed is presented in Figure 2. Using the curve fit based on Kung and Tarifa data, a mass burning rate per unit area of 30 g/s-m^2 is obtained for a 0.2 m diameter fire, which agrees relatively well with the data of Fleischmann et al. of 35 g/s-m^2 .

Fleischmann et al. [1997] measured mass loss rates for liquid fuels that were both larger and smaller than the rates measured for the burning fuel in the open. Burning rates as much as two times larger than those measured in the open were observed for ventilation factors greater than 0.02. The authors also measured mass burning rates that were as low as fifty percent of that measured in the open for ventilation factors below 0.016. In all these tests, the equivalence ratio within the test compartment was relatively constant ($\Phi = 1.7$) over a wide range of opening factors, even for scenarios in which the fuel mass loss rate was less than that measured in open conditions.

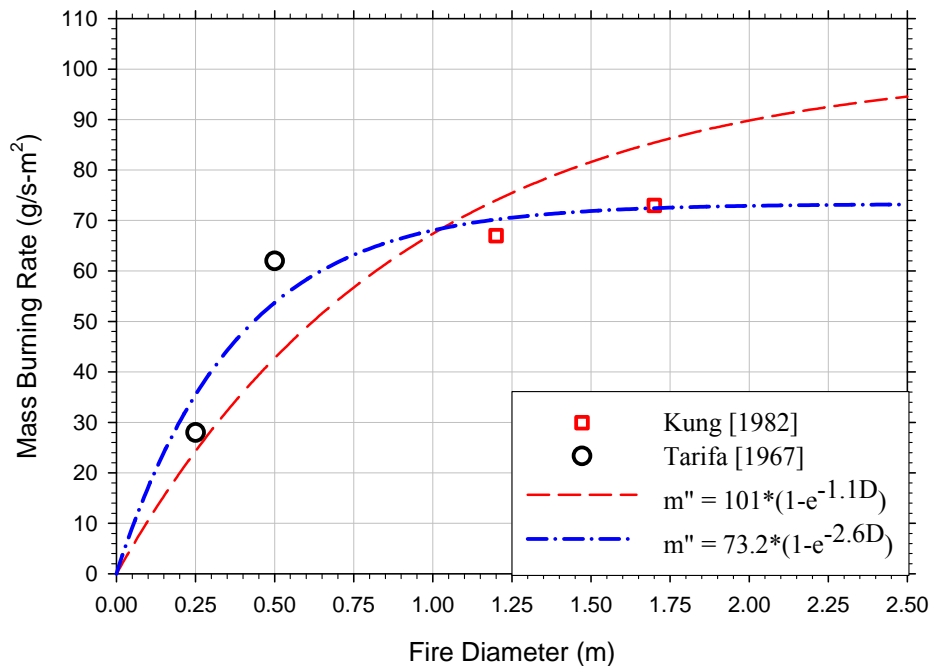


Figure 2. Plot of historical heptane burning rate data and curve fit using Babrauskas [1983] correlation parameters (thin red line) and curve fit based on historical data (thick blue line).

Parkes [2009] conducted a series of fifteen tests using heptane pan fires within an enclosure, which evaluated the impact of vent size, fire location, and fire size. Square 0.2 m (7.9 in.) pans located at three locations along the centerline of a 2.4 m x 3.6 m x 1.2 m (8 ft x 12 ft x 4 ft) enclosure were primarily used. Several larger pans representing areas two and three times that of the standard 0.2 m (7.9 in.) pan were also used. In general, the fires were located in the center, rear, and front (i.e., near the ventilation source) of the enclosure. The fires were continuously fed and permitted to burn for a minimum of one hour such that steady-state burning conditions could be achieved and accurately measured. The impact of fire location was dependent upon the ventilation factor. A summary of the results from the single pan experiments conducted by Parkes [2009] is provided in Table 2.

Except for one scenario (Run ID 13), all tests resulted in higher burning rates in the compartment compared to the open. As shown in Table 2, for all ventilation factors except 0.186, the rear pan had the highest mass burning rate. In general, the increase in mass burning rate compared to open burning diminished with the source moved from the rear to the front of the enclosure. The largest increase in mass burning rate for all scenarios was observed for the front pan with the smallest ventilation opening ($A_o H_o^{1/2} = 0.186$). This ventilation scenario also resulted in the largest average increase for all pans within the enclosure.

Table 2. Summary of single pan experiments conducted by Parkes [2009] with mass loss rate per unit area (MLRPUA) results compared to open burning MLRPUA.

Run ID	Pan Location	$A_o(H_o)^{1/2}$ ($m^{5/2}$)	MLRPUA w.r.t. Open Burning MLRPUA
1	Rear	3.155	1.9
2		2.400	1.3
3		0.400	3.3
4		0.372	2.9
5		0.186	3.3
6	Center	3.155	1.0
7		2.400	1.1
8		0.400	2.8
9		0.372	1.8
10		0.186	2.9
11	Front	3.155	1.1
12		2.400	1.1
13		0.400	0.7
14		0.372	1.1
15		0.186	3.6

3.2 Flashover

Flashover, the relatively fast transition from a single item or localized group of items burning within a space to the widespread involvement of combustibles within the space, has been studied and reviewed by numerous researchers [Waterman 1968, Haggland et al. 1974, Babrauskas 1979, Peacock et al. 1999, Francis and Chen 2012]. Various conditions have been identified as indicators for the occurrence of flashover. A recent comprehensive review conducted by Peacock et al. [1999] concluded that flashover can be reasonably predicted using an upper gas layer temperature threshold of 600°C (1112°F) and heat flux threshold of 20 kW/m² measured at the floor. The most recent review by Francis and Chen [2012] suggest that the most convenient definition is based on the visual observation of flame projecting out of the vent.

4.0 EXPERIMENTAL APPROACH

A total of six test series were conducted to address the research objectives. Tests were conducted at the Alcohol, Tobacco, Firearms and Explosives (ATF) Fire Research Laboratory at the National Laboratory Center beneath the 1 MW and 4 MW hood calorimeters in the medium burn room. Test Series 1–3 were conducted to characterize the fire dynamics of both liquid fuel and Class A fuel fires burning in the open. Unconfined liquid fuel spill fires on two different types of flooring materials were characterized in Test Series 1. Confined liquid fuel spill fires (i.e., pan fires) were evaluated in Test Series 2. The individual burning dynamics of several different Class A fuels were characterized in the third series of tests. Identical fuel packages were used in Test Series 4–6 with the items placed within an enclosure with varying ventilation schemes. A summary of the test series and the rationale for their execution is provided in Table 3.

Table 3. Summary of testing conducted.

Test Series #	Test Series Name	Rationale for Testing
1	Unconfined Liquid Fuel Fires in the Open	Characterize the fire dynamics of the spill, pan, and Class A fire scenarios burning in the open
2	Pan Fires in the Open	
3	Class A Fires in the Open	
4	Enclosure Unconfined Liquid Fuel Fires	Characterize the fire dynamics of the spill, pan, and Class A fire scenarios burning within an enclosure
5	Enclosure Pan Fires	
6	Enclosure Class A Fire	

4.1 Test Floor

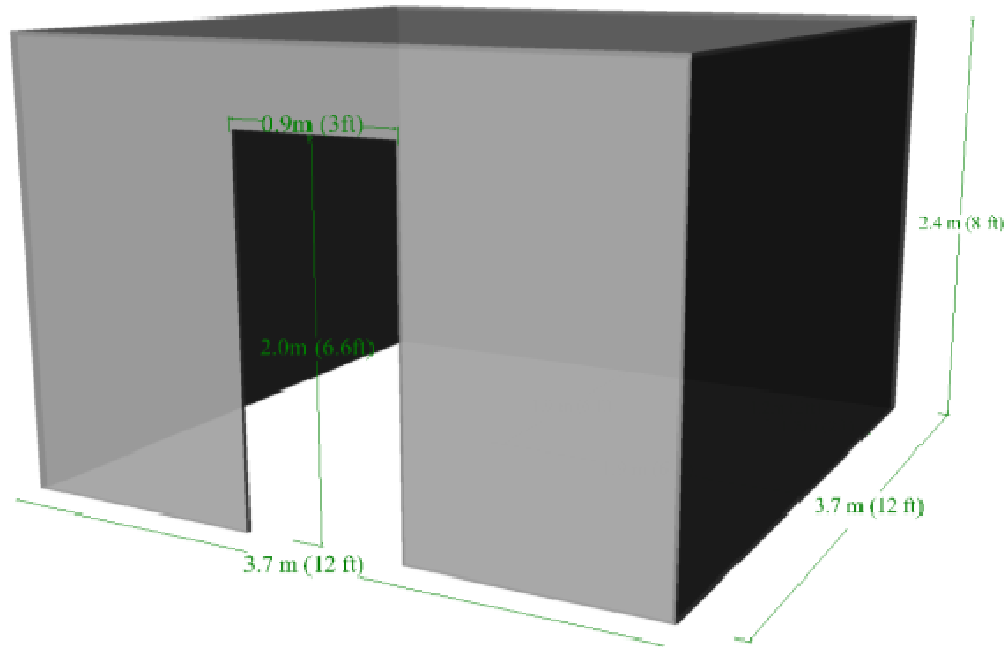
A test floor for conducting unconfined liquid fuel spill fires in the open was framed with 5.1 x 10.2 cm (2 x 4 in.) dimensional lumber spaced 40.6 cm (16 in.) on center, overlaid with a single layer of 12.7 mm (0.5 in.) plywood. The plywood served as the subfloor to either carpet or vinyl flooring. After each spill fire test the plywood substrate was removed and a new sub-floor installed. A photograph of the test floor is provided in Figure 3.



Figure 3. Vinyl floor constructed for open burn testing.

4.2 Test Enclosure

The test enclosure used in Test Series 4–6 was 3.7 m (12 ft) by 3.7 m (12 ft) square. The enclosure had a ceiling elevation of 2.1 m (8 ft) and a total volume of 32.6 m³ (1,152 ft³). Identical room geometries were used by Shanley [1997] for fire pattern research and are recommended in ASTM E603 [2007]. The front wall of the enclosure was identified as the wall containing the vent and all other walls are identified accordingly (i.e., left wall to the left side upon entering through the vent opening, rear wall opposite the vent, and right wall to the right side upon entering the vent opening). Photographs and dimensioned renderings of the test enclosure are provided in Figure 4 and Figure 5.

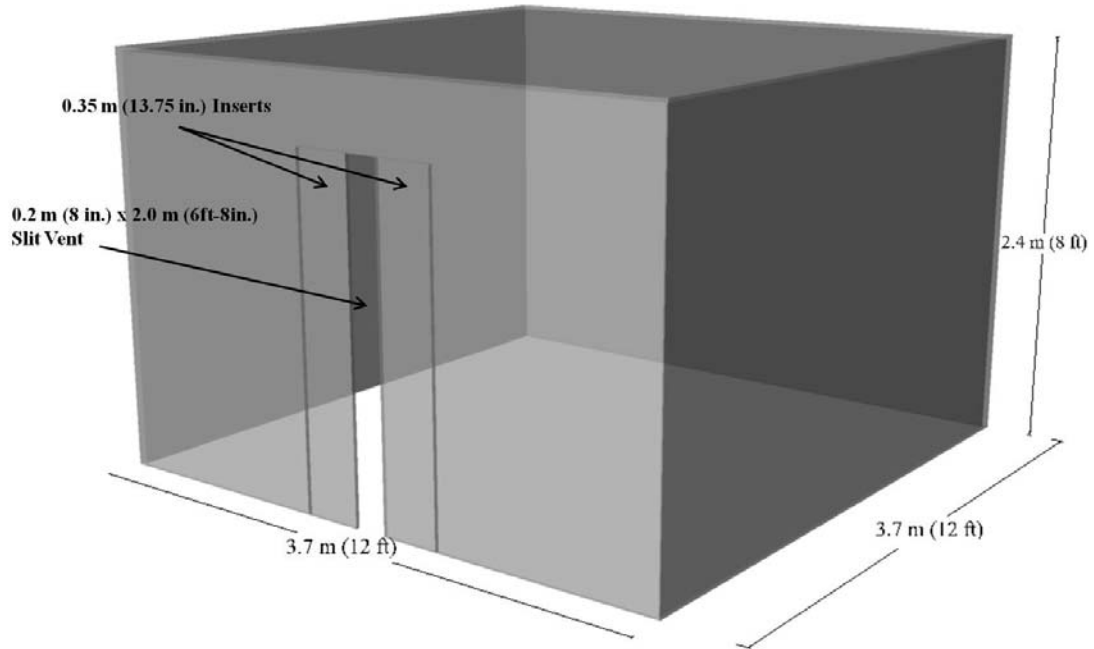


(a) Dimensioned rendering of test enclosure.



(b) Photograph of test enclosure beneath 4MW hood calorimeter.

Figure 4. Test enclosure with full door vent used in Test Series 4–6.



(a) Rendering with slit vent



(b) Photograph of test enclosure beneath 4 MW hood calorimeter

Figure 5. Test enclosure with slit vent used in Test Series 4–6.

This enclosure layout was selected because it provided a height -to-width ratio that was less than one which is representative of typical building spaces (i.e., in typical occupied spaces, the bounding walls are located at a greater distance from the fire than the ceiling [Parkes 2009]). The walls of the test enclosures were framed using 5.1 x 10.2 cm (2 x 4 in.) dimensional lumber while the floor and ceiling joists were constructed from 5.1 x 15.2 cm (2 x 6 in.) dimensional lumber. All framing was spaced 40.6 cm (16 in.) o/c. Depending on the test series being conducted, the interior of the enclosure was lined with either 12.7 mm (0.5 in.) or 15.9 mm (0.625 in.) gypsum wall board (GWB). The thicker GWB was used in Test Series 5 (pan fires) because the thicker material provided more thermal protection to the wood framing of the structure for these prolonged burns. GWB joints were sealed using 3M® intumescent fire barrier sealant (IC 15WB+).

Two different ventilation conditions were evaluated. The first ventilation scheme consisted of an opening in the form of a full-open doorway. The doorway was 0.91 m (3 ft) by 2.0 m (6 ft 8 in.) with a total vent area of 1.85 m² (19.9 ft²). The fully open doorway represented a ventilation factor of 2.63. The second ventilation condition was a 0.2 m (8 in.) by 2.0 m (6 ft 8 in.) slit vent with a total vent area of 0.4 m² (4.3 ft²) as may occur with a partially open door to an office or bedroom. This vent represents a ventilation factor of 0.56 m^{5/2}, which is comparable to most residential window openings. A typical window opening was not used because of the differing flow dynamics created by elevating the vent. These vents were selected because they represent typical ventilation schemes in residential enclosure fire scenarios, such as partially or fully open doorways. There are relatively large data sets for comparison at the two ventilation factors that these vents represent. When transitioning between the full-open doorway vent and the slit vent, the ventilation area was reduced by the addition of 15.9 mm (0.625 in.) gypsum wallboard panels that effectively reduced the width of the full-open doorway.

The floor system of the test enclosures consisted of a base layer of 12.7 mm (0.5 in.) plywood overlaid directly on the floor joists. A secondary layer of 12.7 mm (0.5 in.) gypsum wallboard was laid over top of the plywood to provide a thermal barrier to prevent degradation of the enclosure sub-floor. A second sub-floor that consisted of an additional layer of 12.7 mm (0.5 in.) plywood was installed prior to each test, serving as the 'test' sub-floor that was subjected to the thermal exposure of the enclosure fire.

4.3 Spill Substrates

The substrates used for spill fire testing included vinyl flooring over plywood and carpet / padding over plywood. The vinyl flooring was a Congoleum Prelude® vinyl sheeting having a nominal thickness of 1.2 mm (0.04 in.). The vinyl sheet was applied to 14.7 mm (0.578 in.) plywood using Roberts 2001 felt-back sheet vinyl adhesive. The vinyl adhesive was applied using a 1/16 x 1/16 x 3/32 in. notched trowel. The vinyl was applied in accordance with adhesive manufacturer instructions.

The carpet used in this testing was a Portico Royale Plus® (BP724) 100% nylon cut pile Saxony with an approximate mass per unit area of 0.85 kg/m² (25 oz./yd²) and pile height of 12.5 mm (0.49 in.). The backing material of the carpet was woven polypropylene. This carpeting material complies with all federally mandated flammability standards including 16CFR-1630.4 (Pill Test), ASTM E648 (Critical Radiant Flux), and ASTM E662 (Smoke Density). All carpet

was backed using Mohawk PS53P bonded urethane foam pad with a nominal thickness of 9.5 mm (0.375 in.) and density of 88.1 kg/m³ (5.5 lb/ft³).

4.4 Class A Fuels

The Class A fuels evaluated included an upholstered sofa; an upholstered chair; a coffee table; plastic baby car seats; and flooring materials. Photographs of these materials are provided in Figure 6.



Figure 6. Class A fuels.

The sofa used in these tests was an IKEA® Klippan® style sofa. The overall dimensions of the sofa were 1.8 m (5 ft 10 in.) wide by 0.88 m (2 ft 11 in.) deep by 0.66 m (2 ft 2 in.) high. The seat depth was 0.54 m (1 ft 9 in.) and the seat height was 0.43 m (1 ft 5 in.). The frame of the sofa was constructed of particleboard, solid hardwood, solid softwood, and cardboard. The sofa had steel zigzag springs. The sofa seat, back and armrest were constructed of 91% polyurethane foam (density of 30 kg/m³) and 9% polyester wadding. The lining and cover were 100% cotton. The sofa meets the requirements of the California Bureau of Home Furnishings Technical Bulletin 117.

The chair used in these tests was an IKEA® Tullsta style upholstered chair. The overall dimensions of the chair were 0.8 m (2 ft 6 in.) wide by 0.7 m (2 ft 3 in.) deep by 0.8 m (2 ft 6 in.) high. The seat depth was 0.6 m (1 ft 10 in.) and the seat height was 0.5 m (1 ft 5 in.). The frame of the chair was constructed of expanded polystyrene plastic and oriented strand board (OSB). The chair seat, back and armrest were constructed of polyurethane foam with an average density of 27 kg/m³ (1.7 lbs/ft³). Polyester wadding was used to wrap the polyurethane foam and this

wadding was wrapped with a lining cover, which was constructed from 100% cotton. The chair also meets the requirements of the California Bureau of Home Furnishings Technical Bulletin 117.

The coffee table used in these tests was an IKEA® Lack® style table. The overall dimensions of the table were 0.9 m (3 ft) wide by 0.5 m (1 ft 9 in.) deep with a total height of 0.46 m (18 in.). The top of the coffee table was constructed of particleboard, ABS plastic and acrylic paint. The shelf was constructed of particleboard, ABS plastic and melamine foil. The legs were constructed of particleboard and foil.

For furnished enclosure tests, Class A materials were installed within the test enclosure as shown in Figure 7. The upholstered sofa was positioned in the rear right corner of the room, positioned such that an air gap of 0.1 m (4 in.) was present between the walls and the perimeter of the sofa. The upholstered chair was offset from the rear wall by 1.0 m (39 in.) and 0.1 m (4 in.) from the left wall. The table was positioned so that the long edge was 0.61 m (2 ft) from the edge of the sofa and centered with respect to the sofa. The distance between the table and chair was 0.6 m (24 in.). The baby seat, positioned against the left wall approximately 1.5 m (60 in.) from the upholstered chair provided a multi-component fuel package comprised of both plastic, cloth and padding materials. In some test scenarios, a 100 percent polyester blanket was spread out on top of the carpet. The blanket was used to determine if Class A materials, when consumed by fire, create fire patterns that look similar to liquid fuels.

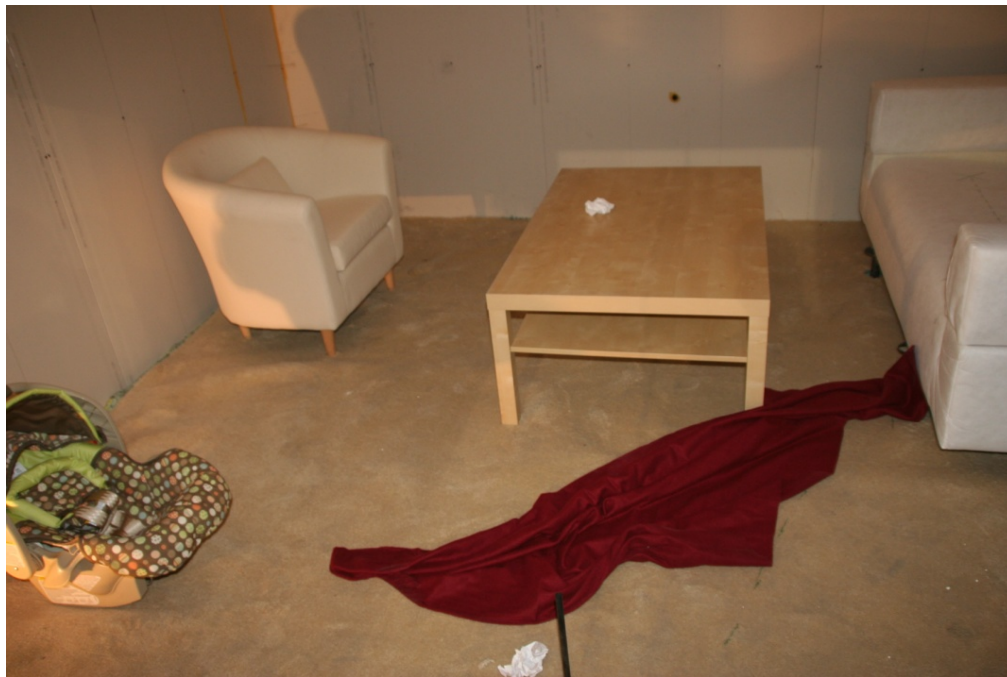


Figure 7. Typical Class A fuel layout in test enclosure.

The vinyl flooring system consisted of vinyl flooring applied to 12.7 mm (0.5 in.) plywood using vinyl adhesive. The vinyl used was a Congoleum Prelude® vinyl sheeting with a nominal thickness of 1.2 mm (0.04 in.). The adhesive used was Robert's Premium vinyl adhesive. The vinyl adhesive was applied using a 1/16 x 1/16 x 3/32 in. notch trowel. Once applied, the adhesive was permitted to become tacky prior to the application of the vinyl sheet.

The carpet system was comprised of carpet and foam padding on 12.7 mm (0.5 in.) plywood. The carpet was a Portico Royale Plus® (BP724) 100% nylon cut pile Saxony with an approximate mass per unit area of 0.85 kg/m² (25 oz./yd²) and pile height of 12.5 mm (0.5 in.). The backing material of the carpet was a woven polypropylene. Foam padding was a PS53P bonded urethane foam pad with a nominal thickness of 9.5 mm (0.375 in.) and density of 88.1 kg/m³ (5.5 lb/ft³).

4.5 Enclosure Instrumentation

Experimental measurements recorded included heat release rate, temperature, heat flux, gas concentration, and fuel mass loss rate. Thermocouples were used to characterize the thermal conditions at various elevations and locations within the test enclosure. Heat flux measurements were used to characterize the heat flux to the walls and floor of the test enclosure. Gas concentrations were used to determine the extent to which combustion efficiency played a role in the burning dynamics of the liquid fuel and Class A materials. Fuel mass loss was measured using a load cell platform, for comparison to fuel burning rates as measured by the hood calorimeter (i.e., heat release rate (HRR)).

All tests were conducted beneath either a 1 MW or 4 MW hood calorimeter. For enclosure fire tests, the enclosure was positioned beneath the 4MW hood such that the door spill plume was centered beneath the calorimeter.

4.5.1 Temperature Measurements

A total of twenty-seven, 24 GA, Type K, Inconel sheathed bare-bead thermocouples were used to characterize the thermal gradients within the test enclosure as well as the enclosure vent. Temperature rakes comprised of nine thermocouples, spaced at 0.3 m (1 ft) intervals, were installed in opposite corners as shown in Figure 8. The point of measurements (i.e., bead) was located 0.15 m (6 in.) from both walls of the test enclosure to minimize the effect of the wall boundary. The bottom and top thermocouple in each rake were located 25.4 mm (1 in.) from the floor and ceiling, respectively. The third rake was installed in the vent opening at the vertical centerline from soffit to sill. The upper and lower thermocouples were located approximately 25.4 mm (1 in.) from the soffit and sill respectively with the remaining six thermocouples installed at equal intervals (i.e., 0.15 m (6 in.)) over the height of the vent.

Corner thermocouple rake locations were selected in an attempt to minimize the impact of direct flame impingement from burning objects within the room as well as flaming that could occur along the centerline of the enclosure due to the vent. This approach has been adopted in previous enclosure fire test series examining the impact of an enclosure on burning rates [Parkes, 2009]. Furthermore, basic modeling simulations (FDS) were conducted and showed minimal gradients between the corner locations used (i.e., 0.15 m offset) and centered locations.

4.5.2 Heat Flux Measurements

Heat flux measurements were collected from a total of eight locations within the test enclosure. Six of these measurement locations were in the walls and the remaining two were at floor level. Three of these measurements were collected from the center of the rear wall directly opposite the ventilation opening, at elevations of 0.6, 1.2, and 1.8 m (2, 4, and 6 ft). The

remaining three wall measurements were collected at the right wall, 1.4 m (4.5 ft) from the front wall, at elevations of 0.45, 1.2, and 2.0 m (2.5, 4, and 6.5 ft). Floor heat flux measurements were collocated with the thermocouple trees. All measurements were collected using water-cooled, Schmidt-Boelter type, heat flux transducers (Medtherm Model 64-xxSB-20 where xx is the range of the instrument). Rear wall transducers had a range of 0–200 kW/m². Right wall transducers had a range of 0–150 kW/m². Floor transducers had a range of 0–100 kW/m².

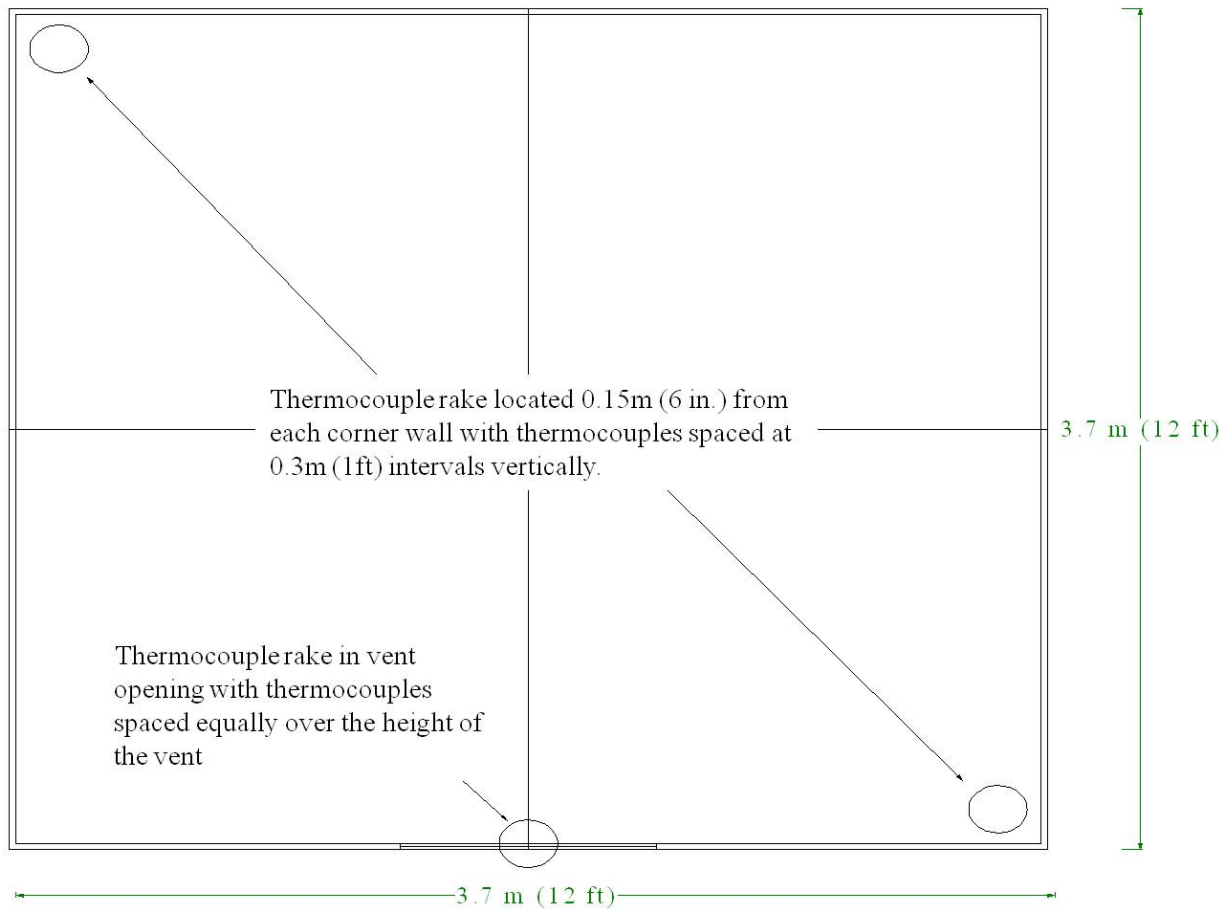


Figure 8. Thermocouple locations within test enclosure.

All transducers were mounted in 2.5 cm (1 in.) diameter holes drilled into the floor/wall of the enclosure. The perimeters of the transducers were sealed using fire caulk to prevent air being entrained into the enclosure at these locations. Water flow to the transducers was provided by a heat flux water bath system designed to ensure constant temperature, constant flow conditions to all gauges. The cooling water temperature provided to each transducer was maintained between 35–40°C (95–104°F), flowing at a nominal flow rate of 0.5 cc/min.

4.5.3 Gas Species Measurements

Gas concentrations were measured at two locations, high and low in the space. These locations were selected to provide representative gas species concentrations for the upper and lower layers during each fire. The upper layer gas probe was located 0.45 m (1.5 ft) from the interior plane of the doorway, 0.3 m (1 ft) below the ceiling. This location was selected because

it provided a characterization of the combustion species present in the enclosure spill plume, generally thought of as an average of the species present in the upper layer of the compartment. The lower layer gas probe was located 0.9 m (3 ft) inside the doorway, 0.3 m (1 ft) above the floor of the test enclosure. This probe sampled incoming air at an elevation representative of the initial burning fuel surfaces. The probes were positioned horizontally, facing the back wall to avoid water spray from suppression activities.

Gas sampling trains for both sampling ports were constructed in the same manner. The probes located within the test enclosure were constructed from 12.7 mm (0.5 in.) diameter stainless steel tubing. An additional 3.0 m (10 ft) of tubing was added downstream of the stainless steel outside the enclosure consisting of 12.7 mm (0.5 in.) polyethylene tubing back to the analyzer rack.

Once extracted from the test enclosure, the amount of CO, CO₂ and O₂ present in the enclosure were measured. The analyzers used in this test series were Siemens Oxymat 61 and Ultramat 23. All samples were conditioned using a soot filter, cold trap, and Drierite desiccator. The O₂ mole fraction was measured using a paramagnetic oxygen purity sensor contained within each of the analyzers. These sensors were operated in the range of 0% to 22%. The analyzers were zeroed using a 100% nitrogen gas and were calibrated with ambient air using a value of 20.95. Non-dispersive infrared gas sensors measured the CO and CO₂ mole fractions present in the gas samples. These analyzers were operated at ranges of 0% to 5% and 0% to 25% for CO and CO₂ concentrations, respectively. The analyzers were zeroed using a 100% nitrogen gas. Calibration was performed with an 8.9% CO, 18.9% CO₂ mixture, with nitrogen balance.

4.5.4 Mass Loss

Fuel mass loss rates were measured using a Sartorius Midrics load cell (Model MW2PU1-150IG) with a maximum capacity of 150 kg (331 lbs) and a measurement accuracy of 0.01 kg (0.0022 lbs). The load cell was selected based on expected mass loss rates for the fuels in these tests. This provided a means of directly measuring changes in fuel mass burning rates resulting from the range of variables evaluated. During liquid fuel fire testing the fuel pan and burning fuel were on top of the load cell. During open burning Class A fire testing, the Class A fuel being tested was placed on top of the load cell and mass loss was measured in real-time. During enclosure fire testing, only the upholstered sofa was placed on top of the load cell. This data in conjunction with the measured HRR values also provided a means of assessing fuel combustion efficiency for various fuels under various ventilation conditions. Due to the thermal environment expected within the test enclosure, the load cell was installed beneath the enclosure during all tests. Fuel mass loss rates were measured remotely using a load cell platform designed to rest atop the load cell and provide steel struts that extended up through the floor of the enclosure to support the burning fuel.

4.5.5 Hood Calorimeters

As mentioned earlier, both a 1 MW and 4 MW hood calorimeter were used to measure heat release rate during testing. A detailed description of the calorimeters and their calibration is provided in Appendix A.

4.5.6 Data Acquisition System

Data acquisition was achieved using the ATF FRL existing system. Control of the acquisition was achieved using iFix Intellution, a Supervisory Control and Data Acquisition system (SCADA). The data collection and cataloging was performed through FireTOSS, a software package unique to the ATF FRL. Instrumentation was connected to the SCADA through Yokogawa DA 100 and DS 600 data acquisition units. A sampling frequency of 1 Hz was used for all tests.

4.6 Video and Thermal Imaging

Video and thermal imaging cameras were used to document all tests conducted. At least two video cameras were used to document the ignition, evolution, and extinction of all fires conducted. For spill fires conducted in the open (Test Series 1), video cameras were offset 90 degrees from one another and mounted 1 m (39 in.) above the floor, viewing the fire horizontally such that the entire flame plume is captured. Additionally, a FLIR ThermaCAM Model P640 infrared camera was positioned to overlook the spill area and document the evolution and final area encompassed by the spill. A similar approach was adopted in Mealy et al. [2011] to evaluate fuel spill areas.

For enclosure fire tests, cameras were positioned to capture both the internal fire dynamics as well as any burning that occurred outside the enclosure. Illustrations of the external and internal view camera locations are provided in Figure 9 and Figure 10, respectively. Two exterior cameras offset 90 degrees from one another characterized vent flow dynamics and flame extension from the vent opening. Both cameras were positioned 1.5 m (5 ft) above the laboratory floor. One camera was positioned directly in front of the enclosure at the centerline of the doorway. This camera was used to characterize the neutral plane in the vent flow as well as record general fire development. The second camera was positioned to view the wall parallel to the enclosure vent. This view provided a means of assessing the flame extension from the doorway during ventilation-limited burning.

In addition to these external views, three different internal views were captured using bullet cameras mounted along the boundaries of the enclosure (see Figure 10). These cameras were mounted in a horizontal orientation (i.e., looking across the width of the compartment) and were installed 0.3 m (1 ft) above the floor of the enclosure. View 1 was installed approximately 0.71 m (28 in.) from the rear wall. View 2 was installed 2.0 m (78 in.) from the rear wall and View 3 was installed 2.9 m (114 in.) from the rear wall. These cameras provided an overall view of the fire dynamics occurring within the enclosure as well as information on spill area, the extent of plume bending resulting from various ventilation schemes, the extent of fuel involvement, and the layer height within the space.

4.7 Qualitative Indicators

In addition to the standard measurements used to characterize the thermal conditions and fire dynamics occurring within the test enclosure, several qualitative indicators were used during the enclosure fire tests conducted. These qualitative indicators consisted of crumpled pieces of newspaper as an indicator of flashover. These crumpled pieces of newspaper were strategically

positioned at different elevations (e.g., floor level, tabletop, etc.) and near the two corner floor level heat flux transducers to characterize the heat flux at which these indicators ignite. The indicators consisted of a single full-size sheet of printer paper, crumpled by hand, into a ball with a nominal diameter of 0.08 m (3 in.).

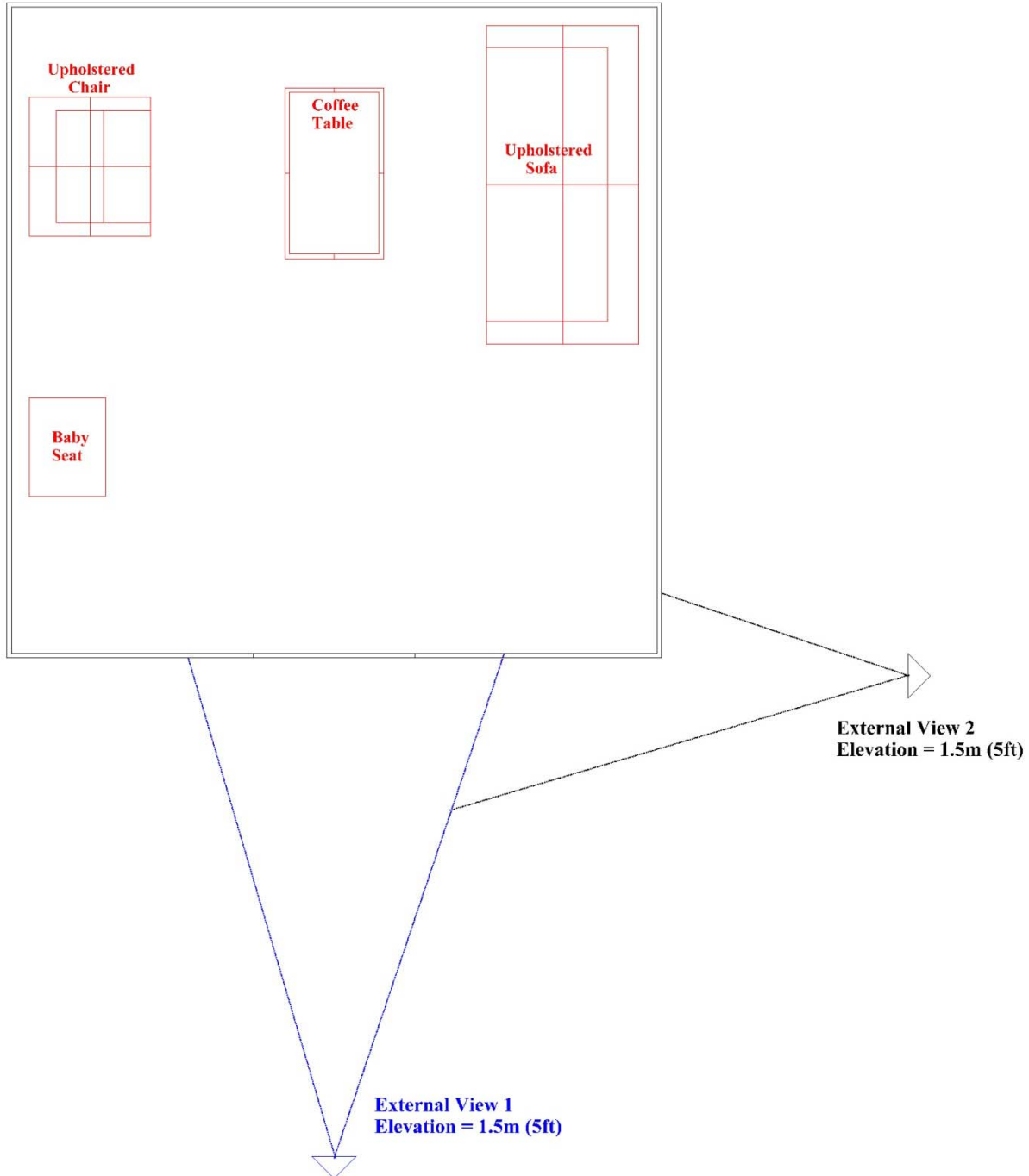


Figure 9. External view camera locations for enclosure fires.

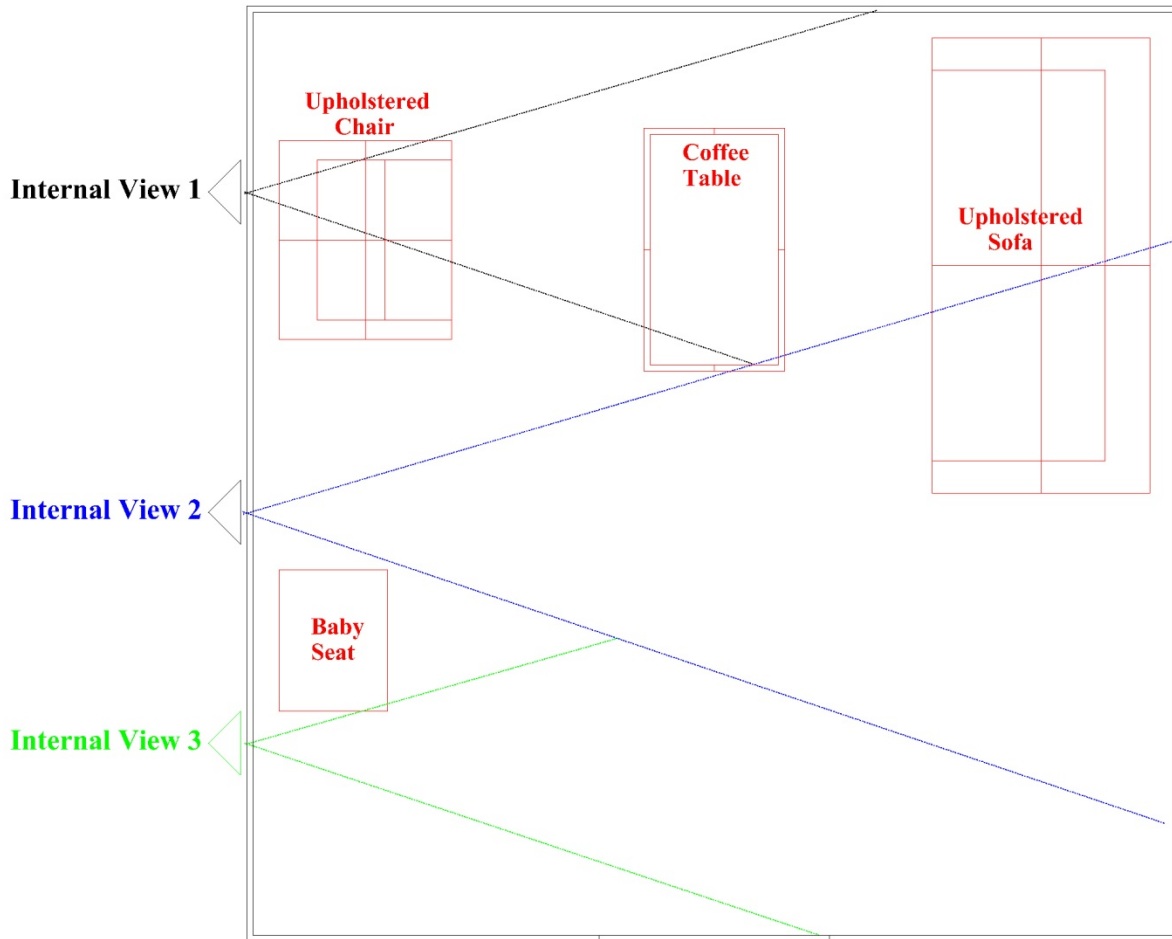


Figure 10. Illustration of internal view camera locations for enclosure fires.

4.8 Liquid Fuels

Three different liquid fuels were used in this test program, gasoline, heptane, and denatured alcohol, as summarized in Table 4. These fuels were selected for various reasons, including differences in volatility and fuel/combustion chemistry. More specifically the denatured alcohol fuel was selected because of its negligible soot yield, which differs from both gasoline and heptane. The gasoline used in this testing was an 87 octane, regular, unleaded gasoline purchased from a local fueling station. The heptane used in these tests was commercial grade heptane that was purchased from Tilley Chemical Company. The denatured alcohol used was KleanStrip SLX Denatured Alcohol purchased from a local hardware store and stored in 3.8 L (1 gal) cans. The fuel was manufactured by W.M. Barr Company. The gasoline used in this testing was purchased at one time from a single location. The gasoline was stored in five 18.9 L (5 gal) plastic gas cans.

Table 4. Summary of fuel properties [Mealy et al. 2011].

Material Property	Gasoline	Denatured Alcohol	Heptane
Density (kg/m³)	742	790	671
Specific Heat Capacity (kJ/kg-K)	2.2	2.5	2.2
Flash Point (°C)	-4	7	13
Boiling Point (°C)	<i>varies</i>	79	99
Heat of Vaporization (kJ/kg)	339	837	365
Effective Heat of Combustion (MJ/kg)	37.6	22.2	40.3

For select test series, (Test Series 5) heptane and denatured alcohol were the fuels used. Heptane was selected because it was a pure hydrocarbon fuel with a relatively well-established mass burning rate and sooting chemistry. Denatured alcohol was used because it represents a fuel chemistry that is different than heptane, thus it will provide a means of establishing how applicable the enclosure effects observed for heptane are for other fuels. The primary differences between the fuels are the soot yield and the heat of combustion. Soot yield can have a significant impact on the emissivity of the hot upper layer within the test enclosure, and thus radiation feedback to the fire. Denatured alcohol has a reported soot yield of 0.004 g/g and heptane has a reported soot yield of 0.037 g/g [SFPE 2008].

5.0 EXPERIMENTAL PROCEDURES & RESULTS

Prior to each test, all instrumentation was checked for operability using the data acquisition system. The hood calorimeters were calibrated using step-wise calibration curves. The hoods were considered calibrated if the measured heat release rate was within ten percent of the known burner output. A description of the calibration procedures and results are provided in Appendix A. Thermocouples were heated using a propane torch to verify response. The load cell was zeroed prior to installing the object being weighed. Heat flux gauge cooling lines were activated and their operation was verified using a propane torch exposure to the measuring surface. Gas analyzers were zeroed and spanned using calibration gases. Once instrumentation operability was confirmed, the volume of liquid fuel required for each test, when appropriate, was measured gravimetrically using a load cell. Once measured, the fuel container was sealed until the test was started. After fuel for a given test had been measured, all video cameras were activated. The recording of all video cameras was verified and the data acquisition system was initiated. The fuel was poured and ignited using an electronic igniter positioned near the fuel surface. The specific location of the igniter was dependent upon the fire scenario being evaluated.

5.1 Test Series 1 – Unconfined Liquid Fuel Fires in the Open

A series of six unconfined liquid fuel fire tests were conducted on two different substrates in open-air conditions (i.e., open burning). A summary of these tests is provided in Table 5. The fuel was released using a mechanical spill arm that discharged the liquid fuel through a 63.5 mm (2.5 in.) orifice under head pressure. Gasoline was used because it is the most prevalent liquid

fuel identified in fire debris analysis. All tests were performed in triplicate. The substrates used were vinyl flooring installed over plywood and carpet flooring with padding installed over plywood. The flooring materials were the same as those used by Mealy et al. [2011] and were selected for three primary reasons: 1) they are generally the most common types of flooring in residential and commercial applications; 2) they represent both a smooth, non-permeable surface as well as a textured, porous surface over which fuel can spread; and, 3) they can both be applied to the test enclosure floor as a continuous surface thus minimizing the probability of fuel escaping through seams in the flooring material.

Table 5. Summary of unconfined gasoline spill fires.

Test ID	Substrate	Spill Volume (L)	Spill Area (m ² [ft ²])	Burning Duration (s)	Peak HRR (kW)	Time to Peak HRR (s)	10s Peak Average HRR (kW)	THR (MJ)	THR by Substrate*
SF1	Vinyl	2.0	2.0 [22]	57	2668	23	2317	64	8
SF2			1.9 [21]	54	2440	23	2116	60	4
SF3			2.1 [23]	69	2729	18	2424	62	6
Avg.			2.0 [22]	60	2612	21	2286	62	6
Std. Dev.			0.1 [1.0]	8	152	3	156	2	2
SF4	Carpet		0.36 [3.9]	300**	599	144	308***	101	73.1
SF5			0.27 [2.9]	300**	619	179	225***	82.8	54.9
SF6			0.45 [4.8]	723**	578	192	453***	229	201
Avg.			0.36 [3.9]	-	599	172	329***	138	110
Std. Dev.			0.1 [1.0]	-	21	25	115	80	80

* Assumes 2.0L of gasoline contains approximately 56 MJ of energy.

** Burning duration measured from time of ignition to time of manual extinguishment, fires did not self-extinguish.

*** Values based on initial 120 seconds of burning to evaluate fire size associated with gasoline spill, not contribution of carpet flooring material

In these tests, the liquid fuel was poured at the center of an appropriately sized square section of the substrate. The fuel was mechanically released through a 64 mm (2.5 in.) orifice from an approximate elevation of 0.3 m (1 ft) above the substrate. Once spilled, the spill area was photographed and the fuel was ignited using a propane torch mounted to an extension pole. Spill areas were quantified using the same approach described by Mealy et al. [2010] whereby image analysis was used to calculate a total coverage area. Once ignited, typically 10 seconds after release, the fire was permitted to burn until it self-extinguished or until the substrate was the only fuel contributing to the fire. Residual flaming, as shown in Figure 13, was observed in all carpet spill fire scenarios and required manual extinguishment using a CO₂ extinguisher after 5–10 minutes of additional burning.

The 2.0 L (0.53 gal) gasoline spills on vinyl resulted in spill areas ranging between 1.9–2.1 m² (21–23 ft²). When ignited, these fires burned for an average of 60 seconds with a 10-second peak average heat release rate of 2.3 MW. Upon ignition, the fire spread rapidly across the fuel surface, burning vigorously for the initial 15–25 seconds. After this, the burning area and flame heights began to regress, eventually transitioning to smaller, localized pockets of burning with independent flame plumes. A photograph of the vinyl spill fire and resulting fire pattern are provided in Figure 11.

For these gasoline fires on vinyl, the 10-second peak burning rate was approximately 31 g/s-m². This value is based on the effective heat of combustion presented in Table 4 divided into the quotient of the 10s peak average fire size presented above (i.e., 2.3 MW) and the average spill area (2.0 m²). This peak burning rate is consistent with the spill fire data reported by Mealy et al. [2010] for similar spill fire scenarios. In this previous work, the 10-second peak burning rates were approximately 29 g/s-m². A comparison of the measured heat release rate curves for the tests in Table 5 is provided in Figure 12.

It should be noted that both the spill fire mass burning rate data measured in this work, as well as that reported in the previous work are approximately 50 percent of the maximum mass burning rate for gasoline pool fires (55 g/s-m²). This is the case even though the effective diameters of the fire scenarios were greater than 1 m (3.3 ft) and is due to the small fuel depth associated with the spill fire scenario [Mealy et al, 2010].



Figure 11. 2.0 L gasoline spill fire (Test SF1) on vinyl (left) and consequent burn pattern (right).

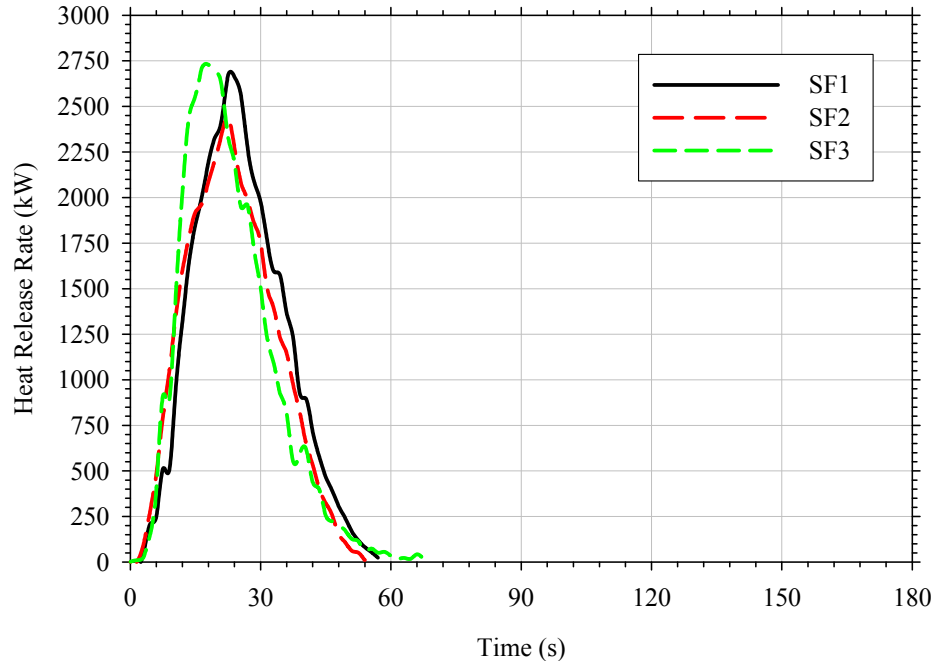


Figure 12. Heat release rates from triplicate testing of 2.0 L gasoline spills on vinyl flooring ignited 10s after release.

The 2.0 L (0.53 gal) gasoline spills on carpet resulted in spill areas ranging between 0.19–0.22 m² (2.0–2.4 ft²). These spill areas are at the lower end of the range of areas measured by Mealy et al. [2010] for all volumes of fuel poured onto carpet (0.21–0.40 m²). During the initial 60–120 seconds of burning, the measured heat release can be attributed primarily to the combustion of the gasoline wicking through the carpet flooring material. This wicking phenomenon was first reported by Ma et al. [2004] and was observed in all gasoline spill fire testing conducted in this work as well as the previous work [Mealy et al. 2010]. During this period, the average peak heat release rate was 330 kW with a standard deviation of 115 kW. After this period of time, the carpet and carpet padding began to thermally degrade and combust, resulting in an increasing fire size. The peak fire sizes measured during this phase of combustion ranged from 500–600 kW. This growth was noticeable for the next 60–90 seconds at which point the fire then began to decay. This decay is attributed to the gradual consumption of the gasoline that had soaked into the flooring material. Consequently, the only fuel remaining to be combusted was the carpet flooring which did not burn as vigorously as the wicking gasoline fuel. Photographs of the various stages of the gasoline spill fire on carpet are shown in Figure 13.

Using the effective heat of combustion presented in Table 4 and dividing this value into the quotient of the 10s peak average fire size presented above (i.e., 329 kW) and the average spill area (0.36 m²) gives a 10-second peak burning rate of approximately 24 g/s-m². This value is consistent with the expected steady-state burning rates for gasoline in pool fire scenarios of the same size. Using Equation 2 and an equivalent diameter of 0.34 m (1.1 ft), a steady-state burning rate of 27 g/s-m² is calculated for a comparable pool fire scenario. The heat release rates per unit area measured in this work were also consistent with the findings of Mealy et al. [2010] for spill fire heat release rates on carpet and liquid fuel pool fire scenarios. Mealy et al. reported heat release rates per unit area of 1354 kW/m² and in the current work these values were 1150 kW/m².

A comparison of the measured heat release rates from the tests presented in Table 5 are provided in Figure 14.



Figure 13. 2.0 L gasoline spill fire on carpet (Test SF4) (left), gasoline burning on carpet (center), burning carpet after gasoline is largely consumed (top right), and resulting burn pattern (lower right).

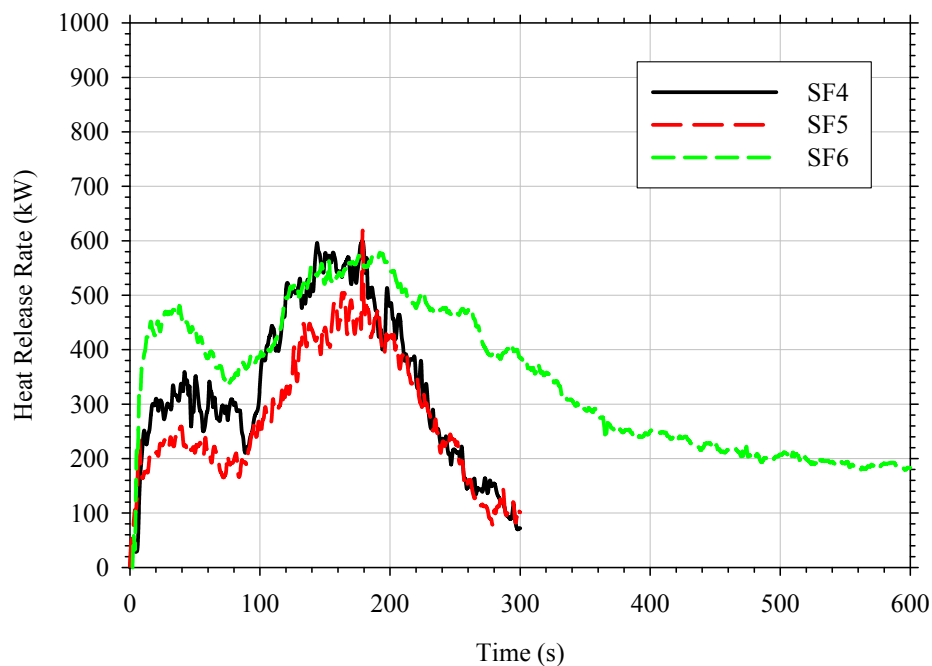


Figure 14. Heat release rates from triplicate testing of 2.0 L gasoline spills on carpet/pad flooring.

5.2 Test Series 2 – Pan Fires in the Open

A series of seven pan fire tests were conducted to characterize the open burning heat release rates in confined areas. These tests provided baseline data for comparison to results obtained for the same pan fires burning within an enclosure. The fuels used were gasoline, heptane, and denatured alcohol. A 0.23 m² (2.5 ft²) pan was used for gasoline and heptane fires. The pan was constructed with a 0.2 m (8 in.) freeboard from 6.35 mm (0.25 in.) thick steel plate. A 1.0 m² (10.4 ft²) pan was used for denatured alcohol fires. The pan was constructed with a 0.1 m (4 in.) freeboard from 3.2 mm (0.125 in.) thick steel plate. Pan sizes were selected to produce a similar size liquid fuel fire scenario using the different fuels. All pan fire tests were conducted in duplicate with the exception of the heptane fires, which were performed in triplicate. For gasoline and heptane tests, a total of 19 L (5 gal) of fuel was used in each test. Denatured alcohol testing was conducted using 21 L (5.5 gal). The fuel quantities used were designed to provide extended steady-state burning durations (i.e., 10–15 minutes). A summary of the pan fire tests conducted is provided in Table 6.

For all pan fire tests, the fuel was manually poured into the pan by fire fighting personnel. In tests using either gasoline or heptane, a 25 mm (1 in.) deep-water sub-layer was added to the pan prior to pouring fuel. The water sub-layer was not added to denatured alcohol testing due to the miscibility of the fuel. Once all fuel was poured, the fuel was ignited using a propane torch mounted to an extension pole. The pan fire was permitted to burn until all fuel was consumed. Representative photographs of the pan fires are presented in Figure 15.

Table 6. Summary of results from pan fires in the open.

Test ID	Pan Size (m ² [ft ²])	Fuel	Mass Loss (kg)	Peak HRRPUA (kW/m ²)	Total Heat Released (MJ)	Eff. Heat of Combustion (MJ/kg)	Average SS HRR (kW/m ²)	Average SS MBR (g/s-m ²)
PF1	0.23 [2.5]	Gasoline	6.9	1962	260	37.7	1697	45
PF2			6.8	1910	254	37.4	1721	46
Avg.			6.9	1936	257	37.6	1709	46
PF3		Heptane	12.2	2344	516	42	2125	51
PF4			10.2	2360	422	41	1915	47
PF5			8.5	2540	336	39	2391	61
Avg.			10.3	2415	425	41	2144	53
PF6	1.0 [10.4]	Denatured Alcohol	18.2	543	396	22	523	24
PF7			18.2	579	412	23	559	25
Avg.			18.3	561	404	23	541	25



Figure 15. Gasoline, heptane, and denatured alcohol pan fires shown left to right, respectively.

The gasoline pan fires were very repeatable with average steady-state heat release rates that were less than 3 percent different. A plot of the measured heat release rates per unit area are provided in Figure 16. Using the mass of fuel consumed and the measured total heat released, an average effective heat of combustion for the gasoline pan fires was determined to be 37.5 MJ/kg. Average steady-state mass burning rates of 45–46 g/s-m² were calculated for these pan fire tests. These values are approximately 15 percent higher than the expected mass burning rate (38 g/s-m²) for a 0.23 m² (2.5 ft²) fuel area as calculated using Equation 2.

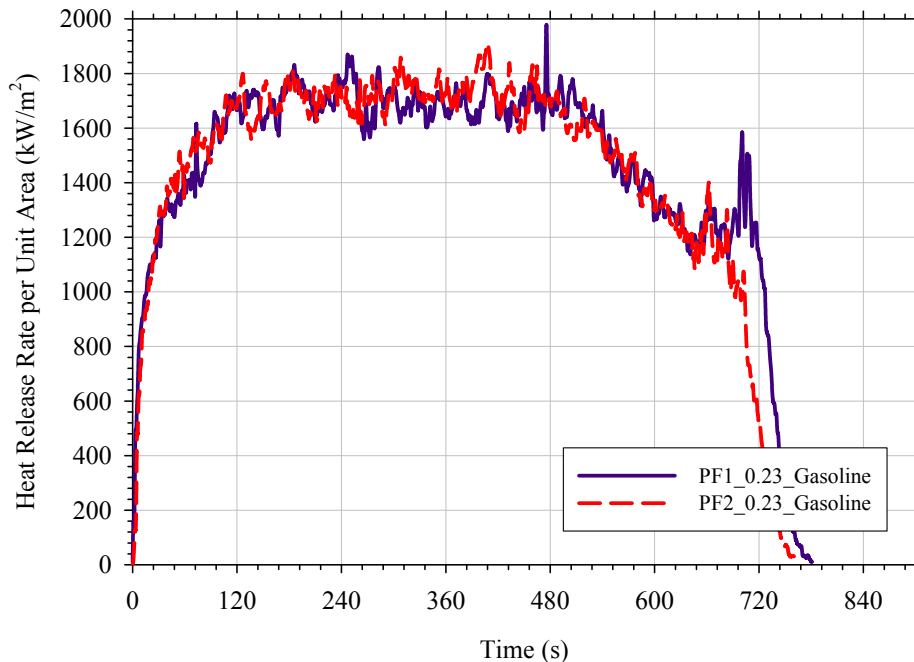


Figure 16. Heat release rate from 0.23 m² (2.5 ft²) gasoline pan fires burning in the open.

The heptane pan fires had average steady-state heat release rates ranging from 2.3–2.5 MW (less than 9% difference). A plot of the measured heat release rates per unit area are provided in Figure 17. The measured heat release rates for these tests generally reached peak values

6–8 minutes after ignition. After this point, relatively steady-state conditions were achieved in two of the three tests with an average steady-state value of 2125 kW. Using the mass of fuel consumed and the measured total heat released, an average effective heat of combustion for the gasoline pan fires was determined to be 40.7 MJ/kg. The average steady-state mass burning rate for all three heptane pan fires conducted was 53 g/s-m². This average value is 13 percent higher than the expected mass burning rate (47 g/s-m²) for a 0.23 m² (2.5 ft²) pan as calculated using Equation 2.

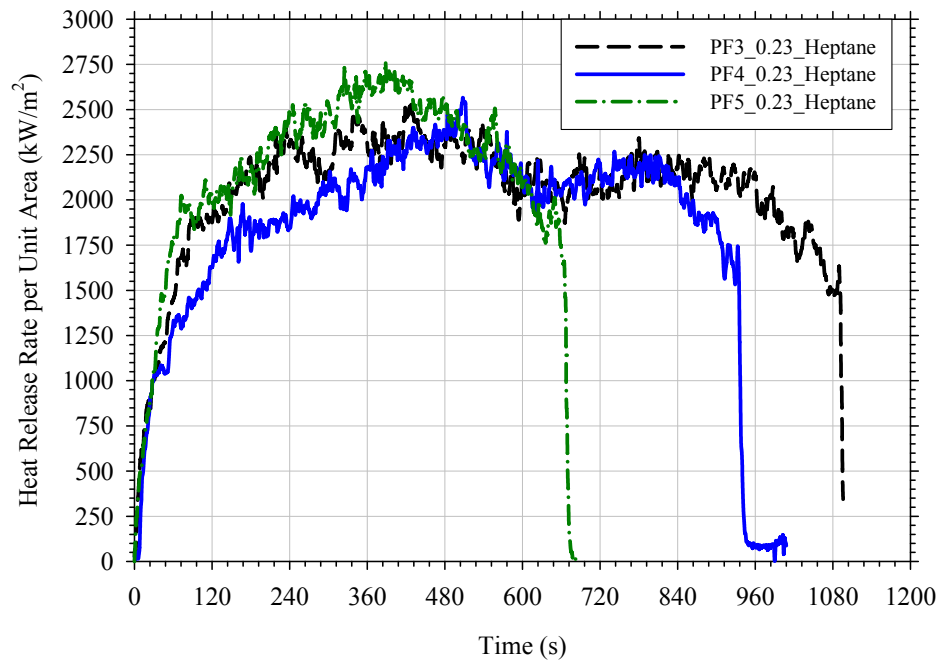


Figure 17. Heat release rate from 0.23 m² (2.5 ft²) heptane pan fires burning in the open.

The two denatured alcohol pan fires were repeatable with average steady-state heat release rates of 543 and 579 kW (about 7 percent different). Steady-state burning conditions were reached within the first two minutes of testing and maintained for the duration of the test. A comparison of the measured heat release rates for these tests is provided in Figure 18. Using the mass of fuel consumed and the measured total heat released, an average effective heat of combustion for the gasoline pan fires was 22.5 MJ/kg. An average steady-state mass burning rates of 24.5 g/s-m² was calculated from the two tests (24 and 25 g/s-m²). These values are 30 percent higher than the peak values (19 g/s-m²) reported by Mealy et al. [2010]. However, the previous test fires [Mealy et al, 2010] did not fully reach steady-state peaks. This difference is due to the fact that the fuel depths used in the previous work were one-fourth that used in this work (5 mm compared to 21 mm). Figure 18 presents the replicate heat release rates for each alcohol pan fire as noted in Table 6.

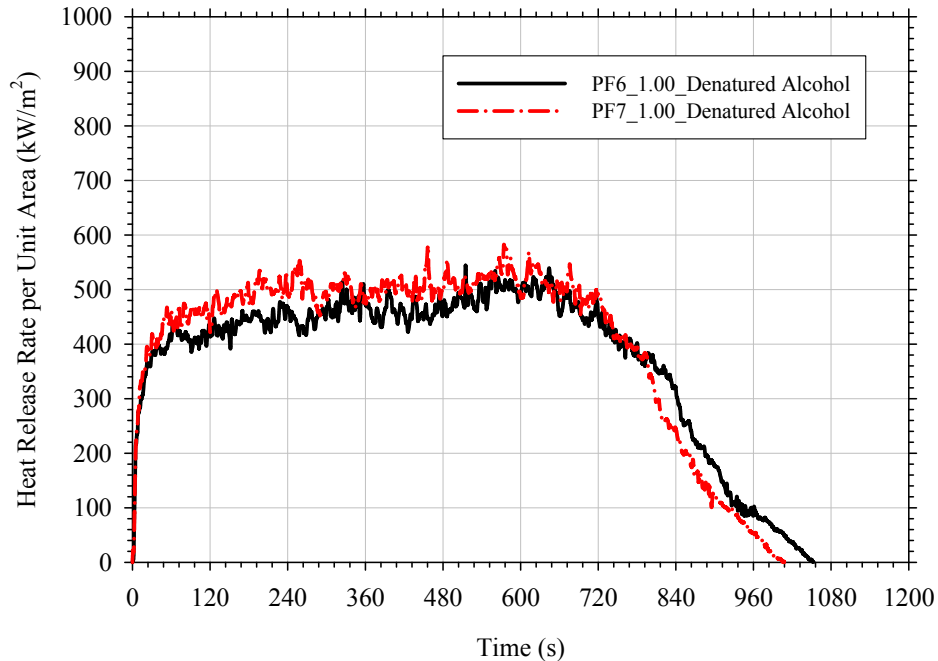


Figure 18. Heat release rate from 1.0 m² (10.8 ft²) denatured alcohol pan fires burning in the open.

As shown in Figure 19, the averaged measured heat release rates for the three different fuel pan fire scenarios had similar steady-state heat release rates as designed. This similarity in fire sizes provides a means of comparing the impact of enclosure effects on liquid fuel fires between sooting and non-sooting fuels. The curves in Figure 19 were developed from the replicate heat release rates for each fuel by averaging at each time step.

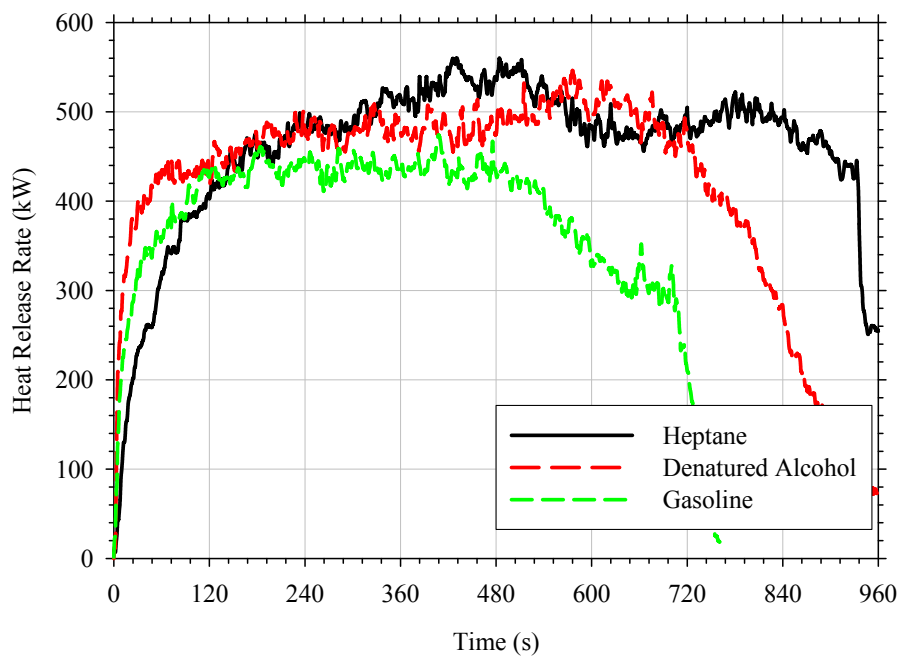


Figure 19. Average heat release rate for Class B or hydrocarbon fuels burning in the open.

5.3 Test Series 3 – Class A Fires in the Open

The open burning characteristics of several different Class A materials were characterized using oxygen consumption calorimetry. These tests provided baseline heat release and mass burning rate data for each of the fuels installed within the test enclosure. Full-scale hood calorimetry was used to characterize the upholstered sofa, upholstered chair, table, and baby seat. Small-scale cone calorimetry was used to characterize the flooring materials on a per unit area basis. The product of the heat release rate per unit area data obtained from the cone calorimeter and the known area of the enclosure was used to estimate the contribution of the flooring material during the test fires. A summary of the heat release data collected in this test series is presented in Table 7.

Except for the flooring, the Class A fires were conducted beneath the 1MW square hood calorimeter. The fuels were ignited using the standard Class A ignition scenario described in Section 5.3.1. The Class A fires were permitted to grow naturally and burn until self-extinguished. Detailed descriptions of the ignition scenarios used for each of the Class A fuels are provided in the sections below.

Table 7. Summary of Test Series 3 results.

Test ID	Fuel Item	Total Heat Released (MJ)	Peak HRR (kW)	Burning Duration (s)	Fraction Consumed (-)
3-1 ¹	Upholstered Sofa	372	1283	1225	0.69
3-2	Upholstered Chair	144	314	564	0.54
3-3	Coffee Table	77	657	1316	0.83
3-4	Car Seat	143	463	840	0.84
3-5	Carpet Flooring System ³	1590 ²	3805 ²	864	0.71
3-6	Vinyl Flooring System ³	1106 ²	2832 ²	1062	0.75

1 – Sofa data collected in previous study [Wolfe et al. 2009]

2 – Values are the product of measured heat release rate per unit area data collected in cone calorimeter and known floor area test enclosure (i.e., 13.4 m² [144 ft²])

3 – Flooring material data from exposure at 25 kW/m²

5.3.1 Class A Ignition Scenario

The Class A ignition scenario described below was developed by Wolfe et al. [2009]. Figure 20 shows a photo of the setup. The source consists of two unopened tissue boxes with a small isopropyl alcohol ignition flame located in the flue space. Four (4) mL of isopropyl alcohol was poured into a nominally 1-inch NPT pipe cap (internal diameter of 0.033 m (1.315 in.)). The cap was positioned between the tissue boxes, oriented vertically, with the bases facing each other. The tissue boxes were Kleenex® Brand 2-ply tissues with box dimensions of 0.12 m (4.75 in.) by 0.225 m (9 in.) by 0.05 m (2 in.). The pipe cap was positioned such that the exterior of the cap was flush with the leading edge of the tissue boxes. The liquid fuel was ignited using a small

diffusion flame from a butane lighter. Once ignited, the alcohol flame typically burned for 6 minutes before the boxes were ignited. The time to ignition for the tissue boxes was relatively repeatable, with a variance from test to test of less than 30 seconds. The box fire then typically burned for 2 minutes before reaching its peak. By itself, the source would generally burn for a total duration of 11 minutes with a peak heat release rate of 2–3 kW.



Figure 20. Photograph of Class A ignition scenario.

5.3.2 Upholstered Sofa

The upholstered sofa and ignition scenario used in this research was the same sofa that was characterized by Wolfe et al. [2009]. Repeat testing was not conducted for this piece of furniture. Instead, the open burning heat release rate data collected in the previous work is presented for reference. The sofa used was an IKEA, Klippan style sofa (see Section 4.4 for details). A series of photos documenting the fire progression is shown in Figure 21 and a plot of the heat release of the sofa is presented in Figure 22.

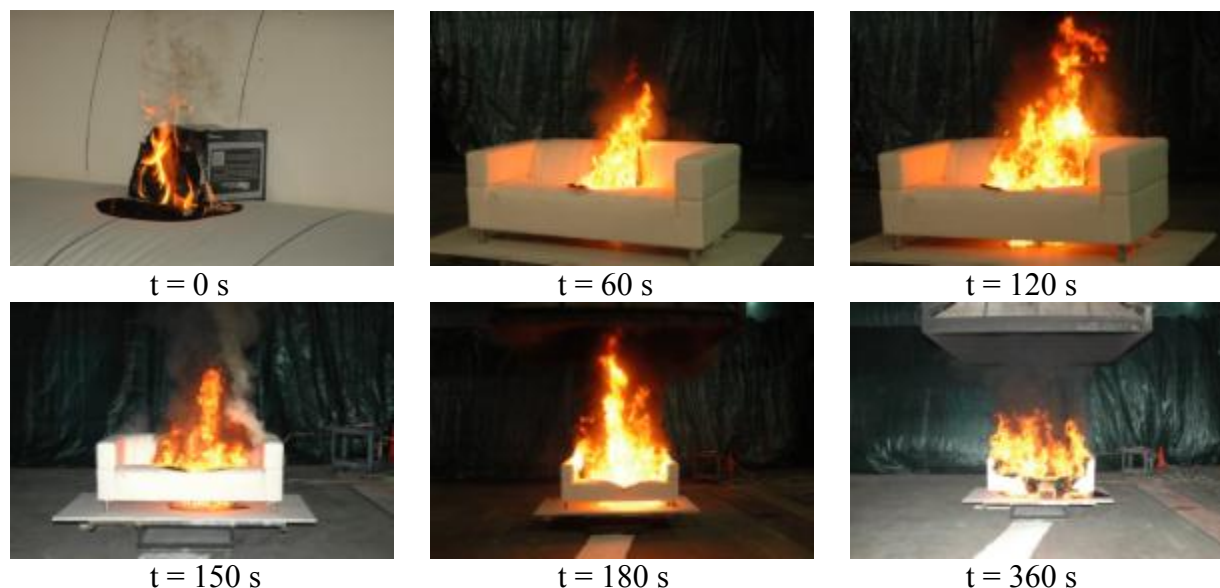


Figure 21. Upholstered sofa fire progression.

The ignition source was placed at the rear of the seat cushion in the middle of the sofa (Figure 21). The upholstered sofa became involved approximately seven minutes after initiation of the ignition scenario. Time zero represented the time at which the sofa was ignited. The fire gradually spread over the top surface of the sofa and burned through the sofa seat, creating a pool fire of molten polyurethane foam beneath the sofa. The fire then spread over the top surface and underneath the sofa gradually involving the entire sofa approximately 180 seconds after being ignited. A peak of heat release rate of 1283 kW was measured and the sofa burned for just over 20 minutes. A plot of the heat release of the sofa is presented in Figure 22.

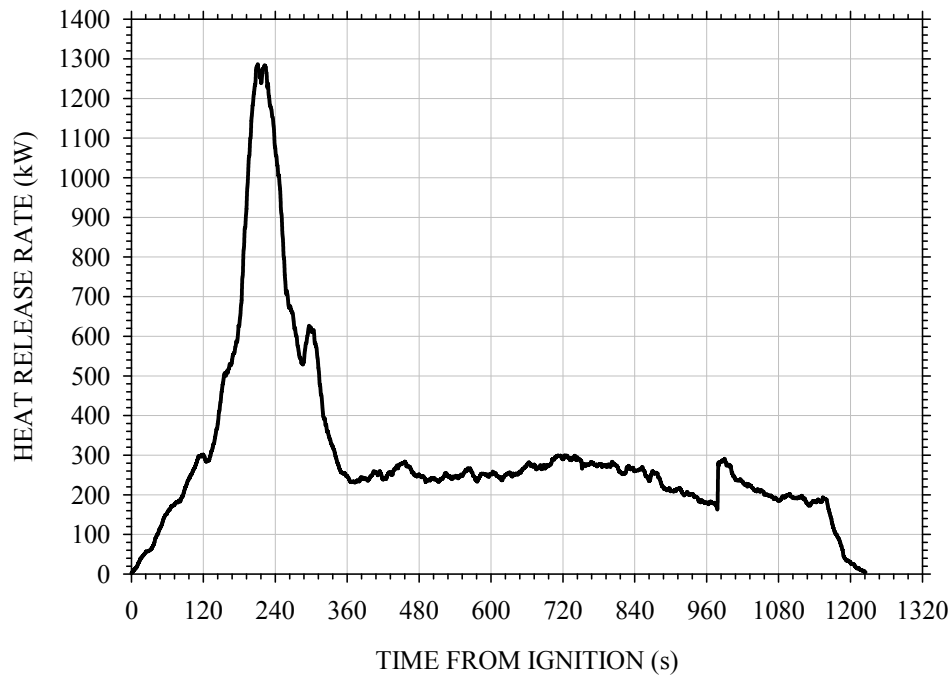


Figure 22. Heat release rate of upholstered sofa.

5.3.3 Upholstered Chair

The upholstered armchair was an IKEA®, Ektorp Tullsta style chair (see Section 4.4 for details). The ignition source was centered along the seat back of the chair. A series of photos documenting the fire progression is shown in Figure 23 and a plot of the heat release of the chair is presented in Figure 24. The upholstered chair became involved approximately seven minutes after initiation of the ignition scenario. Time zero represented the time at which the base of the seat backing was ignited. The fire spread vertically up the seat back and around the perimeter of the seat back/armrests. With the top surface of the seatback/armrests burning, the seat cushion was ignited and the chair became fully-involved. Once fully-involved, the chair burned at a relatively steady-state for a period of approximately seven minutes. The peak heat release rate was 314 kW, and the sofa burned for approximately 22 minutes.

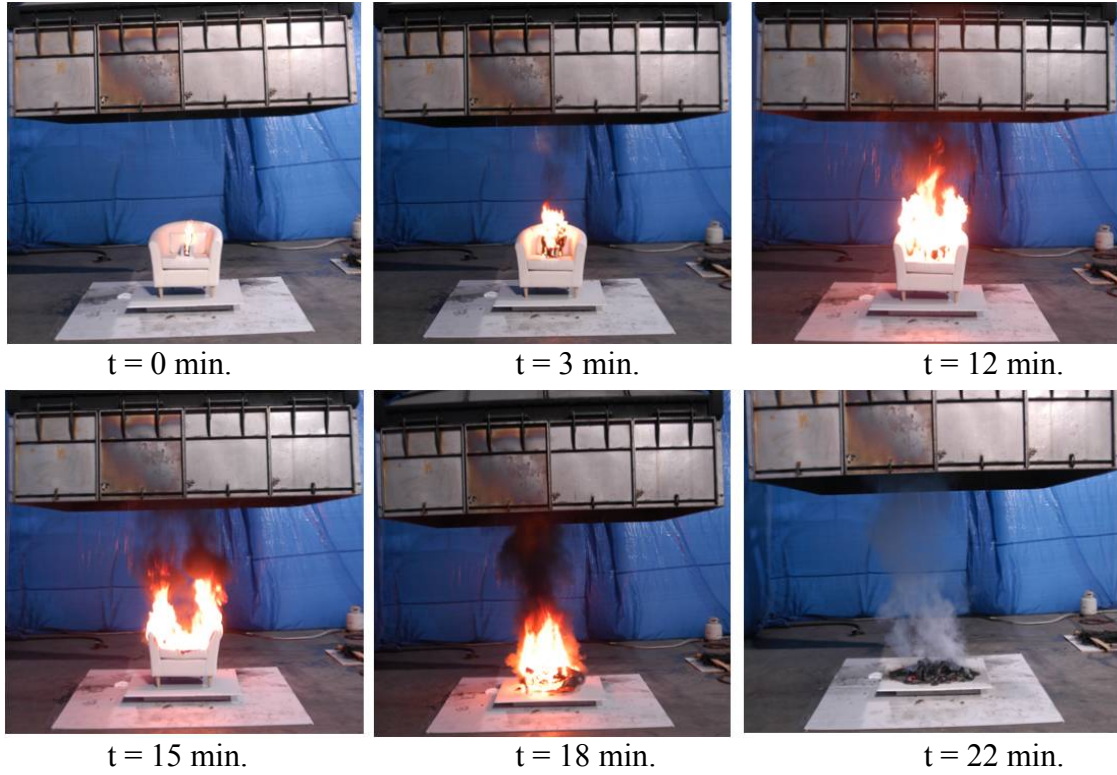


Figure 23. Photographs of upholstered chair fire progression.

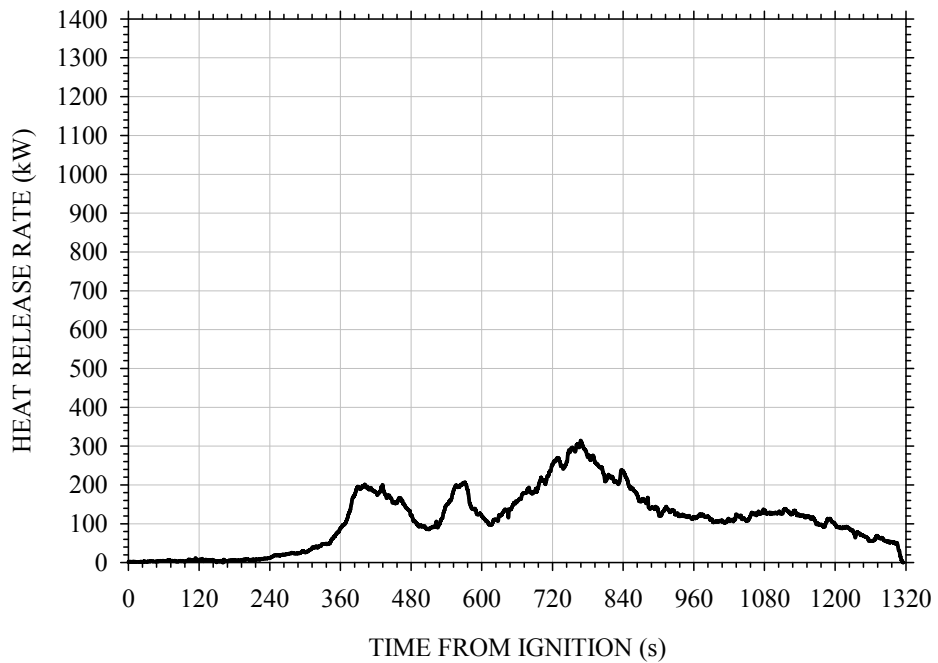


Figure 24. Heat release rate of upholstered chair.

5.3.4 Coffee Table

The coffee table was an IKEA®, Lack style coffee table (see Section 4.4 for details). A series of photos documenting the fire progression is shown in Figure 25 and a plot of the heat release of the table is presented in Figure 26. For this test, the ignition source was centered on the lower level of the coffee table. Once ignited, the fire plume from the ignition source impinged on the underside of the coffee table top and gradually spread along the underside of the table with flame wrapping around the edges. The table became involved approximately ten minutes after initiation of the ignition scenario, which was designated as time zero. Time zero represents the time at which the fire plume from the Class A ignition source started impinging on the underside of the coffee table top. A peak of heat release rate of 657 kW was measured and the coffee table burned for approximately 9 minutes.

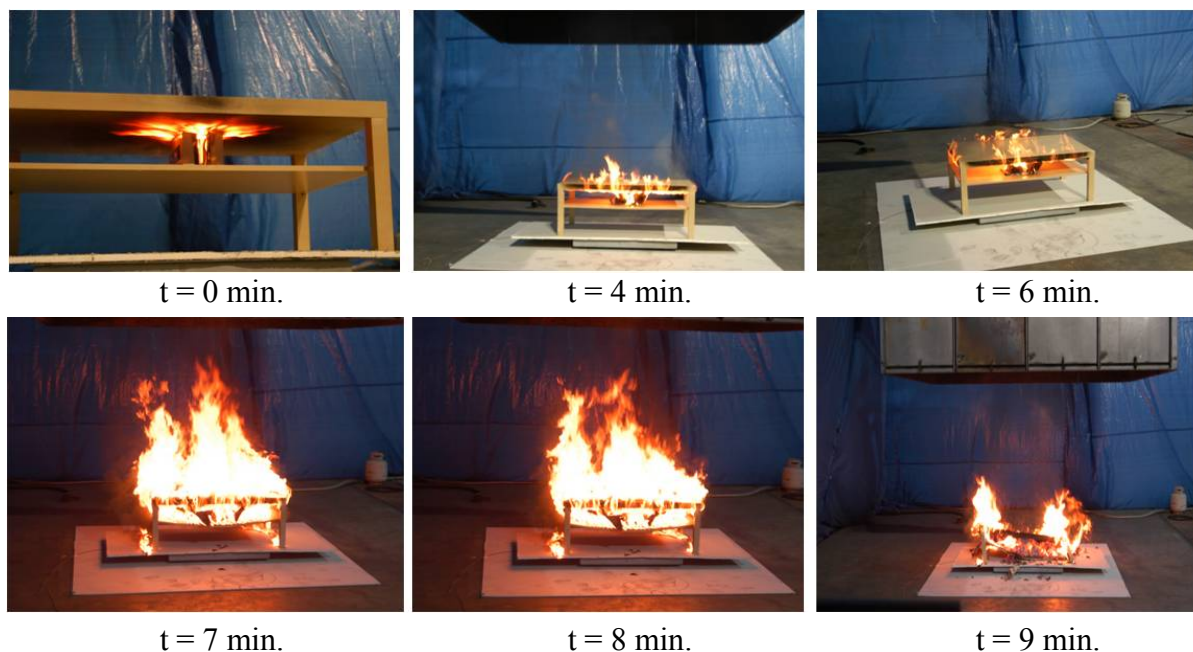


Figure 25. Coffee table fire progression.

5.3.5 Car Seat

The car seat was a Cosco® Model 02-480-BNG car seat (see Section 4.4 for additional details). A series of photos documenting the fire progression is shown in Figure 27 and a plot of the heat release of the table is presented in Figure 28.

In this test, the car seat was tilted forward such that it was resting on the top of the seat back and front of the base (see Figure 27 for photos). The ignition source was placed beneath the car seat in the void space directly beneath the joint where the seat back met the base of the seat. The boxes were oriented across the width of the seat (i.e., side to side). Once ignited, the fire plume from the ignition source impinged on the underside of the baby seat, initially involving the fabric and cushioning but eventually involving the plastic structure of the seat. The seat became involved approximately 8 minutes after initiation of the ignition scenario. Time zero represented

the time at which the base of the seat backing was ignited. A peak of heat release rate of 463 kW was measured and the seat burned for approximately 14 minutes.

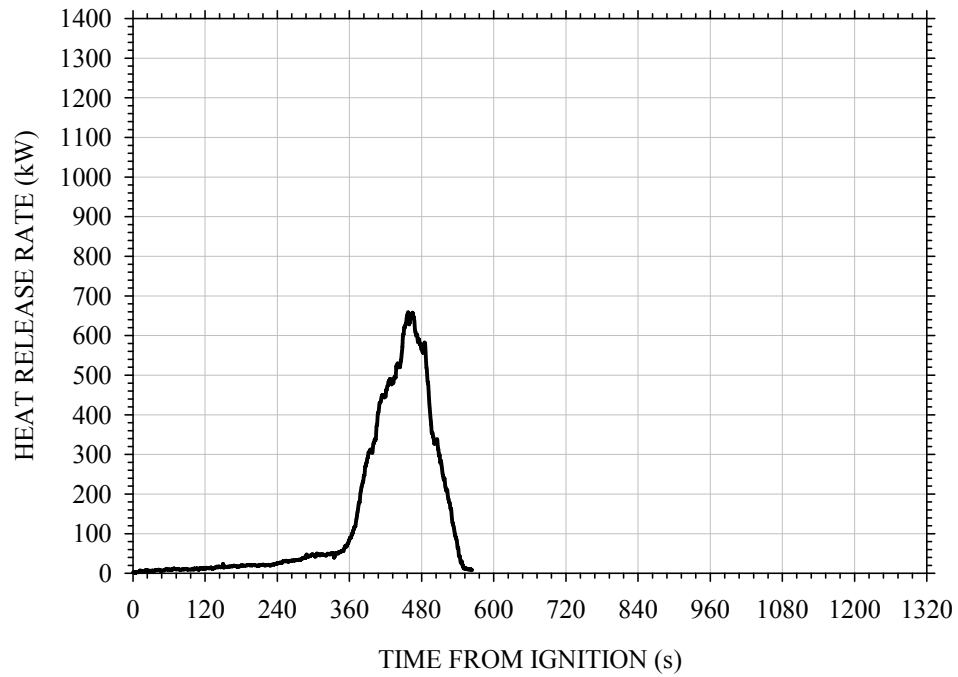


Figure 26. Heat release rate of coffee table.

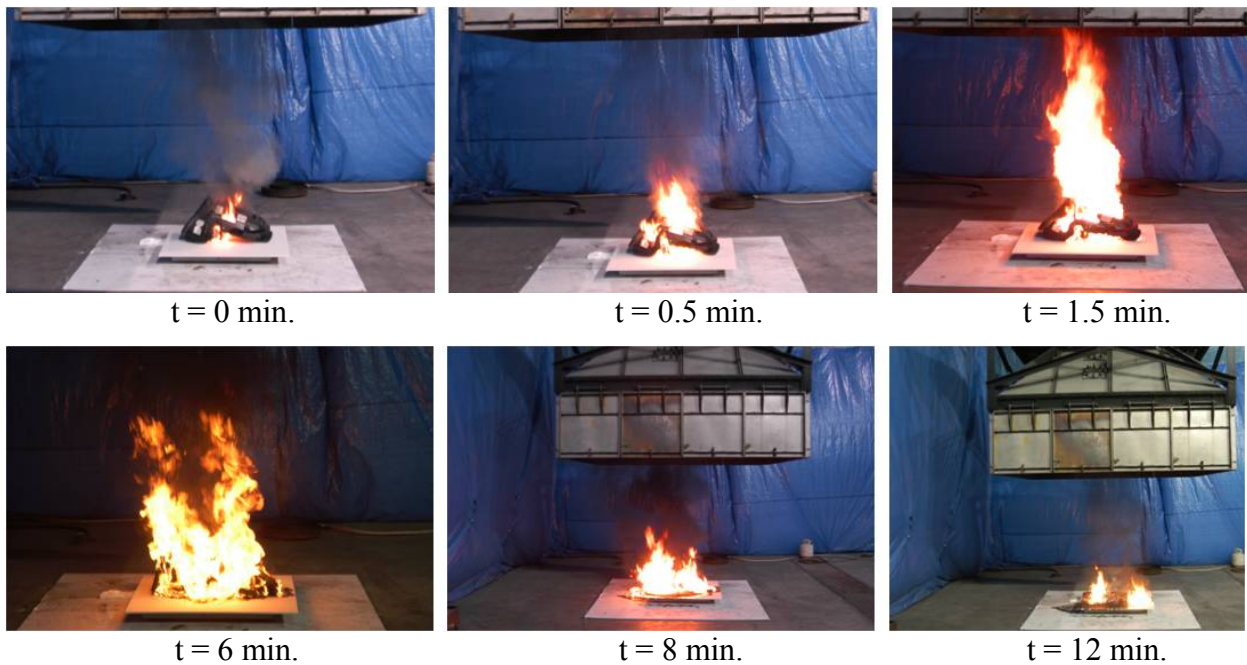


Figure 27. Photographs of car seat fire progression.

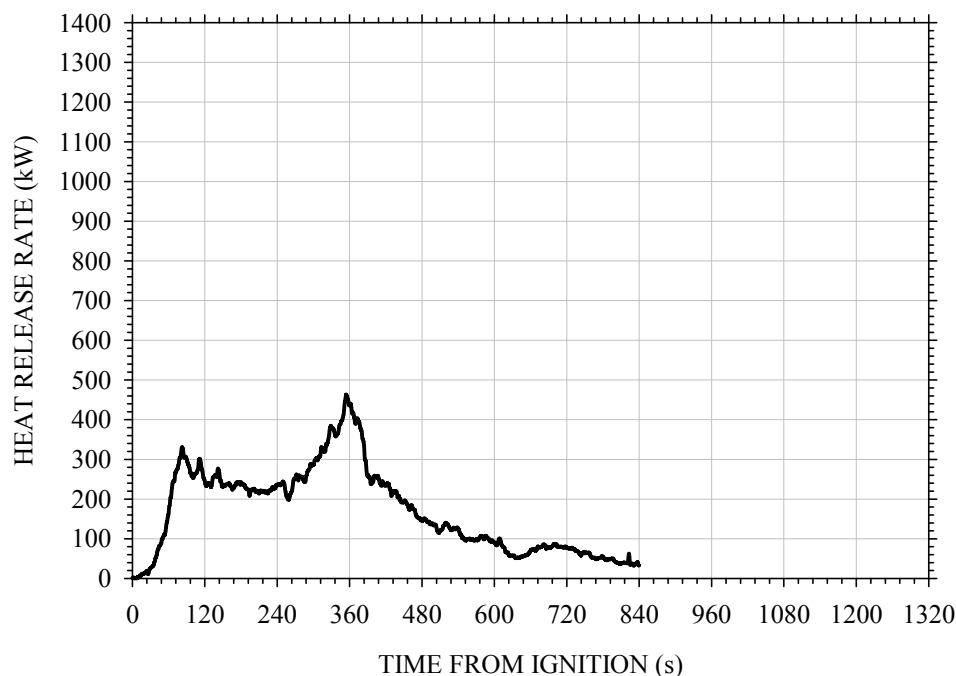


Figure 28. Heat release rate of car seat.

5.3.6 Flooring Material

The heat release of the flooring systems was not characterized at full-scale. The involvement of the carpet in the enclosure fires was primarily a result of the hot upper layer radiating to the carpet. Since it was not feasible to expose full-scale samples in the same manner for calorimetry measurements, the materials were tested using small-scale, standardized fire test methods. The ignitability and heat release of the flooring materials were evaluated using the ASTM E1354 [2010] cone calorimeter at three different incident heat fluxes.

5.3.6.1 Vinyl & Carpet Flooring Systems

The results from the vinyl and carpet flooring fire tests are provided in Table 8, and plots of the average transient heat release rate per unit area are provided in Figure 29 and Figure 30, respectively. The materials exhibited double-peak behavior, whereby an initial rise in heat release was observed early in the test followed by decay in fire size and then another increase. For the vinyl flooring system, the initial peak was consistently smaller than the second peak. While for the carpet flooring system, the opposite was true. For both flooring systems, the average and peak heat release rates increased with incident heat exposure severity. The effective heats of combustion for the vinyl and carpet flooring systems were 13 and 15 MJ/kg, respectively.

Table 8. Summary of heat release rate data for flooring materials.

Sample ID	Incident Heat Flux (kW/m ²)	Time to Ignition (sec)	Flame Duration (sec)	% Mass Loss	Average Effective Heat of Combustion (MJ/kg)	Avg. HRR at 60 sec (kW/m ²)	Avg. HRR at 180 sec (kW/m ²)	Avg. HRR at 300 sec (kW/m ²)	Peak HRR (kW/m ²)	Time of Peak HRR (sec)	Total HRR/A (MJ/m ²)
Vinyl - 1	25	59	1142	0.71	12	78	58	46	188	769	80
Vinyl - 2	25	43	981	0.70	12	76	66	50	236	767	85
Average	25	51	1062	0.71	12	77	62	48	212	768	83
Vinyl - 3	50	8	934	0.74	14	106	89	79	264	637	115
Vinyl - 4	50	14	912	0.76	13	121	81	71	308	573	100
Average	50	11	923	0.75	14	113	85	75	286	605	107
Vinyl - 5	75	3	747	0.76	13	135	102	94	336	467	94
Vinyl - 6	75	4	617	0.75	12	141	111	116	299	440	87
Average	75	4	682	0.76	12	138	106	105	318	453	91
Carpet - 1	25	72	882	0.75	15	266	231	193	289	34	121
Carpet - 2	25	87	848	0.75	15	264	235	174	301	37	112
Carpet - 3	25	99	864	0.75	16	246	224	186	263	35	124
Average	25	86	864	0.75	15	259	230	184	285	35	119
Carpet - 4	50	28	1303	0.80	16	377	294	214	411	20	134
Carpet - 5	50	25	1065	0.79	16	380	279	205	439	25	130
Carpet - 6	50	28	972	0.79	16	373	286	212	426	24	137
Average	50	27	1113	0.80	16	377	286	210	425	23	134
Carpet - 7	75	11	660	0.79	15	513	324	243	609	35	122
Carpet - 8	75	15	649	0.79	15	534	318	245	618	32	120
Carpet - 9	75	13	672	0.80	16	534	320	262	607	25	125
Average	75	13	660	0.79	15	527	321	250	611	31	123

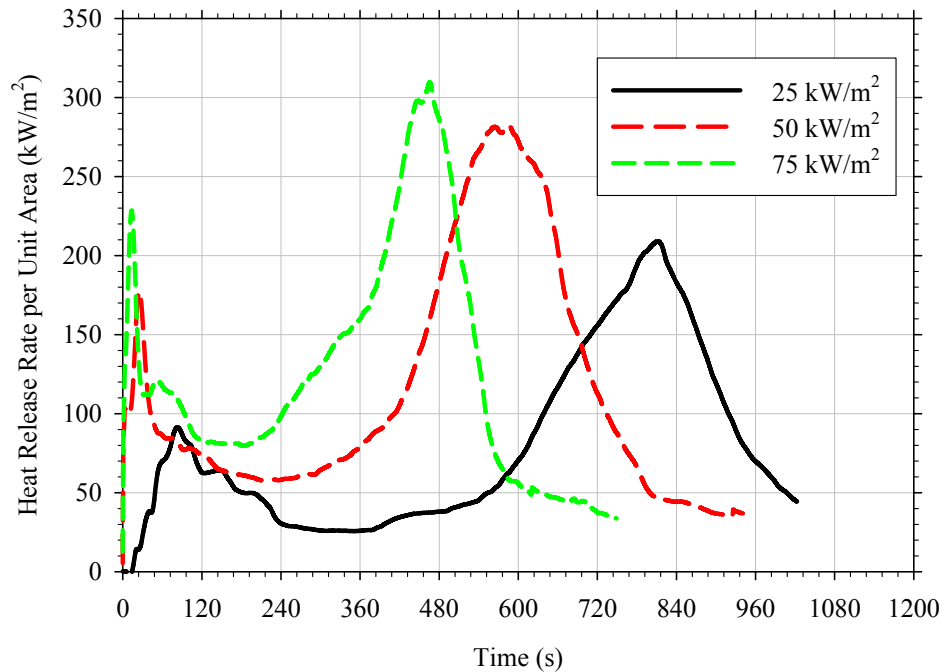


Figure 29. Average transient heat release rates for vinyl flooring at different exposure fluxes.

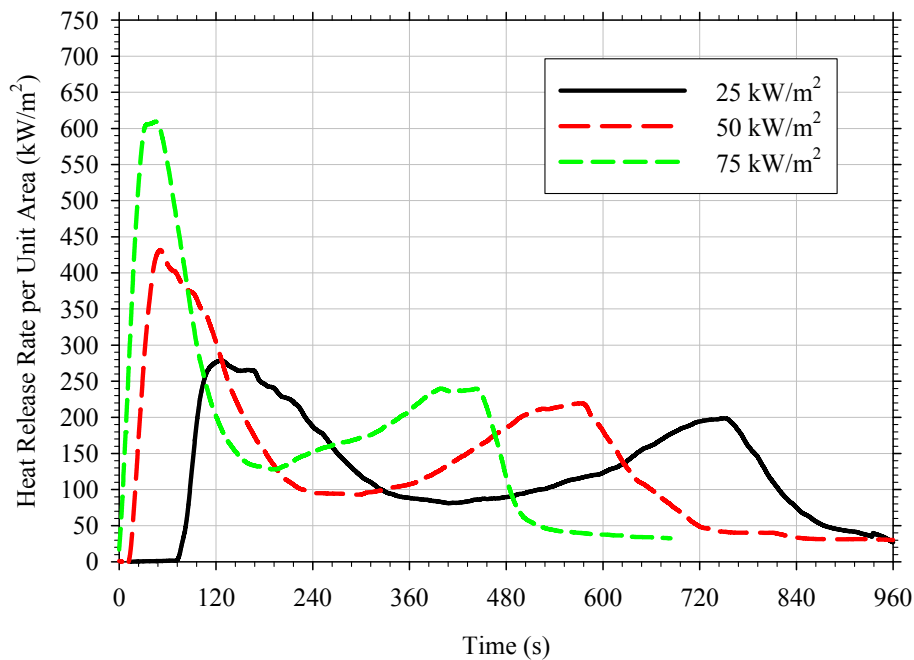


Figure 30. Average transient heat release rates for carpet flooring at different exposure fluxes.

5.4 Test Series 4 – Unconfined Liquid Fuel Fires in Enclosure

Two spill fire tests were conducted within the test enclosure without any Class A materials present. These tests were used to determine whether or not the presence of the enclosure altered (e.g., enhanced/reduced) the burning dynamics of the spill fire on the two types of substrates

being used in this study. The tests consisted of 2.0 L (0.26 gal) gasoline spills in the center of the enclosure on both vinyl and carpet. The fuels were manually poured in the center of the enclosure from a 3 L (0.8 gal) pitcher from an elevation of approximately 0.3 m (1 ft). Prior to ignition, images of the spill area were collected for spill area analysis. Analysis was conducted using the same procedure developed by Mealy et al. [2010]. The gasoline spill on vinyl was conducted with a full-open doorway. The slit vent was used when the spill on carpet flooring was conducted. These specific fuel/ventilation combinations were selected because they represent two different types of exposures that could generate thermal conditions severe enough to enhance fuel-burning dynamics. The carpet scenario represented a long duration, relatively small fire scenario, which could produce a hot upper layer over time without requiring significant ventilation. The vinyl scenario represents a relatively short duration, large fire scenario, which could rapidly develop a hot upper layer and require a large ventilation source. These test scenarios were intended to bound whether or not a spill fire scenario without other combustibles was capable of producing conditions within an enclosure that enhance/reduce the burning rate of the liquid fuel. A summary of the results obtained from these tests is provided in Table 9.

Table 9. Summary of 2.0 L gasoline spill fires in an enclosure.

Flooring Type	Spill Area (m² (ft²))	Burning Duration (s)	Peak HRR (kW)	10s Peak HRRPUA (kW/m²)
Vinyl	2.5 [27]	88	3023	1199
Carpet	0.2 [2.2]	330	218*	1090*

* Peak and 10s peak HRRPUA values based on initial 90 seconds of burning (i.e., gasoline spill fire), not peak measured due to involvement of flooring material

5.4.1 Gasoline Spill Fire on Vinyl

As shown in Figure 31, the 2.0 L gasoline spill in this test covered an approximate floor area of 2.5 m² (27 ft²). After ignition, the fire grew rapidly across the fuel layer. In total, the fire burned for approximately 90 seconds reaching a peak heat release rate of 3023 kW. The limited ventilation condition (i.e., full-open doorway) resulted in the flame plume tilting away from the vent 10–15 seconds after ignition. As a result, the vinyl flooring began to thermally degrade and almost immediately ignite. Figure 32 shows the thermal degradation/ignition of the vinyl in the lower half of the image. Steady-state burning was observed at the peak HRR value for a period of approximately 25 seconds before the fire decayed for approximately 45 seconds (Figure 33). A plot of the measured heat release rate during this fire is presented in Figure 33. The thermal and gas species conditions within the enclosure during the test are presented in Figure 34–Figure 37. In Figure 34, the average temperature from both the front and rear thermocouple trees are presented at four different elevations. It should be noted that carbon monoxide concentration data was corrupted for upper layer measurements during this test and are therefore not reported.

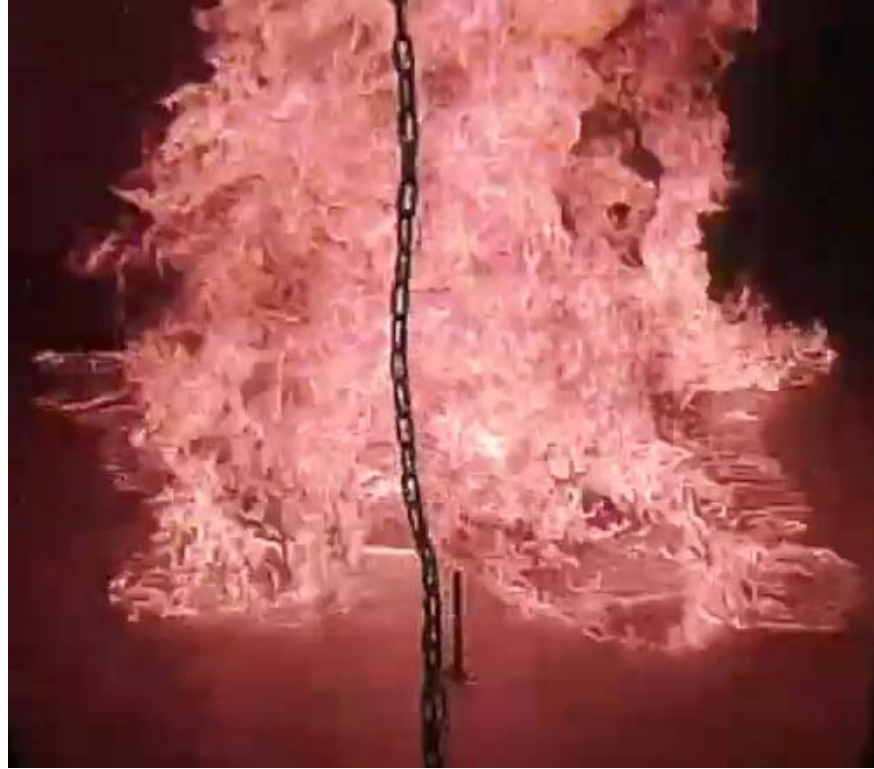


Figure 31. 2.0 L gasoline spill fire conducted in test enclosure.



Figure 32. Thermal degradation to vinyl sub-flooring occurring less than 10 seconds after ignition of the spill fire.

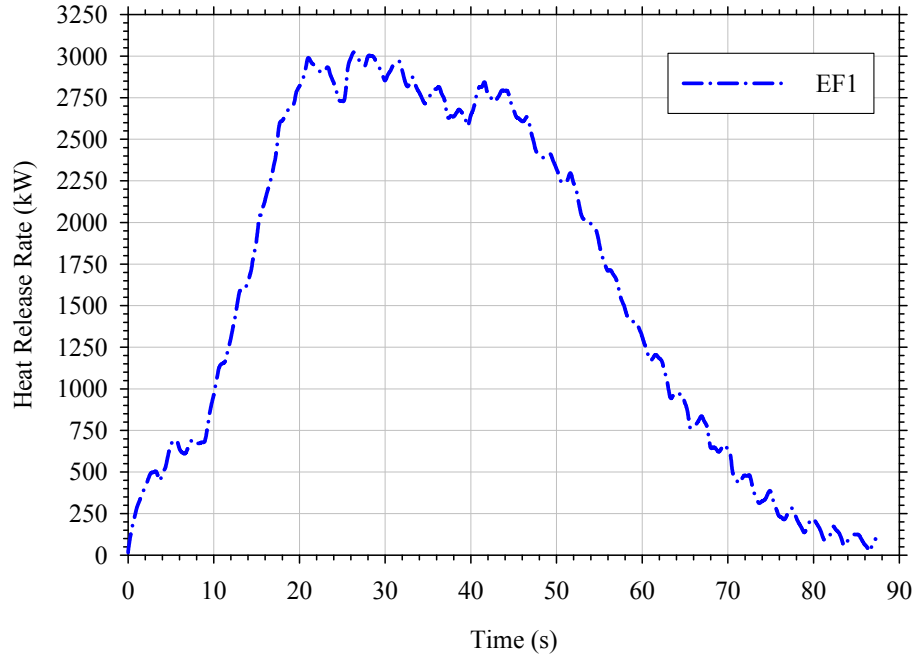


Figure 33. Heat release rate for 2.0 L gasoline spill on vinyl flooring within an enclosure.

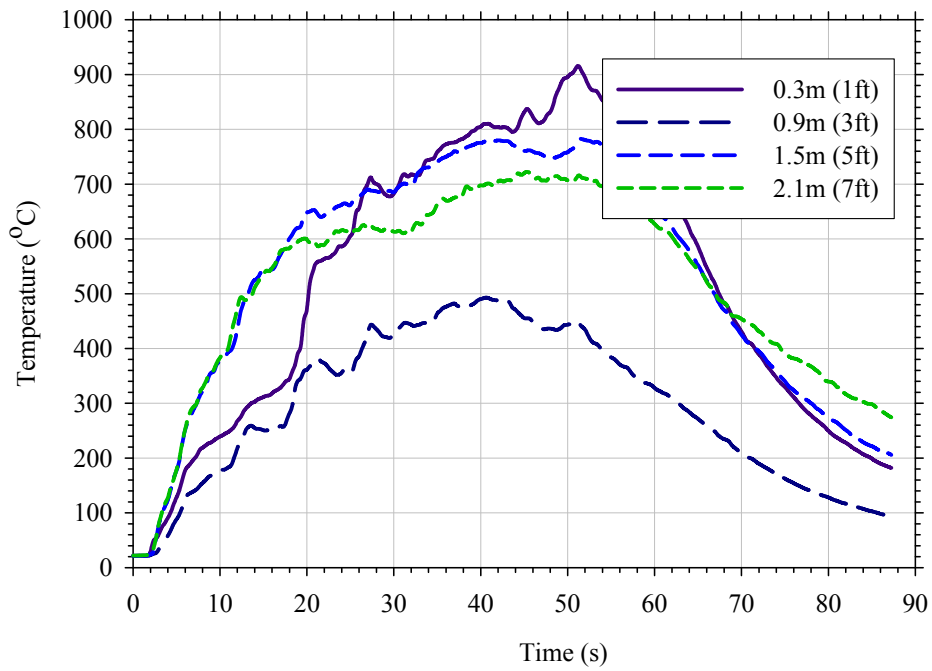


Figure 34. Average enclosure temperatures measured during 2.0 L gasoline spill fire on vinyl.

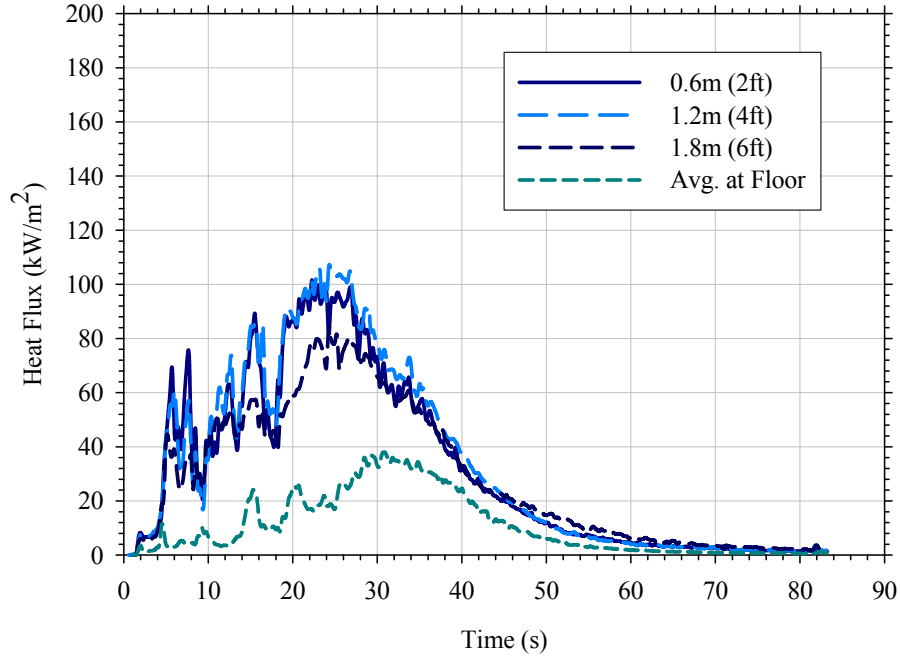


Figure 35. Enclosure heat fluxes measured during 2.0 L gasoline spill fire on vinyl.

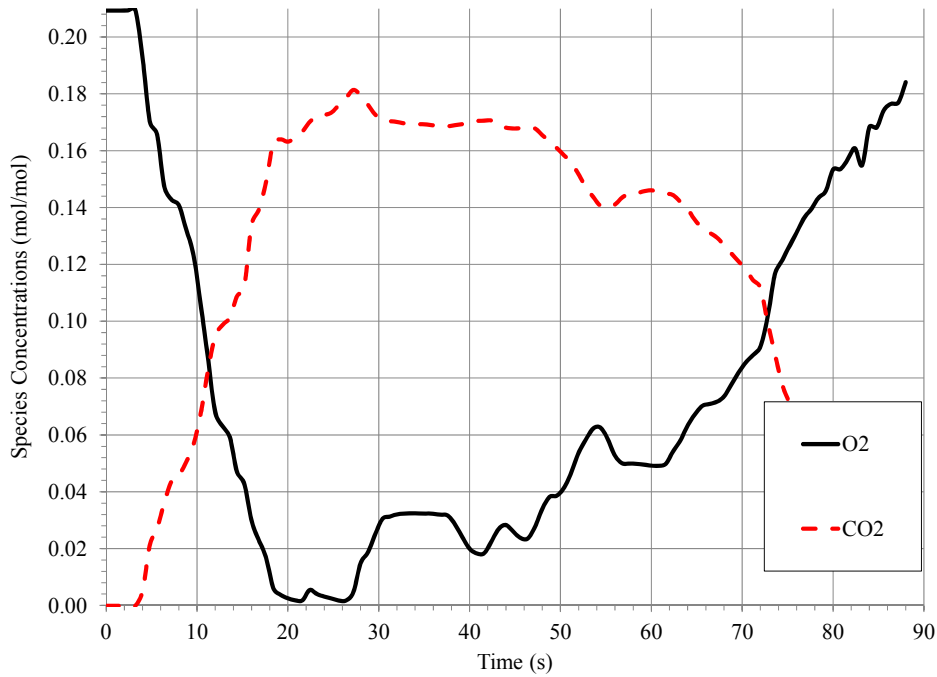


Figure 36. Gas species measurements collected high in the enclosure during 2.0 L gasoline spill fire on vinyl.

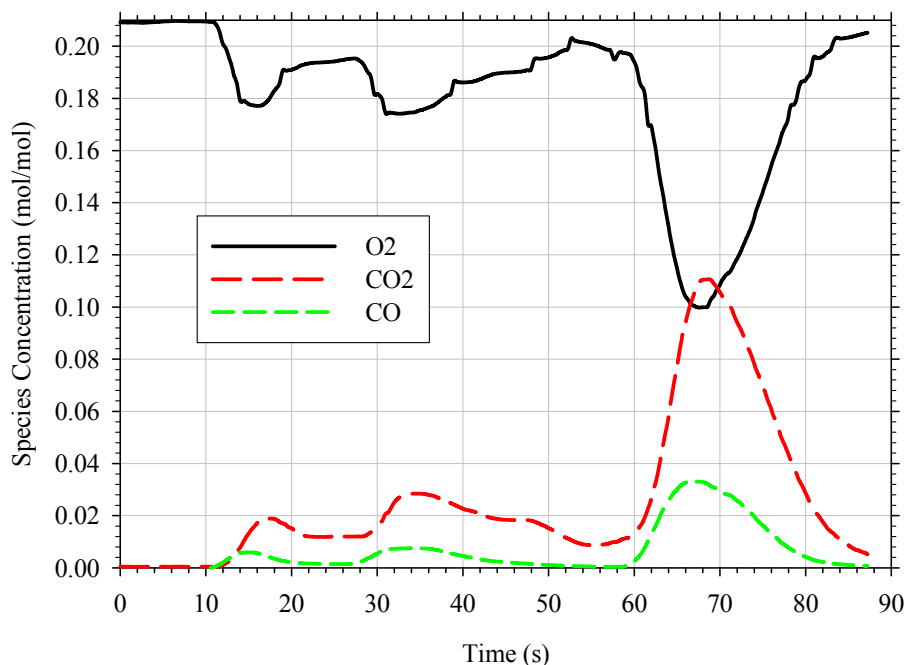


Figure 37. Gas species measurements collected low in the enclosure during 2.0 L gasoline spill fire on vinyl.

As a result of the size of the gasoline spill, flashover conditions were reached very quickly in this test. In this work, flashover was assessed as the transition of the fire from the initial fuel items burning to the relatively rapid involvement of the flooring. In addition, the thermal criteria of a temperature threshold of 600°C (1112°F) and a heat flux threshold of 20 kW/m² at the floor were evaluated as indicators of flashover [Peacock et al. 1999]. Thermal conditions in the upper layer of the enclosure exceeded 600°C (1112°F) less than 20 seconds after ignition. Heat fluxes to the walls of the enclosures increased to near 100 kW/m² within the first 30 seconds of the test, with exposures to the floor as high as 35 kW/m². This intense thermal exposure to the floor of the enclosure resulted in the early involvement of flooring material that was not originally part of the initial fuel spill. Although upper layer oxygen concentrations dropped to near zero within the initial 20 seconds of the test, lower layer gas concentrations remained above 0.16 mol/mol (i.e., 16% by volume) for the majority of the test, until the flooring material was completely involved.

5.4.2 Gasoline Spill Fire on Carpet

The 2.0 L gasoline spill on carpet flooring created a spill area of approximately 0.20 m² (2.2 ft²). A plot of the measured heat release rate during this fire is presented in Figure 38. During the initial 90 seconds of this test, the gasoline spill fire maintained a relatively steady-state heat release rate of approximately 170 kW. This steady-state fire is primarily attributed to the combustion of the gasoline wicking through the carpet flooring. After 90 seconds, the fire size gradually increased at a rate of approximately 200 kW per minute until reaching a peak value of 916 kW. This growth was associated with the spread of flame over the flooring material and the involvement of the carpet and padding material, not the enhanced burning from the liquid fuel. In total, the fire burned for 330 seconds (5.5 minutes) before being manually extinguished. The fire was manually extinguished because it had become a carpet flooring material fire as opposed to a

fuel spill fire, which was the original intent of the test. The thermal and gas species conditions within the enclosure during the test are presented in Figure 39–Figure 42.

The heat release, temperature, and upper layer gas species plots presented in Figures 38, 39, and 41 illustrate the transition between gasoline spill fire on carpet and the gradual involvement of larger areas of carpeting material. During the initial 90 seconds, specifically 45–90 seconds after ignition, the heat release rate stabilizes at approximately 170 kW, upper layer temperatures at 200°C (392°F), and upper layer oxygen concentration at 0.18 mol/mol. This initial fire size corresponds to a heat release rate per unit area of 850 kW/m². This value is generally consistent with the values measured during the early stages of the open burning carpet fires conducted in this test program and the data reported by Mealy et al. [2010] (see Section 6.2.1 for comparison analysis). It should be noted that carbon monoxide concentration data was corrupted for upper layer measurements during this test and are therefore not reported.

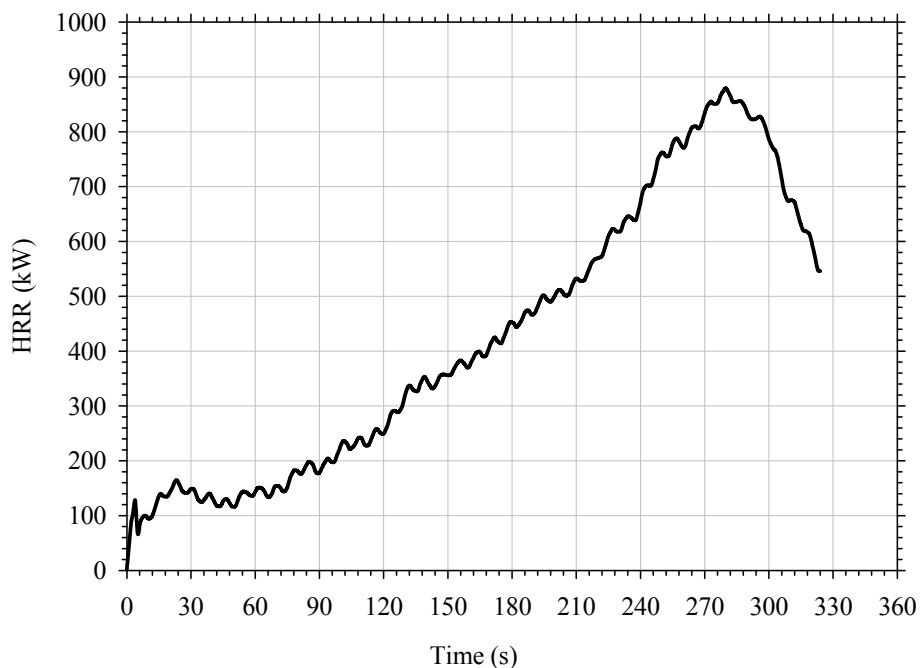


Figure 38. Heat release rate for 2.0 L gasoline spill on carpet flooring within an enclosure.

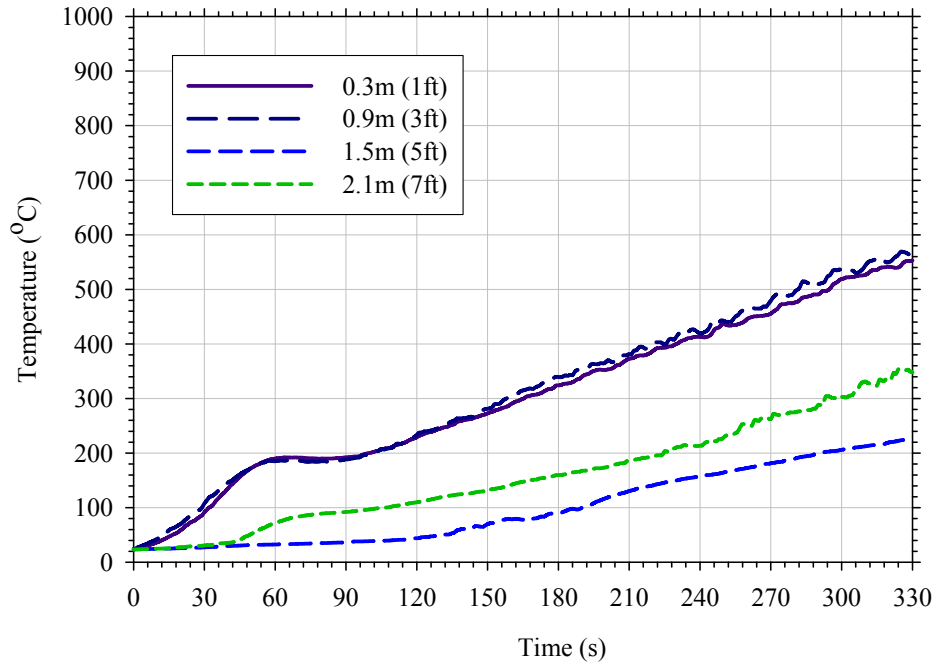


Figure 39. Enclosure temperatures measured during 2.0 L gasoline spill fire on carpet.

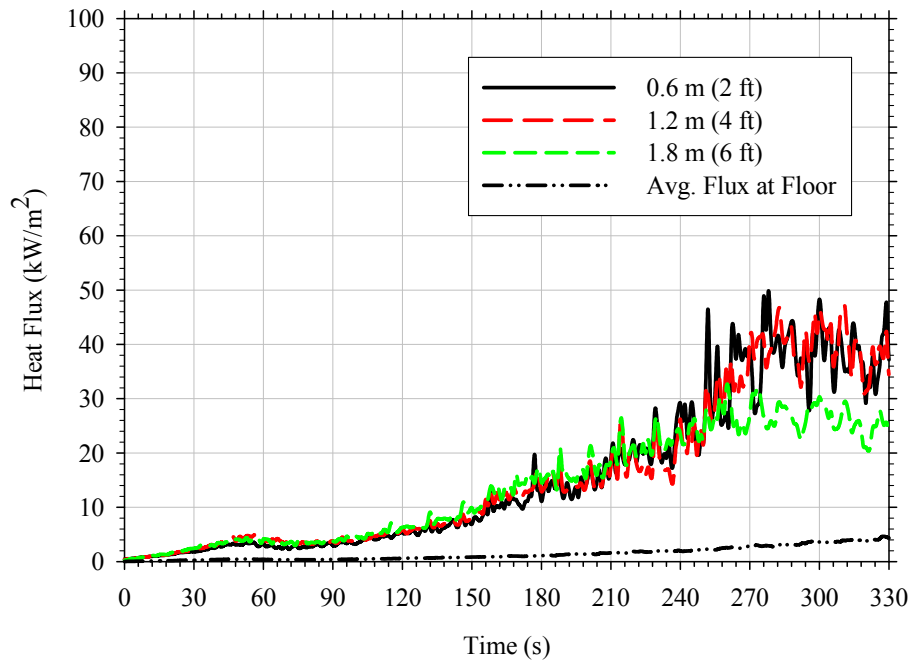


Figure 40. Enclosure heat fluxes measured during 2.0 L gasoline spill fire on carpet.

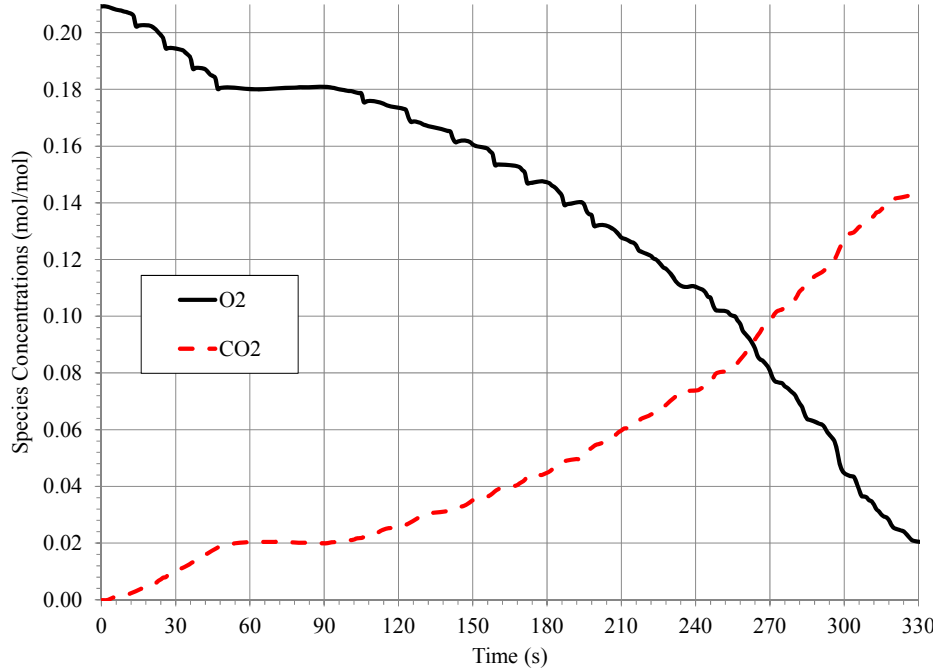


Figure 41. Gas species measurements collected high in the enclosure during 2.0 L gasoline spill fire on carpet.

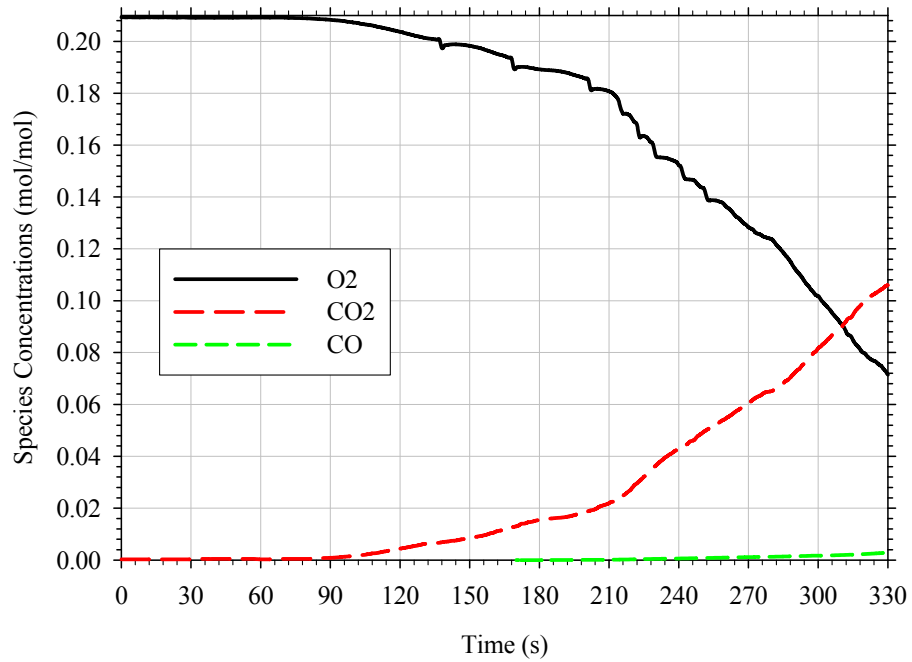


Figure 42. Gas species measurements collected low in the enclosure during 2.0 L gasoline spill fire on carpet.

5.5 Test Series 5 – Pan Fires in Enclosure

A total of eight pan fire tests were conducted within the test enclosure. Individual tests were run to explore three different variables: fuel type, fire location, and ventilation condition. All of these parameters were being explored to determine the varying effects of the enclosure on the overall fire dynamics of the liquid fuel fire. The pan fires evaluated in these tests were identical to those tested in Test Series 1 so that direct comparisons could be made to characterize the impact of the enclosure on the burning rate of liquid fuel for both pre- and post-flashover conditions.

As described in Test Series 1, two different pan sizes were used to create similar fire sizes (HRR) using different fuel types (i.e., sooting and non-sooting fuels). These fires were conducted in both the center and rear corner of the enclosure. Only one pan was present within the test enclosure for any given test. An illustration of the pan locations is provided in Figure 43. A summary of the tests conducted and summary data from these tests are provided in Table 10. The center and corner locations were selected to quantify the impact on burning rate due to fire location with respect to the vent opening. Fuel pans were offset from the enclosure wall 0.1 m (4 in.) for corner configurations. Tests of both ventilation conditions (i.e., full-open door and slit vent) were performed for each fuel type and fuel location. The test procedures outlined in Section 5.2 for pan fires conducted in the open were used in this series of tests as well.

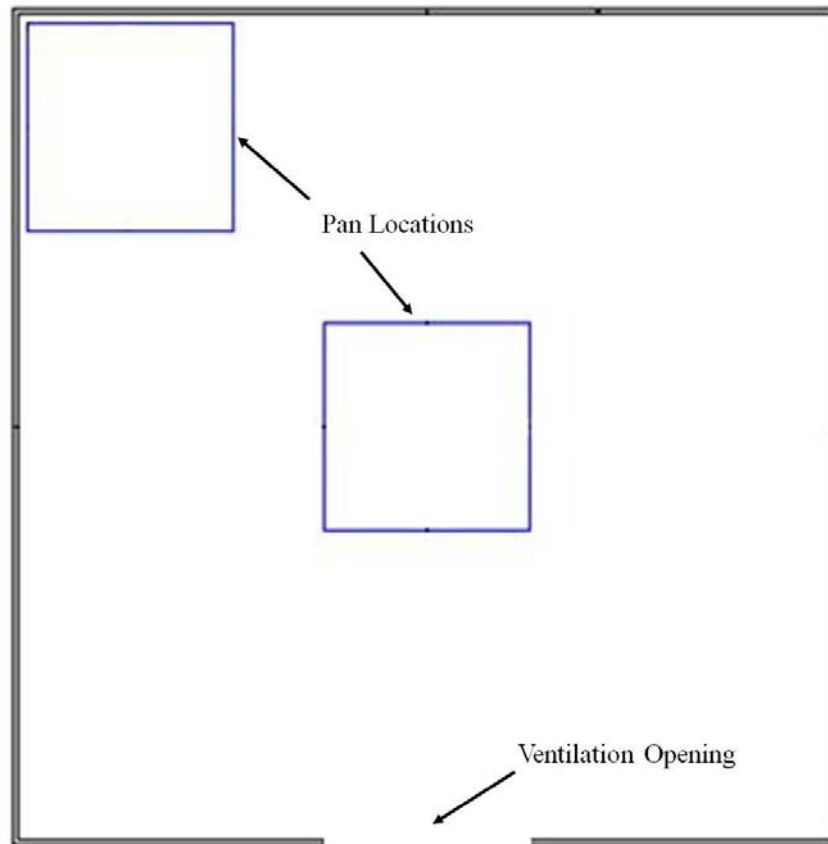


Figure 43. Pan locations within test enclosure.

Table 10. Summary of pan fire testing in enclosure.

Fuel	Fire Location	Ventilation Condition	Avg. HRR (kW)	Avg. Layer Height (m [ft])	Average Upper Layer Temperature (°C)	Avg. Heat Flux to Floor (kW/m²)	Flame Extension from Vent Opening (Yes/No)	Flame Tilt (Yes/No)
Heptane	Open	Open Burn	531	N/A	N/A	N/A	N/A	N/A
	Corner	Full Door	899	1.5 [5]	558	5	No	No
		Slit Vent	611	0.9 [3]	737	2.5	No	No
	Center	Full Door	791	1.2 [4]	752	7	No	Yes (~15°)
		Slit Vent	857	0.9 [3]	786	25*	No	Yes (Complete Detachment)
Denatured Alcohol	Open	Open Burn	540	N/A	N/A	N/A	N/A	N/A
	Corner	Full Door	527	1.5 [5]	412	2.5	No	No
		Slit Vent	779	0.9 [3]	710	10	No	No
	Center	Full Door	532	1.5 [5]	496	<2	No	No
		Slit Vent	530	0.9 [3]	556	<2	No	No

*See discussion in Section 5.5.4

5.5.1 Rear Corner – Full Door Scenario

When burning in the corner of the enclosure with a full-open doorway, enhanced burning of the heptane pan fire was observed approximately 60 seconds after ignition. A comparison of the enclosed and open burning pan fire heat release rates is provided in Figure 44. The enhanced burning continued for the duration of the test and was on average 69 percent higher than that measured in open burning conditions. Transient temperature measurements and thermal gradients within the enclosure are provided in Figure 45 and Figure 46. An average upper layer height of 1.5 m (5 ft) was observed for the majority of the test. As shown in Figure 45 and Figure 46, after the initial period of fire development (i.e., initial 120 seconds) upper layer temperatures ranged from between 350–800°C (662–1472°F) for the duration of the test. Temperatures in the lower layer of the compartment remained below 300°C (572°F) for the duration of the test. Average heat fluxes at the floor during this test remained relatively low with values ranging from 3–7 kW/m². A photograph of the pan fire burning in the corner of the enclosure is provided in Figure 47. The full-open doorway prevented the layer from descending below 1.5 m (5 ft), the gas species in the lower layer of the compartment did not vitiate at any point in time. Upper layer oxygen concentrations did drop to approximately ten percent after three minutes of burning and remained at this level for the duration of the test. No exterior flaming or flaming in the upper layer was observed. The flame plume remained above the fuel surface for the duration of the test with only a small amount of vapor spillover outside the compartment at the very end of the test, as shown in Figure 44, i.e., increase in HRR just prior to burn out.

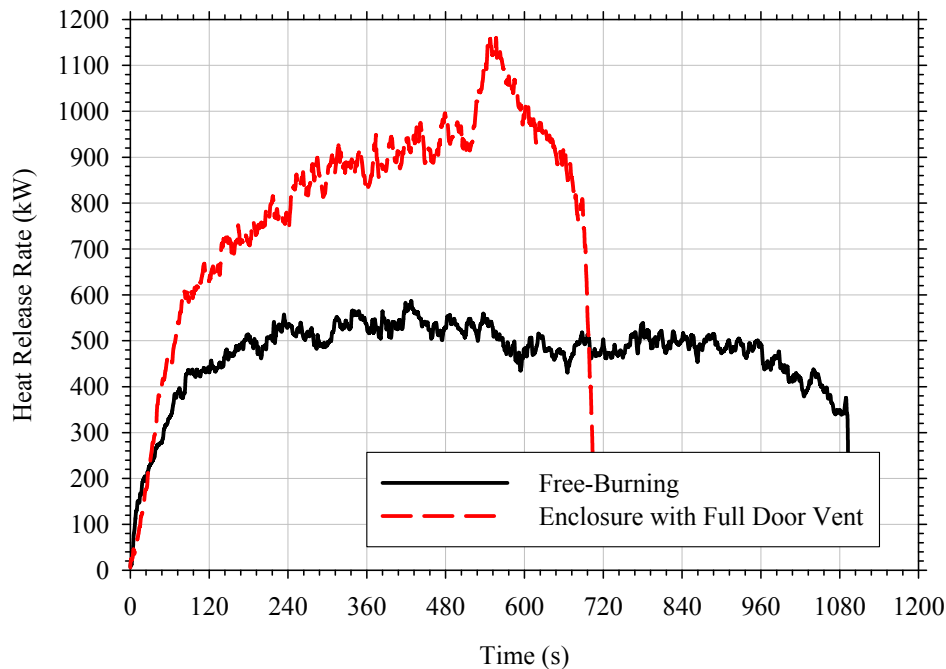


Figure 44. Measured heat release rate from heptane pan fire burning in corner of enclosure with full-open doorway compared to open burning fire.

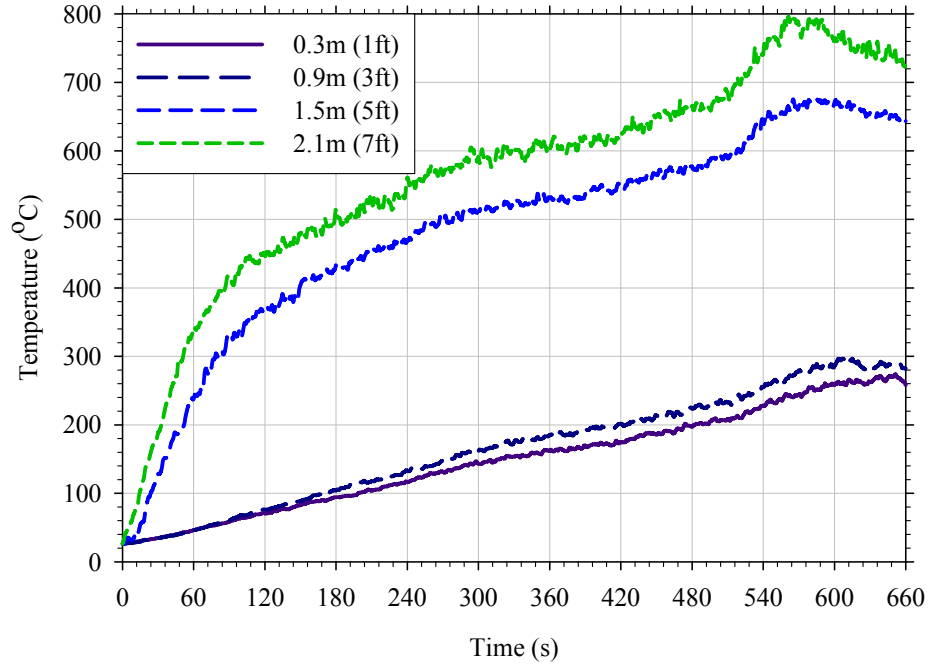


Figure 45. Enclosure temperatures during heptane pan fire burning in corner of enclosure with full-open doorway.

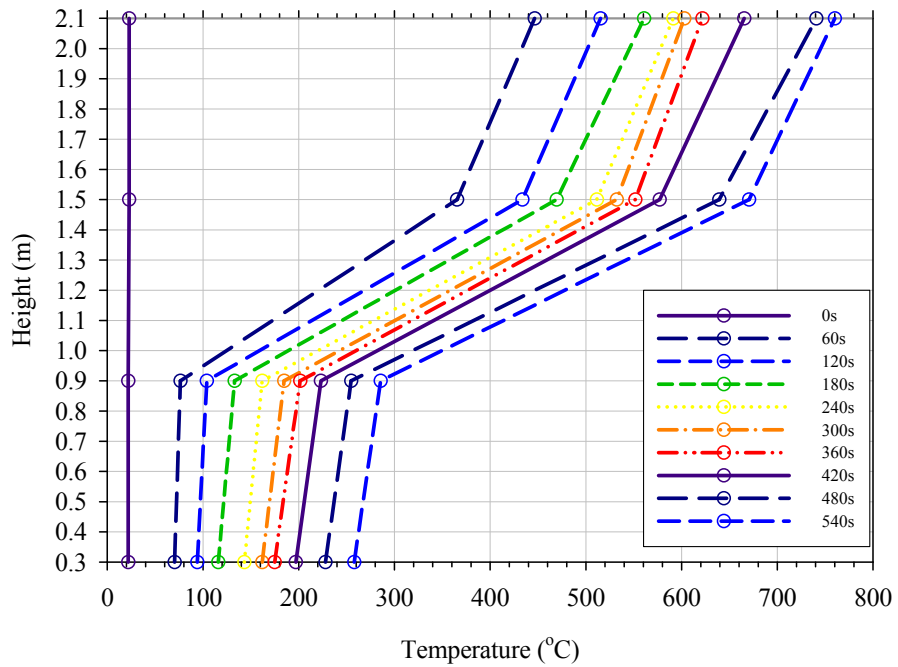


Figure 46. Thermal gradients at 1-minute intervals for heptane pan fire burning in corner of enclosure with full-open doorway.



Figure 47. Steady-state 0.23 m² (2.5 ft²) heptane pan fire burning in the corner of the enclosure.

Contrary to the heptane fires, the denatured alcohol pan fire burning in the corner of the enclosure with a full-open doorway did not result in enhanced burning. Both visually as well as from a measured heat release rate (Figure 48), no differences were observed between the pan fires burning in the open versus in the enclosure. Although not visually observed, an average upper layer depth of approximately 1.5 m (5 ft) is evident in both Figure 49 and Figure 50 approximately two minutes after ignition. As shown in Figure 49, average upper layer temperatures remained between 250–440°C (482–842°F) for the duration of the test. Heat fluxes at the floor during this test remained relatively low with values ranging from 2–3 kW/m². Temperatures in the lower layer of the compartment remained below 200°C (392°F) for the duration of the test. The full-open doorway prevented the layer from descending below 1.5 m (5 ft); therefore, the lower layer did not vitiate at any point in time. Upper layer oxygen concentrations did drop to between 15–17 percent after three minutes of burning and remained at this level for the duration of the test. No exterior flaming or flaming in the upper layer was observed and no flame tilt was observed. A photograph of the denatured alcohol pan fire burning in the corner of the enclosure is provided in Figure 51.

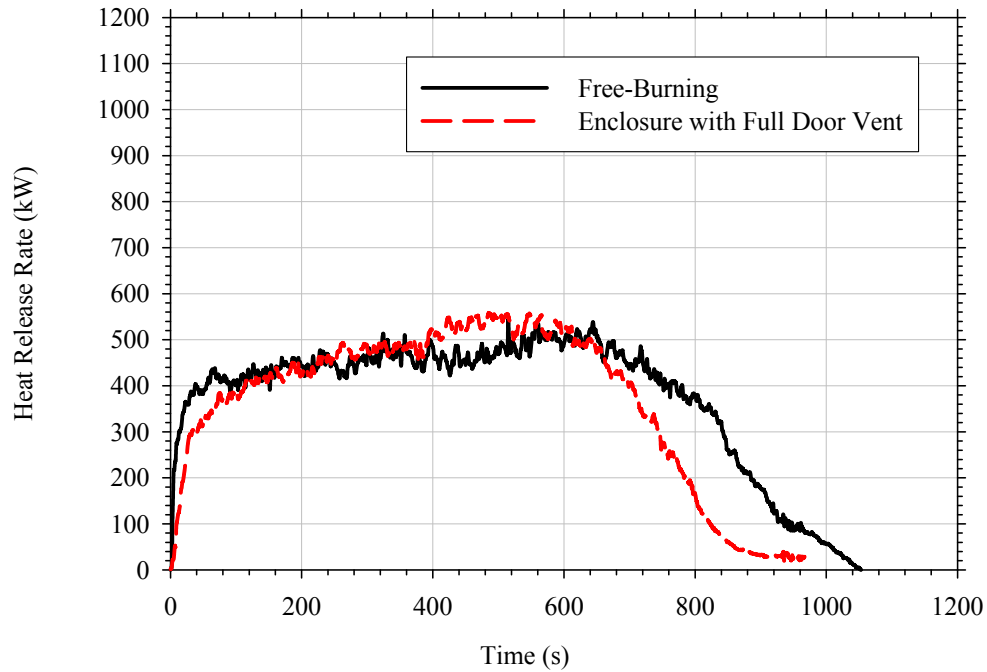


Figure 48. Measured heat release rate from denatured alcohol pan fire burning in corner of enclosure with full-open doorway compared to open burning fire.

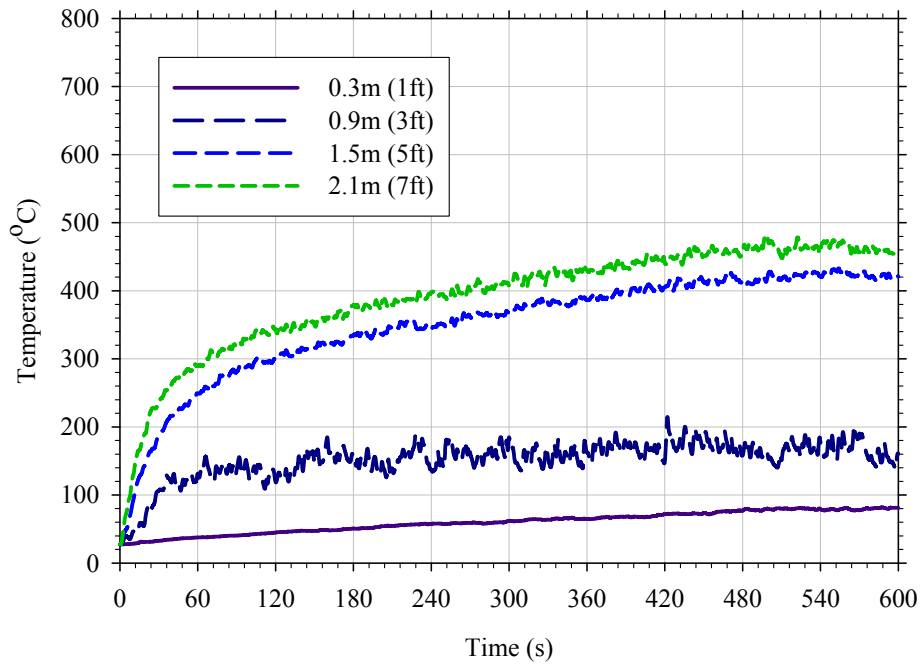


Figure 49. Compartment temperatures measured during denatured alcohol pan fire burning in corner of enclosure with full-open doorway.

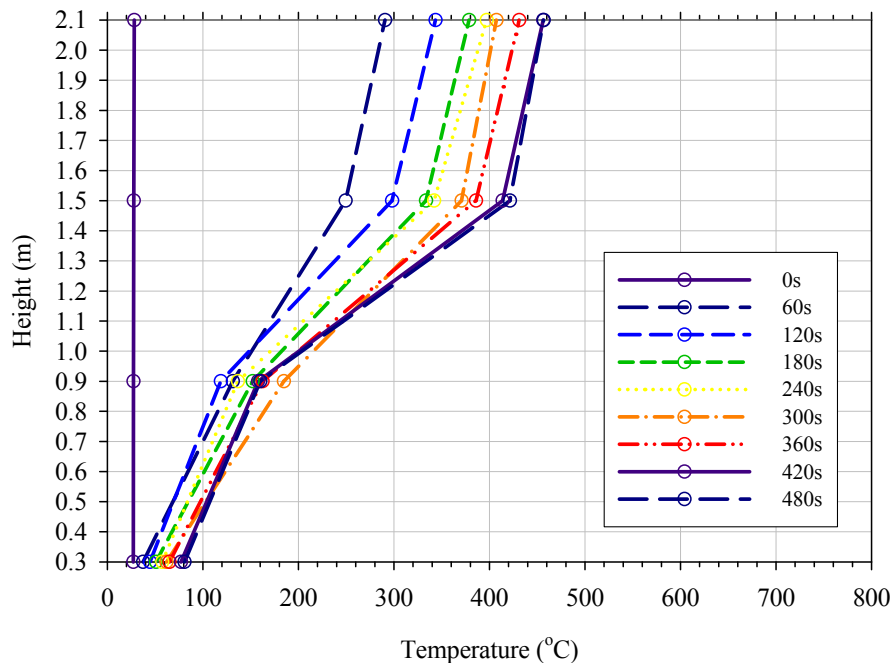


Figure 50. Vent opening thermal gradients at 1-minute intervals for denatured alcohol pan fire burning in corner of enclosure with full-open doorway.



Figure 51. Steady-state 1.0 m² (10.4 ft²) denatured alcohol pan fire burning in the corner of the enclosure.

5.5.2 Rear Corner – Slit Vent Scenario

With the slit ventilation scheme and a heptane pan fire burning in the corner of the enclosure, a minimal degree of enhanced burning of the heptane pan fire was observed after approximately 200 seconds. A comparison of the open burning and enclosed heptane pan fires is provided in Figure 52. The enhanced burning continued for the duration of the test and was on average 10 percent higher than that measured in open burning conditions. Thermal conditions within the test enclosure over the course of this test are presented in Figure 53 and Figure 54. Despite the fact that the hot upper layer had an average depth of approximately 0.9 m (3 ft) and an average temperature 470–570°C (878–1058°F), an increased rate of combustion was not observed. Heat fluxes at the floor during this test ranged from 7–10 kW/m². Although the slit vent allowed the upper layer to descend further than with a full-open doorway, the lower layer did not vitiate at any point in time. Upper layer oxygen concentrations dropped to around five percent after three minutes of burning and remained at this level for the duration of the test. No exterior flaming or flaming in the upper layer was observed. The flame plume remained above the fuel surface for the duration of the test. A photograph of the corner heptane pan fire with a slit ventilation condition is provided in Figure 55.

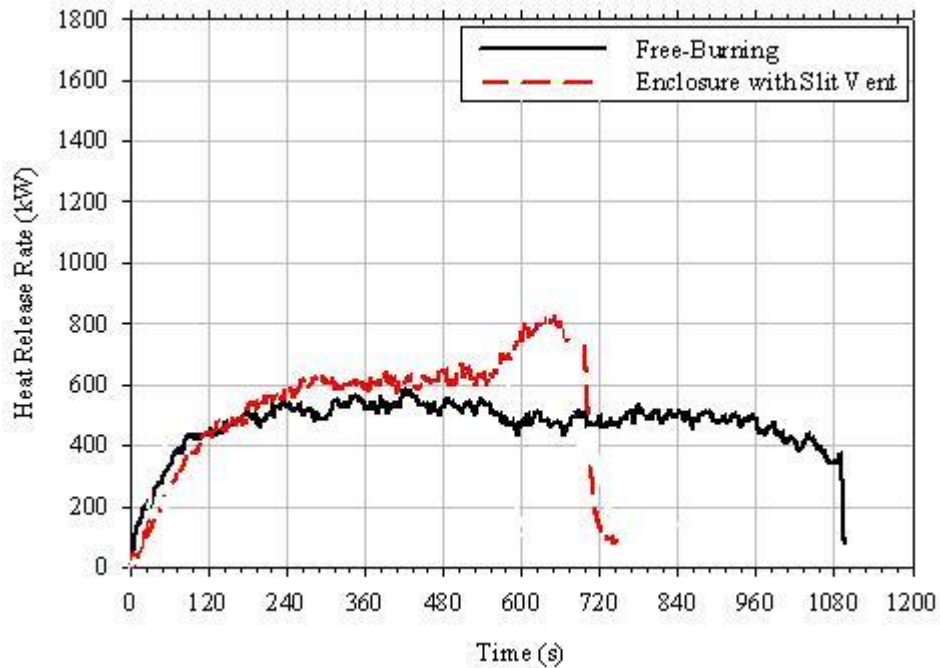


Figure 52. Measured heat release rate from heptane pan fire burning in corner of enclosure with slit vent compared to open burning fire.

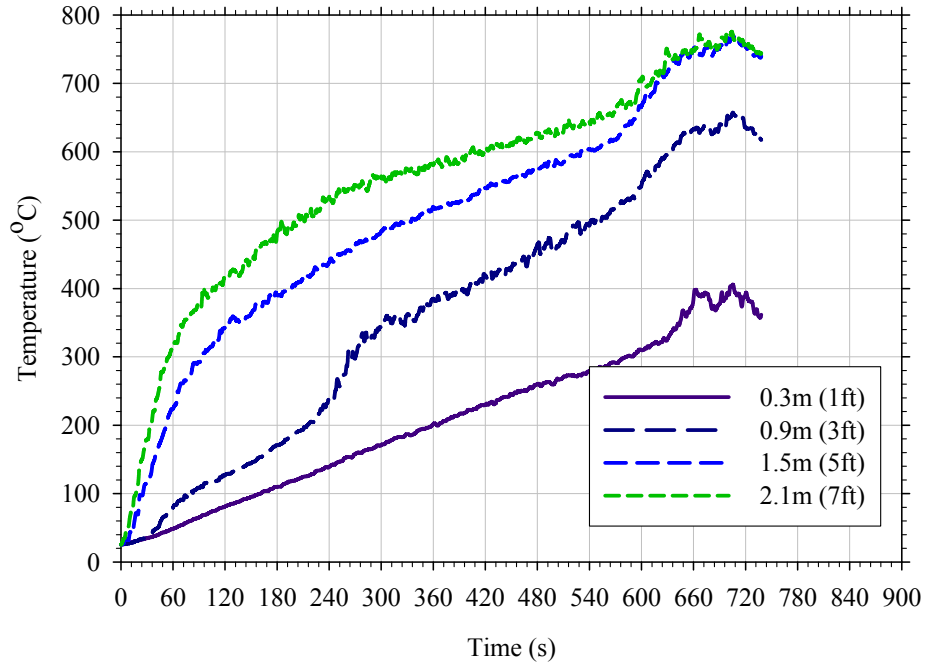


Figure 53. Enclosure temperatures during heptane pan fire burning in corner of enclosure with slit vent.

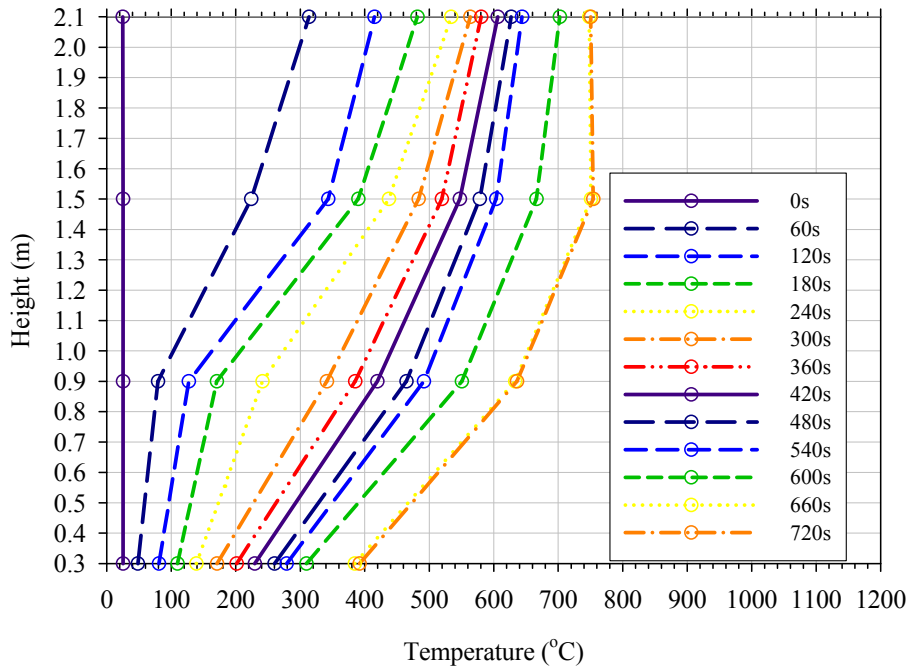


Figure 54. Thermal gradients at 1-minute intervals for heptane pan fire burning in corner of enclosure with slit vent.



Figure 55. Steady-state 0.23 m² (2.5 ft²) heptane pan fire burning in the corner of the enclosure with a slit vent scenario.

With the slit ventilation scheme and a denatured alcohol pan fire burning in the corner of the enclosure, enhanced burning was observed for the majority of this test. As shown in Figure 56, heat release rates measured for this scenario were approximately 50 percent higher than that measured under open burning conditions. The hot upper layer that developed within the enclosure had an average depth of 0.9 m (3 ft) and an average temperature that ranged from 350°C (662°F) early in the test up to approximately 675°C (1247°F) late in the test. Temperatures at four different elevations and thermal gradients at 60-second time steps are provided in Figure 57 and Figure 58, respectively. Heat fluxes at the floor ranged from 8–12 kW/m² once the upper layer developed. Although the slit vent allowed the upper layer to descend further within the compartment, the lower layer of the compartment did not vitiate at any point in time. Upper layer oxygen concentrations dropped to approximately ten percent after three minutes of burning and remained at this level for the duration of the test. No exterior flaming or flaming in the upper layer was observed. The flame plume remained above the fuel surface for the duration of the test. A photograph of this test scenario is provided in Figure 59.

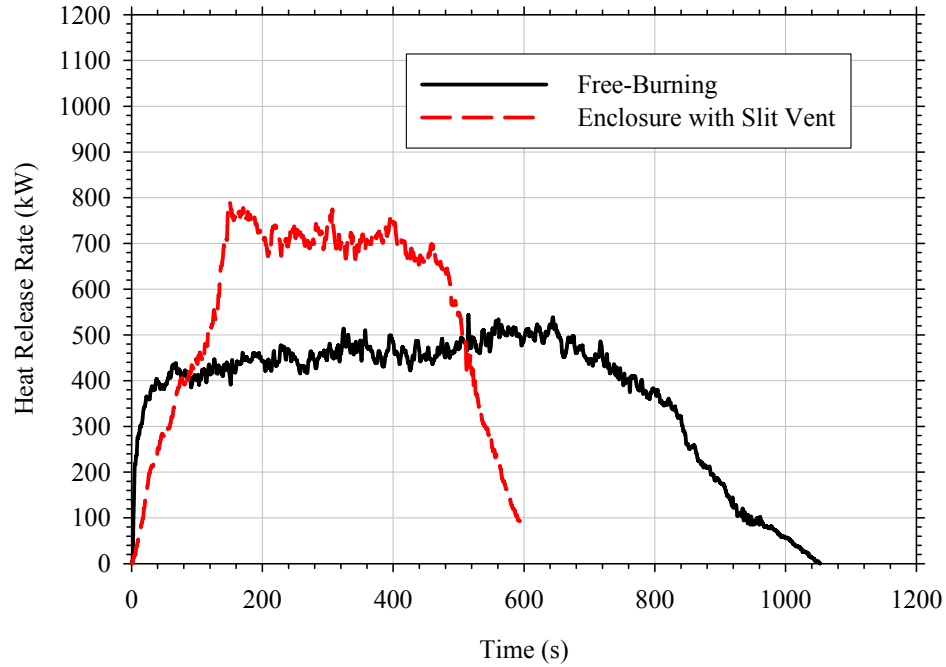


Figure 56. Measured heat release rate from denatured alcohol pan fire burning in corner of enclosure with slit vent compared to open burning fire.

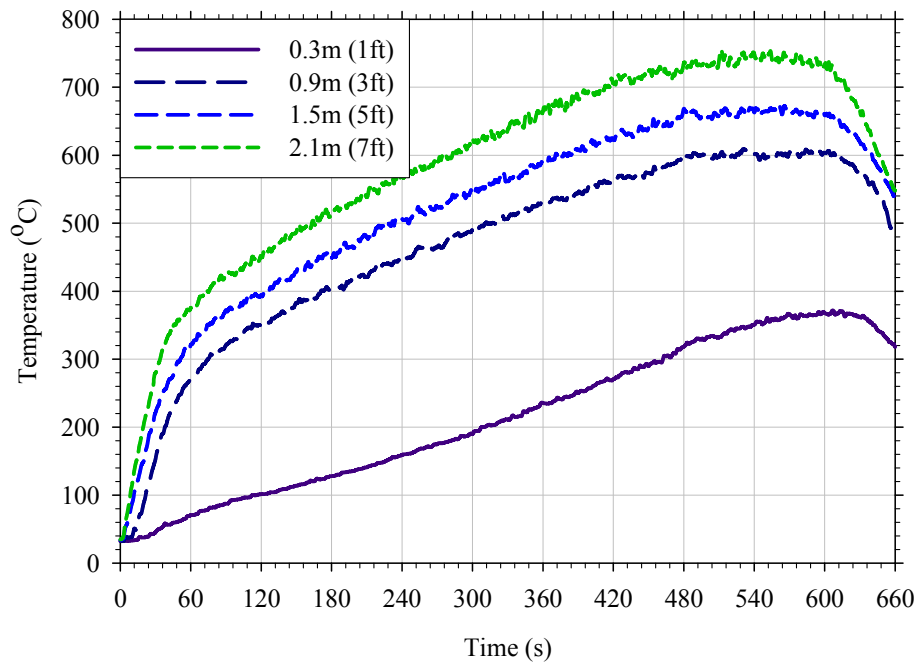


Figure 57. Enclosure temperatures during denatured alcohol pan fire burning in corner of enclosure with slit vent.

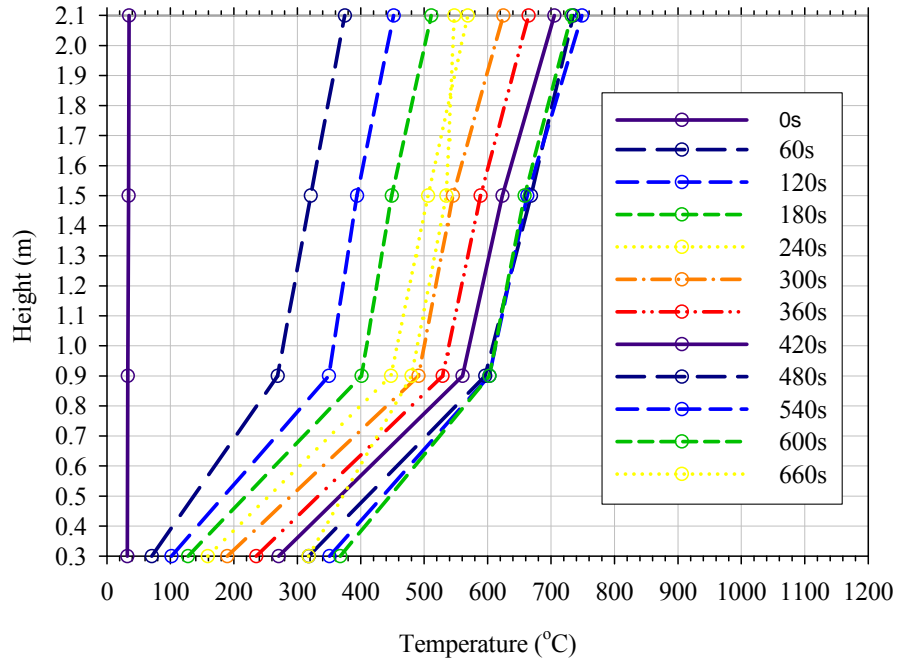


Figure 58. Thermal gradients at 1-minute intervals for heptane pan fire burning in corner of enclosure with slit vent.



Figure 59. Steady-state 1.0 m² (10.8 ft²) denatured alcohol pan fire burning in the corner of the enclosure with a slit vent scenario.

5.5.3 Center of Compartment – Full Door Scenario

As shown in Figure 60, when burning in the center of the enclosure with a full-open doorway, enhanced burning of the heptane pan fire was observed approximately 60 seconds after ignition. The enhanced burning continued for the duration of the test and was on average 50 percent higher than that measured in open burning conditions. During this test, an average upper layer depth of 1.2 m (4 ft) was observed for the majority of the test. As shown in Figure 61, after the initial 120 seconds of fire development upper layer temperatures remained between 300–500°C (572–932°F) for the duration of the test. Temperatures in the lower layer of the compartment remained below 150°C (302°F). Vertical temperature gradients at 60-second time intervals are provided in Figure 62. Average heat fluxes at the floor during this test remained relatively low with values ranging from 6–8 kW/m². No exterior flaming or flaming in the upper layer was observed. However, due to the location of the pan fire relative to the ventilation opening, a flame tilt of approximately 15 degrees from vertical, toward the rear of the room, was noted 150 seconds after ignition. In general, this tilt was maintained for the duration of the test. A still image of the pan fire flame tilting is provided in Figure 63.

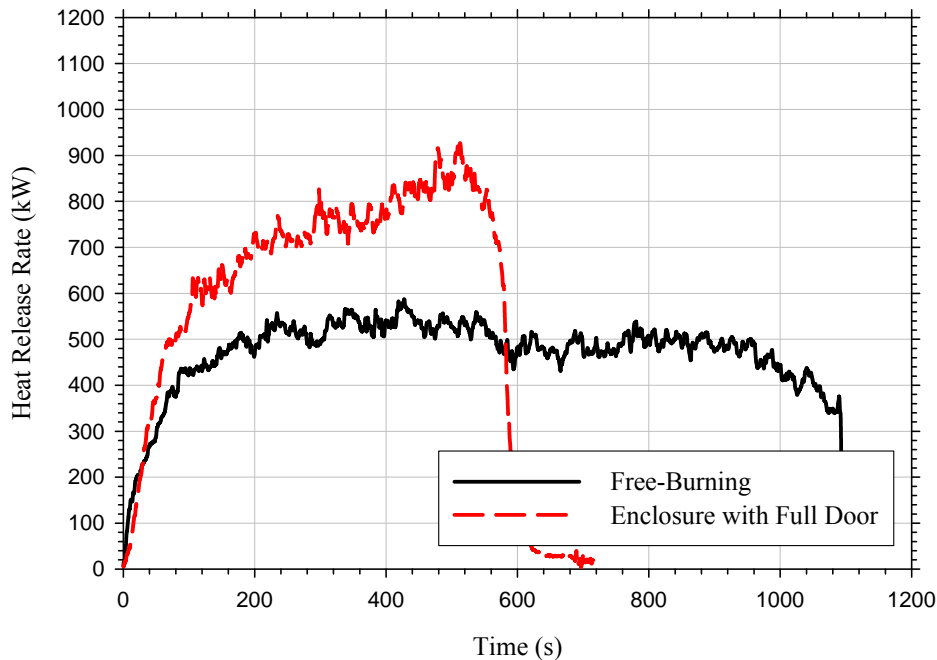


Figure 60. Measured heat release rate from heptane pan fire burning in center of enclosure with full open door compared to open burning fire.

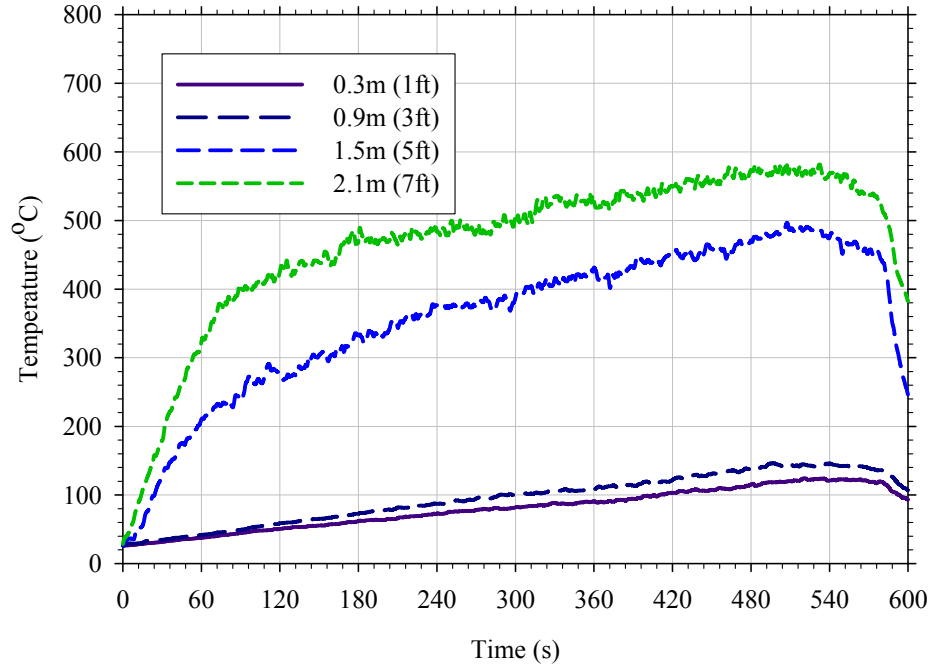


Figure 61. Enclosure temperatures during heptane pan fire burning in center of enclosure with full-open doorway.

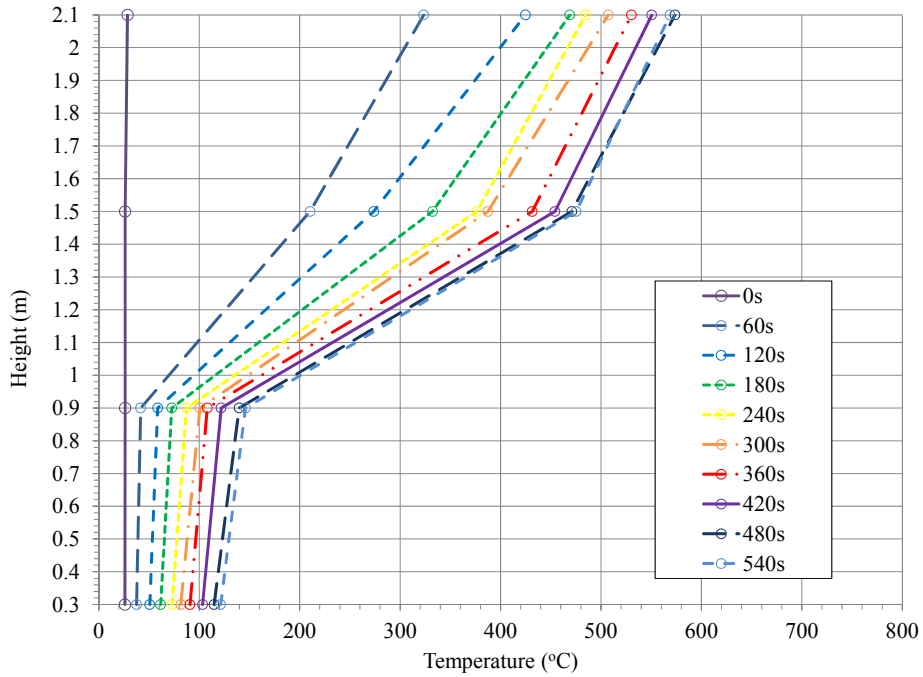


Figure 62. Thermal gradients at 1-minute intervals for heptane pan fire burning in center of enclosure with full-open doorway.

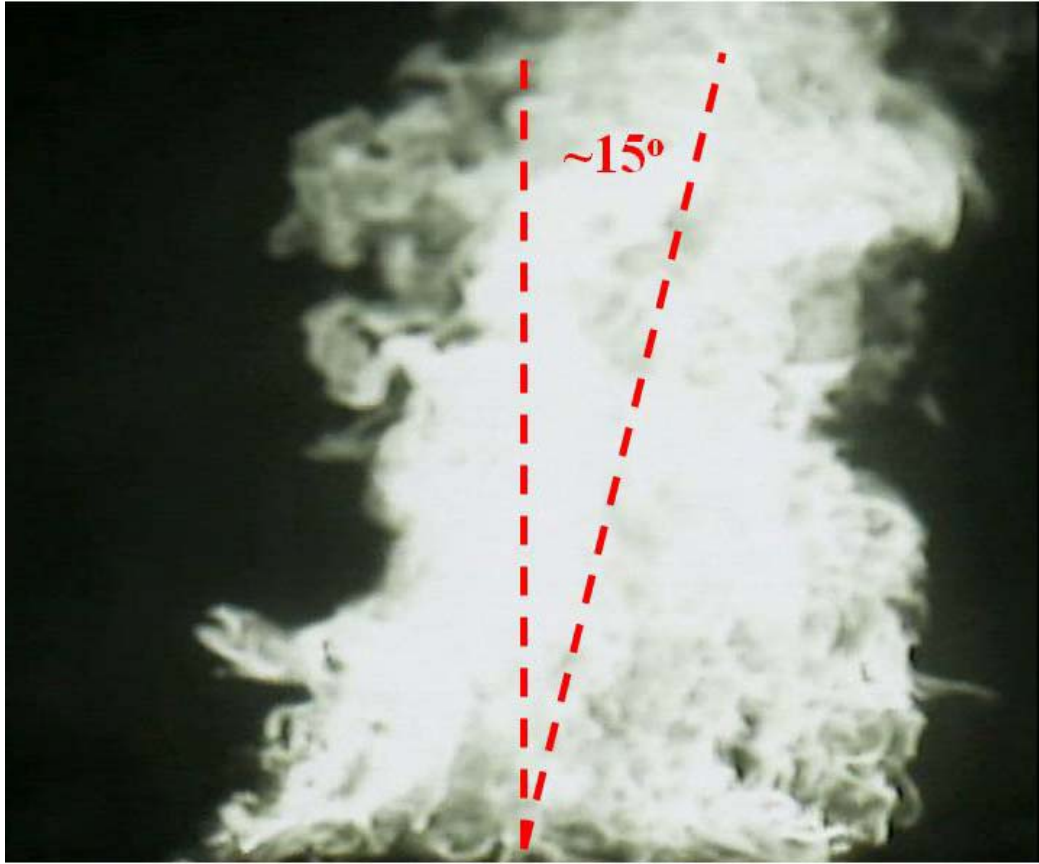


Figure 63. Flame tilt (towards the rear of the enclosure – away from vent) observed during heptane pan fire in center of enclosure with full-open doorway.

Contrary to the heptanes fires, the denatured alcohol pan fire burning in the center of the enclosure with a full-open doorway did not result in enhanced burning. Both visually as well as from a measured heat release rate, no differences were observed between the pan fires burning in the open versus in the enclosure. A comparison of the open burning and enclosed heat release rates is provided in Figure 64. Based on the thermal data presented in Figure 65 and Figure 66, the average layer interface depth was approximately 1.5 m (5 ft). As shown in these figures, the average upper layer temperature remained between 250–400°C (482–752°F) for the majority of the test. Heat fluxes at the floor during this test remained less than 2 kW/m². No exterior flaming or flaming in the upper layer was observed. The flame plume remained above the fuel surface for the duration of the test.

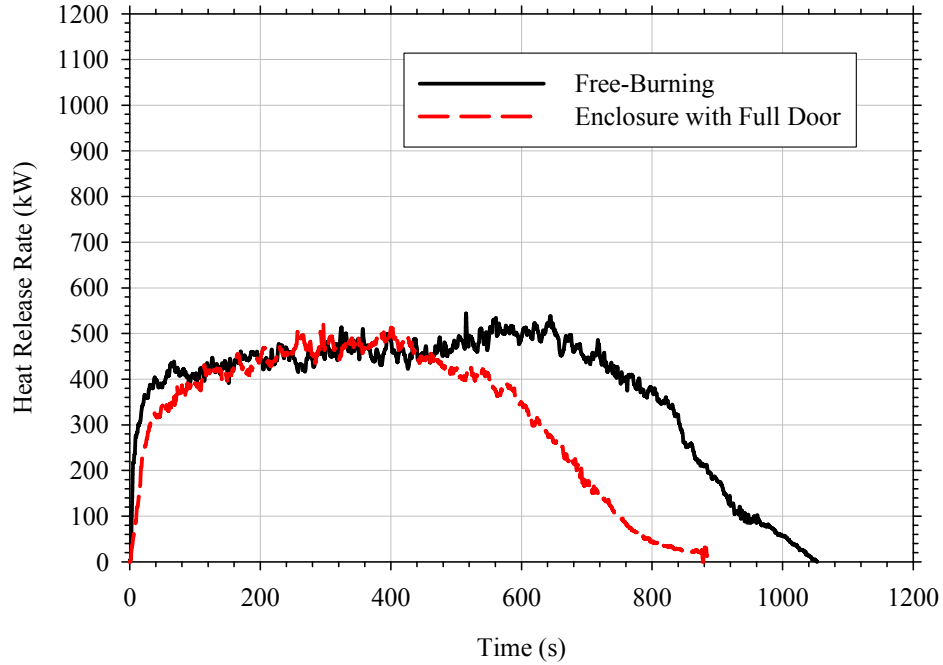


Figure 64. Measured heat release rate from denatured alcohol pan fire burning in center of enclosure with full open door compared to open burning fire.

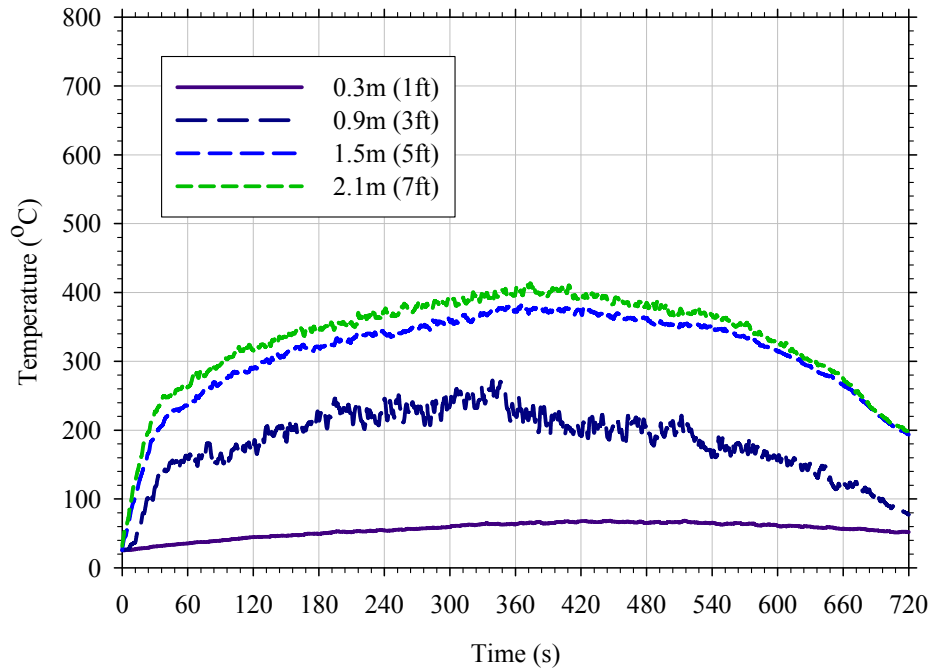


Figure 65. Enclosure temperatures during denatured alcohol pan fire burning in center of enclosure with full open door.

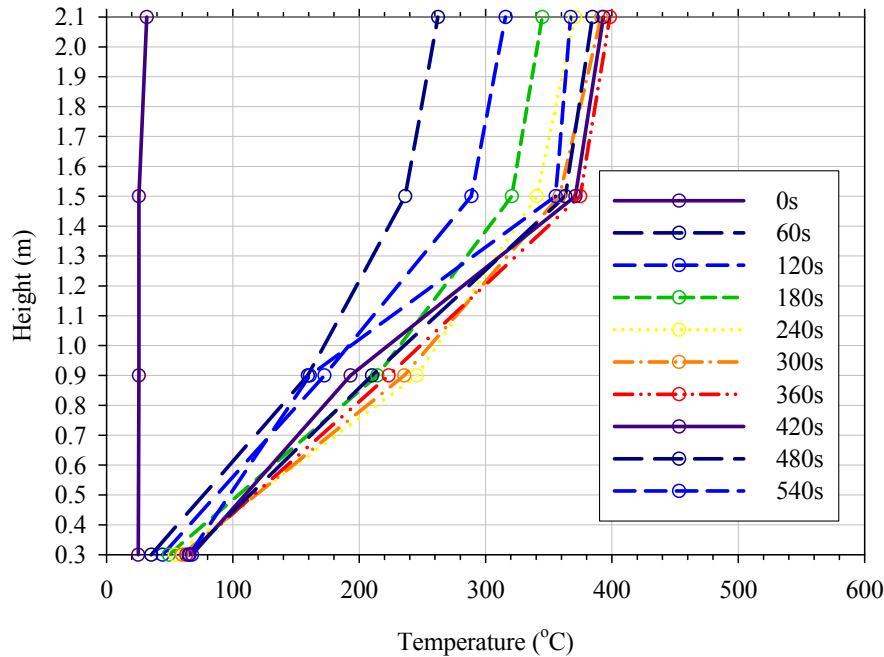


Figure 66. Thermal gradients at 1-minute intervals for denatured alcohol pan fire burning in corner of enclosure with full open door.

5.5.4 Center of Compartment – Slit Vent Scenario

When burning in the center of the enclosure with a slit vent, enhanced burning of the heptane pan fire was observed approximately 60-seconds after ignition. A comparison of the open burning and enclosed pan fires is presented in Figure 67. The enhanced burning continued for the duration of the test and was on average 70 percent higher than that measured in open burning conditions. An average upper layer interface depth of 0.6–0.9 m (2–3 ft) was observed for the majority of the test. As shown in Figure 68 and Figure 69, after the initial period of fire development (i.e., initial 120 seconds) average upper layer temperatures ranged from between 450–750°C (842–1382°F) for the duration of the test. Average heat flux values to the floor of the enclosure during steady-state conditions were 20–30 kW/m². However, it should be noted that due to the flame detachment observed in this test, the severity of the floor level heat fluxes could be skewed and not representative of the flux being imposed strictly by the radiant upper layer. No exterior flaming or flaming in the upper layer was observed. However, severe flame tilt and eventual flame detachment from the evaporating fuel surface were observed in this test. The flame began to tilt towards the rear of the enclosure after approximately 90 seconds of burning. Five minutes after ignition, the flame plume detached from the fuel surface and began combusting in various locations throughout the rear of the enclosure (Figure 70). The migration of the flame plume through the test enclosure was relatively random; often times combustion occurred in areas up to 1.8 m (6 ft) from the fuel surface.

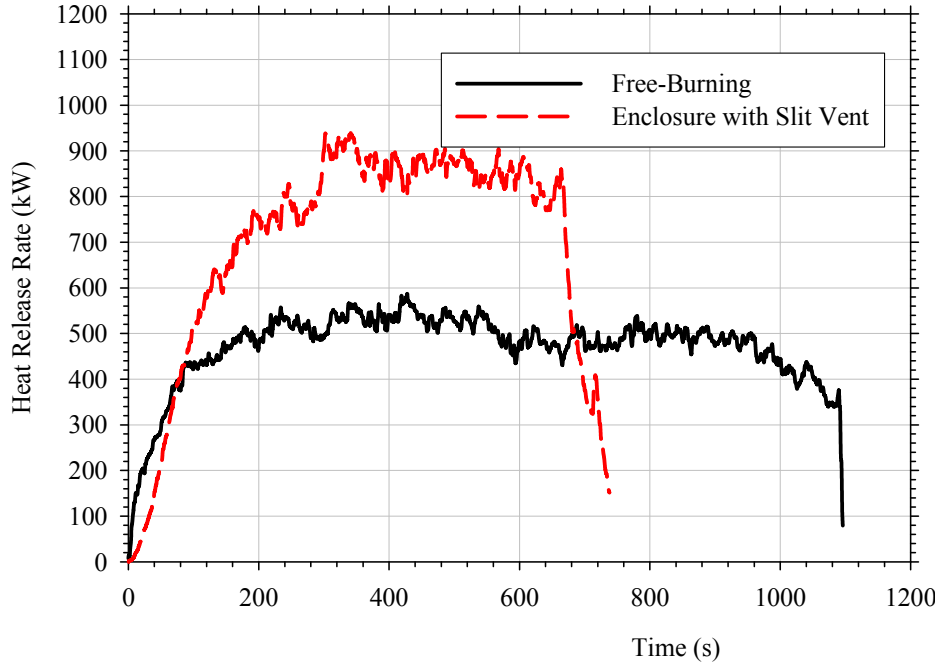


Figure 67. Measured heat release rate from heptane pan fire burning in center of enclosure with slit vent compared to open burning fire.

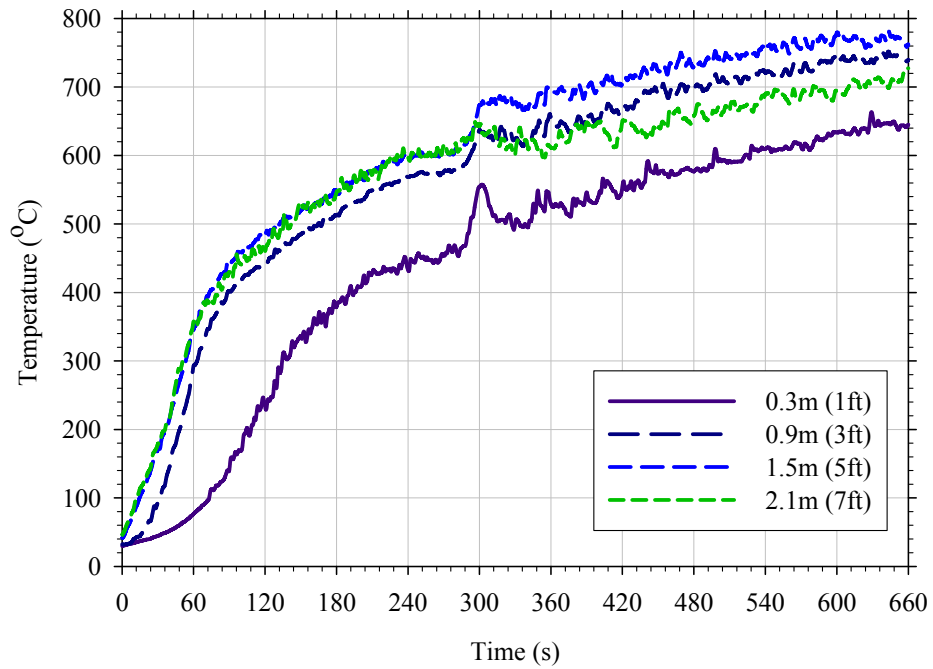


Figure 68. Enclosure temperatures during heptane pan fire burning in center of enclosure with slit vent compared to open burning fire.

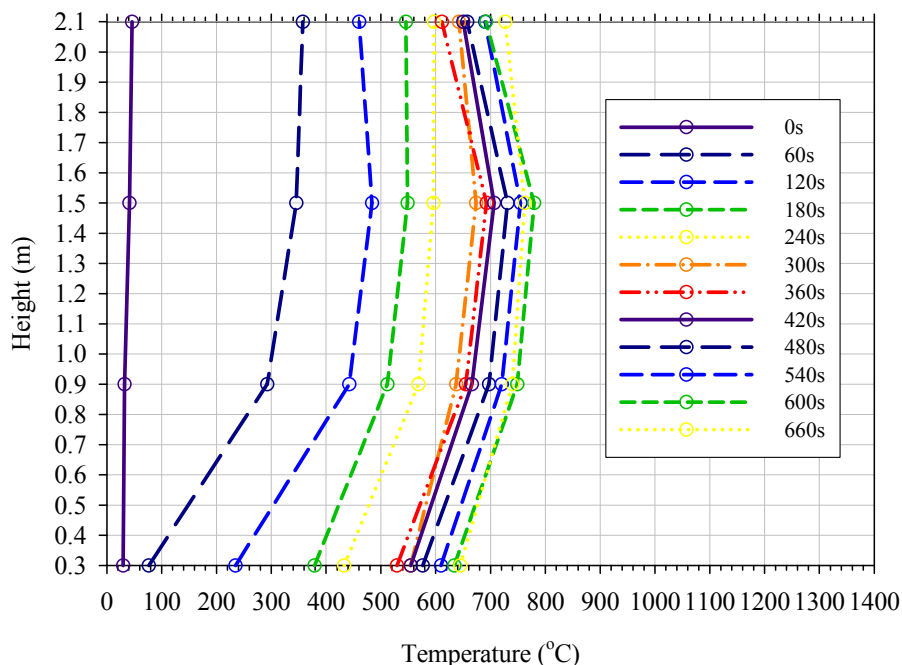


Figure 69. Thermal gradients at 1-minute intervals for heptane pan fire burning in center of enclosure with slit vent compared to open burning fire.



Figure 70. Gradual migration of the heptane pan fire to the rear of the test enclosure. The dashed line indicates the corner of the pan

As shown in Figure 71, contrary to the heptanes fire, enhanced burning of the denatured alcohol pan fire in the center of the enclosure did not occur with a slit vent. Both visually as well as from a measured heat release rate, no differences were observed. Thermal conditions within the enclosure are presented in Figure 72 and Figure 73. Based on data from these figures, an average upper layer interface depth of 0.9 m (3 ft) was established approximately two minutes after ignition. As shown in Figure 72, average upper layer temperatures remained between 350–550°C (662–1022°F) for the duration of the test. Heat fluxes at the floor during this test remained less than 2 kW/m². No exterior flaming or flaming in the upper layer was observed. The flame plume remained above the fuel surface for the duration of the test.

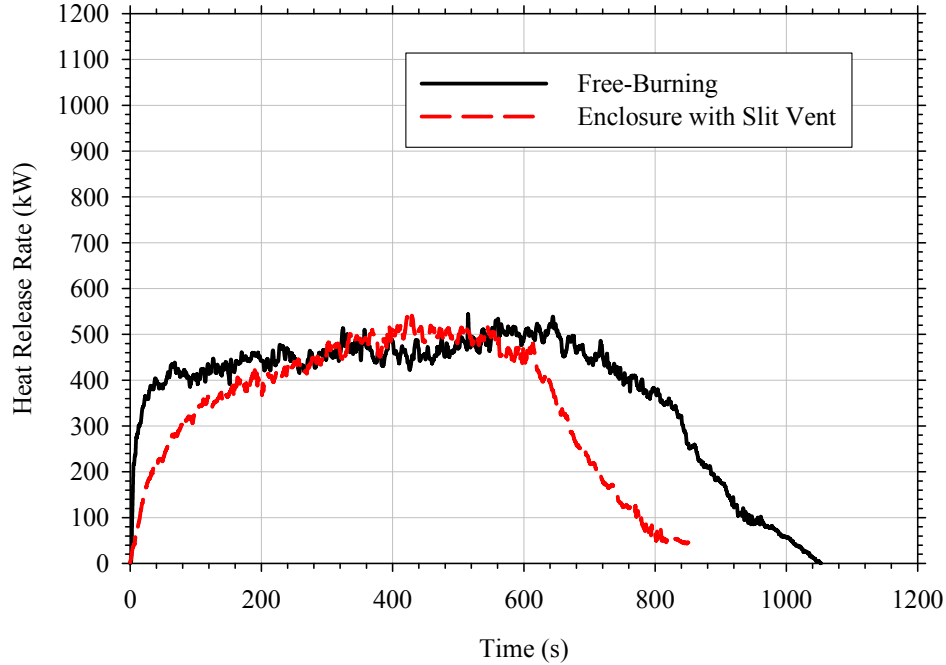


Figure 71. Measured heat release rate from denatured alcohol pan fire burning in center of enclosure with slit vent compared to open burning fire.

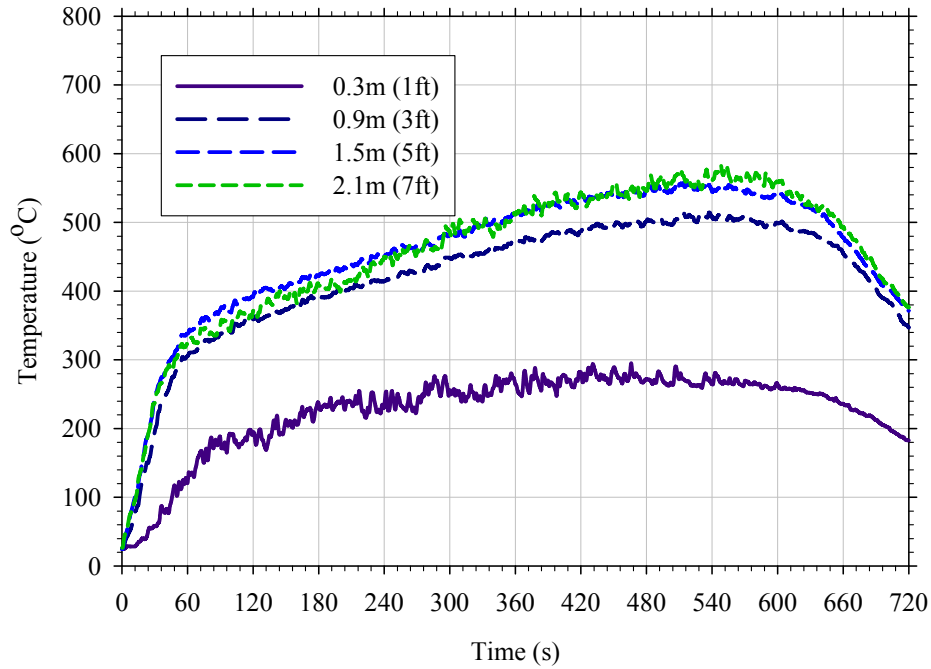


Figure 72. Enclosure temperatures during denatured alcohol pan fire burning in center of enclosure with slit vent.

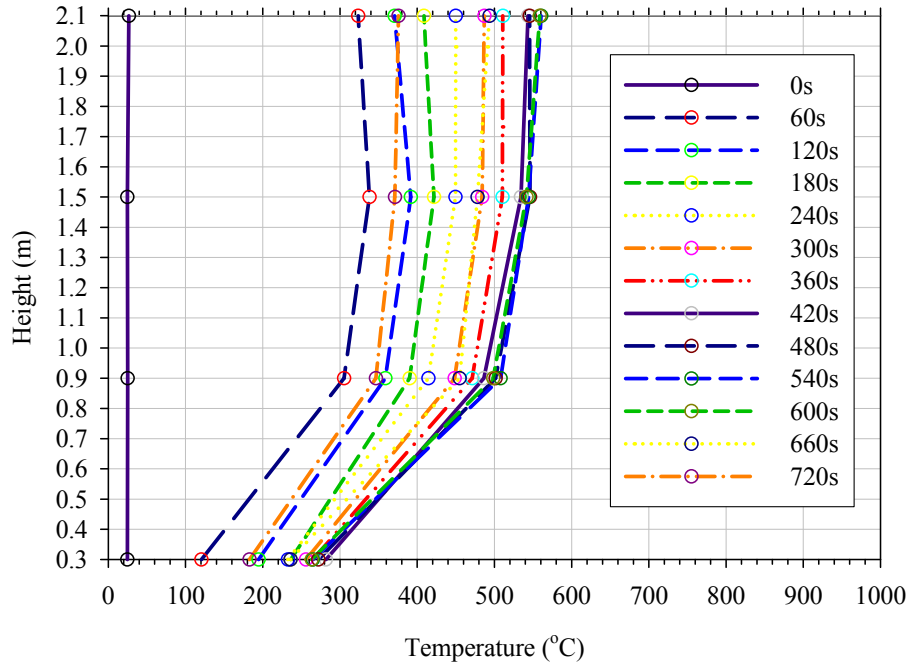


Figure 73. Thermal gradients at 1-minute intervals for denatured alcohol pan fire burning in corner of enclosure with slit vent.

5.6 Test Series 6 – Class A Fires in an Enclosure

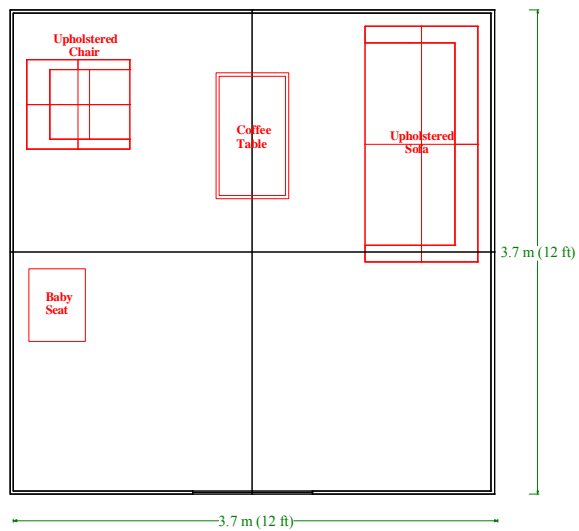
The burning dynamics of Class A fuels installed within the test enclosure were characterized in Test Series 6. A summary of the Class A enclosure fires, with and without accelerants, is provided in Table 11. Both Class A and liquid fuel ignition scenarios were explored. The Class A furnishings used in these tests were identical to those used in previous test programs [Mealy et al. 2006, Wolfe et al. 2009]. The Class A fuel items were installed as shown in Figure 74. The first test in this series was ignited using a small (<10 kW) Class A ignition source (described in Section 5.3.1). As shown in Figure 75, the ignition source was placed in the center rear of the seat of the upholstered sofa.

The remainder of the tests conducted in this test series were ignited using a 2.0 L (0.26 gal) gasoline spill fire. In half of the tests, the entire 2.0 L (0.52 gal) of fuel was spilled directly onto the floor as shown in Figure 76. In the remaining four tests, 1.5 L (0.40 gal) of gasoline was spilled onto the upholstered chair and 0.5 L (0.12 gal) was used to create a trailer leading from the foot of the upholstered chair to the doorway. A photograph of this fuel spill scenario is provided in Figure 77.

Table 11. Summary of Class A enclosure fire tests.

Test ID	Ventilation Scenario	Flooring Type	Ignition Scenario	Peak HRR (MW)	Time to Peak HRR (s)	Avg. Upper Layer Temperature (°C [°F])	Time to Exterior Flaming (s)	Test Duration (s)
6-0	Full Door	Carpet	Class A	6.1	429	800 [1472]	408	755
6-1	Full Door		Fuel Spill on Floor	6.3	218	655 [1211]	192	260
6-2	Slit Vent			0.9	272	415 [779]	N/A	480
6-3	Full Door		Fuel Spill on Upholstered Chair	7.2	158	715 [1319]	120	264
6-4	Slit Vent			1.8	723	500 [932]	270*	713
6-5	Full Door	Vinyl	Fuel Spill on Floor	5.0	64	755 [1391]	59	186
6-6	Slit Vent			1.1	221	413 [775]	N/A	506
6-7	Full Door		Fuel Spill on Upholstered Chair	3.7	121	715 [1319]	115	190
6-8	Slit Vent			0.9	139	605 [1121]	N/A	566

*Intermittent exterior flaming observed during test.



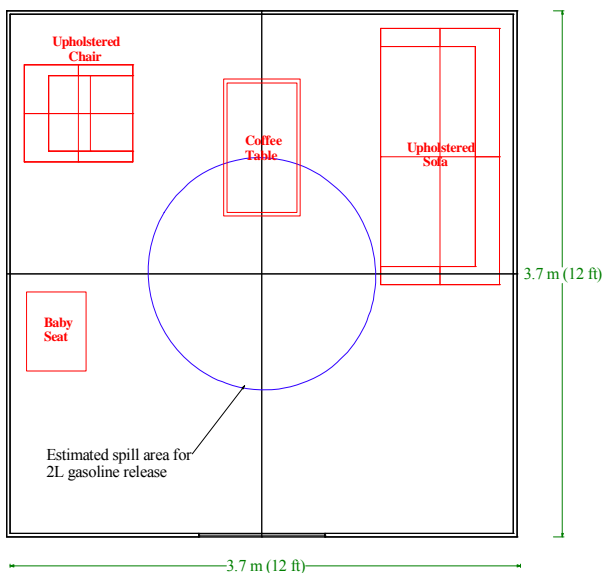
(a)

(b)

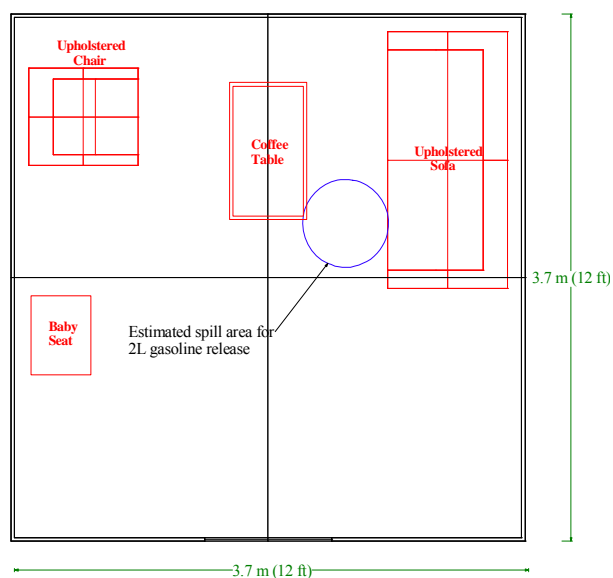
Figure 74. (a) Class A fire test layout and (b) photograph of Class A fuels from the doorway of the enclosure.



Figure 75. Class A ignition source on upholstered sofa.



(a) Vinyl Spill Scenario with unconfined gasoline spill fire.



(b) Carpet Spill Scenario, photograph from Test 6-1.

Figure 76. Target spill area and Class A material locations within test enclosure (left) and representative photograph of the spill fire when initially ignited (right).



Figure 77. Gasoline spill on seat of upholstered chair (left) and trailer leading from front of chair to doorway (right).

After ignition, the enclosure fire was permitted to grow and burn naturally. The ventilation scheme remained fixed during each test. The duration of the tests varied based on a variety of parameters. With the exception of the first test, tests involving full-door ventilation were permitted to burn for an additional 60–120 seconds after the doorway plume was ignited (i.e., exterior flaming at the vent opening). The first test was allowed to burn for 300 seconds (5 min.) after ignition of the doorway plume. For tests involving the slit ventilation scenario, the fires were permitted to burn for between 8–12 minutes. The decision to suppress these limited ventilation scenarios was primarily based on the development of the thermal conditions within the enclosure. Once relatively steady-state conditions were achieved within the enclosure an additional 6–10 minutes of data were collected.

5.6.1 Class A Ignition Scenario

Test scenario 6-0 was a fully furnished, carpeted room with a full-open doorway. The first item ignited in this test was the upholstered sofa with a Class A source on top of the sofa. Approximately 438 seconds (7 minutes 18 seconds) after ignition of the source, the upholstered sofa became involved (ignited). The point at which the sofa ignited was considered as time zero in the synopsis of the test provided below.

Burn-through of the sofa was observed 185 seconds (3 minutes 5 seconds) after the sofa was ignited. As a result of this burn-through, flames were observed both on top of and beneath the sofa. Over the next two minutes, the fire spread across the seat of the sofa and beneath the sofa on the carpet. Gradually, the entire sofa was involved and produced an upper layer within the space that was approximately 1.2 m (4 ft) deep. Six minutes after ignition of the sofa, the upper layer within the room reached floor level; at this point, there was still no flame extension out of

the doorway until approximately seven minutes. Flame extension out of the doorway continued for 335 seconds (5 minutes 35 seconds) until manual suppression was initiated. Suppression was achieved using a 2.5 in. manual hose line. The progression of fire in this test is illustrated in Figure 78.

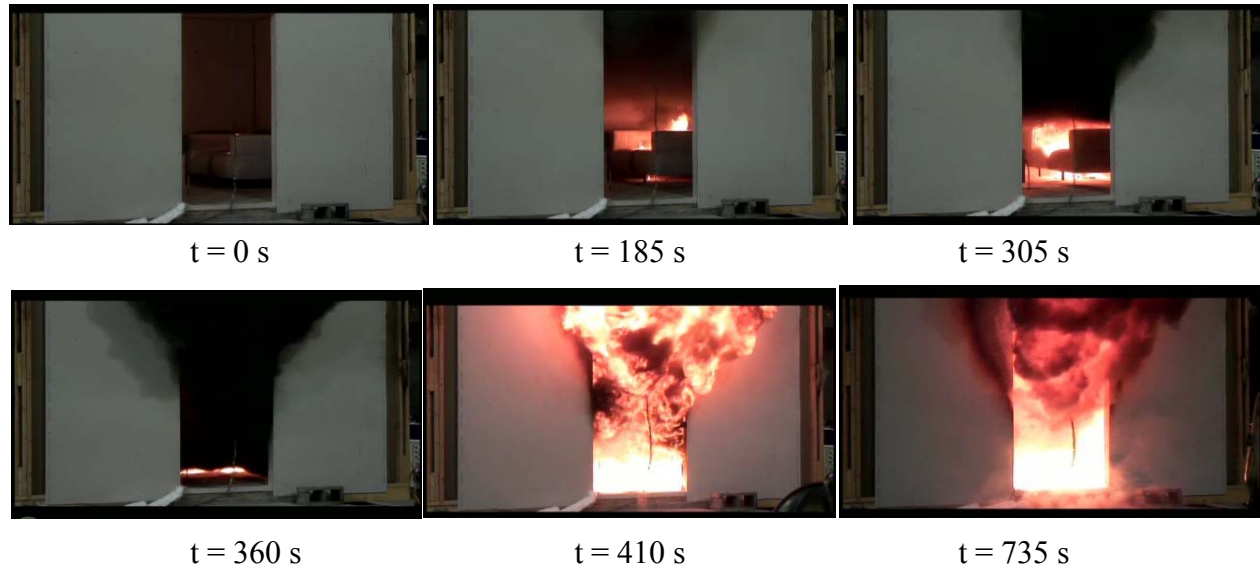


Figure 78. Fire progression observed in Test 6-0 for fully furnished, carpeted room with a full-open doorway. Sofa ignited by Class A source on top of seat.

A summary of the heat release rate from the enclosure fire is presented in Figure 79. The peak heat release measured in this test was 6.1 MW. The heat release rate grew exponentially at two different points during the test. The first occurred over the course of 40 seconds between 300–340 seconds and was attributed to the complete involvement of the upholstered sofa and initial involvement of neighboring contents of the room burning within the enclosure. The second period of rapid growth occurred over the course of 11 seconds between 408–419 seconds and was attributed to the ignition of the door plume resulting in flames extending from the enclosure vent.

The total heat released was 1.35 GJ over the 755 seconds (12 minute 35 second) burning duration. In that time, the contents of the test enclosure lost approximately 168.5 kg (371.5 lbs), or seventy percent of the original mass. A breakdown of the total mass loss from each of the combustibles within the enclosure is provided in Table 12.

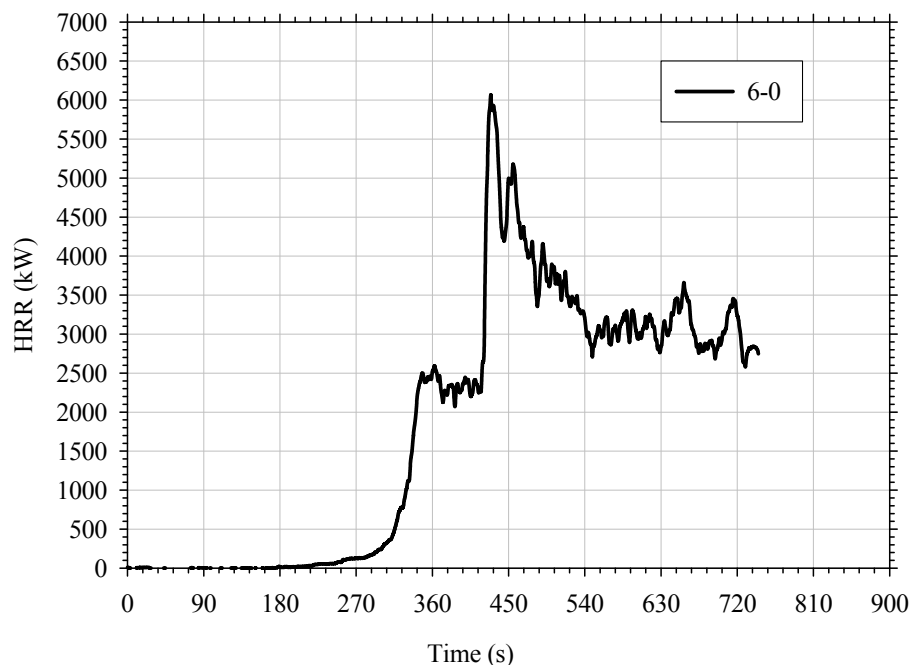


Figure 79. Heat release rate from Test 6-0.

Table 12. Summary of mass loss of combustibles within Test 6-0.

Item	Total Mass Loss (kg [lbs])	Mass Loss Fraction
Upholstered Sofa	31.9 [70.3]	0.69
Upholstered Chair	5.8 [12.8]	0.54
Table	9.1 [20.1]	0.83
Baby Seat	5.2 [11.5]	0.84
Flooring Material	116.6 [257.1]	0.69
Total	168.5 [371.5]	0.70

The average temperature (i.e., front and rear) measured at four elevations is presented in Figure 80. The average temperature gradient over the height of the test enclosure at five different times is presented in Figure 81. As shown in Figure 80, shortly after the involvement of the upholstered sofa around 270 seconds after ignition, average enclosure upper layer temperature increased rapidly reaching temperature greater than 600°C (1112°F) at elevations as low as 0.9 m (3 ft). Layer temperatures gradually increased from this point forward in the test, eventually reaching maximum temperatures as high as 1050°C (1922°F) at the 2.1 m (7 ft) elevation and 800°C (1472°F) at the 0.3 m (1 ft) elevation. The thermal gradients presented in Figure 81 illustrate the fact that approximately 360 seconds after ignition; the enclosure became a relatively well-mixed, uniform temperature space.

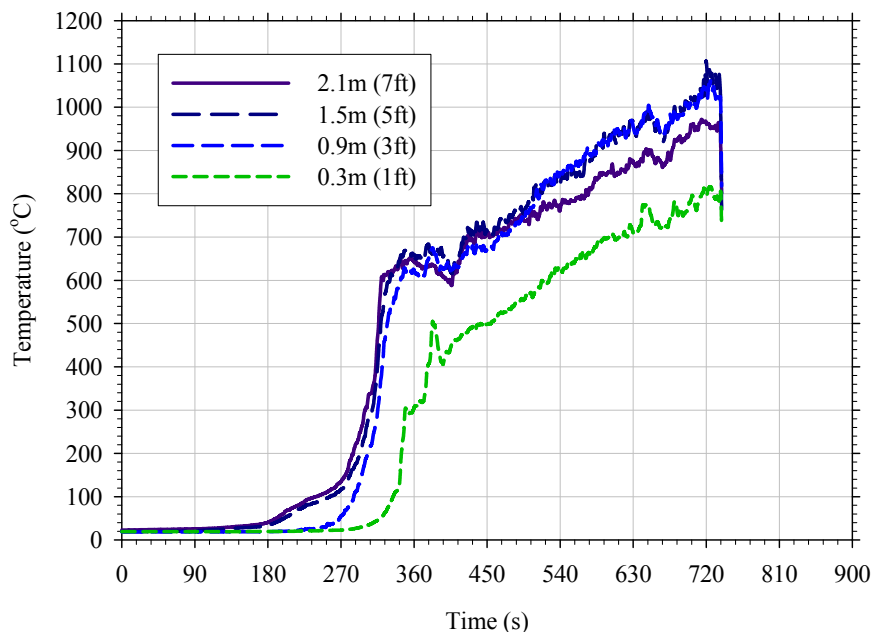


Figure 80. Average temperature measured at four elevations in Test 6-0.

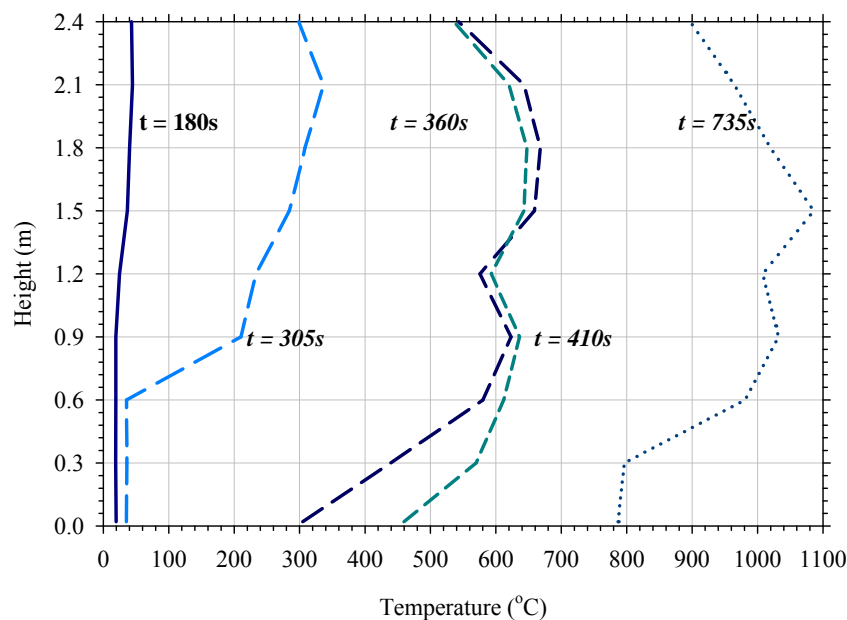


Figure 81. Temperature gradients measured in Test 6-0.

Heat flux measurements were collected at five locations, three wall and two floor locations during this test. The data collected at the wall and floor locations are presented in Figure 82 and Figure 83, respectively. The heat flux to the rear wall increases sharply at approximately 330 seconds with values at the 1.8 m (6 ft) increasing first and lower levels following shortly thereafter. This increase corresponds to the rise in HRR, but then plateaus around 360 seconds due to the thick black, vitiated smoke layer that descends toward the floor (see photo in Figure 78) temporarily suppressing the fire. This vitiation of the fire reduces fluxes to the rear wall of the enclosure over the following 90 s (i.e., 360–450 seconds after ignition). After this period of decay, fluxes to the

wall again increased eventually reaching fluxes between 170–200 kW/m². However, as materials continue to heat and additional materials become involved, floor level heat fluxes continuously increase exceeding 20 kW/m², 346 seconds after ignition and reaching peak values of 70 kW/m². This increase in floor level heat flux corresponds to a distinct rise in lower layer gas temperatures (Figure 80). The brief increase in heat flux measured in the rear corner of the enclosure at approximately 380 seconds (6 minutes 20 seconds) is most likely due to the radiant ignition of the upholstered chair located in this corner.

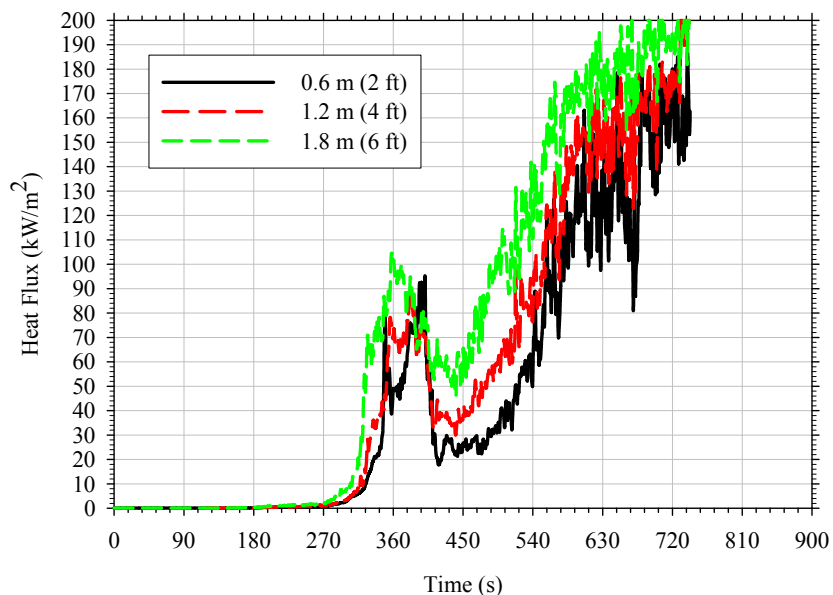


Figure 82. Heat flux on rear wall of enclosure opposite doorway in Test 6-0.

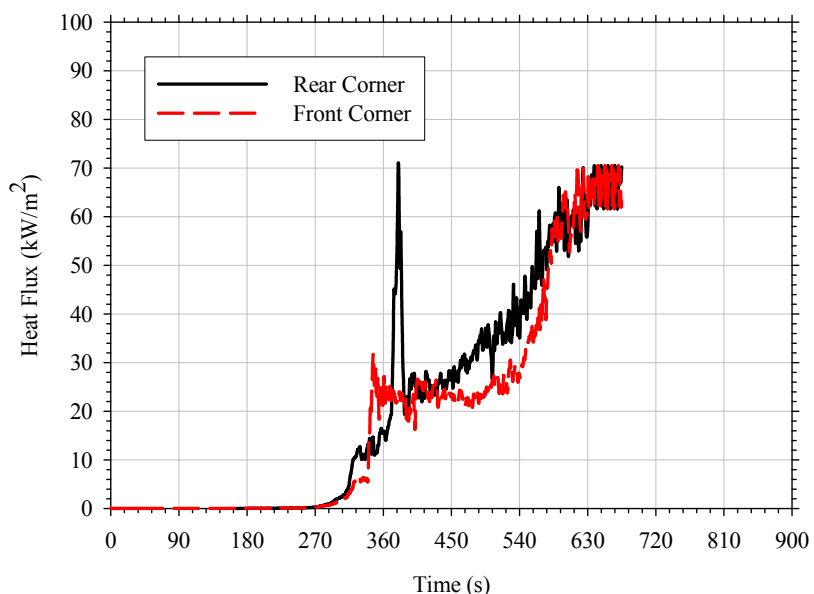


Figure 83. Average heat flux measured at floor in Test 6-0.

The gas species measured during the test are presented in Figure 84 and Figure 85. Although two point measurements were collected during the test, only the lower layer measurements were

reported for the entire test duration. Upper layer measurements were only reported for the initial 422 seconds (7 minutes 2 seconds) of this test because flow to the upper layer gas train was obstructed resulting in erroneous data. Gas species concentrations in the upper layer of the enclosure began to fall four minutes after ignition, which corresponds with the initial fire growth shown in Figure 79. Changes in lower layer species concentrations did not occur until approximately 7 minutes after ignition, at which point oxygen decreased rapidly to values below 0.06. At the same time, carbon dioxide value increased dramatically (i.e., greater than 0.12). Carbon monoxide concentrations initially increased to concentrations of approximately 0.04 mol/mol but decreased to values of less than 0.02 after approximately 90 seconds and remained at these values for the remainder of the fire.

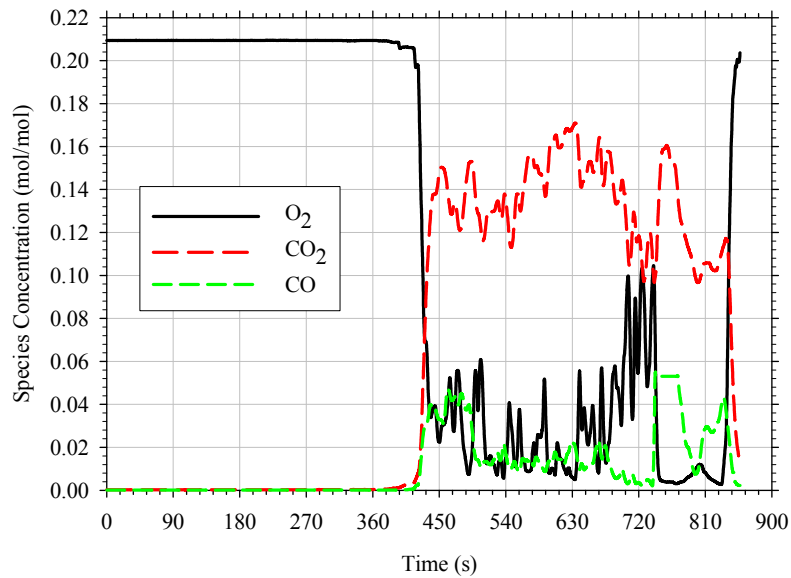


Figure 84. Gas concentrations measured 0.45 m (18 in.) above the floor in Test 6-0.

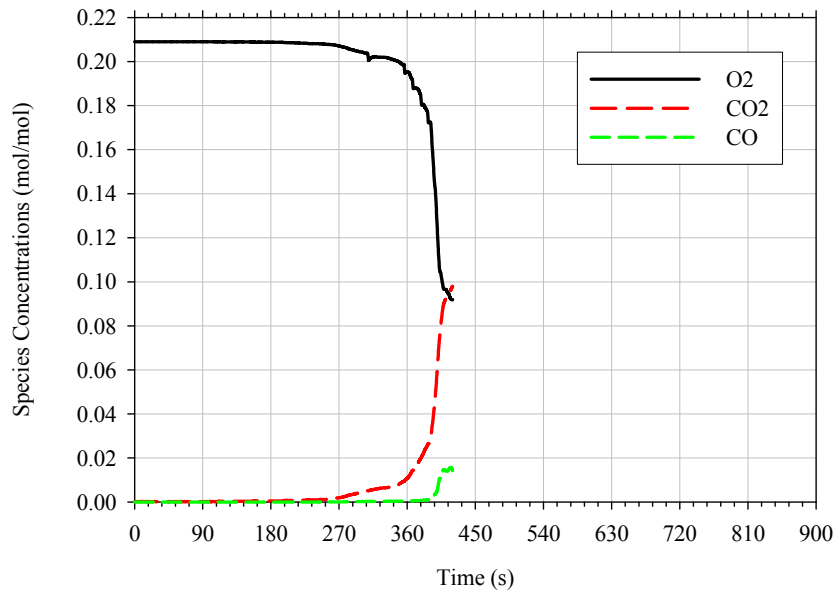


Figure 85. Gas concentrations measured 0.45 m (18 in.) below the ceiling in Test 6-0.

5.6.2 Gasoline on Carpet Floor with Full Door Opening

Test scenario 6-1 was a fully furnished, carpeted room with a full-open doorway. The first item ignited in this test was the upholstered sofa. The ignition scenario was the 2.0 L (0.53 gal) gasoline spill fire located on the carpet between the upholstered sofa and coffee table as described in Section 5.6. As shown in Figure 86, a spill area of approximately 0.14 m² (1.5 ft²) was created. Approximately 20 seconds after ignition of the gasoline spill, the upholstered sofa became involved, considered as time zero.



Figure 86. Test 6-1 2.0 L (0.53 gal) gasoline spill fire ignition scenario.

The progression of fire in this test is illustrated in Figure 87. The gasoline spill fire ignited the front center portion of the sofa leg rest. The fire gradually spread up and across the seat of the sofa. Forty-five seconds after the sofa was ignited, the layer interface depth descended to 1.2 m (4 ft). At this time, the fire began to migrate to the rear of the enclosure. As the sofa fire grew and spread to adjacent combustibles, the upper layer descended to the floor of the enclosure 128 seconds (2 minutes 8 seconds) after ignition of the sofa. The filling smoke layer within the enclosure resulted in the entire door vent filling with escaping effluent. This type of venting was observed for approximately one minute before ignition of the door plume occurred at 192 seconds. After ignition of the door plume, the fire burned for an additional 67 seconds (1 minute 7 seconds) before manual suppression was initiated. Firefighters suppressing the fire were instructed to use a minimal amount of water to extinguish the fire and to the extent possible not directly impact the walls of the test enclosure. These procedures were adopted for all tests and were primarily done to preserve forensic data being collected for pattern analysis.

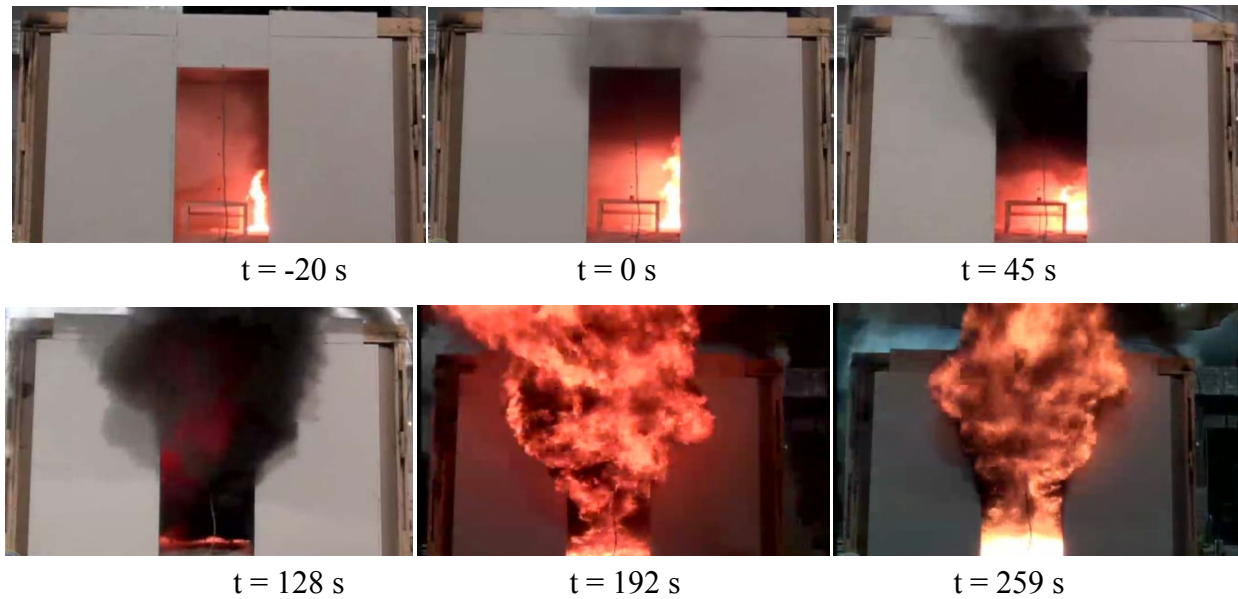


Figure 87. Fire progression observed in Test 6-1.

A plot of the heat release rate from the enclosure fire is presented in Figure 88. The peak heat release was 6.3 MW. It grew exponentially at two different points in time during the test. The first period occurred over the course of 100 seconds between 40–140 seconds and was attributed to the complete involvement of the upholstered sofa as well as the involvement of neighboring combustibles within the enclosure. The fire flashed over around the 140 second time frame as evidenced by the temperature and heat flux measurements discussed below. The second period of measured fire growth (as measured by the heat release rate external to the enclosure) occurred over the course of 20 seconds between 193–213 seconds and was attributed to the ignition and combustion of the unburned effluent escaping from the test enclosure through the door vent. This ignition resulted in flames extending from the enclosure vent. The total heat released was 699 MJ over the 260 second (4 minute 20 second) burning duration. In that time, the contents of the test enclosure lost approximately 70.5 kg (155 lbs), or twenty-seven percent of their original mass. A further breakdown of the total mass loss from each of the combustibles within the enclosure is provided in Table 13.

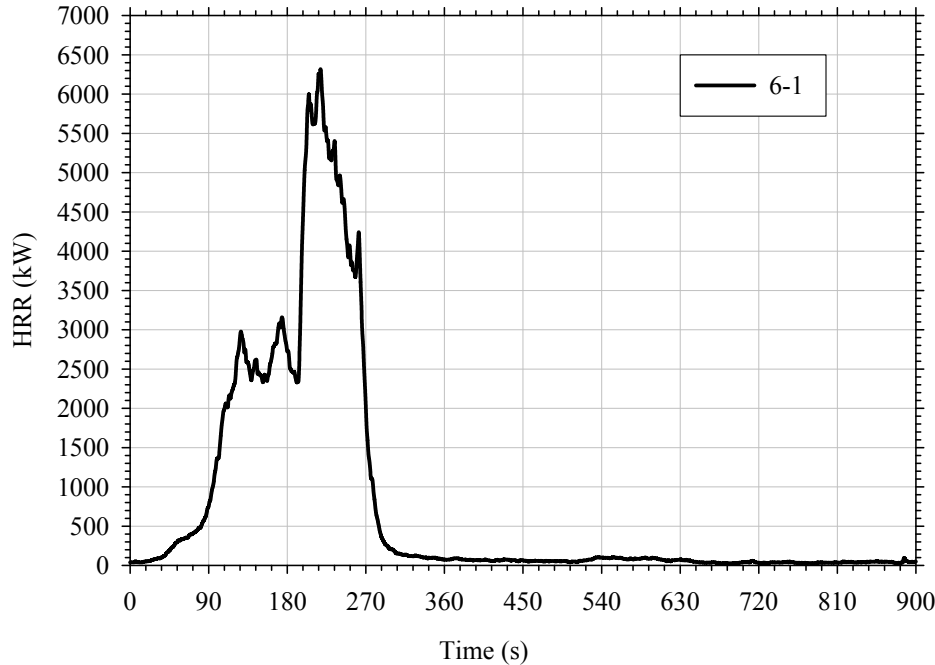


Figure 88. Heat release rate from Test 6-1.

Table 13. Summary of mass loss of combustibles within Test 6-1.

Item	Total Mass Loss (kg [lbs])	Mass Loss Fraction
Upholstered Sofa	12.8 [28.2]	0.28
Upholstered Chair	2.8 [6.2]	0.27
Table	6.6 [14.6]	0.42
Baby Seat	1.1 [2.4]	0.18
Flooring Material	47.2 [104]	0.28
Total	70.5 [155]	0.27

The average temperature measured at four elevations, from the two-thermocouple tree locations, is presented in Figure 89. The average temperature gradient over the height of the test enclosure for the duration of the test is presented in Figure 90. A result of the gasoline spill ignition scenario was that average enclosure temperature increased soon after ignition and did so relatively rapidly. As shown in Figure 89, upper layer temperature rose from ambient conditions to 600–700°C (1112–1292°F) within the first two minutes of the test with an average upper layer temperature of 600°C (1112°F) being reached 119 seconds after ignition. It should be noted that lower layer gas temperatures increased dramatically around this same time in the test. It should also be noted that approximately 150 seconds after ignition, gas temperatures at both the 0.9 (3 ft) and 1.5 m (5 ft) were greater than those measured at higher elevations within the enclosure. Although not visually observable, this change in thermal gradient within the enclosure was due to layer burning effects as a result of the flame extension from the enclosure vent. This change is evident in Figure 90 for times greater than 150 seconds.

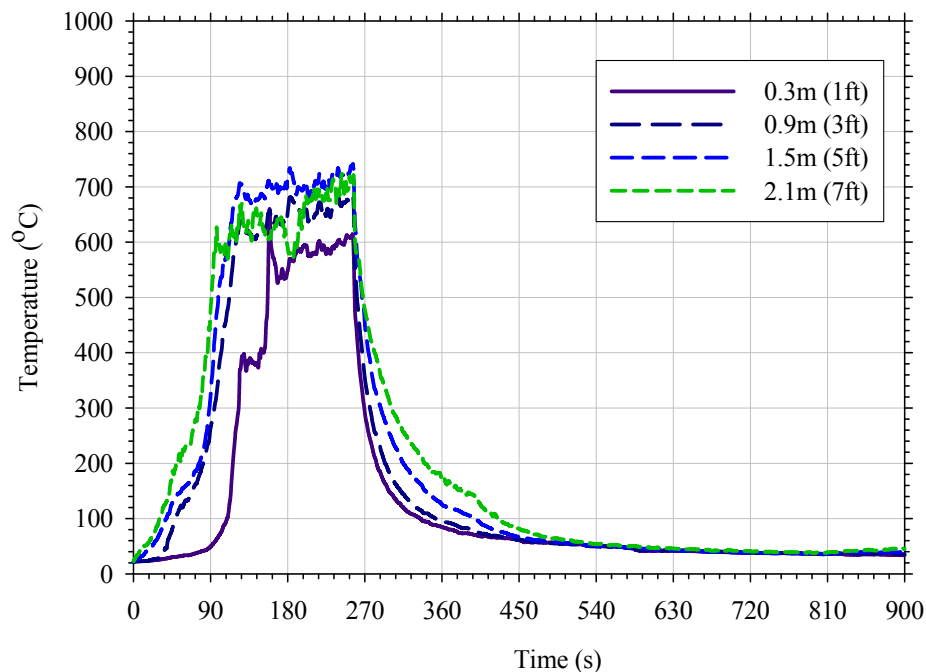


Figure 89. Average temperature measured at four elevations in Test 6-1.

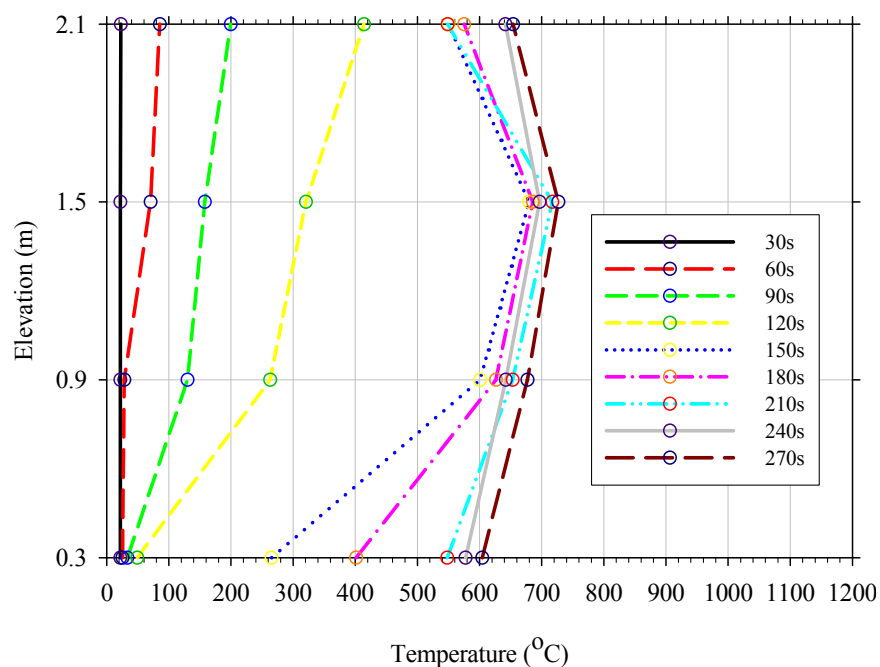


Figure 90. Average temperature gradients measured during Test 6-1.

Heat flux was collected at five locations, three wall and two floor locations. The data collected at the wall and floor locations are presented in Figure 91 and Figure 92, respectively. Heat fluxes to the rear wall of the enclosure began to increase shortly after ignition due to the migration of the initiating fire to the rear of the enclosure. This migration is attributed to the flow dynamics within the space due to the ventilation opening airflows toward the back. Incident heat

fluxes to the rear wall of the enclosure remained around 5 kW/m^2 during the initial minute of burning and then gradually began to increase as the fire on the upholstered sofa and the fire on the carpet flooring began to grow. This initial period of increasing heat flux to the rear wall peaked with values ranging from $60\text{--}130 \text{ kW/m}^2$ approximately 120 seconds after ignition. After a short period of decay, the heat flux measurements at 0.6 m (2 ft) and 1.2 m (4 ft) rapidly increased to 100 kW/m^2 before returning to relatively steady-state fluxes of 20 and 40 kW/m^2 for the duration of the test. The brief increase in lower level heat flux at approximately 140 seconds ($2 \text{ minutes } 20 \text{ seconds}$) corresponds to some flaming in the layer that was observed during review of test video from this location.

The two measured floor heat fluxes in this test were very comparable, growing at a similar rate and reaching a steady-state value of approximately 30 kW/m^2 . The heat flux trace for the gauge located in the front of the enclosure showed a brief spike in flux at approximately 140 seconds ($2 \text{ minutes } 20 \text{ seconds}$). Again, this spike corresponds to the observation of intermittent flaming in the upper layer of the enclosure.

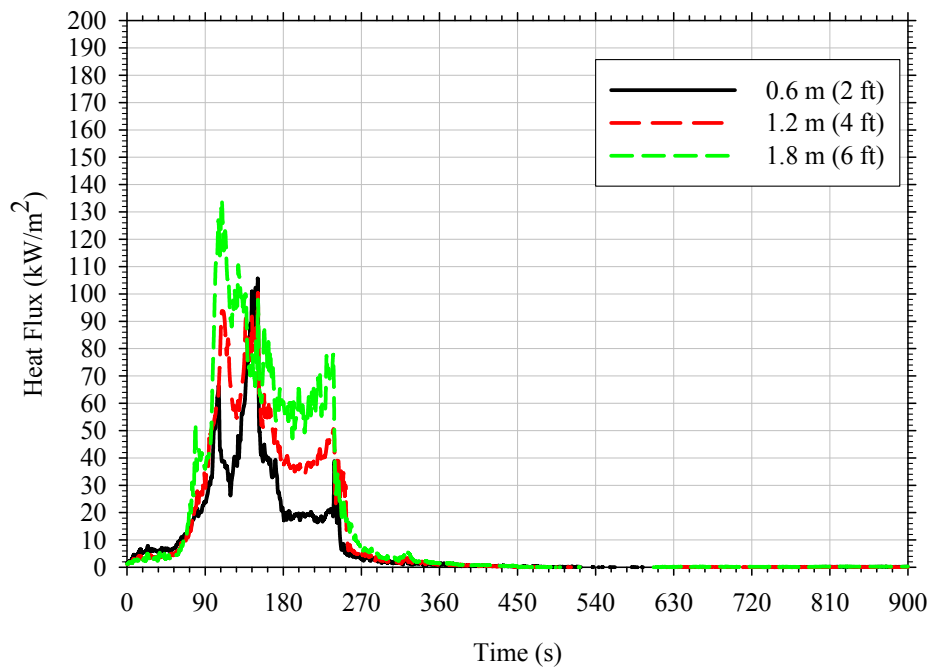


Figure 91. Heat flux on rear wall of enclosure opposite doorway.

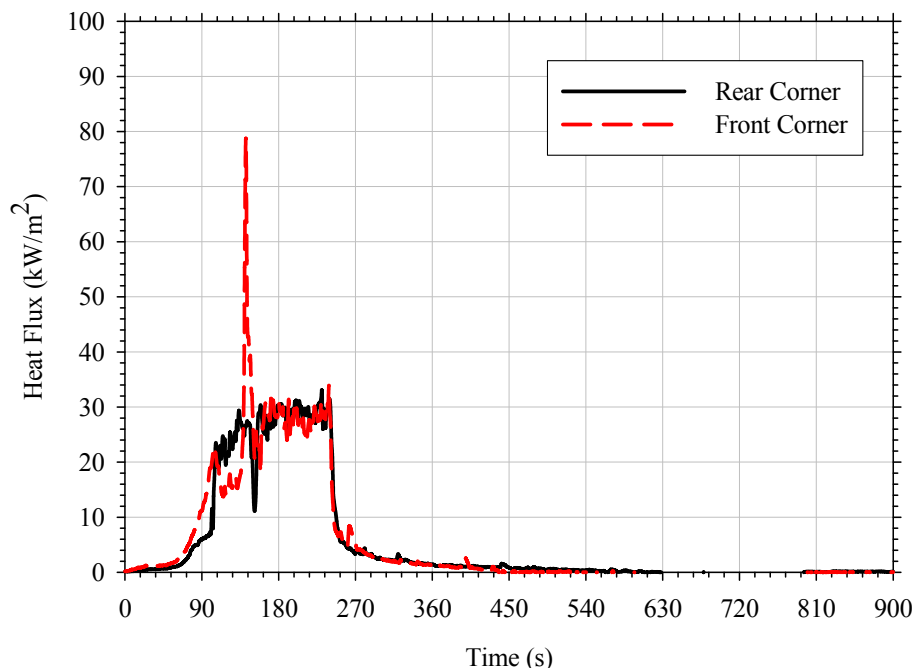


Figure 92. Average heat flux measured at floor in Test 6-1.

The gas species measured low and high in the enclosure are presented in Figure 93 and Figure 94, respectively. In this test, upper layer gas concentrations decreased rapidly reaching concentrations less than 0.02 mol/mol within the first two minutes. Carbon dioxide and carbon monoxide concentrations reaching average values of 0.15 mol/mol and 0.04 mol/mol, respectively between 120–240 seconds. The two periods of burning (i.e., interior burning and exterior burning) were more evident in the lower layer gas species concentrations. During the initial stage of burning, oxygen decreased while carbon dioxide and carbon monoxide increased. However, when the fire transitioned to burning on the exterior of the vent, these lower layer gas concentrations reversed with oxygen concentrations increasing and CO₂/CO concentrations decreasing. This reversal was attributed to the upper layer within the enclosure decreasing in depth once flaming combustion in the door plume began.

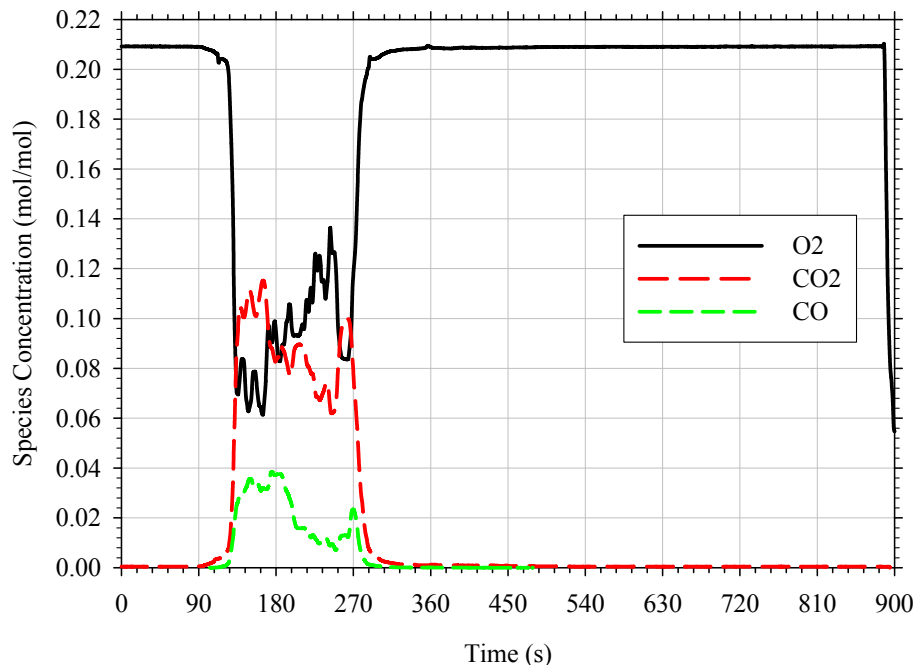


Figure 93. Gas concentrations measured 0.45 m (18 in.) above the floor in Test 6-1.

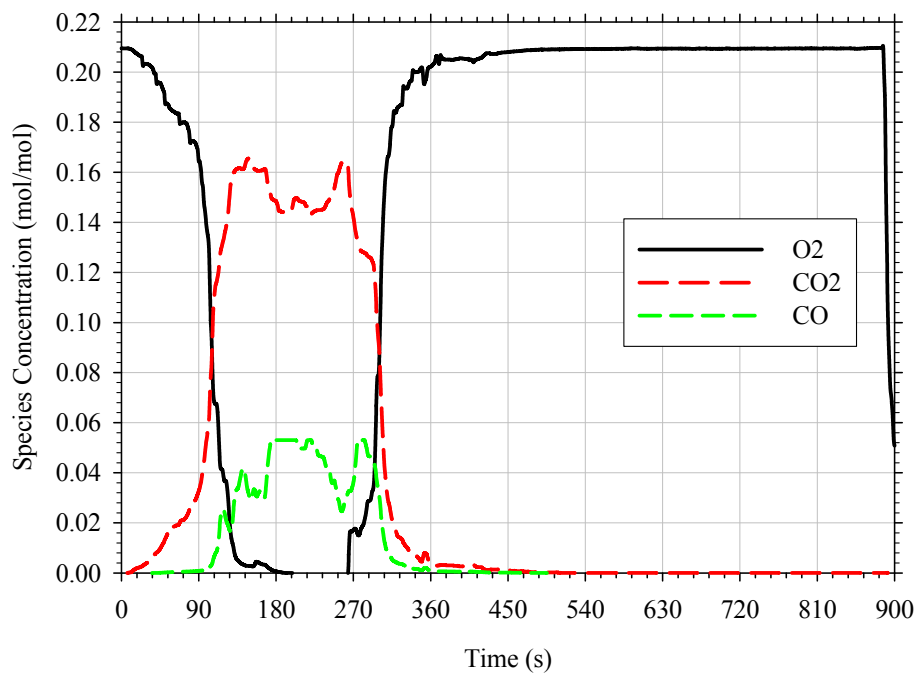


Figure 94. Gas concentrations measured 0.45 m (18 in.) below the ceiling in Test 6-1.

5.6.3 Gasoline on Carpet Floor with Slit Vent Opening

Test scenario 6-2 was a fully furnished, carpeted room with a slit vent. The upholstered sofa was ignited using the same gasoline pour ignition scenario used in Test 6-1. Approximately

25 seconds after ignition of the gasoline spill, the upholstered sofa became involved, considered as time zero.

The gasoline spill fire ignited the front leg rest and quickly grew onto the seat of the sofa. The fire gradually spread up and across the seat of the sofa. Approximately 15 seconds after the sofa was ignited, the layer interface descended to a depth of 1.2 m (4 ft). Twenty-one seconds later, the rear corner of the table was ignited. The smoke layer within the test enclosure and the slit vent reached the floor approximately two minutes after the sofa became involved. Once the room filled with smoke to floor level, the slit vent served primarily as exhaust with the majority of flow through the vent being outward flowing. This type of venting was observed for the duration of the test (i.e., 360 seconds longer). Flashover was not observed in this test. Suppression was achieved using a 2.5 in. manual hose line using the same procedures as described in Section 5.6.2. The fire was suppressed 480 seconds (8 minutes) after ignition of the sofa. Due to the deep smoke layer being present for the majority of this test, a photographic progression was only provided for the first two minutes of the test (Figure 95) after which visibility within the enclosure was lost.

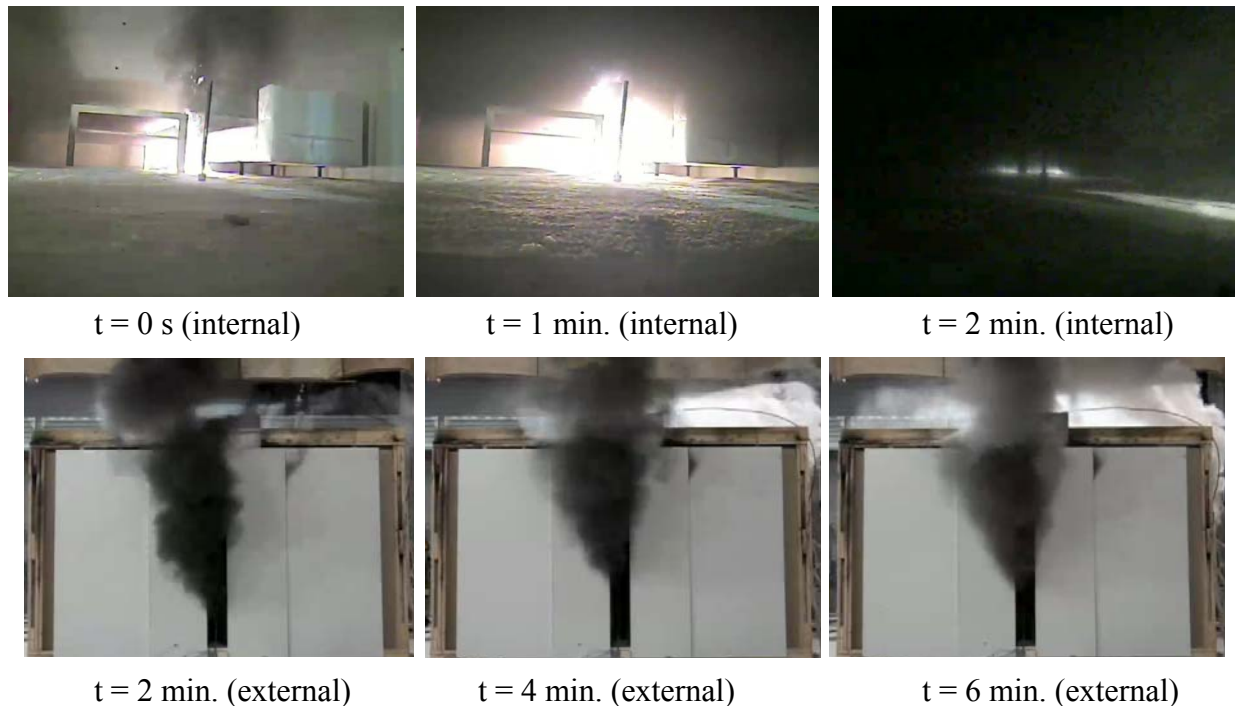


Figure 95. Fire progression observed in Test 6-2 (view from doorway).

A plot of the heat release rate from the enclosure fire is presented in Figure 96. The peak heat release was 904 kW with an average steady-state heat release rate of 761 kW. The heat release rate grew exponentially during the initial three minutes of the test and then reached a quasi-steady-state burning condition that was maintained for the duration of the test. This steady-state burning continued for approximately six minutes before manual suppression. The total heat released was 318 MJ over the 480 second (8 minute) burning duration. In this time, the contents of the test enclosure lost approximately 44.4 kg (97.9 lbs), or sixteen percent of their original

mass. A breakdown of the total mass loss from each of the combustibles within the enclosure is provided in Table 14.

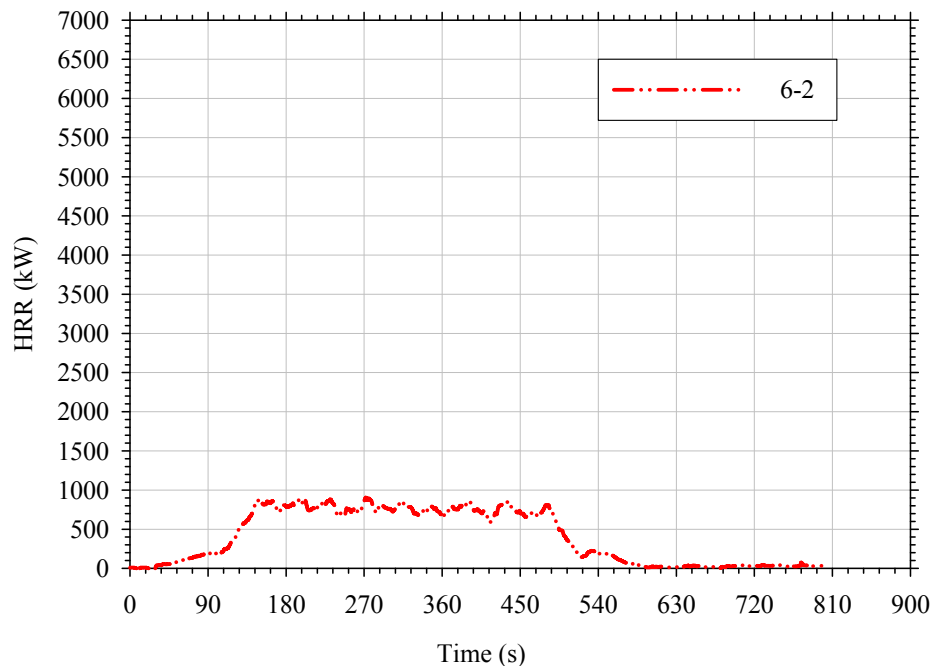


Figure 96. Heat release rate from Test 6-2.

Table 14. Summary of mass loss of combustibles within Test 6-2.

Item	Total Mass Loss (kg [lbs])	Mass Loss Fraction
Upholstered Sofa	15.0 [33.1]	0.32
Upholstered Chair	1.4 [3.1]	0.14
Table	2.5 [5.5]	0.16
Baby Seat	2.3 [5.1]	0.37
Flooring Material	23.2 [51.1]	0.14
Total	44.4 [97.9]	0.16

The average temperature measured at four elevations is presented in Figure 97. The average temperature gradient over the height of the test enclosure for the duration of the test is presented in Figure 98. As shown in Figure 97, gas temperatures within the enclosure at each elevation presented steadily increased during the initial 150 seconds of the test. After this period of increase, temperatures reached a quasi-steady-state with the exception of temperatures at the 0.3 m (1 ft) elevation. In this test, no gas temperatures exceeded 600°C (1112°F). Approximately 300 seconds after ignition, the gas temperatures at the 0.3 m (1 ft) elevation began to increase at an increased rate. Thirty seconds later, these temperatures exceeded those measured at the 0.9 m (3 ft) elevation. This increase in temperature low in the enclosure is attributed to the ignition of the carpet flooring material. The low-level burning material locally increased and changed the thermal gradient within the enclosure, as shown in Figure 98.

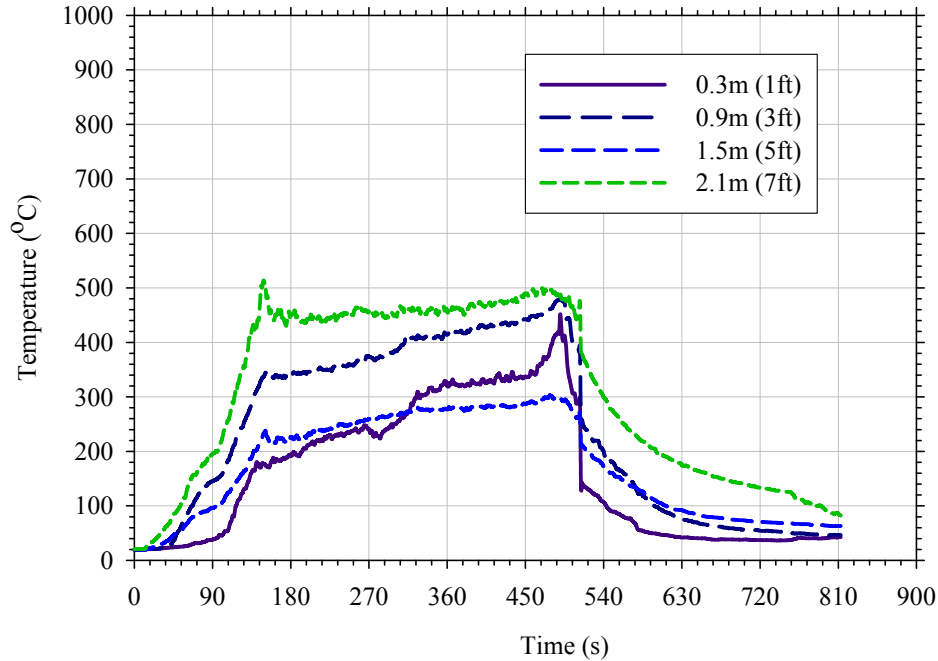


Figure 97. Average temperature measured at four elevations in Test 6-2.

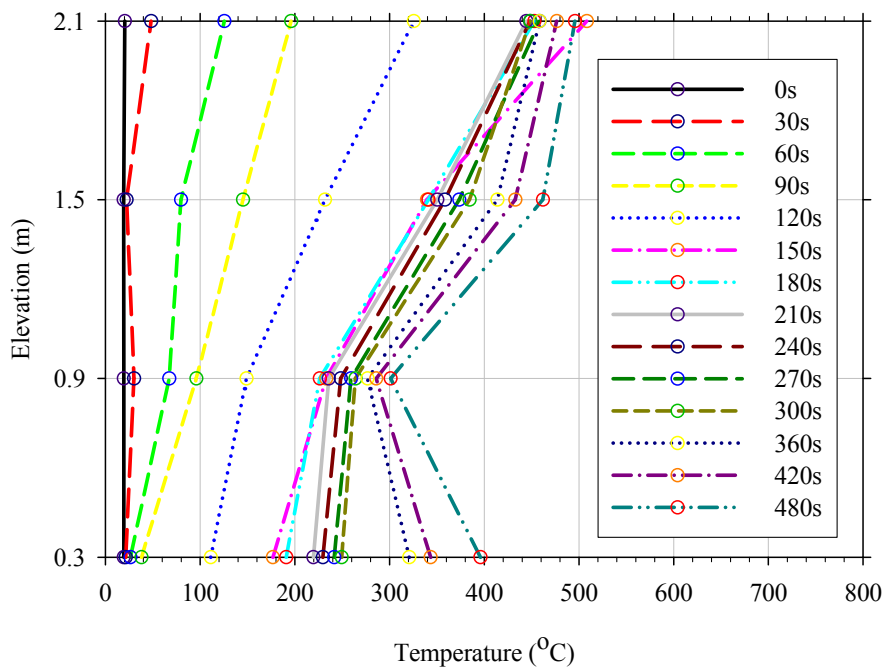


Figure 98. Average temperature gradients measured during Test 6-2.

Heat flux was collected at eight locations, six wall and two floor locations. Wall mounted heat flux transducers were located in the rear wall opposite the vent and in the sidewall perpendicular to the vent. Transducers mounted in the rear and side wall were mounted at heights of 0.6 m (2 ft), 1.2 m (4 ft), and 1.8 m (6 ft). The data collected at the wall and floor locations is presented in Figure 99, Figure 100 and Figure 101.

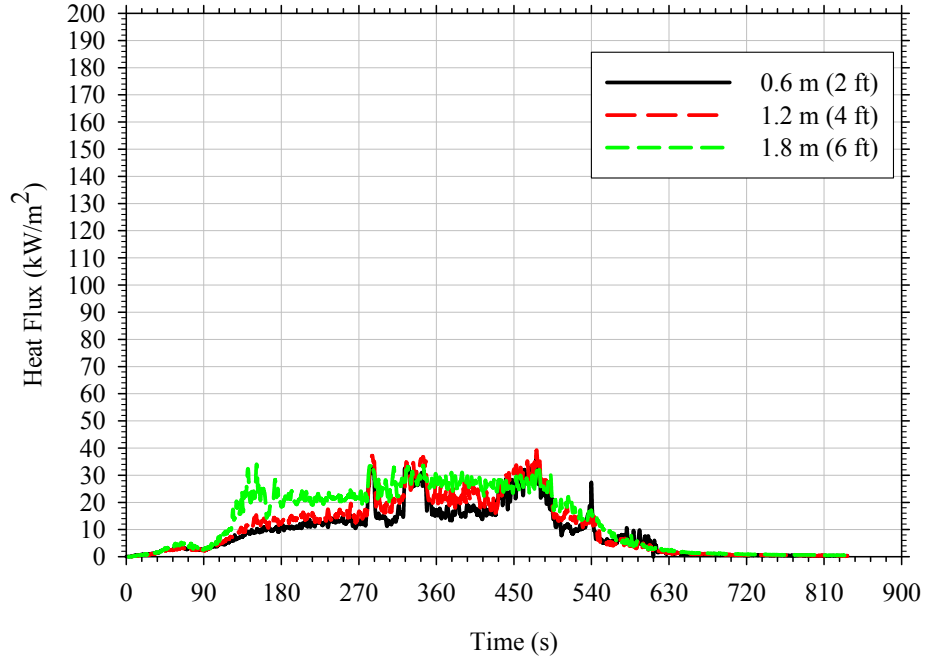


Figure 99. Heat flux on rear wall of enclosure opposite doorway in Test 6-2.

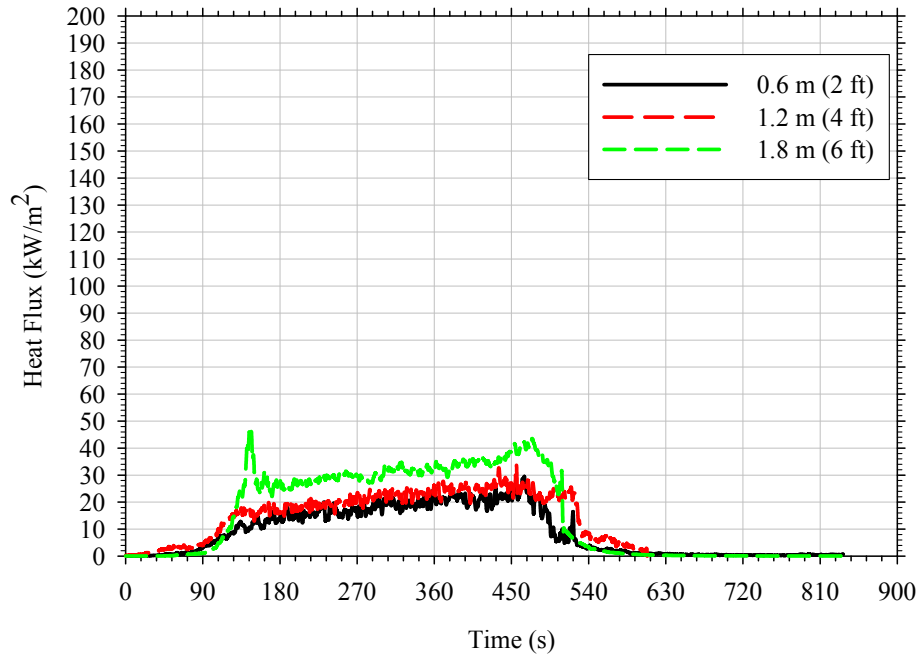


Figure 100. Heat flux on sidewall of enclosure perpendicular to vent in Test 6-2.

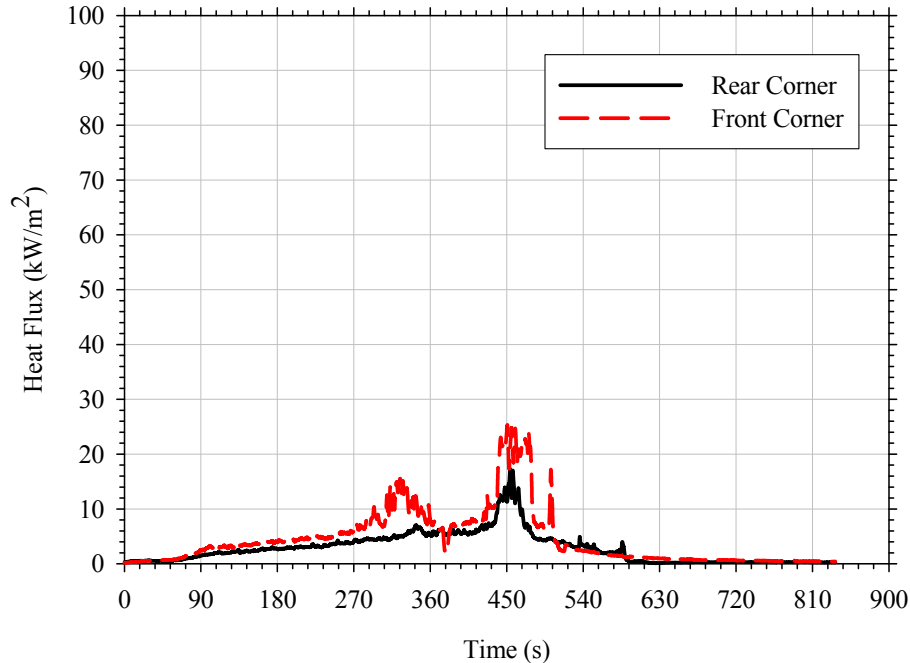


Figure 101. Heat fluxes measured at floor in Test 6-2.

Heat fluxes to the walls in this test were generally similar with no fluxes greater than 50 kW/m². Low-level heat fluxes (i.e., 0.6 and 1.2 m (2 and 4 ft) were comparable when compared against both location and elevation. The highest heat fluxes were measured at the 1.8 m (6 ft) elevation on the wall perpendicular to the wall containing the vent. They were 5–10 kW/m² greater than the fluxes to the rear wall. With the exception of approximately 60 seconds later in the test, both floor mounted heat flux gauges did not exceed 20 kW/m² in this test. Based on review of video, the elevated floor heat fluxes measured between 440–490 seconds were due to the localized burning of the flooring material and not a result of radiant heating from the upper layer.

The gas species measured low and high in the enclosure are presented in Figure 102 and Figure 103, respectively. Note that carbon monoxide levels at the 1.9 m (78 in.) elevation exceeded analyzer limits between 300–480 seconds after ignition in this test. With the exception of carbon monoxide, both upper and lower layer gas concentration measurements were relatively steady during this test. Oxygen concentrations in the lower layer and upper layer reached 0.12 mol/mol and 0.04 mol/mol (i.e., 12 and 4%), respectively, within the first three minutes of the test and remained at this level for the duration of the test. Similarly, carbon dioxide concentrations reached values of 0.08 mol/mol and 0.15 mol/mol in the lower and upper layer, respectively, and sustained at this level. Carbon monoxide concentrations did not exhibit the same behavior. In the lower layer, concentrations increased from 0.01 mol/mol to 0.04 mol/mol between 300 and 360 seconds. In the upper layer, concentrations increased from 0.02 mol/mol to values greater than 0.05 mol/mol during the same time frame. Lack of visibility during this test prevented any visual observations from being collected to explain this change.

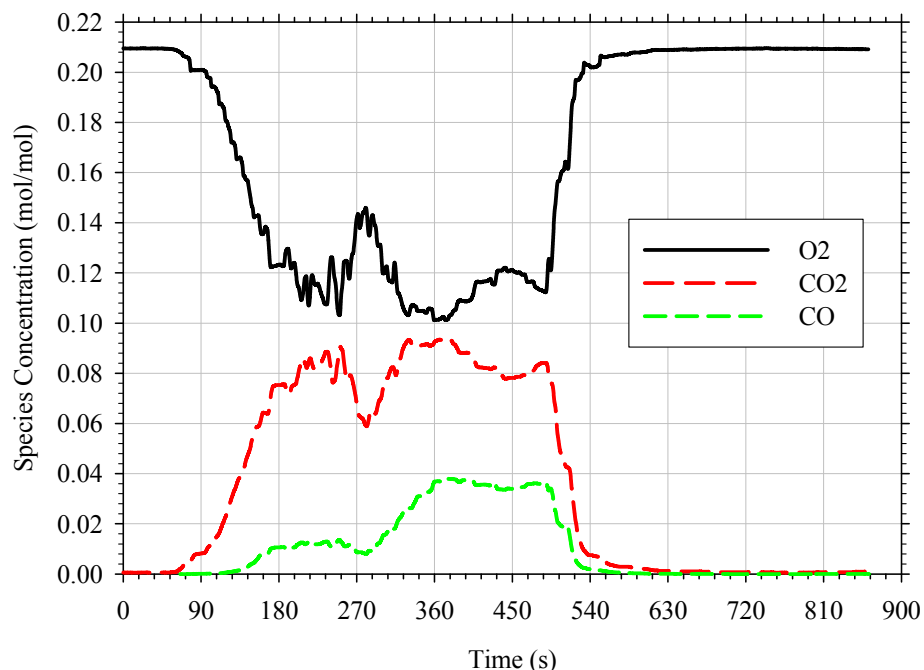


Figure 102. Gas concentrations measured 0.45 m (18 in.) above the floor in Test 6-2.

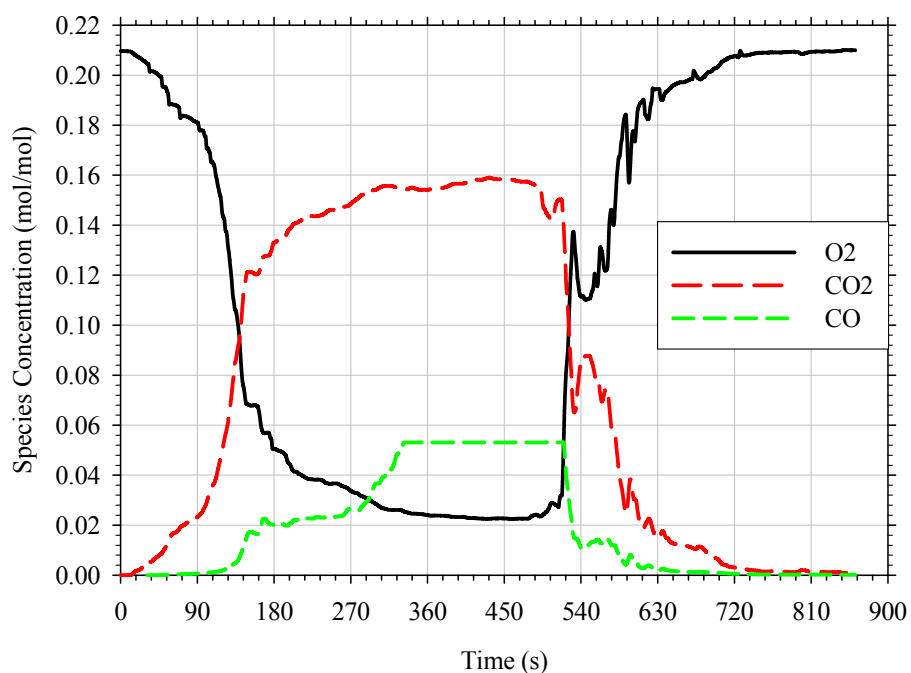


Figure 103. Gas concentrations measured 0.45 m (18 in.) below the ceiling in Test 6-2.

5.6.4 Gasoline on Upholstered Chair with Full Door Opening (w/Carpet)

Test scenario 6-3 was a fully furnished, carpeted room with a full open doorway. The upholstered chair was ignited using 1.5 L (0.40 gal) of gasoline poured on the chair and 0.5 L (0.13 gal) poured on the carpet as a trailer to the doorway. The gasoline was poured onto the seat

of the chair and allowed to run off the seat onto the floor. The fire was ignited at the end of the trailer nearest the doorway. The fire was ignited less than ten seconds after it was poured. The trailer quickly spread back to the front of the upholstered chair. The trailer burned for approximately six seconds before involving the gasoline poured onto the seat of the chair.

One minute after ignition, the corner of the coffee table nearest to the trailer fire became involved. Ignition of the top of the table occurred 45 seconds after the corner became involved. One minute and forty-seven seconds (107 s) after ignition, the contents of the room became involved and the room reached flashover conditions. Approximately 45 seconds later, two minutes 38 seconds after ignition (158 s), flame extension out of the open doorway was observed. The enclosure fire was suppressed two minutes later, four minutes 38 seconds after the start of the test (278 s). Suppression was achieved using a 2.5 in. manual hose line using the same procedures as described in Section 5.6.2. Photographs showing the evolution of this fire are presented in Figure 104.

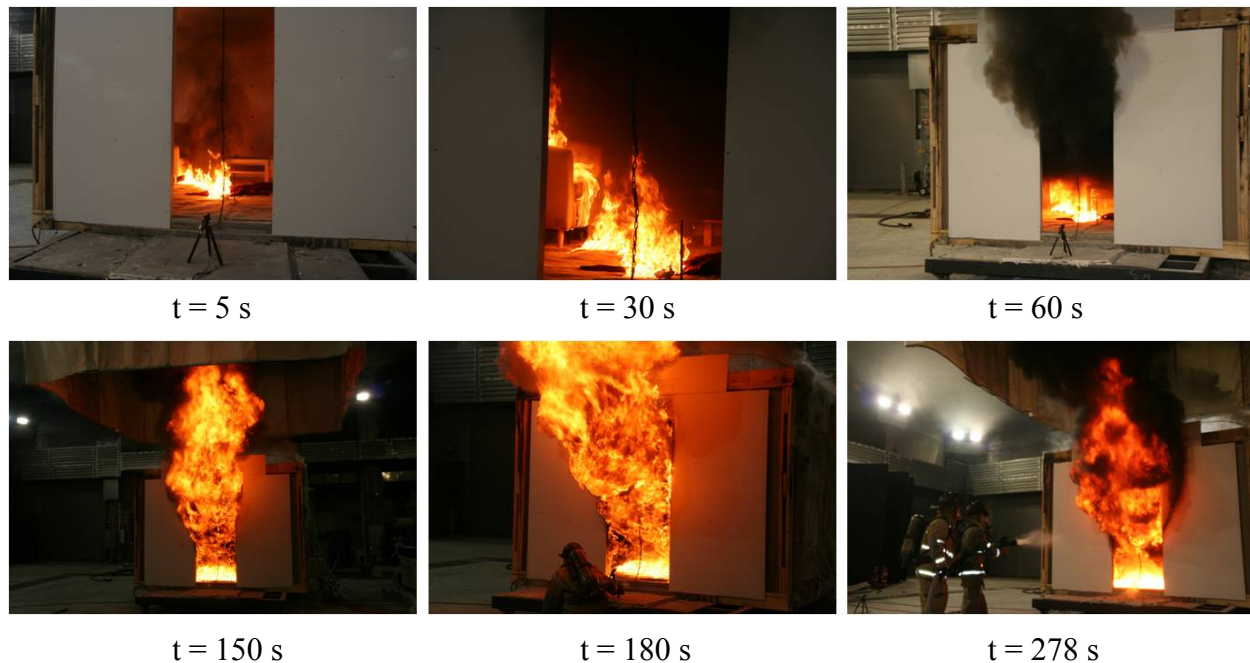


Figure 104. Fire progression in Test 6-3.

A plot of the heat release rate from the enclosure fire is presented in Figure 105. The peak heat release was 7.2 MW. During the initial 60 seconds of this test, the fire grew to approximately 600 kW. This fire growth is primarily attributed to the combustion of the gasoline spill on the upholstered chair and carpet flooring. After this initial fire growth, the fire spread to adjacent combustibles with all flaming combustion occurring within the enclosure (i.e., no flame extension from the enclosure vent). During this period of time the fire grew from approximately 600 kW to approximately 2.5 MW. Two minutes after the start of the test, the unburned combustion products exiting the enclosure were ignited and the entire door plume became involved. This event resulted in the rapid increase in heat release from 2.5–4.5 MW with a brief peak as high as 7.2 MW. After this initial peak but still during the period of time where the door plume was combusting, the average heat release rate was on the order 4.5 MW. This sustained

exterior burning lasted for approximately seventy-five seconds. The total heat released during this test was 856 MJ over the 264 seconds (4 minute 24 second) burning duration. In this time, the contents of the test enclosure lost approximately 83.2 kg (183 lbs), or thirty-two percent of their original mass. A further breakdown of the total mass loss from each of the combustibles within the enclosure is provided in Table 15.

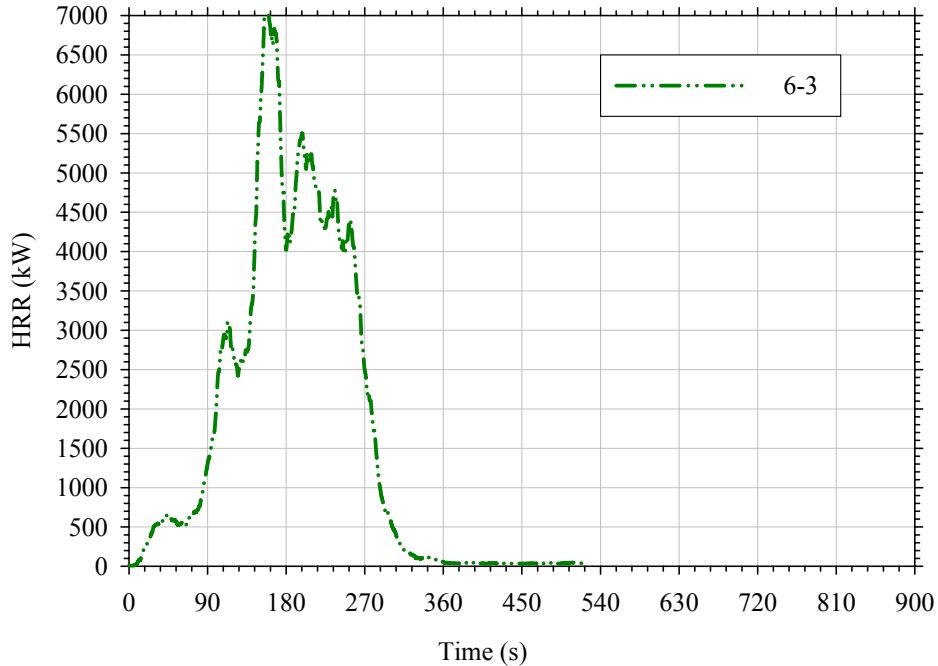


Figure 105. Heat release rate from Test 6-3.

Table 15. Summary of mass loss of combustibles within Test 6-3.

Item	Total Mass Loss (kg [lbs])	Mass Loss Fraction
Upholstered Sofa	10.8 [23.8]	0.23
Upholstered Chair	4.3 [9.5]	0.41
Table	2.5 [5.5]	0.16
Baby Seat	2.8 [6.2]	0.45
Flooring Material	62.8 [138]	0.37
Total	83.2 [183]	0.32

The average temperature measured at four elevations is presented in Figure 106. The average temperature gradient over the height of the test enclosure for the duration of the test is presented in Figure 107. Upper layer temperatures during the initial 60 seconds of fire growth reached temperatures between 200–300°C (392–572°F) with the layer remaining relatively high in the space (i.e., 1.5 m (5 ft)). As the fire spread to adjacent combustibles, eventually involving the upholstered sofa, enclosure temperatures increased rapidly to temperatures greater than 600°C (1112°F) 101 seconds after ignition. At this point in time and for the duration of the test, there was no temperature gradient over the height of the enclosure (as shown in Figure 107).

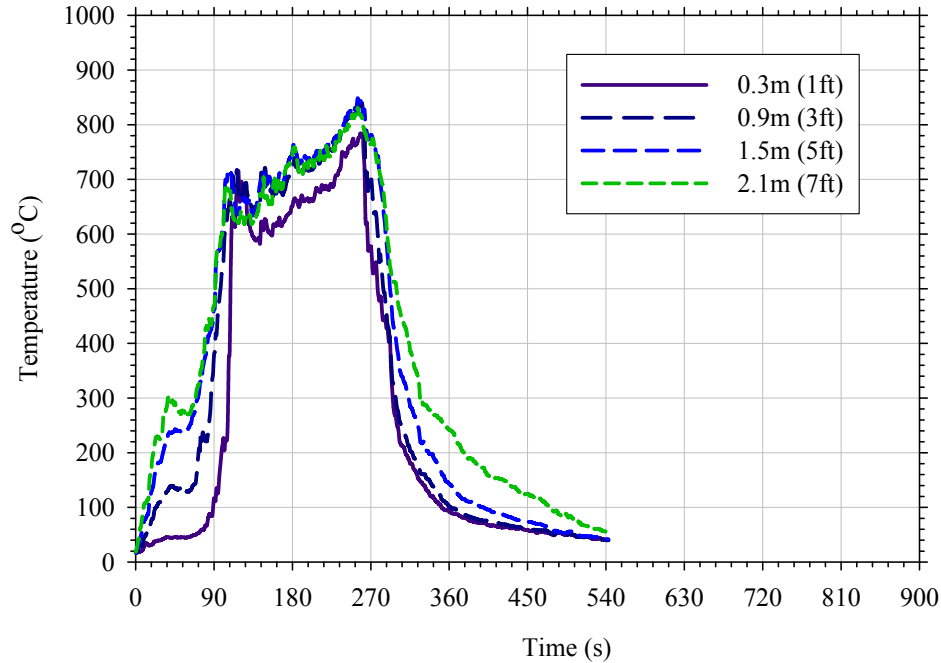


Figure 106. Average temperature measured at four elevations in Test 6-3.

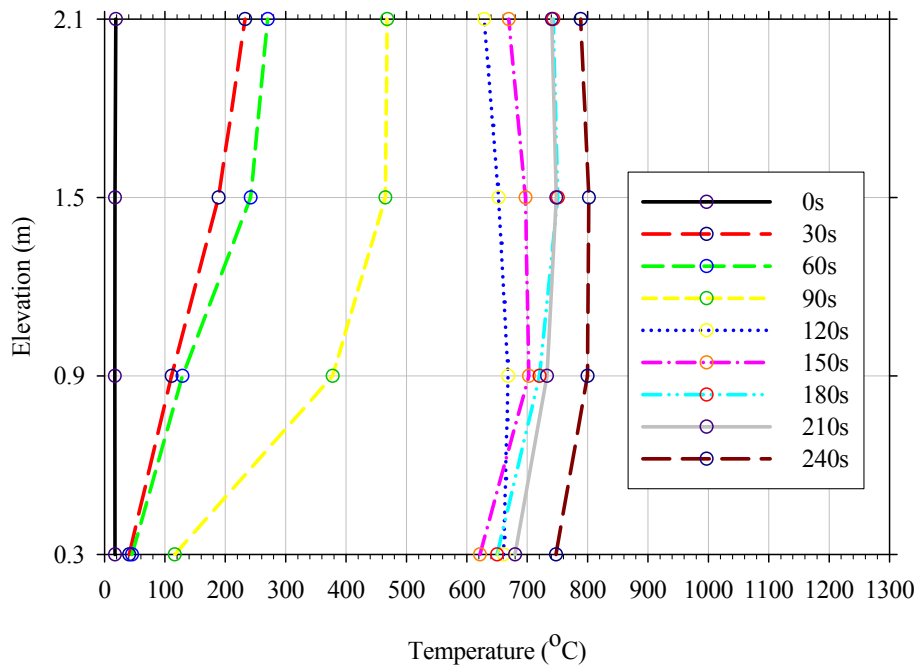


Figure 107. Average temperature gradients measured during Test 6-3.

Heat flux was collected at eight locations, six wall and two floor locations. Wall mounted heat flux transducers were located in the rear wall opposite the vent and in the sidewall perpendicular to the vent. Transducers mounted in the rear wall were mounted at heights of 0.6 m (2 ft), 1.2 m (4 ft), and 1.8 m (6 ft). Those mounted in the sidewall were mounted at

0.45 m (1.5 ft), 1.2 m (4 ft), and 1.95 m (6.5 ft). The data collected at the wall and floor locations is presented in Figure 108, Figure 109 and Figure 110.

As shown in Figure 108 and Figure 109, the heat fluxes to the rear and sidewalls, respectively, were different during the initial 180 seconds of the test. Both locations saw an increase in incident heat flux after the initial 90 seconds of burning but the exposures after this point in time were generally different. Heat fluxes to the rear wall were generally uniform over the height of the enclosure and increased at a more rapid rate during the initial 180 seconds of the test. Rear wall heat fluxes also reached higher peak values (100–115 kW/m²). Heat fluxes to the sidewall increased at a much more gradual rate with no period of decay as was seen at the rear wall location. During the last 90 seconds of the test, the heat fluxes at both locations were increasing. However, a larger gradient between elevations was observed at the rear wall, with values ranging from 45–90 kW/m², than was observed at the sidewall, with values ranging from 80–95 kW/m². Similar differences were observed for the floor heat flux measurements, when comparing rear and front locations. The rear floor gauge measured more severe heat fluxes earlier in the test while the front gauge measured a gradual increase in flux to the enclosure floor. Heat fluxes greater than 20 kW/m² were measured in both locations.

The differences noted during the initial 180 seconds of the test are most likely due to the proximity of the initiating fire to the rear gauge locations. As the upholstered chair fire grew in size and vent flow conditions were established within the enclosure, the fire most likely began to migrate across the rear wall of the enclosure (i.e., towards the heat flux gauge locations) resulting in a more severe, localized exposure.

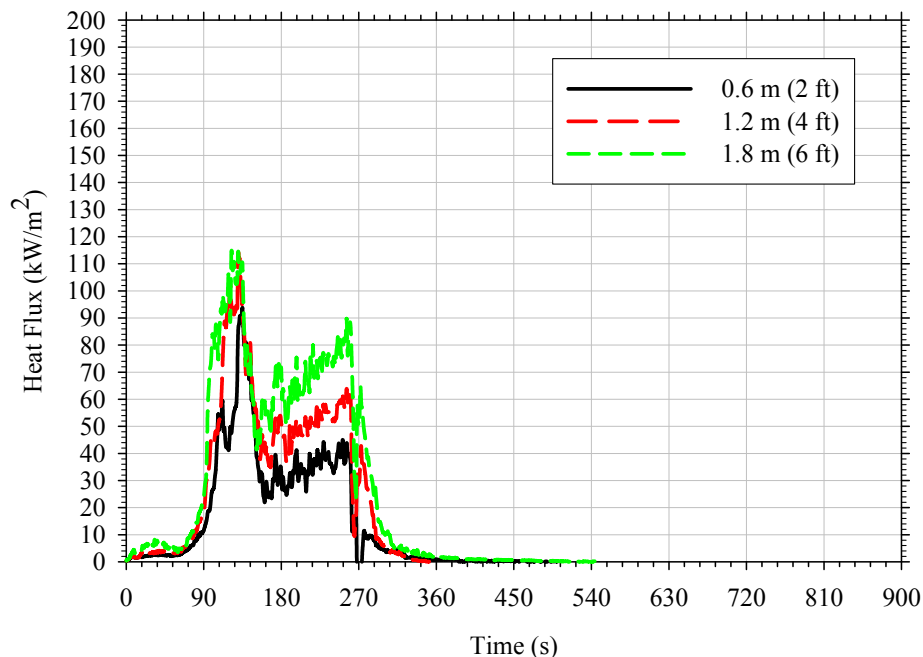


Figure 108. Heat flux on rear wall of enclosure opposite doorway in Test 6-3.

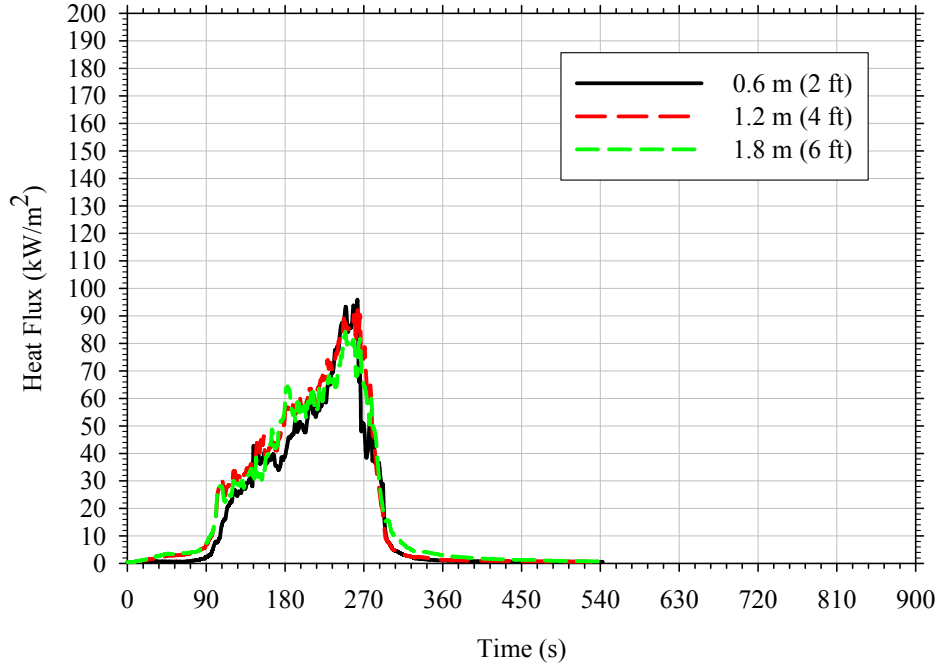


Figure 109. Heat flux on sidewall of enclosure perpendicular to vent in Test 6-3.

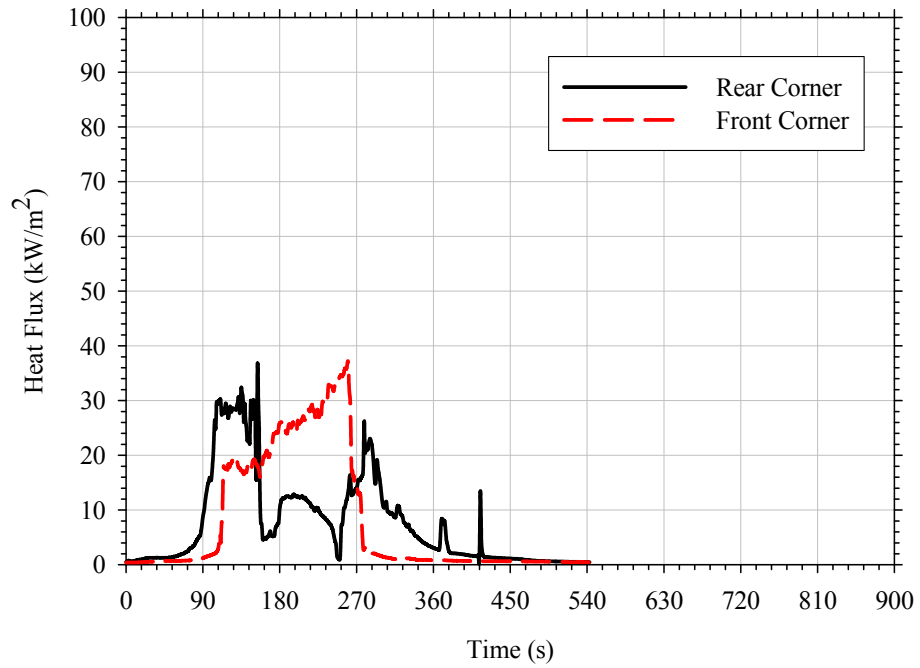


Figure 110. Average heat flux measured at floor in Test 6-3.

The gas species measured low and high in the enclosure are presented in Figure 111 and Figure 112, respectively. Note that carbon monoxide levels at the 1.9 m (78 in.) elevation exceeded analyzer limits between 120–180 seconds after ignition in this test. Once the fire developed in this test, both upper and lower layer oxygen concentration measurements were relatively steady for the duration of the test. Oxygen concentrations in the lower layer and upper layer reached 0.11 mol/mol and essentially 0, respectively. Similar to what was observed in previous full open door ventilation tests the carbon dioxide and carbon monoxide concentrations exhibited two stages during this test. After the initial fire development but before the transition to exterior burning (i.e., 90–120 seconds) carbon monoxide concentrations were increasing both high and low in the enclosure while carbon dioxide concentrations were decreasing. However, after the door plume ignited and exterior burning was occurring, these trends reversed with carbon monoxide concentrations decreasing and carbon dioxide concentrations increasing. This reversal is first noticed in the lower layer gas species measurements then in the upper layer measurements and is most likely a result of changing combustion efficiency associated with the occurrence of exterior flaming. At the onset of exterior flaming, visual observations noted the upper layer depth decreasing (i.e., the layer interface rising within the enclosure) suggesting that additional air was being entrained into the space.

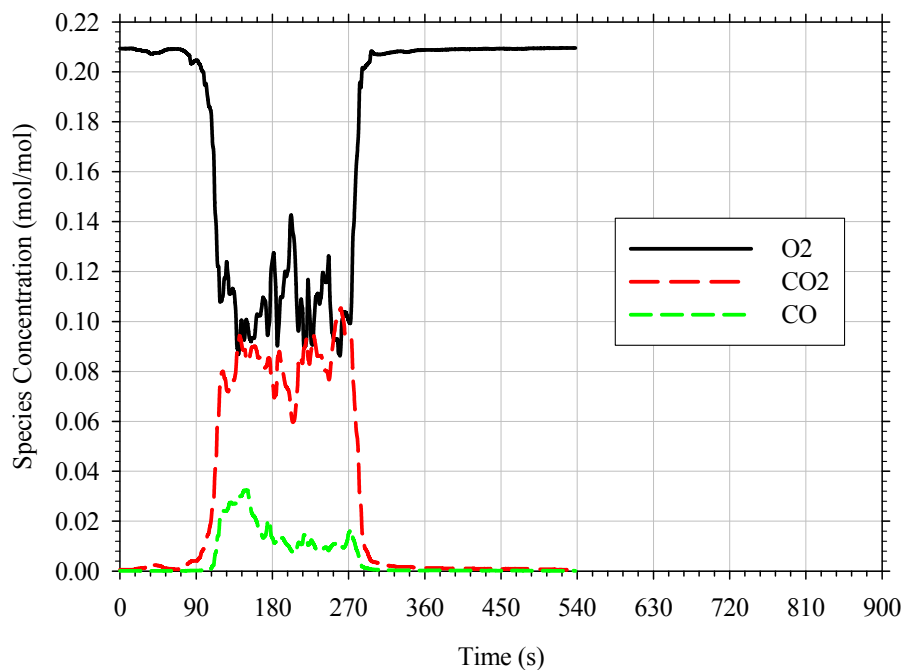


Figure 111. Gas concentrations measured 0.45 m (18 in.) above the floor in Test 6-3.

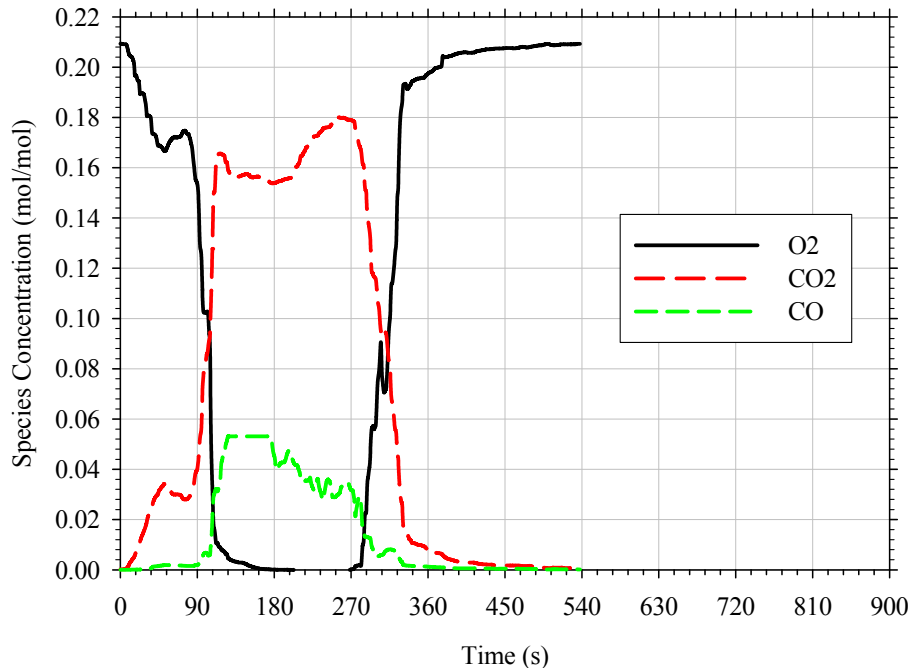


Figure 112. Gas concentrations measured 0.45 m (18 in.) below the ceiling in Test 6-3.

5.6.5 Gasoline on Upholstered Chair with Slit Vent Opening (w/Carpet)

Test scenario 6-4 was a fully furnished, carpeted room with a slit vent. The ignition scenario in this test was identical to that in Test 6-3. The upholstered chair was ignited using 1.5 L (0.40 gal) of gasoline poured on the chair and 0.5 L (0.13 gal) poured on the carpet as a trailer to the doorway. Upon ignition of the trailer, the liquid fuel fire spread quickly back to the upholstered chair which became involved. Due to the limited ventilation in this test, the upper layer within the enclosure reached floor level within 30 seconds of ignition. Approximately five minutes after ignition, the smoke leaving the test enclosure began to increase and decrease at 1–2 second intervals (i.e., puffing was observed). This oscillation in smoke production continued for approximately 60 seconds before the door plume ignited. This external burning continued for 30 seconds before transitioning back to burning within the enclosure. Three minutes later the door plume began to burn once more and continued to burn for 150 seconds (2 minutes 30 seconds) before manual suppression was started. Suppression was achieved using a 2.5 in. manual hose line using the same procedures as described in Section 5.6.2. Photographs showing the evolution of this fire are presented in Figure 113.

A plot of the heat release rate from the enclosure fire is presented in Figure 114. The peak heat release was 1.8 MW with an average steady-state of 839 kW. A quasi-steady-state burning condition was reached within 90 seconds of ignition. The fire burned under these conditions for a total of 270 seconds (4 minutes 30 seconds) before burning outside the vent. This initial period of external burning continued for approximately thirty seconds reaching a peak heat release rate of 1.6 MW. For the remainder of the test, the fire transitioned between burning within the compartment and burning at the vent. The fire was eventually suppressed after 720 seconds of total burn time. The total heat released during this test was 661 MJ over the 713 seconds (11 minute 53 second) burning duration. In this time, the contents of the test enclosure lost

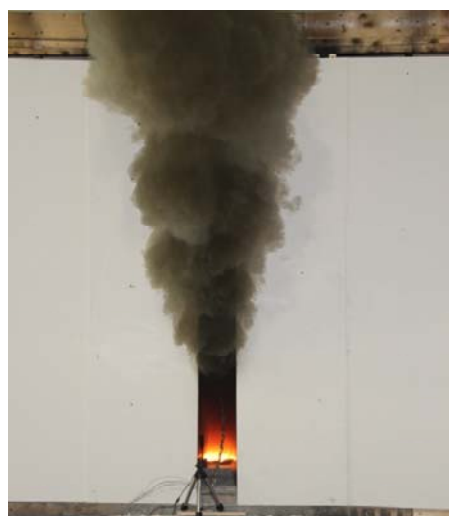
approximately 85 kg (187 lbs), or thirty-three percent of their original mass. A further breakdown of the total mass loss from each of the combustibles within the enclosure is provided in Table 16.



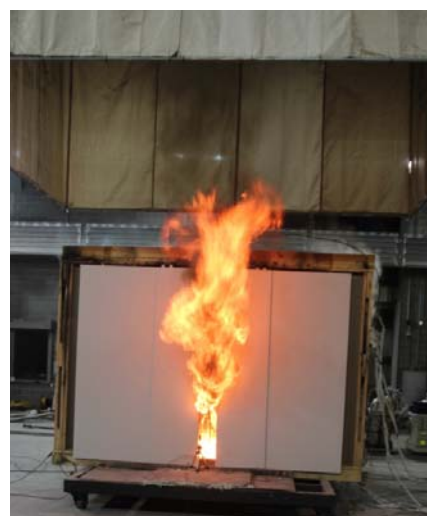
t = 5 s



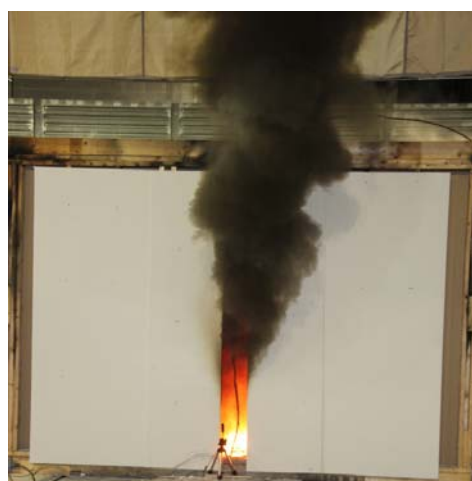
t = 10 s



t = 270 s



t = 366 s



t = 399 s



t = 735 s

Figure 113. Fire progression observed in Test 6-4.

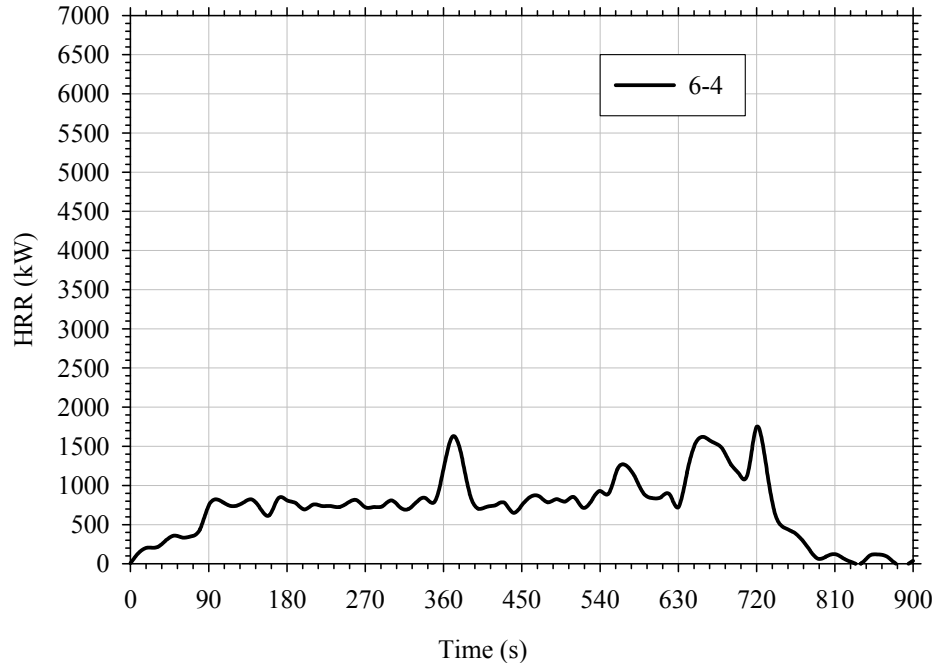


Figure 114. Heat release rate from Test 6-4.

Table 16. Summary of mass loss of combustibles within Test 6-4.

Item	Total Mass Loss (kg [lbs])	Mass Loss Fraction
Upholstered Sofa	13.6 [30.0]	0.29
Upholstered Chair	4.6 [10.1]	0.44
Table	7.5 [16.5]	0.48
Baby Seat	2.0 [4.4]	0.32
Flooring Material	57.3 [126]	0.34
Total	85.0 [187]	0.33

The average temperature (front and back) measured at four elevations is presented in Figure 115. The average temperature gradient over the height of the test enclosure for the duration of the test is presented in Figure 116. As shown in Figure 115 and Figure 116, the upper layer developed quickly in this test due to the slit ventilation scenario. Approximately 210 seconds after ignition, there was essentially no thermal gradient within the enclosure. Temperatures from floor to ceiling within the space were approximately 500°C (932°F) and remained at this temperature for the next 240 seconds (i.e., from about 450 seconds on). At this point in time, the temperatures within the enclosure started increasing at a rate of approximately 20°C/minute, eventually exceeding 600°C (1112°F) at 725 seconds (12 minutes 5 seconds) after ignition. It should be noted that at the 60 and 180 second time frames in Figure 116, temperatures measured at the 0.9 and 1.5 m (3 and 5 ft) elevations are slightly greater than those measured at the 2.1 m (7 ft) elevation. This is due to the proximity of the lower level temperature measurement locations being close to the burning chair.

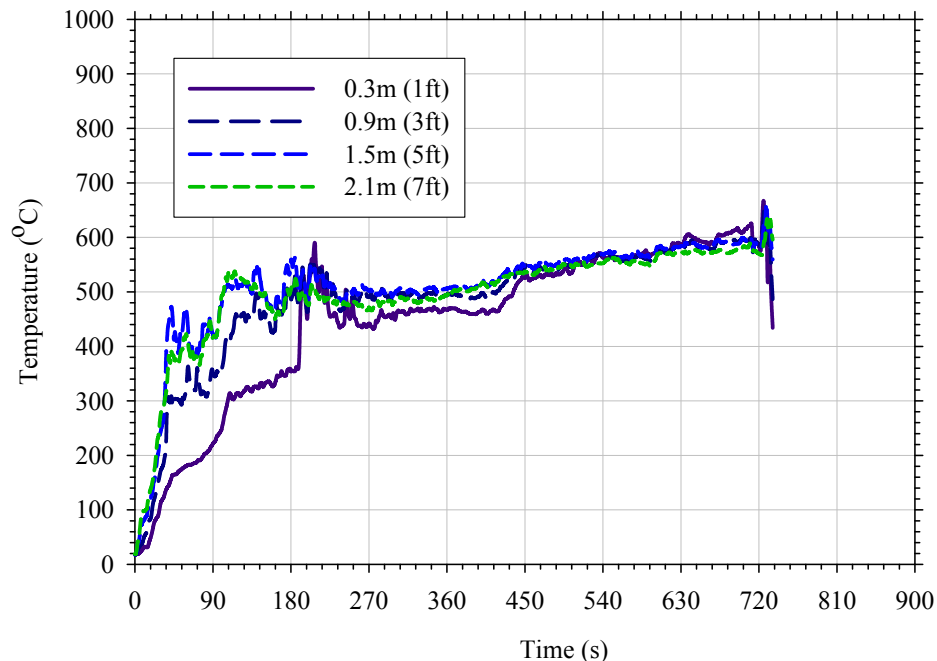


Figure 115. Average temperature measured at four elevations in Test 6-4.

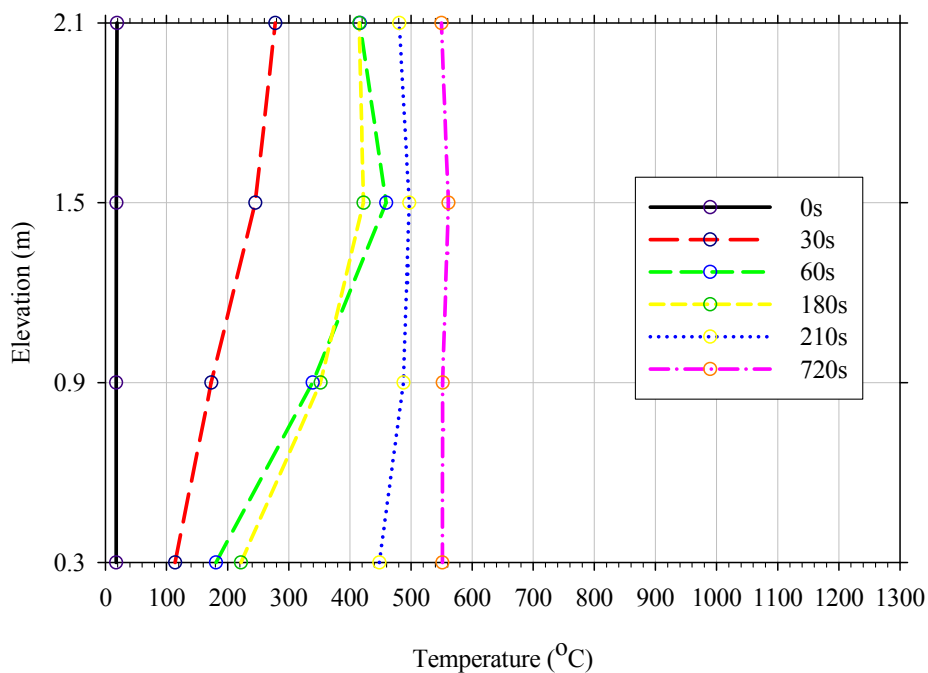


Figure 116. Average temperature gradients measured during Test 6-4.

Heat flux was collected at eight locations, six wall and two floor locations. Wall mounted heat flux transducers were located in the rear wall opposite the vent and in the sidewall perpendicular to the vent. Transducers mounted in the rear wall were mounted at heights of 0.6 m (2 ft), 1.2 m (4 ft), and 1.8 m (6 ft). Those mounted in the sidewall were mounted at 0.45 m (1.5 ft), 1.2 m (4 ft), and 1.95 m (6.5 ft). The data collected at the wall and floor locations is

presented in Figure 117, Figure 118, and Figure 119. Heat fluxes to the walls of the enclosure behaved similarly during the initial 360 seconds (6 minutes) of the test. Both locations saw an increase in incident heat flux during the first 120 seconds of burning followed by a period of steady-state conditions. However, the intensity of the incident heat fluxes during this period of time was different, with the rear wall having a more severe exposure. Rear wall heat fluxes during the steady-state period ranged from 15–35 kW/m² with the more severe exposures being higher in the enclosure. Sidewall heat fluxes were approximately the same over the different heights of the enclosure and had values of approximately 10 kW/m².

Whereas the heat fluxes to the rear wall were greater than the front during the start of the fire, the severity of wall heat flux reversed during the second half of the test (i.e., 360–720 seconds). In the rear of the enclosure, steady-state conditions were maintained at approximately 20 kW/m², while at the forward sidewall location, the fluxes steadily increased from 15–50 kW/m². The differences in incident flux measured during the first half of the test were due to the proximity of the initiating fire to the rear wall mounted gauges. The higher heat fluxes toward the front during the second half of the test are attributed to the ventilation conditions and the consequent migration of the fire towards the vent (i.e., movement of fire from the rear to the front of enclosure, particularly around 360 s). This migration is supported by visual observations made during the test as well as the fact that intermittent vent burning was noted in the test synopsis provided above. The migration of the fire towards the vent is also supported by the increased floor heat fluxes measured in the front corner (shown in Figure 119) and follows from the vitiation of the upper layer as shown in Figure 121.

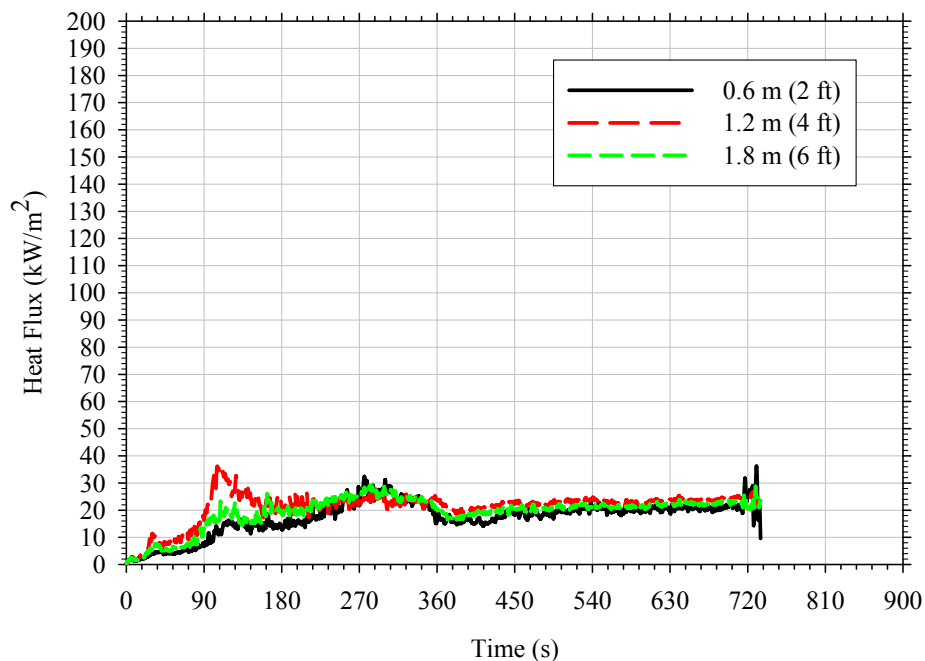


Figure 117. Heat flux on rear wall of enclosure opposite doorway in Test 6-4.

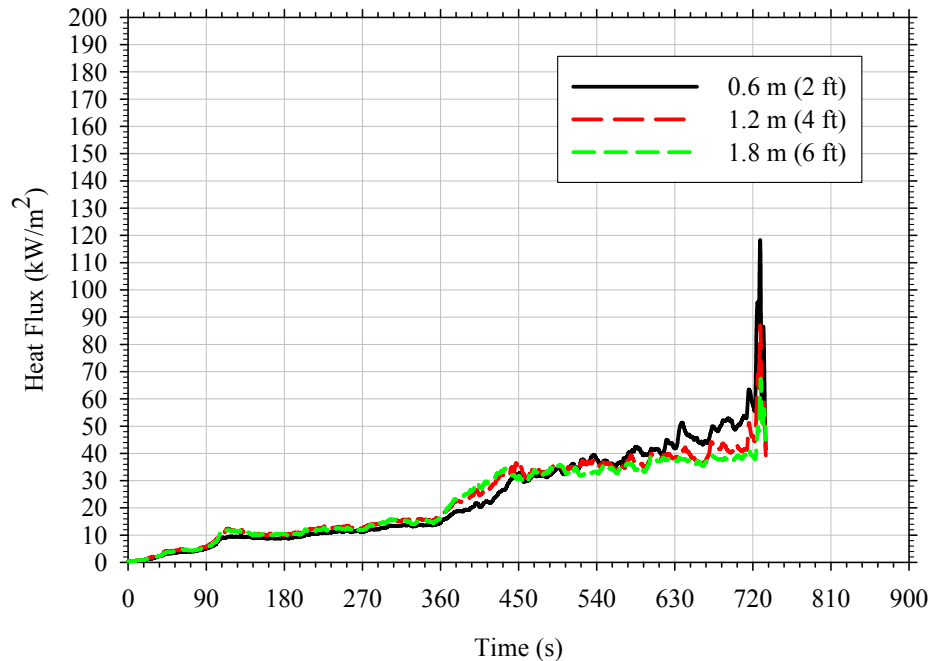


Figure 118. Heat flux on sidewall of enclosure perpendicular to vent in Test 6-4.

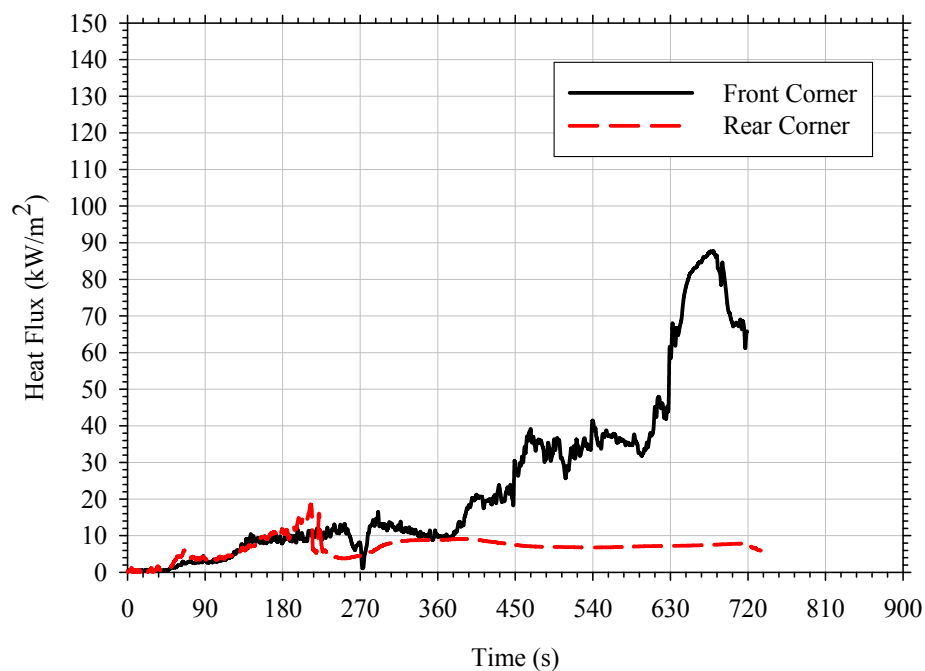


Figure 119. Average heat flux measured at floor in Test 6-4.

The gas species measured low and high in the enclosure are presented in Figure 120 and Figure 121, respectively. Note that carbon monoxide levels at the 1.9 (78 in.) elevation exceeded analyzer limits between 210–410 seconds after ignition in this test. Figure 120 and Figure 121 illustrate the early development of a highly vitiated upper layer in this test. The plots also illustrate the impact this vitiation had on fire development. The reversal of lower layer oxygen concentrations (from a low of 13% at about 160 s back up to ambient) reflects a shift in the

ventilation dynamics and more air being drawn into the fire. This is consistent with the corresponding plateau of enclosure temperatures at approximately 500°C (932°F) noted in Figure 115. After this point in time, lower layer gas concentrations begin to revert back to ambient conditions and upper layer concentrations level out with the upper layer becoming completely oxygen deprived.

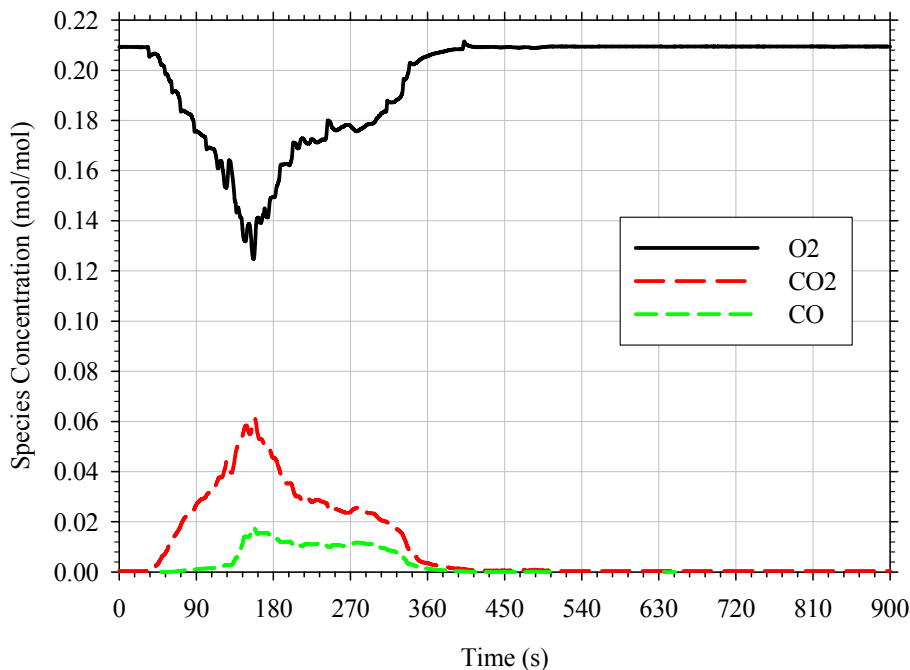


Figure 120. Gas concentrations measured 0.45 m (18 in.) above the floor in Test 6-4.

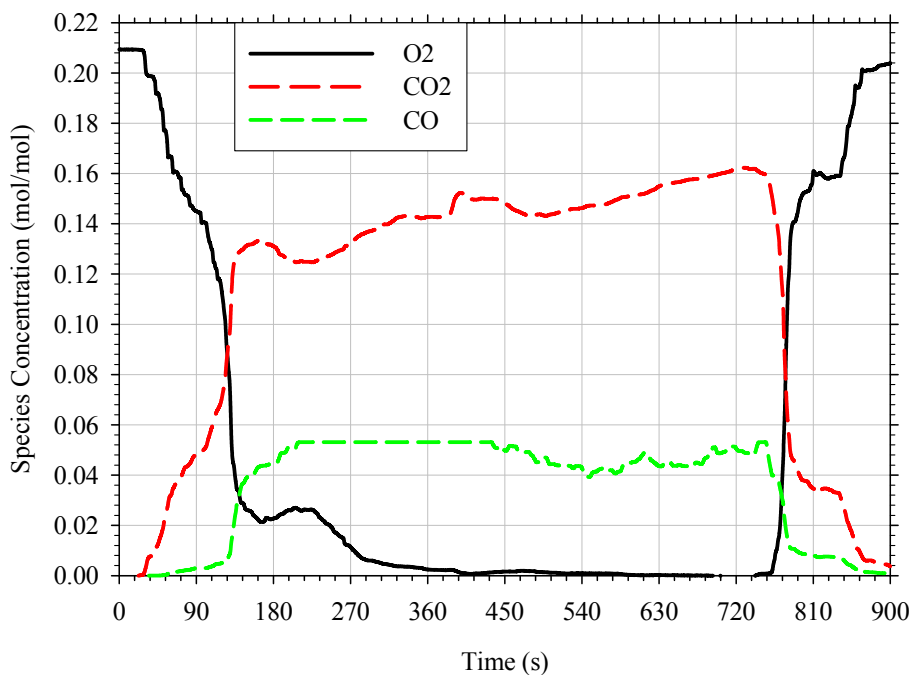


Figure 121. Gas concentrations measured 0.45 m (18 in.) below the ceiling in Test 6-4.

5.6.6 Gasoline on Vinyl Floor with Full Door Opening

Test scenario 6-5 was a fully furnished room with a full-open doorway and vinyl flooring. The ignition scenario used in this test consisted of a 2.0 L (0.53 gal) gasoline spill on the vinyl flooring in the center of the test enclosure. The fuel release created a 1.6 m² (17 ft²) spill area. Due to the size of the gasoline spill on the vinyl, all combustibles within the test enclosure were ignited at nominally the same time. The upper layer reached floor level in approximately 15 seconds and burning at the vent occurred after 60 seconds. After two minutes of additional burning, manual suppression was started. Photographs showing the evolution of this fire are presented in Figure 122.

A plot of the heat release rate from the enclosure fire is presented in Figure 123. The peak heat release was 5.0 MW. The gasoline spill resulted in rapid-fire growth up to between 2.5–3.0 MW. All other combustibles within the enclosure were quickly involved and the door plume was ignited approximately 60 seconds after ignition. The ignition of the door plume resulted in a rapid spike in heat release, peaking at approximately 5.0 MW. The fire then maintained a heat release between 2.5–4.0 MW for the duration of the test. The total heat released during this test was 611 MJ over the 186 seconds (3 minute 6 second) burning duration. The contents of the test enclosure lost approximately 85.6 kg (189 lbs), or thirty-three percent of their original mass. A further breakdown of the total mass loss from each of the combustibles within the enclosure is provided in Table 17.

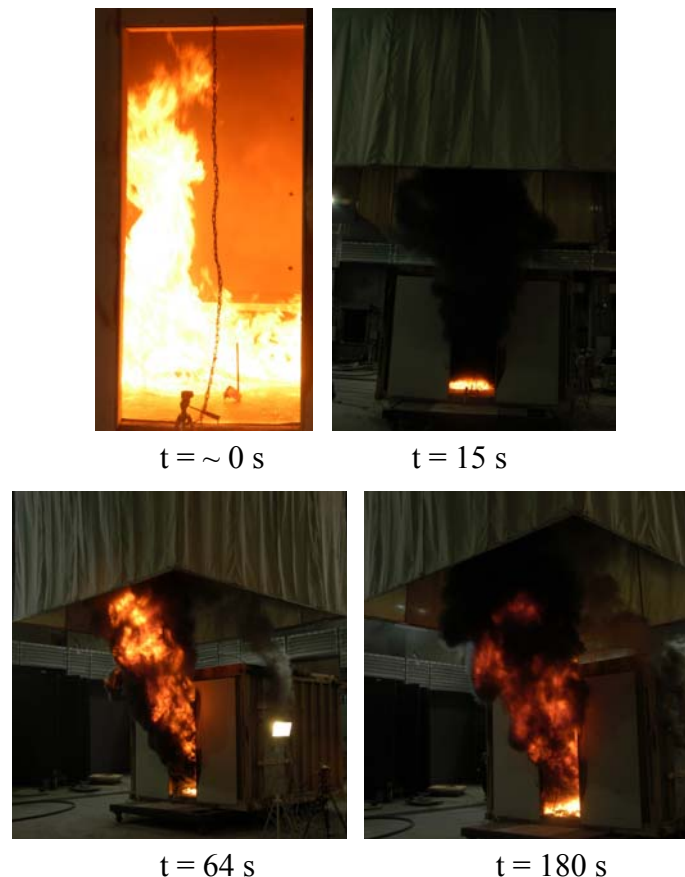


Figure 122. Fire progression observed in Test 6-5.

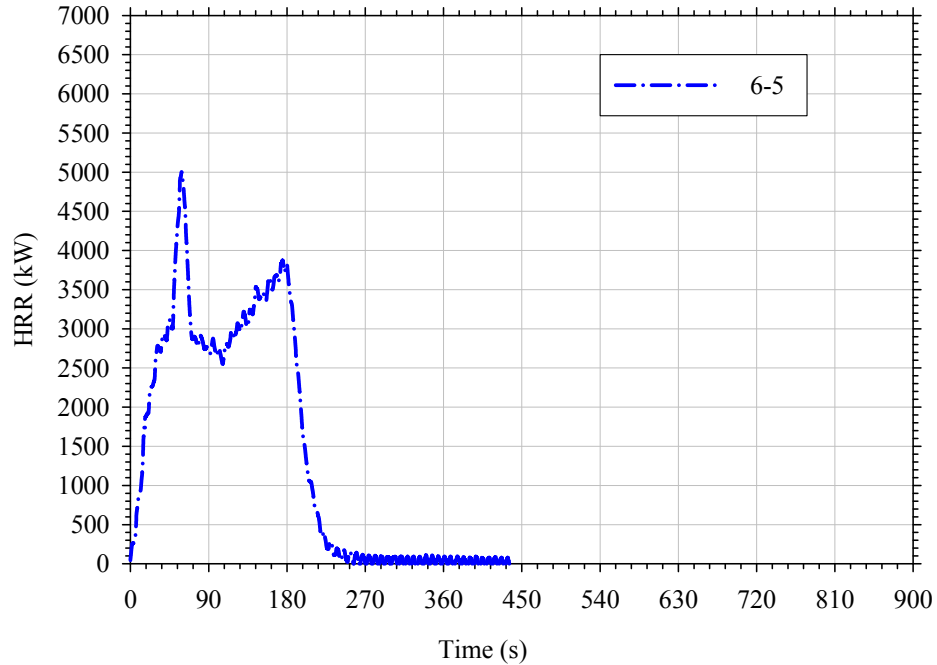


Figure 123. Heat release rate from Test 6-5.

Table 17. Summary of mass loss of combustibles within Test 6-5.

Item	Total Mass Loss (kg [lbs])	Mass Loss Fraction
Upholstered Sofa	13.7 [30.2]	0.30
Upholstered Chair	4.4 [9.7]	0.42
Table	4.2 [9.3]	0.27
Baby Seat	3.3 [7.3]	0.53
Flooring Material	60.0 [132]	0.36
Total	85.6 [189]	0.33

The average temperature (back and front) measured at four elevations is presented in Figure 124. The average temperature gradient over the height of the test enclosure for the duration of the test is presented in Figure 125. The large initiating fire used in this test produced temperatures within the enclosure from floor to ceiling in excess of 600°C (1112°F) within 33 seconds of ignition. The rapid-fire development resulted in a minimal thermal gradient within the enclosure for the entire test.

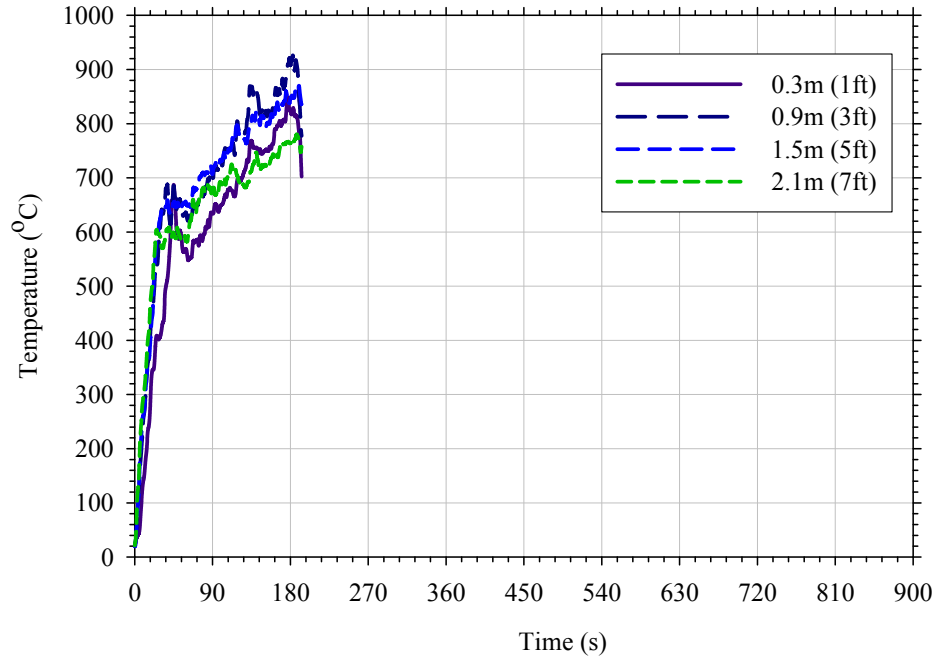


Figure 124. Average temperature measured at four elevations in Test 6-5.

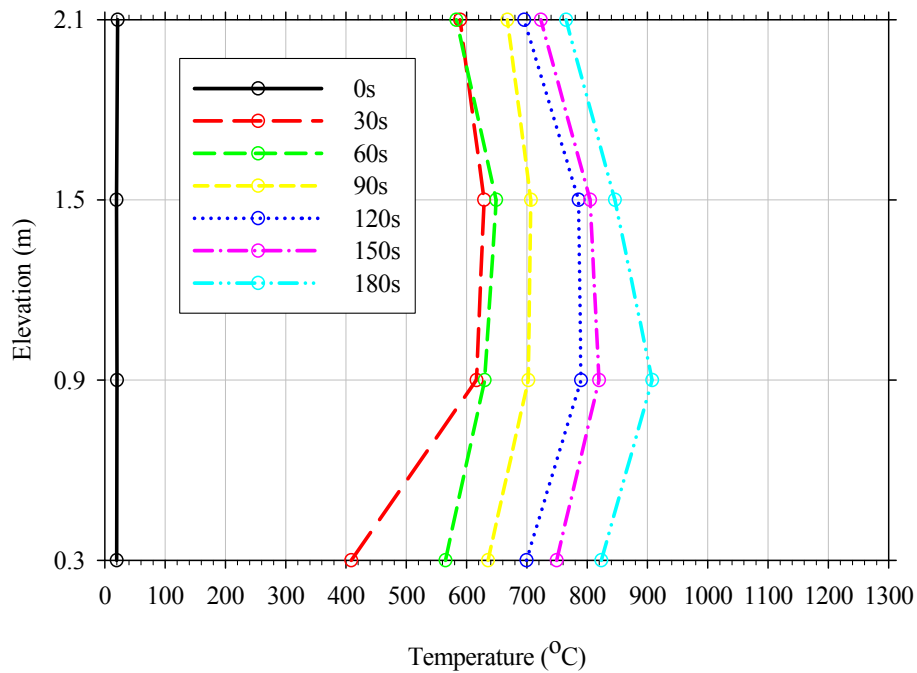


Figure 125. Temperature gradients measured during Test 6-5.

Heat flux was collected at eight locations, six wall and two floor locations. Wall mounted heat flux transducers were located in the rear wall opposite the vent and in the sidewall perpendicular to the vent. Transducers mounted in the rear wall were mounted at heights of 0.6 m (2 ft), 1.2 m (4 ft), and 1.8 m (6 ft). Those mounted in the sidewall were mounted at 0.45 m (1.5 ft), 1.2 m (4 ft), and 1.95 m (6.5 ft). The heat flux data collected at the wall and floor

locations is presented in Figure 126, Figure 127, and Figure 128. In this test, wall heat fluxes reached as high as 140 kW/m^2 with the highest heat fluxes being measured at the rear wall. The initial spike in rear wall heat fluxes occurring around 45 seconds was due to the migration of the fire toward the rear of the enclosure as a result of the vent flow into the enclosure. After the initiating fire self-extinguished and only Class A materials were burning, wall heat flux measurements grew at a comparable rate to similar levels. Rear wall heat fluxes were slightly greater than those measured on the sidewall. A larger gradient between heat flux measurement elevations was also noted at the sidewall location. Average floor heat fluxes exceeded 20 kW/m^2 34 seconds after ignition in this test and reached peak values of approximately 80 kW/m^2 .

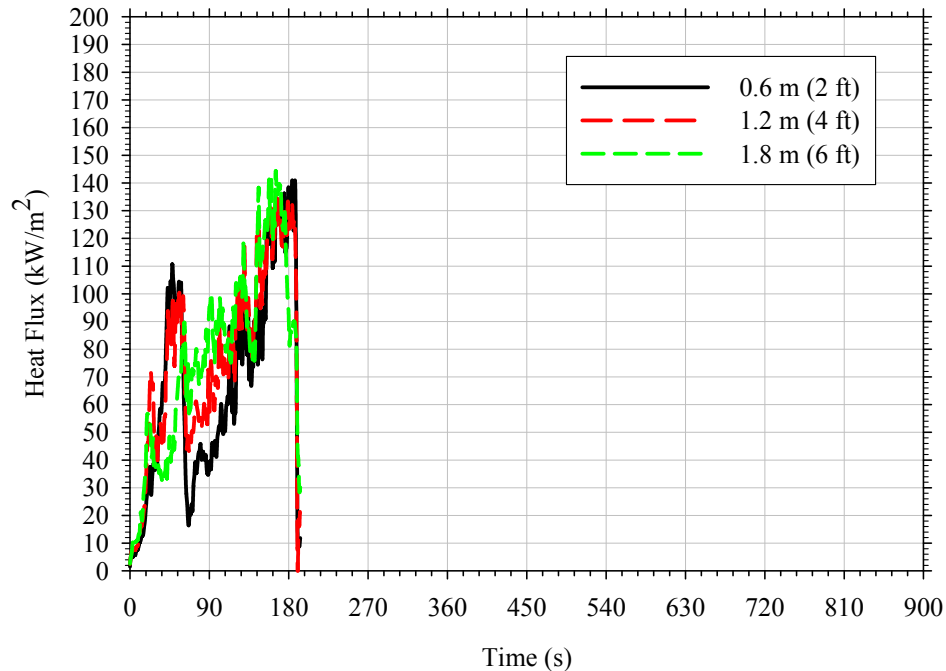


Figure 126. Heat flux on rear wall of enclosure opposite doorway in Test 6-5.

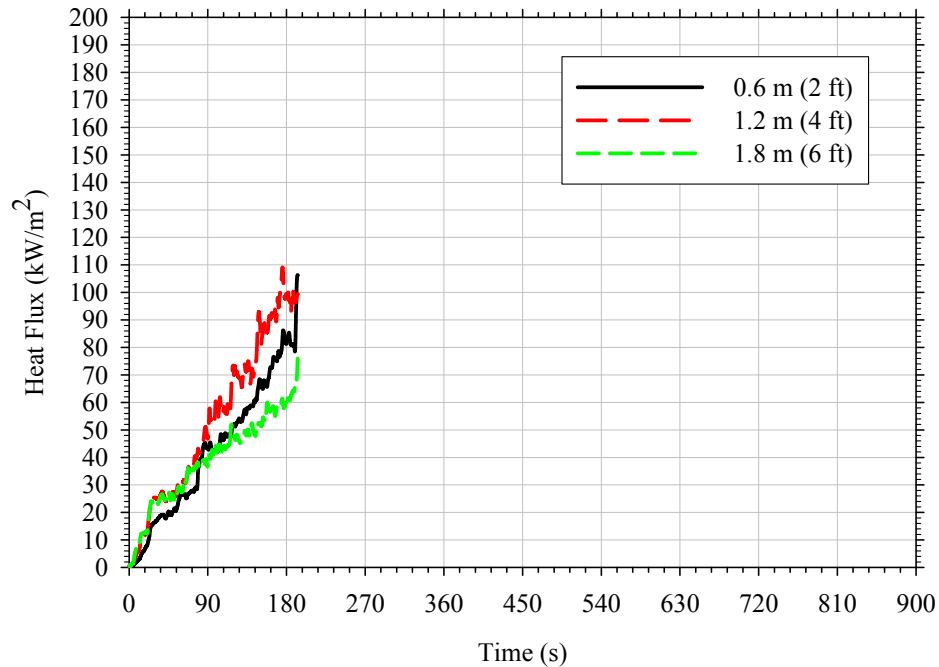


Figure 127. Heat flux on sidewall of enclosure perpendicular to vent in Test 6-5.

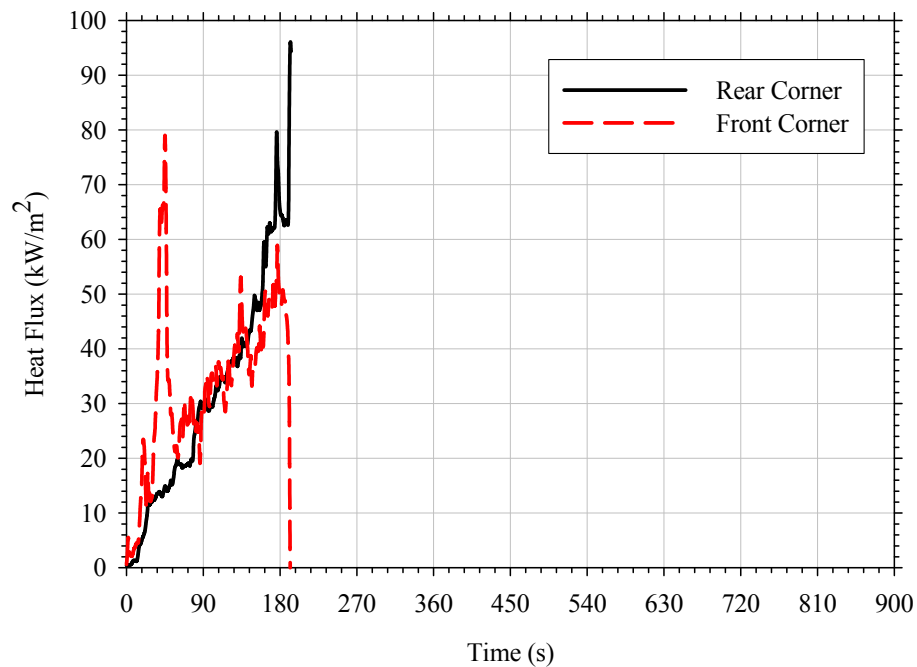


Figure 128. Average heat flux measured at floor in Test 6-5.

The gas species measured low and high in the enclosure are presented in Figure 129 and Figure 130, respectively. Note that carbon monoxide levels at the 1.9 m (78 in.) elevation exceeded analyzer limits between approximately 35 and 85 seconds after ignition in this test. The rapid-fire growth observed in this test produced a vitiated upper layer within the first 30 seconds of burning. Upper layer oxygen concentrations fell below 0.02 mol/mol, carbon dioxide rose

above 0.15 mol/mol, and carbon monoxide was greater than 0.05 mol/mol during this short time. Conditions in the lower layer were slightly less vitiated with average concentrations of 0.14, 0.06, and 0.02 for oxygen, carbon dioxide, and carbon monoxide, respectively. Changes in the trends of both carbon dioxide and carbon monoxide were again observed at the onset of external burning at the vent opening.

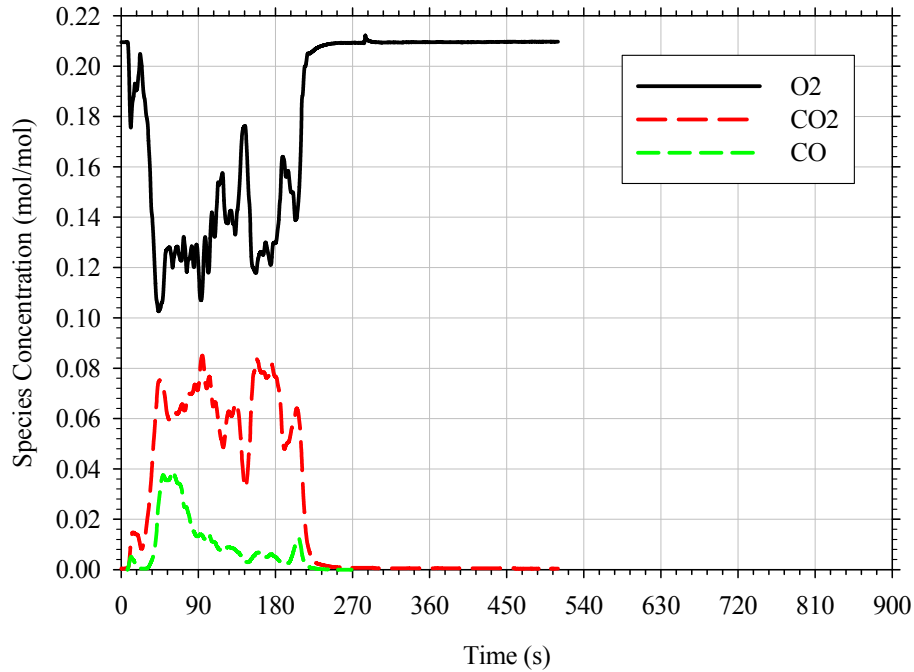


Figure 129. Gas concentrations measured 0.45 m (18 in.) above the floor in Test 6-5.

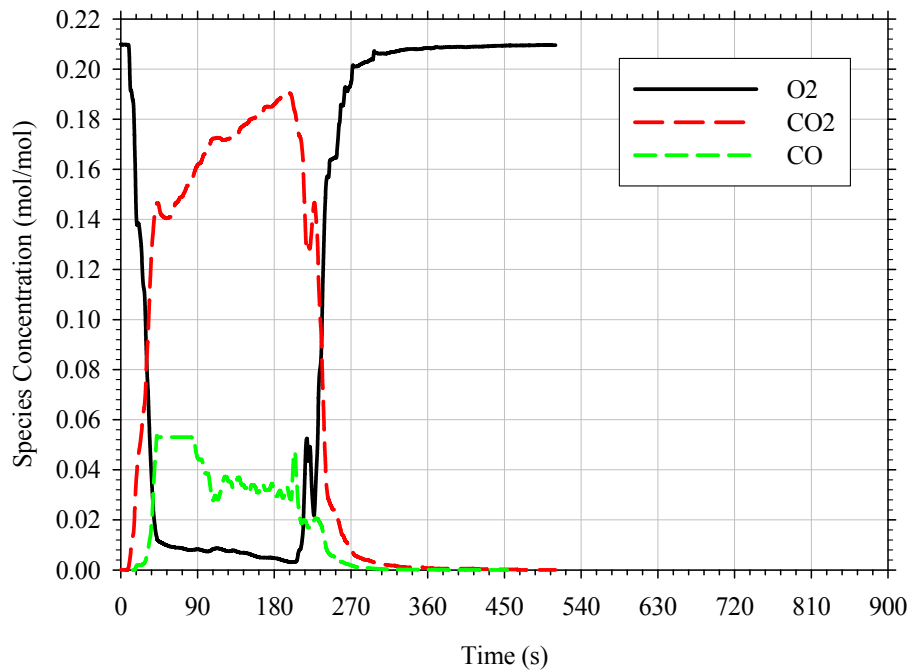


Figure 130. Gas concentrations measured 0.45 m (18 in.) below the ceiling in Test 6-5.

5.6.7 Gasoline on Vinyl Floor with Slit Vent Opening

Test scenario 6-6 was a fully furnished room with a slit vent and vinyl flooring. The ignition scenario used in this test was identical to that used in Test 6-5, a 2.0 L (0.53 gal) gasoline spill in the center of the test enclosure. Due to the limited ventilation from the slit vent, the upper layer reached floor level in approximately 10 seconds. As a result, the extent to which the upholstered chair and other Class A combustibles within the enclosure could burn was limited. Approximately 180 seconds after ignition, the layer interface began to rise allowing the upholstered chair to burn more vigorously, eventually involving both the coffee table and the sofa. Burning at the vent was not observed in this test. Suppression was started 510 seconds (8 minutes 30 seconds) after ignition. Photographs showing the evolution of this fire are presented in Figure 131.

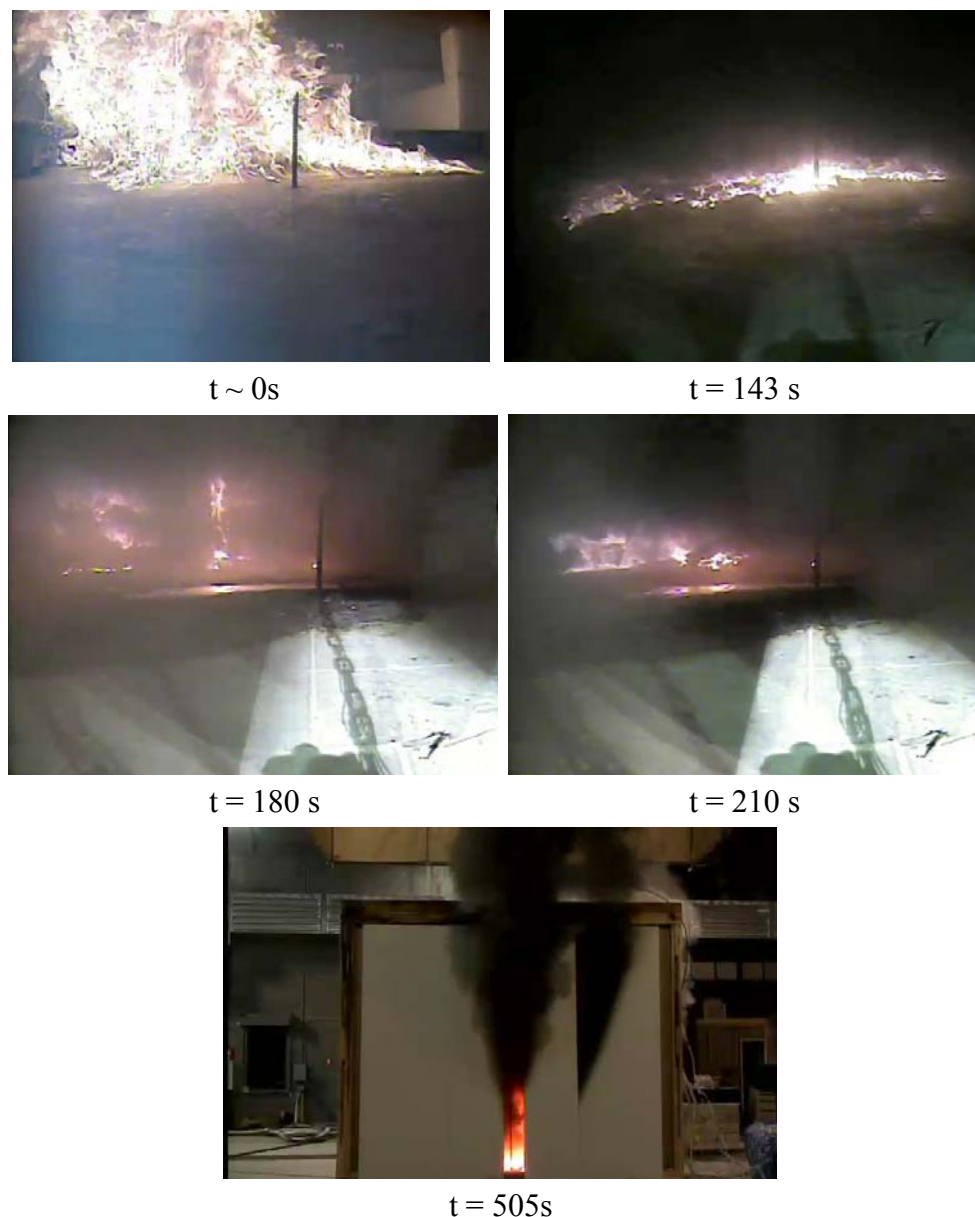


Figure 131. Fire progression observed in Test 6-6.

A summary of the heat release rate from the enclosure fire is presented in Figure 132. The peak heat release measured in this test was 1.1 MW with an average steady-state heat release rate of 856 kW. As shown in the plot, the spill fire quickly grew to 750 kW in the initial 45 seconds of the test. However, the ventilation opening inhibited further growth as the vitiated upper layer descended quickly to the floor, resulting in the gradual decrease in heat release over the next 150 seconds (2 minutes 30 seconds). After this period of decay, the fire on the chair and table began to grow as oxygen levels increased. Eventually the fire involved the upholstered sofa, and reaching a peak heat release of 1.1 MW. After this period of growth, the fire maintained a relatively steady-state heat release for the duration of the test. The total heat released during this test was 356 MJ over the 506 seconds (4 minute 36 second) burning duration. The contents of the test enclosure lost approximately 93.6 kg (206 lbs), or thirty-eight percent of their original mass. A further breakdown of the total mass loss from each of the combustibles within the enclosure is provided in Table 18.

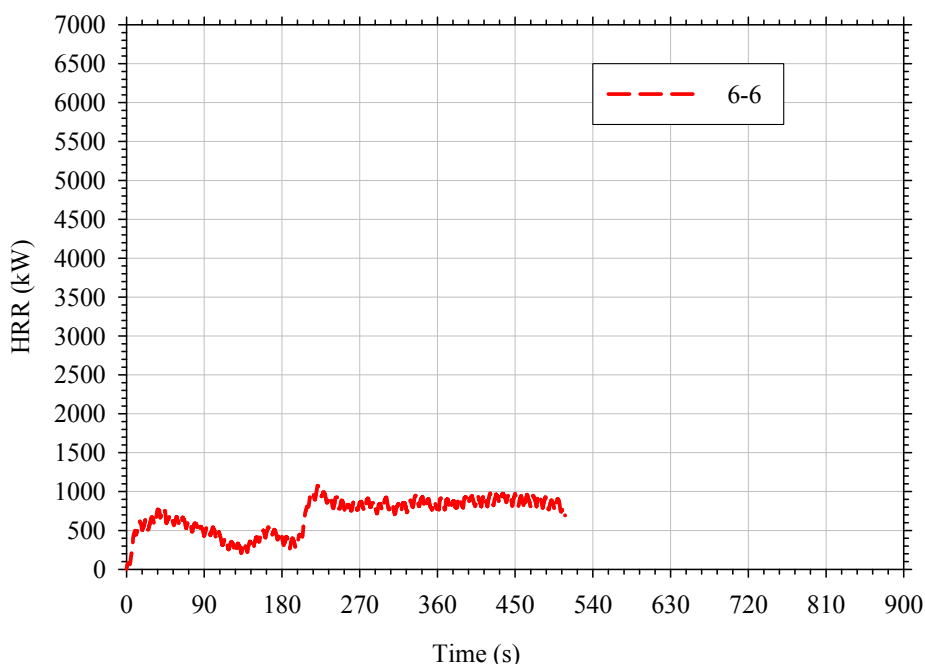


Figure 132. Heat release rate from Test 6-6.

Table 18. Summary of mass loss of combustibles within Test 6-6.

Item	Total Mass Loss (kg [lbs])	Mass Loss Fraction
Upholstered Sofa	8.5 [18.7]	0.18
Upholstered Chair	6.7 [14.8]	0.64
Table	10.4 [23.0]	0.66
Baby Seat	2.8 [6.2]	0.45
Flooring Material	65.2 [144]	0.39
Total	93.6 [206]	0.37

The average temperature (front and back) measured at four elevations is presented in Figure 133. The average temperature gradient over the height of the test enclosure for the duration of the test is presented in Figure 134. Temperatures within the enclosure grew rapidly to peak values ranging from 325–500°C (617–932°F) within the initial 60 seconds of the test. This increase was a result of the large initiating fire used in this test. However, due to the limited ventilation condition, the enclosure quickly became highly vitiated and the fire was suppressed. The associated decay in temperatures over the next 120–150 seconds can be seen in Figure 133. After reaching some equilibrium between fire size and air inflow, the fire became re-established and burned at decreased size leading to a second increase in temperatures. This secondary increase eventually reached a steady-state condition with enclosure temperature, from floor to ceiling, at temperatures of approximately 600°C (1112°F).

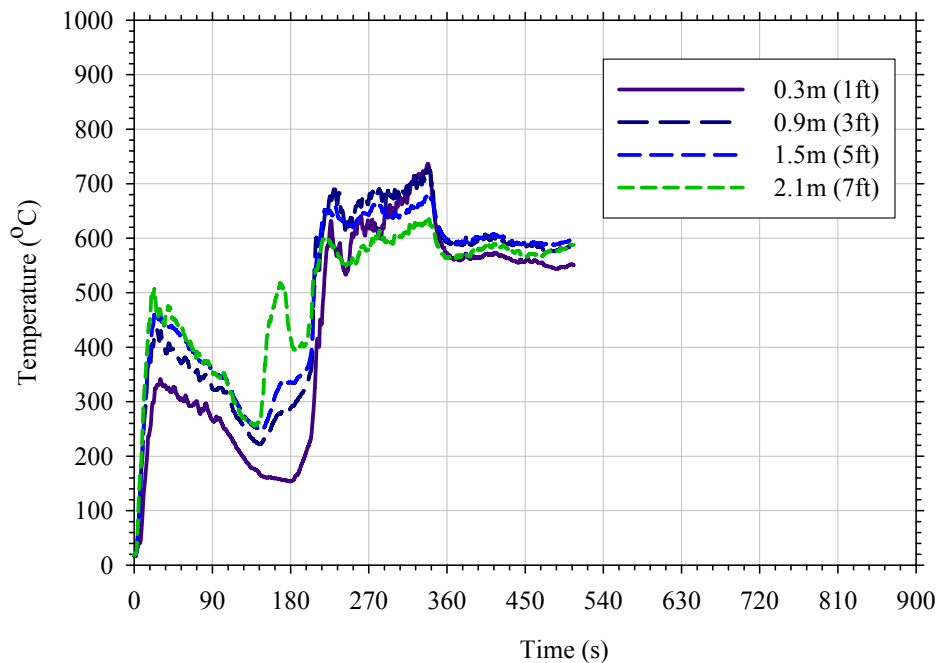


Figure 133. Average temperature measured at four elevations in Test 6-6.

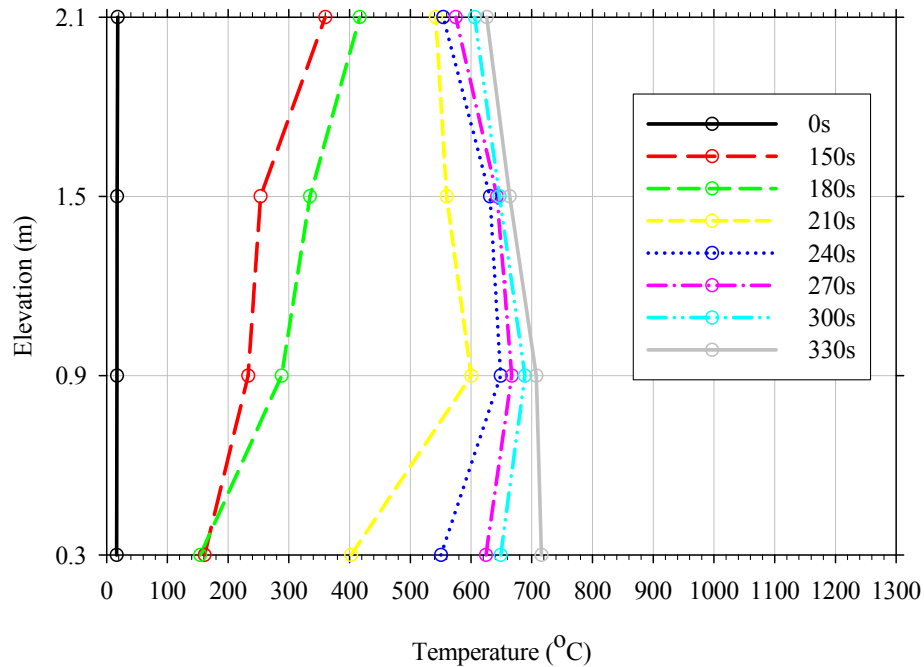


Figure 134. Average temperature gradients measured during Test 6-6.

Heat flux was collected at eight locations, six wall and two floor locations. Wall mounted heat flux transducers were located in the rear wall opposite the vent and in the sidewall perpendicular to the vent. Transducers mounted in the rear wall were mounted at heights of 0.6 m (2 ft), 1.2 m (4 ft), and 1.8 m (6 ft). Those mounted in the sidewall were mounted at 0.45 m (1.5 ft), 1.2 m (4 ft), and 1.95 m (6.5 ft). The heat flux data collected at the wall and floor locations is presented in Figure 135, Figure 136, and Figure 137. The wall heat fluxes measured in this test, in both rear and side locations, were generally comparable over the entire test duration. Initial wall heat fluxes ranged from 10–35 kW/m² depending upon the elevation of the instrument. The measurements later stabilized to values that were on average 20 kW/m². Fluxes measured on the rear wall were slightly erratic than those measured on the sidewall but this was associated with the migration of the fire to the rear of the enclosure as a result of the ventilation condition. Heat fluxes to the floor in this test differed dramatically. However, this difference is again most likely due to the fire moving to the rear of the enclosure and corresponding proximity of the fire to the rear floor heat flux gauge. The measurements collected by the front floor gauge are much more representative of the incident heat flux that was imposed by the upper layer during this test.

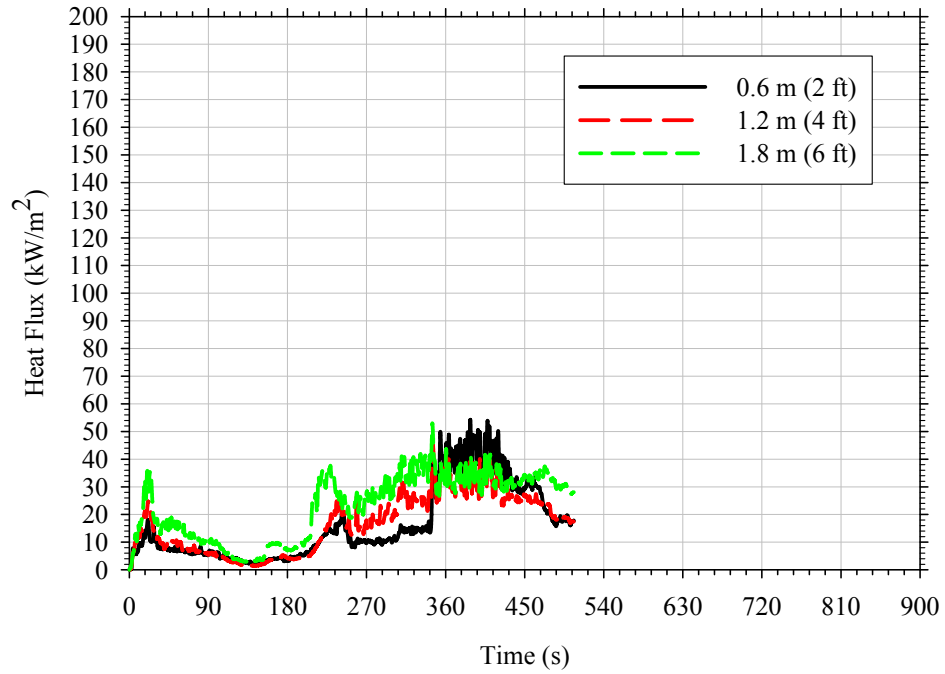


Figure 135. Heat flux on rear wall of enclosure opposite doorway in Test 6-6.

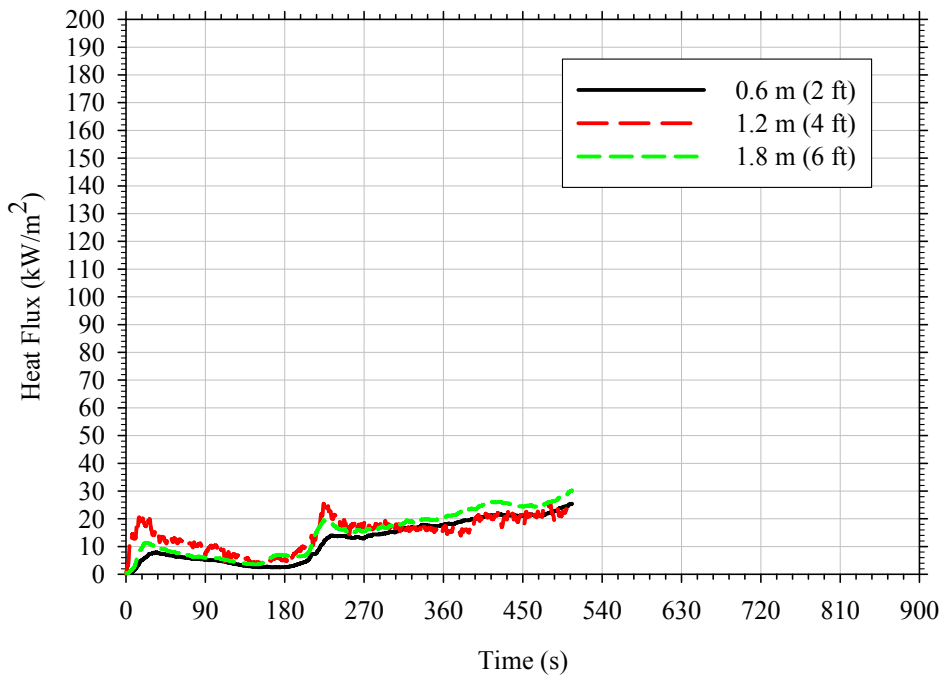


Figure 136. Heat flux on sidewall of enclosure perpendicular to vent in Test 6-6.

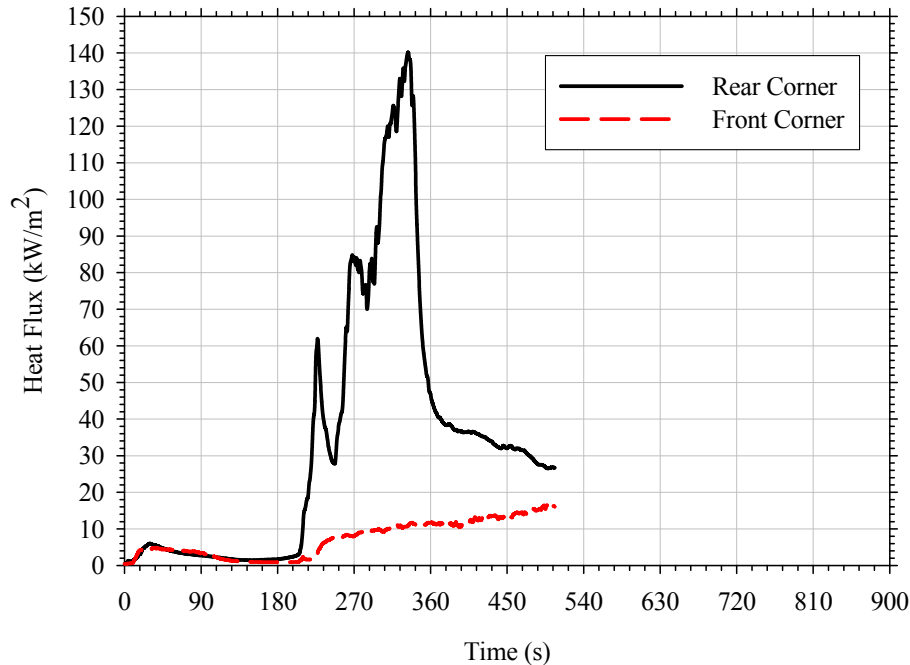


Figure 137. Average heat flux measured at floor in Test 6-6.

The gas species measured low and high in the enclosure are presented in Figure 138 and Figure 139, respectively. Note that carbon monoxide levels at the 1.9 m (78 in.) elevation exceeded analyzer limits approximately 225 seconds (3 minutes 45 seconds) after ignition in this test. The gas species trends presented in Figure 138 and Figure 139 show the highly vitiated conditions that were created as a result of the initiating fire and the slit ventilation scenario. Lower layer oxygen concentrations fell below 0.10 mol/mol, which limited the extent to which both the initiating fire and the upholstered chair could burn. Oxygen concentrations increased after this initial decrease with lower layer conditions returning to nearly ambient conditions and upper layer concentrations of approximately 0.15 mol/mol. With sufficient oxygen available for combustion, the fuels began to burn again, but at a more controlled rate such that sustained burning was established and an equilibrium condition was achieved (approx. 240 s). During this period of equilibrium, upper layer gas species concentrations were approximately zero for oxygen, 0.15 mol/mol for carbon dioxide, and greater than 0.05 mol/mol for carbon monoxide. Lower layer conditions were only slightly less vitiated with average oxygen concentrations between 0.03–0.05 mol/mol, carbon dioxide conditions of 0.13 mol/mol, and carbon monoxide conditions of 0.05 mol/mol.

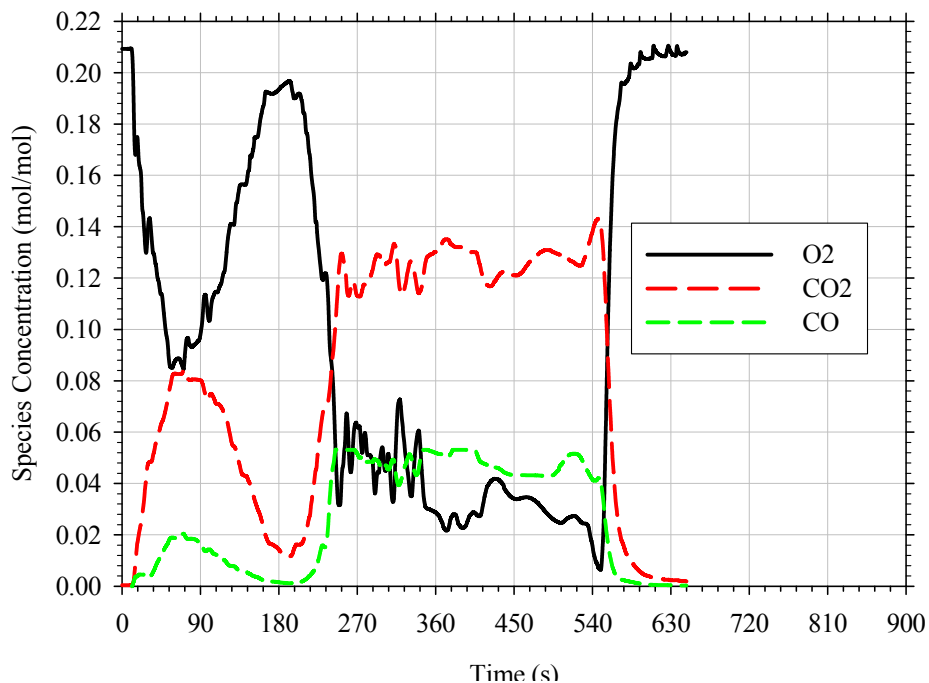


Figure 138. Gas concentrations measured 0.45 m (18 in.) above the floor in Test 6-6.

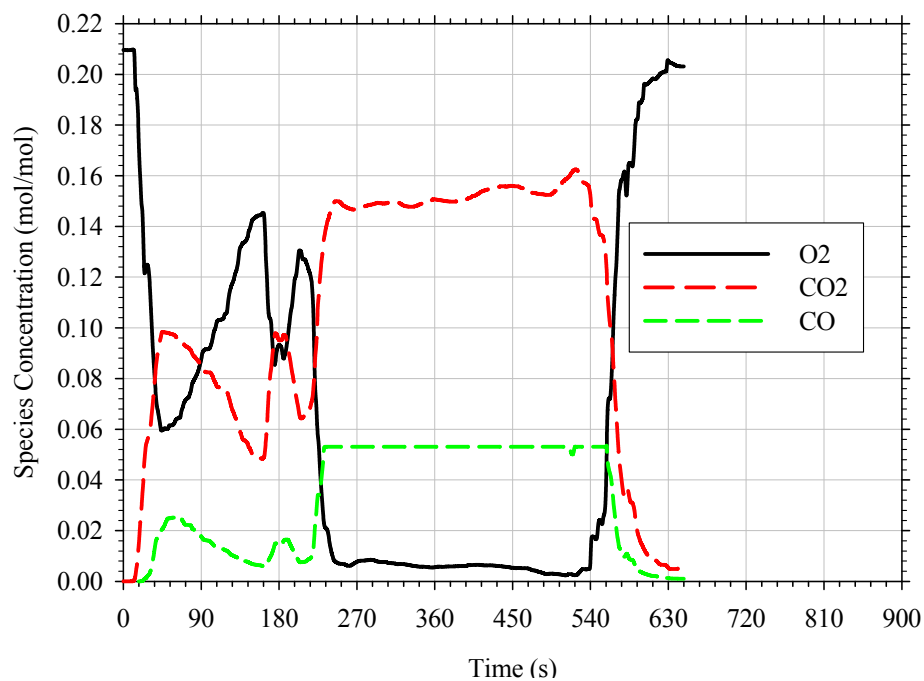


Figure 139. Gas concentrations measured 0.45 m (18 in.) below the ceiling in Test 6-6.

5.6.8 Gasoline on Upholstered Chair with Full Door Opening (w/Vinyl)

Test scenario 6-7 was a fully furnished room with a full open doorway and vinyl flooring. The first item ignited in this test was the upholstered chair using 1.5 L (0.40 gal) gasoline poured onto the seat of the chair. The fuel was allowed to run off the seat onto the floor. The fire was

ignited using a 0.5 L (0.13 gal) gasoline trailer leading from the front of the chair, near the coffee table in the center of the room, and ending at the doorway of the enclosure. The trailer was ignited using a propane torch immediately after it was poured. The trailer quickly spread back to the front of the upholstered chair. As a result of the gasoline spill, the upholstered chair and front left leg of the coffee table were immediately involved. After 110 seconds of burning, the top of the coffee table ignited as intermittent flaming in the upper layer started. Five seconds later (about two minutes after ignition), the door plume ignited. However, this external burning only continued for approximately 10 seconds. The fire was permitted to burn for an additional 60 seconds before manual suppression was started. Photographs showing the evolution of this fire are presented in Figure 140.

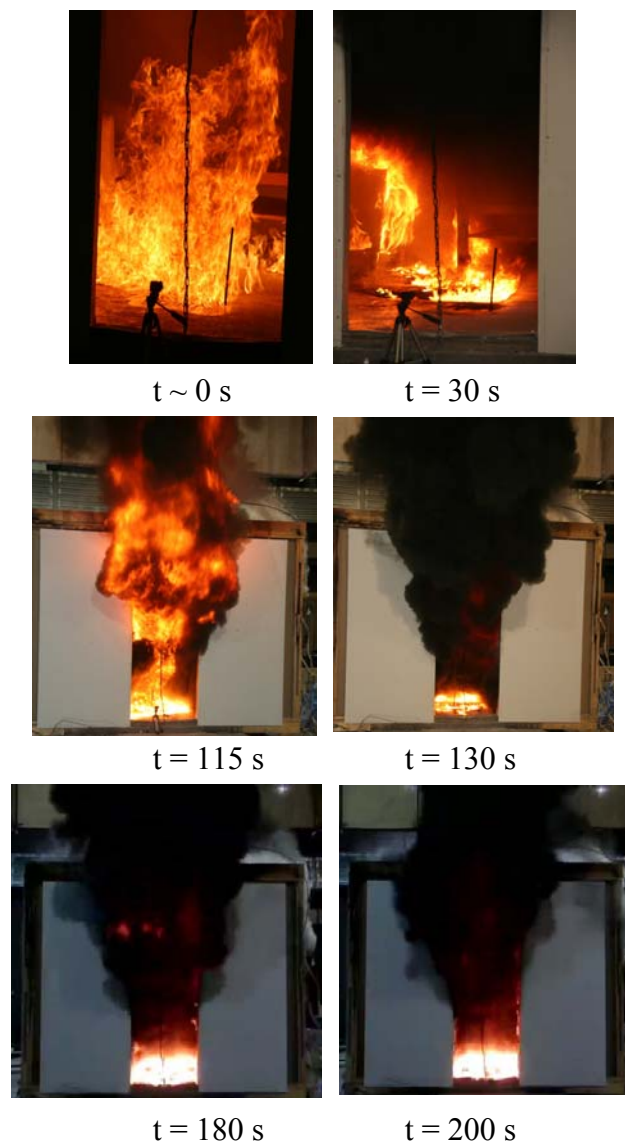


Figure 140. Fire progression observed in Test 6-7.

A plot of the heat release rate from the enclosure fire is presented in Figure 141. The peak heat release was 3.7 MW. The gasoline poured on the vinyl flooring resulted in a 1.2 m² (13 ft²) spill area. Once ignited, the gasoline spill fire produced a peak fire size of approximately

800 kW. This initial peak was reached 45 seconds after ignition. The fire growth began to decay as the gasoline was consumed, leaving the upholstered chair as the only burning combustible within the test compartment. During these 45 seconds of decay, the fire size briefly fell below 500 kW. Eventually, the upholstered chair fire spread to the other combustibles within the enclosure via radiant heating from the upholstered chair fire plume. After 115 seconds of burning within the enclosure, the fire transitioned to burning at the full doorway vent, which produced a peak fire size of 3.7 MW. Approximately 15 seconds after ignition of the door plume, external burning ceased for the duration of the test. The fire continued to burn at a quasi-steady-state fire size of 2.8 MW. The total heat released during this test was 339 MJ over the 190 seconds (3 minute 10 second) burning duration. In this time, the contents of the test enclosure lost approximately 70.0 kg (183 lbs), or twenty-seven percent of their original mass. A further breakdown of the total mass loss from each of the combustibles within the enclosure is provided in Table 19.

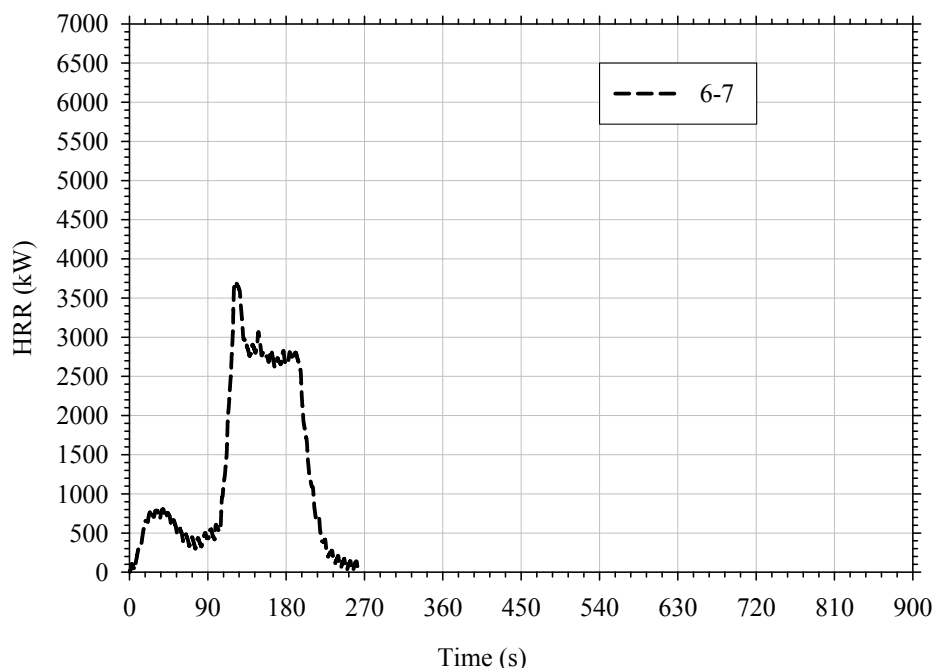


Figure 141. Heat release rate from Test 6-7.

Table 19. Summary of mass loss of combustibles within Test 6-7.

Item	Total Mass Loss (kg [lbs])	Mass Loss Fraction
Upholstered Sofa	8.8 [19.4]	0.19
Upholstered Chair	4.0 [8.8]	0.38
Table	2.9 [6.4]	0.18
Baby Seat	3.0 [6.6]	0.49
Flooring Material	51.3 [113]	0.31
Total	70.0 [154]	0.27

The average temperature (front and back) measured at four elevations is presented in Figure 142. The average temperature gradient over the height of the test enclosure for the duration of the test is presented in Figure 143. Immediately after ignition, there was a rise in enclosure temperatures with a 200°C (392°F) gradient between the 0.3 m (1 ft) and 2.1 m (7 ft) elevation. This brief period of increase was followed by a decay period. The decay in heat release rate, shown in Figure 141, was associated with the extinguishment of the initiating fire, leaving only the burning upholstered chair, which is supported by the heat release rate data provided in Figure 24. Once established, the upholstered chair fire grew in size and eventually spread to neighboring combustibles causing an increase in overall enclosure temperatures. In this test, average upper layer temperatures reached 600°C (1112°F) 110 seconds after ignition.

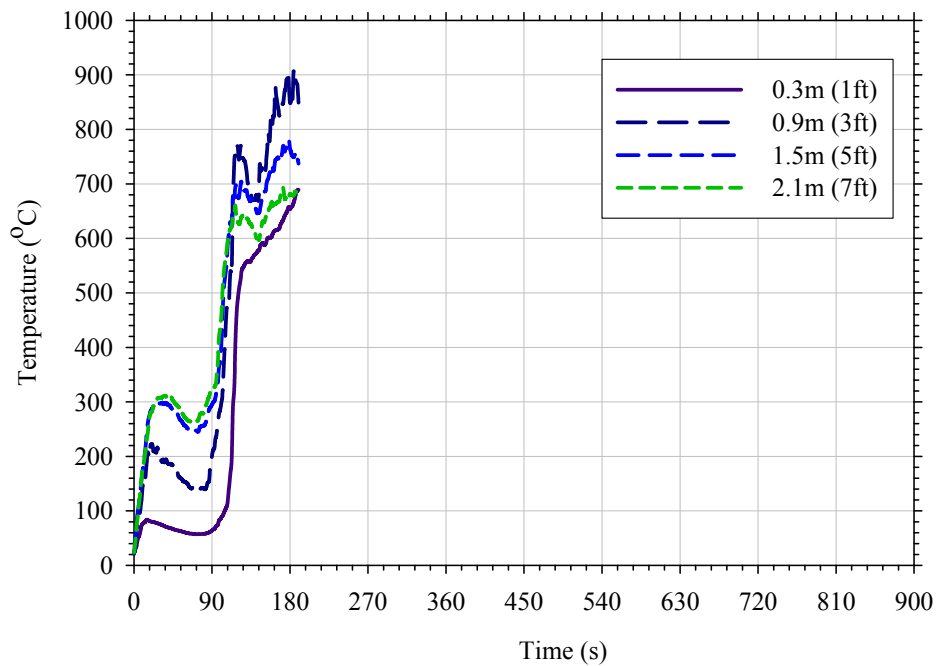


Figure 142. Average temperature measured at four elevations in Test 6-7.

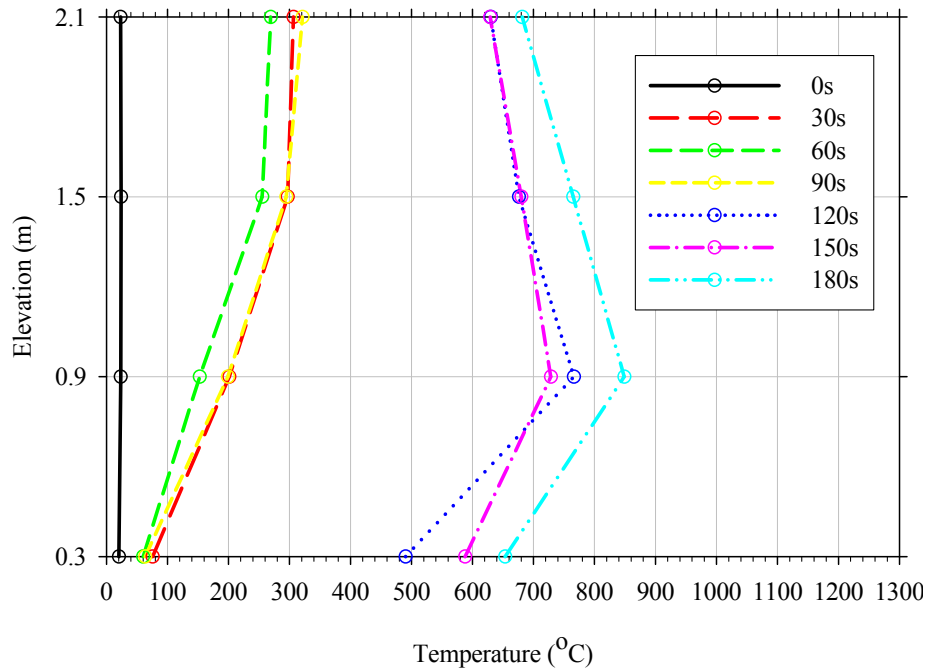


Figure 143. Temperature gradients measured during Test 6-7.

Heat flux was collected at eight locations, six wall and two floor locations. Wall mounted heat flux transducers were located in the rear wall opposite the vent and in the sidewall perpendicular to the vent. Transducers mounted in the rear wall were mounted at heights of 0.6 m (2 ft), 1.2 m (4 ft), and 1.8 m (6 ft). Those mounted in the sidewall were mounted at 0.45 m (1.5 ft), 1.2 m (4 ft), and 1.95 m (6.5 ft). The data collected at the wall and floor locations is presented in Figure 144, Figure 145, and Figure 146. The rear and side location wall heat fluxes were generally comparable over the entire test duration. Heat fluxes did not begin to increase until approximately 90 seconds after ignition. In general, the differences in heat flux over the height of the enclosure were negligible with the exception of the 0.6 m (2 ft) elevation at the sidewall location, which lagged slightly behind. Heat fluxes to the floor in this test differed dramatically. However, this difference is attributed to the initiating fire and upholstered chair being close to the rear gauge which caused the spike in incident heat flux approximately 120 seconds after ignition.

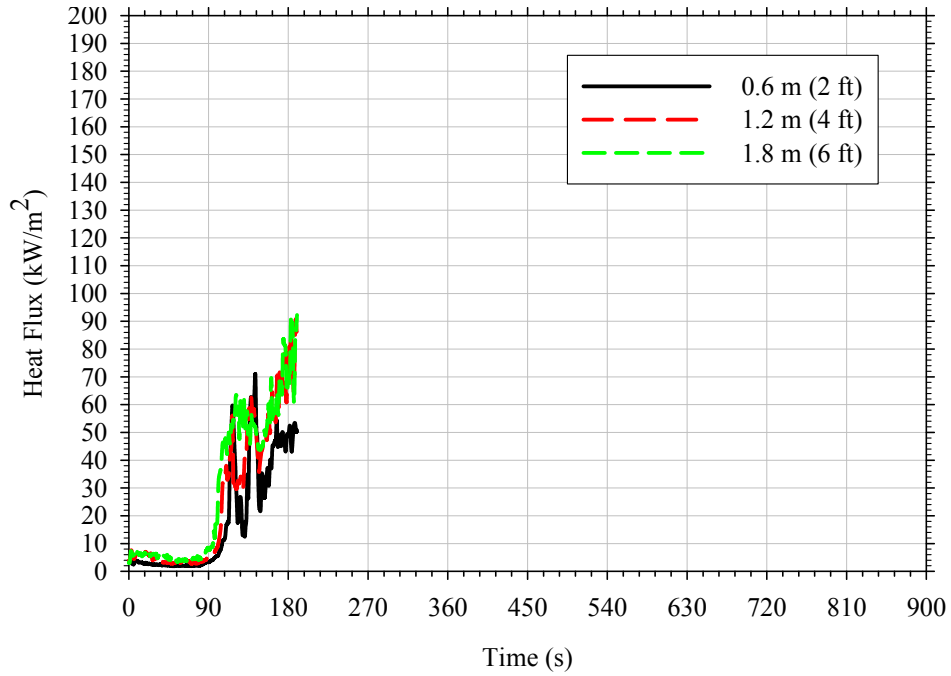


Figure 144. Heat flux on rear wall of enclosure opposite doorway in Test 6-7.

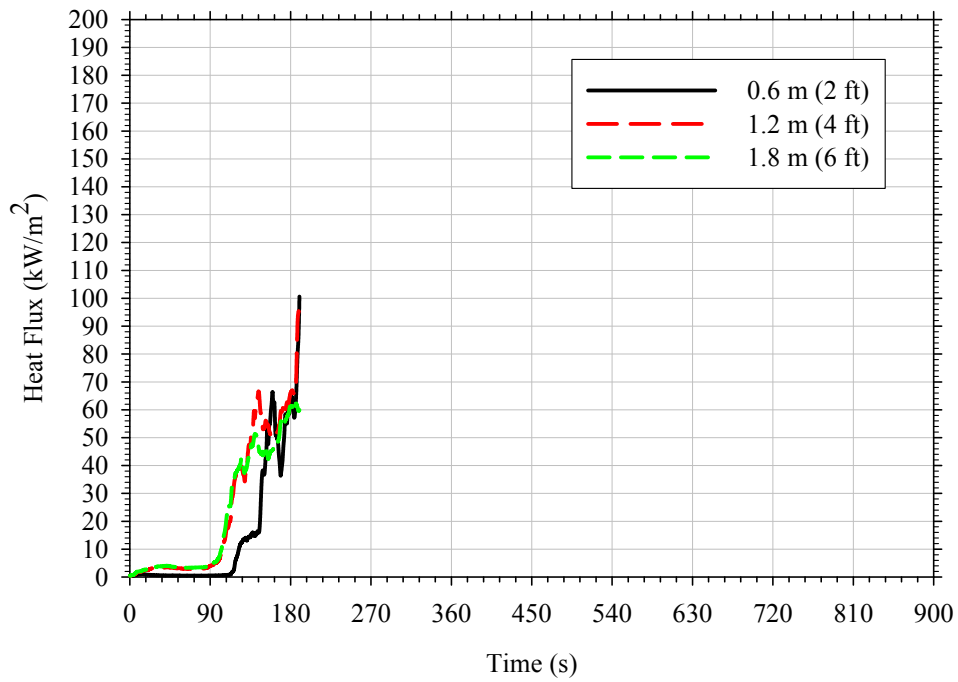


Figure 145. Heat flux on sidewall of enclosure perpendicular to vent in Test 6-7.

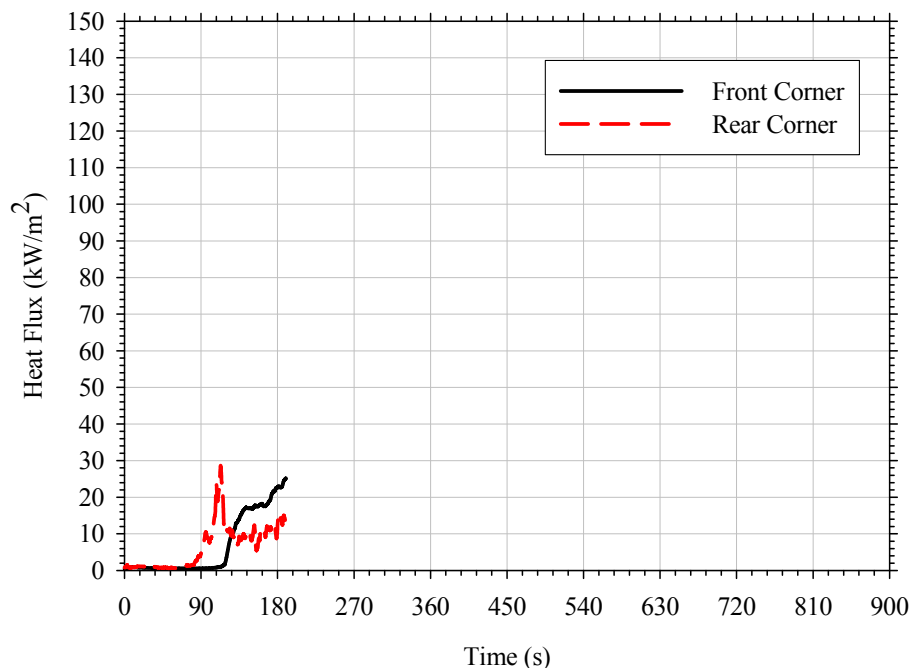


Figure 146. Average heat flux measured at floor in Test 6-7.

The gas species measured low and high in the enclosure are presented in Figure 147 and Figure 148, respectively. The initial fuel spill fire dynamics within the enclosure caused the oxygen concentrations high in the space to briefly fall to 0.16 mol/mol, rebound to a value of approximately 0.18 mol/mol, and finally decrease to around zero for the remainder of the test. Carbon dioxide concentrations in the upper layer exhibited similar behavior reaching peak values of 0.16–0.17 mol/mol. Carbon monoxide concentration did not increase early in the test, but later reached values between 0.03–0.05 mol/mol. Lower layer gas species concentrations showed no signs of the initial changes in the enclosure environment, but later in the test oxygen, carbon dioxide, and carbon monoxide values reached peak values of 0.03, 0.14, and 0.025, respectively. Differences in gas concentration behavior are consistent with the layer heights shown in Figure 148.

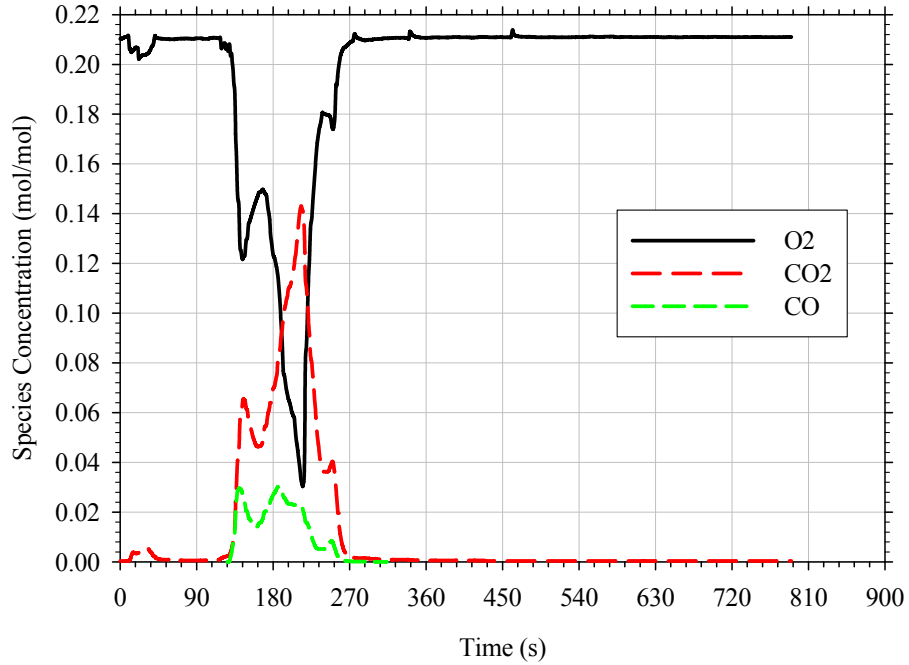


Figure 147. Gas concentrations measured 0.45 m (18 in.) above the floor in Test 6-7.

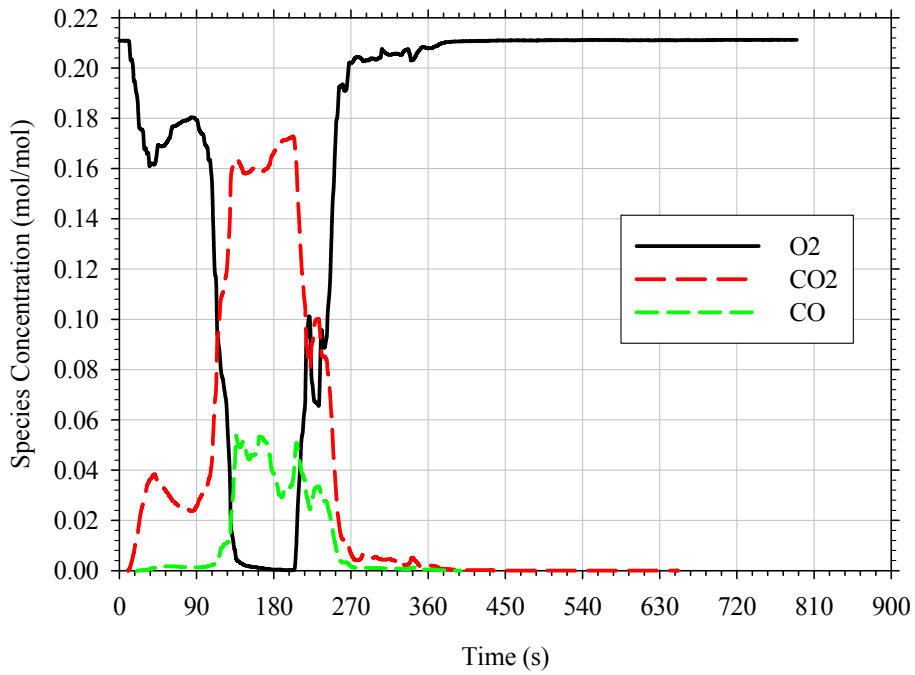


Figure 148. Gas concentrations measured 0.45 m (18 in.) below the ceiling in Test 6-7.

5.6.9 Gasoline on Upholstered Chair with Slit Vent Opening (w/Vinyl)

Test scenario 6-8 was a fully furnished room with a slit vent and vinyl floor. The ignition scenario used in this test was identical to that used in Test 6-7 except for the fact that the gasoline trailer was not ignited until sixty seconds after being poured. Thirty seconds later the upholstered chair became fully-involved. The upper layer gradually descended to the floor and remained at this level for the duration of the test. The enclosure fire was suppressed ten minutes after the start of the test. Photographs showing the evolution of this fire are presented in Figure 149.

A plot of the heat release rate from the enclosure fire is presented in Figure 150. The peak heat release measured in this test was 872 kW, with an average steady-state value of 755 kW. The fire grew to a steady-state value over the initial two minutes. Both the gasoline trailer and gasoline soaked upholstered chair contributed to this initial growth. However, after the initial 60 seconds, the gasoline trailer self-extinguished leaving only the upholstered chair burning. Peak burning of the upholstered chair occurred approximately four minutes after ignition. In general, the chair, baby seat, and flooring material were the primary fuels that contributed to this fire. Damage to the upholstered sofa and coffee table were minimal because the fire was started on the opposite side the enclosure and shortly after ignition, this fire was suppressed due to vitiation of the enclosure. This steady-state burning continued for approximately eight minutes before being manually suppressed. The total heat released during this test was 414 MJ over the 566 second (9 minute 26 second) burning duration. In this time, the contents of the test enclosure lost approximately 83.2 kg (183 lbs), or thirty-two percent of their original mass. A further breakdown of the total mass loss from each of the combustibles within the enclosure is provided in Table 20.

The average temperature measured at four elevations is presented in Figure 151. The average temperature gradient over the height of the test enclosure for the duration of the test is presented in Figure 152. In general, temperatures within the enclosure increased during the first 180 seconds of this test. The upper layer in this test descended to around the 0.9 m (3 ft) elevation and remained at this elevation for the duration of the test. Average upper layer temperatures exceeded 600°C (1112°F) 589 seconds (9 minutes 49 seconds) after ignition. Temperatures within the enclosure peaked at around 360 seconds and slowly decayed after this point in time.



t ~ 0 s



t = 60 s



t = 90 s



t = 420 s



t = 540 s

Figure 149. Fire progression observed in Test 6-8.

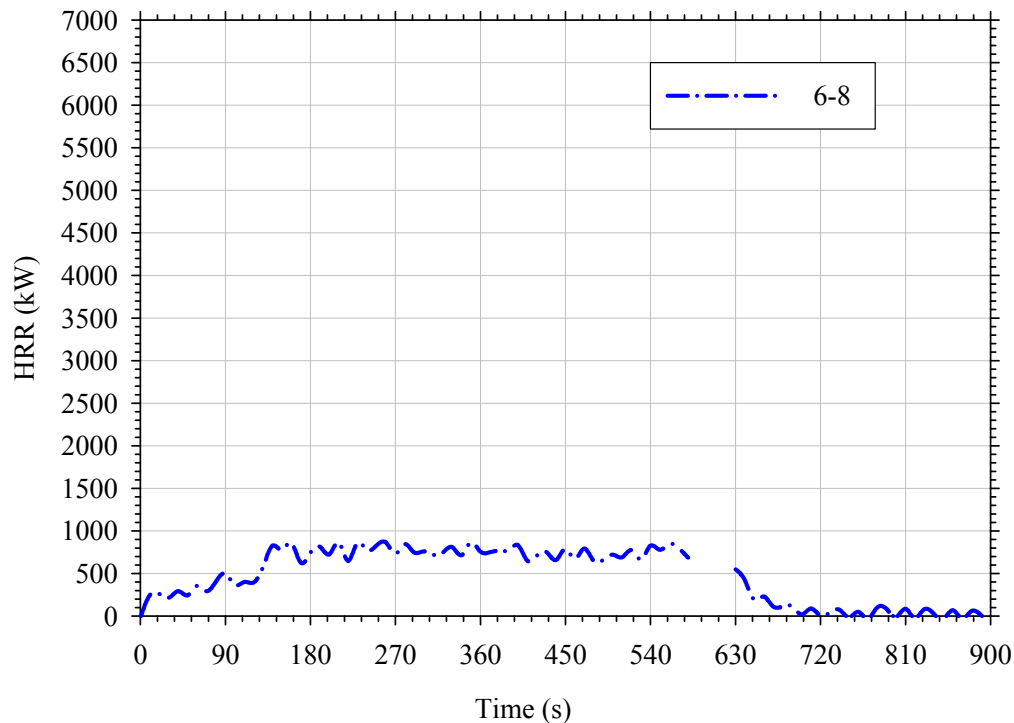


Figure 150. Heat release rate from Test 6-8.

Table 20. Summary of mass loss of combustibles within Test 6-8.

Item	Total Mass Loss (kg [lbs])	Mass Loss Fraction
Upholstered Sofa	2.7 [6.0]	0.06
Upholstered Chair	5.9 [13.0]	0.56
Table	1.2 [2.6]	0.08
Baby Seat	3.2 [7.1]	0.52
Flooring Material	50.2 [111]	0.30
Total	63.2 [139]	0.24

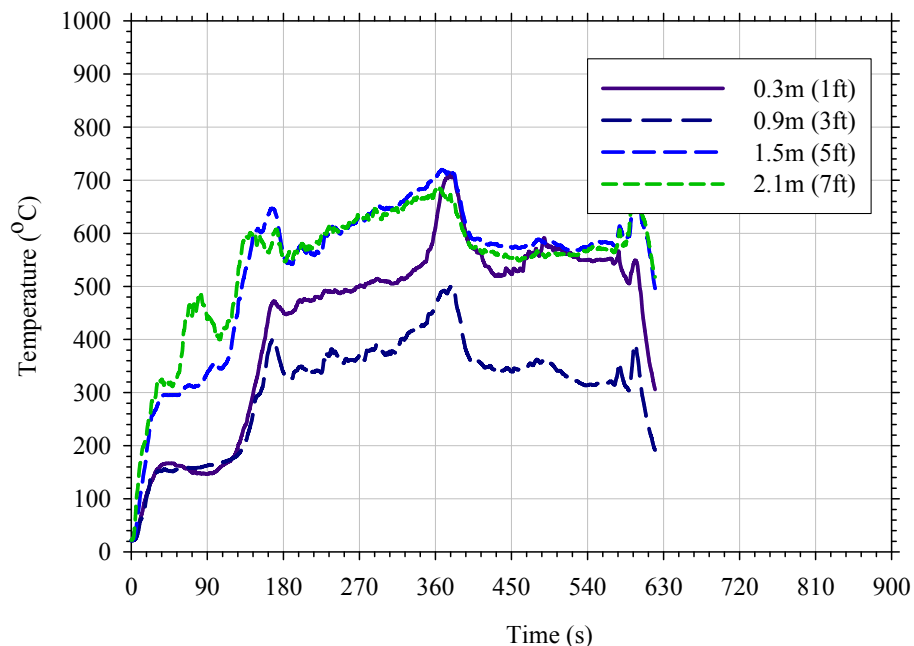


Figure 151. Average temperature measured at four elevations in Test 6-8.

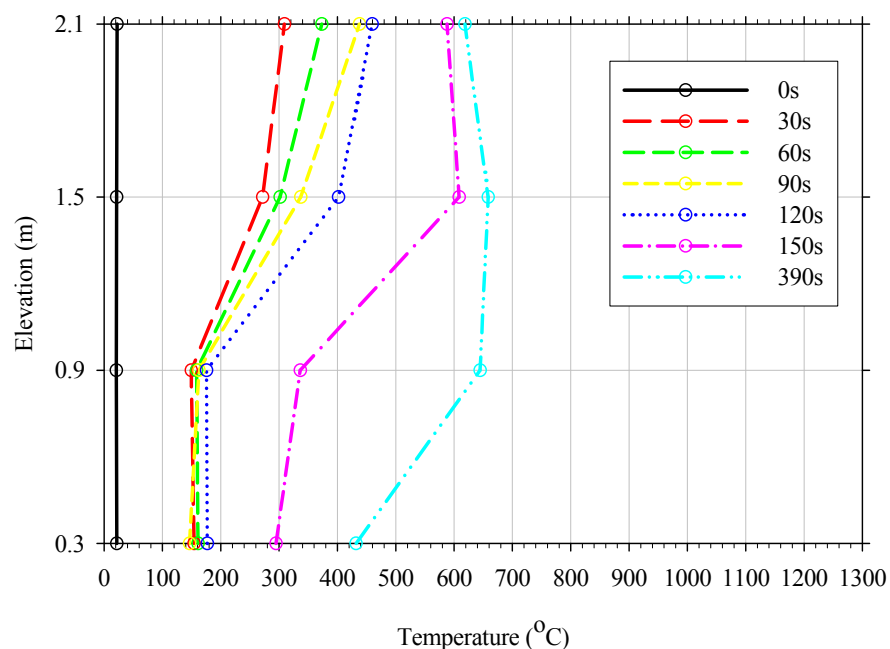


Figure 152. Temperature gradients measured during Test 6-8.

Heat flux was collected at eight locations, six wall and two floor locations. Wall mounted heat flux transducers were located in the rear wall opposite the vent and in the sidewall perpendicular to the vent. Transducers mounted in the rear wall were mounted at heights of 0.6 m (2 ft), 1.2 m (4 ft), and 1.8 m (6 ft). Those mounted in the sidewall were mounted at 0.45 m (1.5 ft), 1.2 m (4 ft), and 1.95 m (6.5 ft). The heat flux data collected at the wall and floor locations is presented in Figure 153, Figure 154 and Figure 155. In general, wall heat fluxes

measured at both the rear wall and sidewall locations were comparable in this test. In both locations, the 1.8 m (6 ft) gauge measured consistently higher heat fluxes than the two lower gauges. After the initial 180 seconds of fire growth, heat fluxes at the highest locations ranged from 20–40 kW/m². Heat fluxes to the floor in this test differed dramatically with the rear gauge increasing sooner and to a higher heat flux than the front mounted gauge. However, this difference was attributed to the initiating fire and upholstered chair being close to the rear gauge. The front gauge increased gradually after the first 150 seconds, to a peak value slightly less than 20 kW/m² at the end of the test.

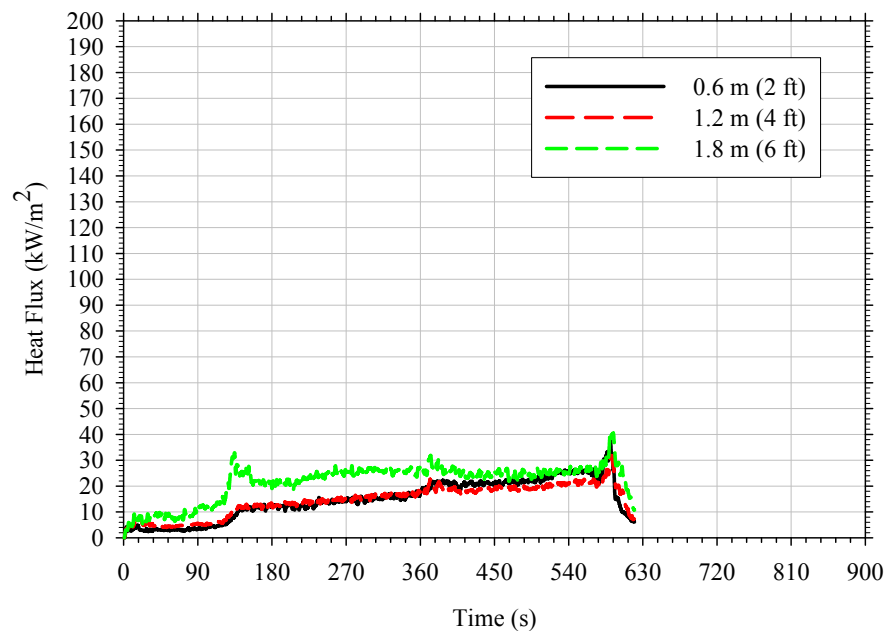


Figure 153. Heat flux on rear wall of enclosure opposite doorway in Test 6-8.

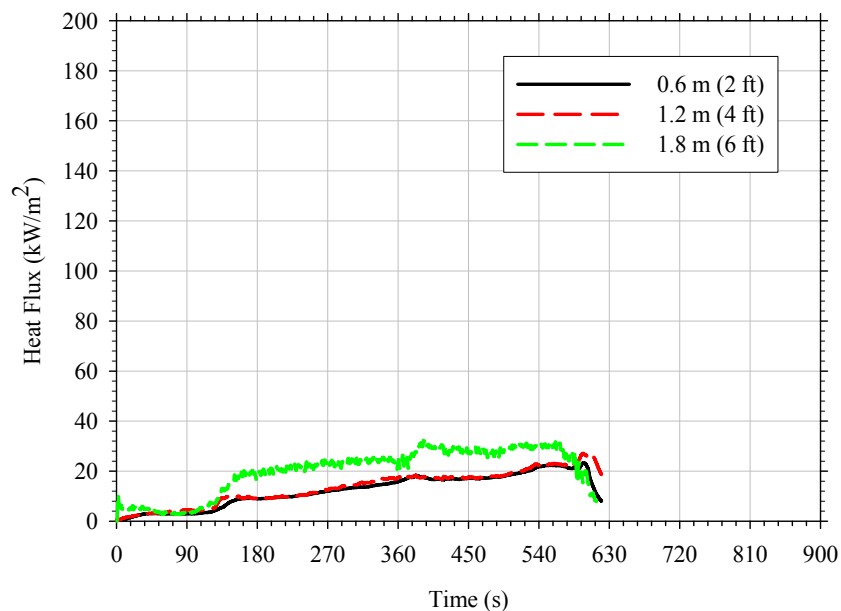


Figure 154. Heat flux on sidewall of enclosure perpendicular to vent in Test 6-8.

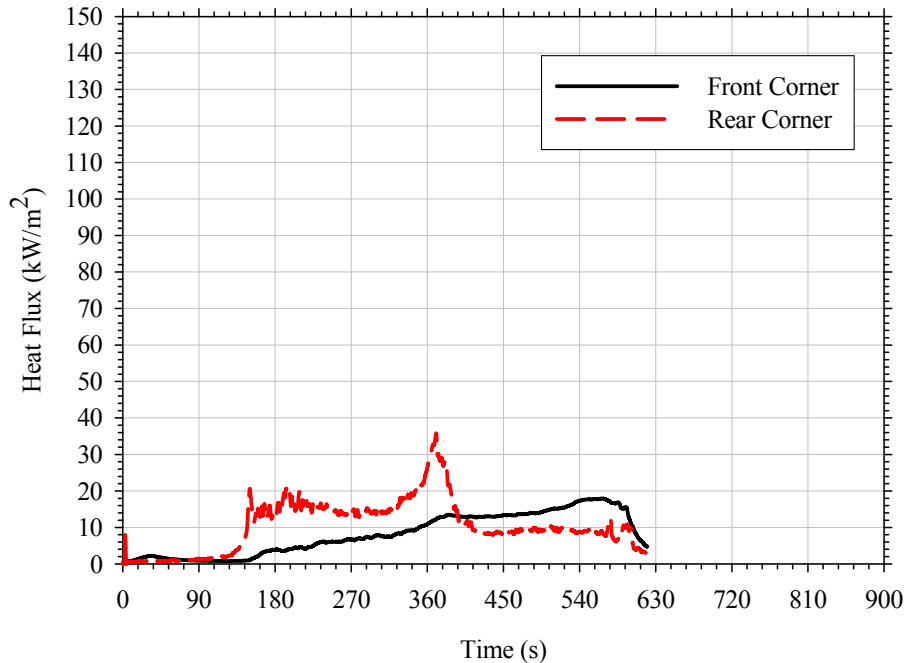


Figure 155. Average heat flux measured at floor in Test 6-8.

The gas species measured low and high in the enclosure are presented in Figure 156 and Figure 157, respectively. Note that carbon monoxide levels at the 0.45 m (18 in.) elevation exceeded analyzer limits approximately 450 seconds (7 minutes 30 seconds) after ignition in this test. Oxygen concentrations in the upper layer gradually decreased to a value of 0.01 mol/mol during the initial 180 seconds and remained at this low level throughout the fire. Lower level oxygen concentrations fell to similar values over the course of the entire test. Initially, lower level oxygen concentration briefly fell to 0.18 mol/mol, which was attributed to the ignition and burning of the initiating spill fire. Once this gasoline fire was consumed, concentrations returned to nominally ambient conditions. Approximately 120 seconds after ignition, lower layer concentrations began to decrease once more reaching concentrations between 0.10 and 0.12 mol/mol. The final decrease in oxygen concentrations in the lower layer occurred 420 seconds after ignition. However, this decrease was an artifact of the flooring material in the vicinity of the sample probe igniting which immersed the probe, making the data non-representative of the lower layer. Carbon dioxide concentrations followed similar trends as that of oxygen with upper layer concentrations reaching average steady-state values of approximately 0.15 mol/mol and lower layer concentrations of 0.07 mol/mol. Carbon monoxide the lower layer and at this location steady-state values of 0.02 mol/mol were achieved.

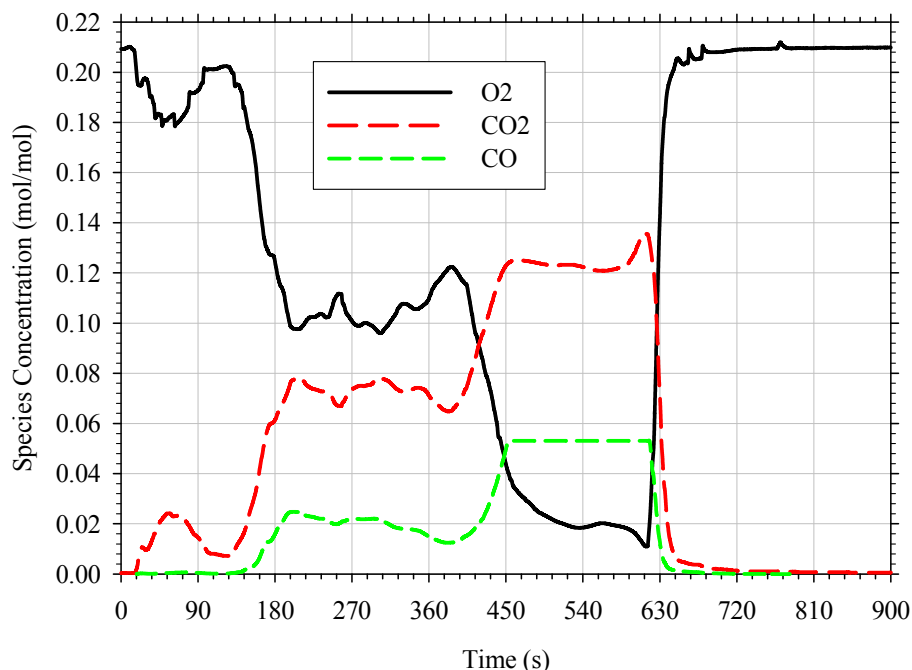


Figure 156. Gas concentrations measured 0.45 m (18 in.) above the floor in Test 6-8.

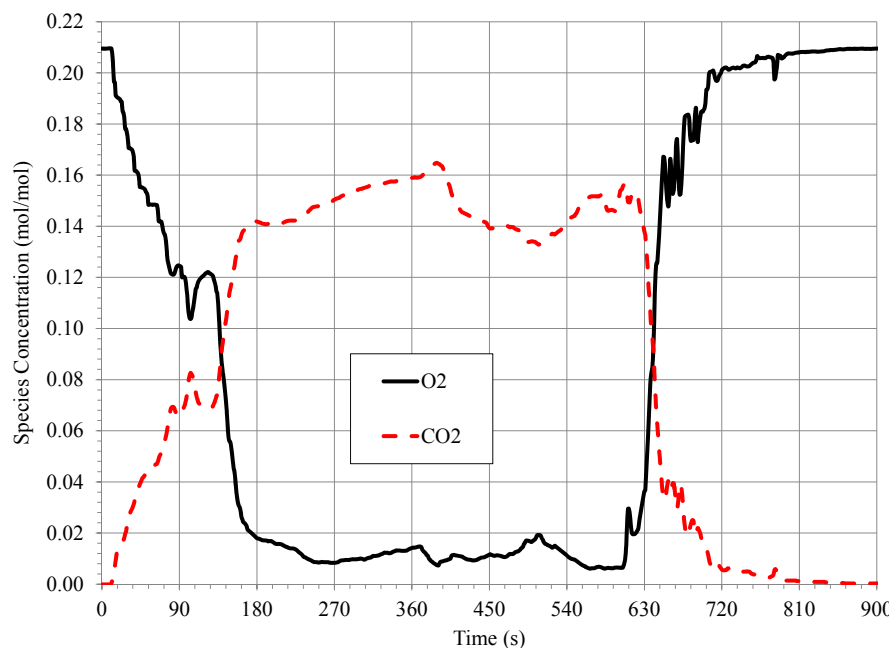


Figure 157. Gas concentrations measured 0.45 m (18 in.) below the ceiling in Test 6-8. Note that in this test the CO concentrations were not measured due to instrumentation error.

6.0 ANALYSIS

6.1 Enclosure Fire Dynamics – Flashover

The occurrence of flashover was evaluated for each of the nine enclosure fires conducted with Class A fuels present. Flashover is defined as the relatively fast transition from a localized

fire to the widespread involvement of combustible material within the room. Thermal data and visual indicators were evaluated and summarized in Table 21. The measured heat release rates at the times the thermal thresholds were reached are also provided in Table 21. Thermal data consisted of calculating peak average upper layer temperature and floor level heat flux to determine the time at which pre-determined thresholds [Peacock et al, 1999] were reached. Average upper layer temperature was calculated based on a visual observation of an upper layer depth in each test and the average of the temperature data collected from within this depth at each time step. The thresholds used were an average upper layer temperature of 600°C (1112°F) and an average floor level heat flux of 20 kW/m² (based on back and front floor heat flux gauges). Visual indicators included the extension of flame out of the vent of the enclosure, the radiant ignition of crumpled printer paper located at various elevations within the enclosure, and the radiant ignition of the flooring material present in the enclosure. Based on the four thresholds described above, flashover occurred in all but one of the enclosure fire tests conducted with Class A fuels present. In Test 6-2, none of the indicators, thermal data or visual, were reached.

In all of the full door ventilation tests, the upper layer temperature threshold was reached first, followed by the floor level heat flux threshold, followed by flame extension from the vent. However, it should be noted that the occurrence of all three of these indicators typically occurred within 60 seconds. On average, the upper layer temperature threshold was reached less than ten seconds prior to the floor level flux threshold being reached. The extension of the flame plume through the ventilation opening occurred less than 60 seconds after the upper layer threshold was reached. The occurrence of flashover was quite clear and indisputable for the full door fires. Visual observations of the ignition of paper indicators and the flooring material were clearly definable. The ignition of floor level combustibles always occurred after both the 600°C (1112°F) and 20 kW/m² criteria were achieved, but before ignition of the door plume. The time differences between the two criteria and floor level ignition ranged from 5 to 43 seconds. In general, these criteria appear to be reasonably representative and conservative in that they predict flashover (ignition of all combustibles in the space) slightly earlier than may occur in actuality. The occurrence of external flames lagged behind the occurrence of flashover.

For the slit vent condition, the occurrence of flashover was not as clearly defined (visually) or consistent as was observed for full door ventilation. Three of the four tests with the slit vent reached the thermal thresholds. The radiant ignition of paper indicators was only observed in one of the tests, despite always being consumed based on post-test observations. Due to the reduced visibility in these limited ventilation tests (i.e., upper layer depths near the floor) the time of ignition of the indicators could not be determined. In two of three tests where thermal thresholds were reached, floor level heat fluxes were reached first. On average, this threshold was reached four minutes prior to upper layer temperatures reaching 600°C (1112°F). In the third test, the temperature and heat flux thresholds were reached simultaneously. Flame extension from the vent was only observed for one test (Test 6-4) with the slit vent scenario. In this test, the flame extension was intermittent with periods of vent burning lasting between 30–60 seconds. The lack of sustained flame from the vent is consistent with the visual definition proposed by Francis and Chen [2012].

Table 21. Summary of Flashover Indicators.

Test ID	Vent Condition/ Flooring/Ign. Scenario	Time to Reach 20kW/m ² at Floor Level (s)	Fire Size at Time Heat Flux Threshold was Reached (kW)	Time to Reach Average UL Temperature of 600°C (s) ¹	Fire Size at Time UL Temperature Threshold was Reached (kW)	Time to Ignition of Door Plume (s)	Time to Ignition of Paper Indicators (s)	Time to Radiant Ignition of Flooring in Enclosure (s)	Fire Size at Time Radiant Ignition of Flooring Occurs (kW)
6-0 ²	Full Door/ Carpet /Class A	346	2417	333	2265	358	N/A	399	2387
6-1	Full Door/Carpet/ Spill on Floor	123	2654	119	2296	192	101 ³ / 163 ⁴	163	2700
6-2	Slit Vent/Carpet/ Spill on Floor	N/R	-	N/R	-	N/R	N/R	N/R	N/A
6-3	Full Door/Carpet/ Spill on Chair	114	3080	101	2235	146	89 ³	134	2748
6-4	Slit Vent/Carpet/ Spill on Chair	464	884	725	1327	366 ⁵	N/O	N/O	N/A
6-5	Full Door/Vinyl/ Spill on Floor	34	2735	33	2762	63	- ⁶	57	4876
6-6	Slit Vent/Vinyl/ Spill on Floor	217	944	216	993	N/R	N/O	N/O	N/A
6-7	Full Door/Vinyl/ Spill on Chair	N/R	-	110	1267	120 ⁷	110 ³	115	2332
6-8	Slit Vent/Vinyl/ Spill on Chair	362	683	286	832	N/R	N/O	N/O	N/A

N/R – not reached

N/O – not observed due to smoke layer

1 – Average upper layer temperature taken from measurements 1.5–2.4 m (5–8 ft) above the floor in two locations

2 – Time zero based on ignition of sofa, not ignition source

3 – Indicator placed on top of coffee table (0.45 m [18 in.] above floor)

4 – Indicator placed on floor

5 – Intermittent ignition/extinguishment of door plume was observed

6 – Indicators were ignited by flash fire created when igniting gasoline spill

7 – Flame extension from vent only observed for 10s

It should be noted that although the two thermal criteria for flashover were achieved in three of the four slit ventilation tests conducted, it is expected that flashover did not actually occur. In these tests, fire growth was inhibited by the limited ventilation condition. The vent condition created a vitiated upper layer that extended almost to the floor of the enclosure causing the fire to bank down and burn primarily at low levels. Over time, fire spread to adjacent combustibles and involved the whole room as evidenced post-test by fire damage across the whole space. The instantaneous involvement of all combustibles within the enclosure was not visually observed as the deep smoke layer prevented a clear view of the flooring and paper indicators. Although the average floor level heat flux reached a value of 20 kW/m^2 , this was due to a high reading above the criteria in only one of the two measurement locations. Consequently, this non-uniformity indicates that the thermal conditions throughout the space were not sufficient to cause a rapid transition from localized burning to wide spread ignition of combustibles throughout the room. In other words, flashover did not actually occur. The upper layer temperature measurements were generally consistent with this conclusion in that upper layer values were only slightly above 600°C (1112°F) and usually for only short periods of time. Test 6-6 was the most notable exception (Figure 133) and temperatures ranged from 600 to 700°C for approximately two minutes.

The conclusion from the limited ventilation fire tests is that full room involvement occurred, but without clearly flashing over. Instead, fire spread across combustibles, and pyrolysis (not necessarily flaming combustion) of materials exposed to a hot environment caused thermal damage throughout the enclosure. The importance of this conclusion is that the post-fire damage alone cannot be used as a determination of whether flashover occurred (i.e., a relatively rapid transition from local to widespread involvement of combustible material within the room). Depending on the fire circumstances (e.g., ventilation, occupant egress, etc), the impact of this conclusion for fires that may have limited ventilation is that temperatures and heat fluxes may not have reached as high levels as frequently associated with flashover conditions.

As shown in Table 22, the fire size needed to produce upper layer temperatures greater than 600°C (1112°F) and floor level heat fluxes greater than 20 kW/m^2 varied depending on the ventilation opening. For full door scenarios, the average fire size was approximately 2.4 MW . For the slit vent scenarios, an average fire size of approximately 1.0 MW was needed. Compared to the data set compiled by Babrauskas et al. [2003], these values fall within one standard deviation of the mean value that was established as the heat release rate value needed to reach flashover (i.e., $1975 \pm 1060 \text{ kW}$). It should be noted that Brabauskas' data set is based on tests conducted in a room with slightly smaller dimensions (i.e., $2.4 \text{ m} \times 3.6 \text{ m} \times 2.4 \text{ m}$ ($8 \text{ ft} \times 12 \text{ ft} \times 8 \text{ ft}$)) than evaluated in this program. However, the difference in effective surface area for heat transfer (i.e., total area of enclosure surfaces) between the enclosure used in this work and the enclosures considered by Babrauskas et al. [2003] was only 6 m^2 (65 ft^2). This difference constitutes an increase of less than 100 kW in fire size to reach flashover conditions based on Equation 6 of Peacock et al. [1999].

Various correlations have been developed to predict the heat release rate needed to produce flashover conditions within an enclosure. Table 22 shows the calculated heat release rate based on three of these correlations compared to the average heat release rate at flashover for the full door fires and the average peak values for the slit vent fires. It should be noted that the heat

release rate values presented for Babrauskas [1980], Thomas [1981], and McCaffrey [1981] are all based on correlations developed generally from the same database of fires.

Table 22. Comparison of heat release rates required to produce flashover conditions to average values measured in enclosure tests.

Ventilation Conditions	Avg. Measured HRR (Std Dev)	Babrauskas [1980]	Thomas [1981]	McCaffrey [1981]
Full Door	3177±1143	1973	1362	1893
Slit Vent	944±216*	420	592	416

*Value represents average of peak HRR achieved since flashover did not occur.

The correlations were also developed using the same thermal flashover criteria (i.e., upper layer temperature of 600°C (1112°F) and and/or 20 kW/m² at floor level). The correlation-based heat release rate estimates were consistently lower than that measured at the onset of flashover in these tests. On average, for the full door ventilation conditions, the correlation predictions were 55 percent of the measured value. For the slit vent condition, the predictions were approximately 50 percent of the measured peak values. The conservative values obtained from the correlations are consistent with the results of other researchers [Babrauskas et al. 2003] who found that these predictions were generally a lower bound (i.e., minimum heat release at which flashover would occur in a given enclosure). Babrauskas concluded that the development of flashover and the corresponding fire size was dependent on the relationship between fire growth and time. Shorter duration fires required larger fire sizes to achieve flashover because of the need to quickly develop a hot, radiative upper layer. Contrary to this, lesser fire sizes are required to achieve flashover for prolonged fire durations because time is available for a sufficiently hot upper layer to develop. These generalizations are consistent with the findings presented in Table 22, in that for the full door ventilation scenarios, rapid-fire development was observed and increased heat release rates needed for flashover were measured.

Since the correlations are based on fires with full door ventilation, it is not surprising that they predict heat release rates for flashover in limited ventilation fires even though flashover may not occur, as seen in the slit vent tests. This work serves to demonstrate that ventilation conditions must be considered when evaluating the fire dynamics of a fire event relative to the post-fire damage. As noted above, a limited ventilation compartment may become fully involved and result in widespread fire damage across all flooring and furniture. In addition, a generic correlation for flashover may yield a required heat release rate that is well within reason given the fuel loads in the room. For example, in the testing in this program, the correlations predict that heat release rates for flashover in the slit-vent fires of approximately 400 to 600 kW. These heat release rates are in the range of the upholstered chair and coffee table, respectively. Based on this calculation and the post-fire damage, one may conclude that the fire flashed over early in the fire development and reached temperatures well in excess of 600°C (1112°F). However, the same fire damage can occur without flashover due to limited ventilation that can actually limit fire growth to progress over a longer timeframe with temperatures below 600°C (1112°F).

6.2 Enclosure Effects

The impact of an enclosure on the burning rates and overall fire dynamics of three different fire scenarios was evaluated. The scenarios were unconfined, liquid fuel spill fires; fixed-area (pan), liquid fuel fires; and Class A fuel fires ignited using liquid fuels. Spill fires were conducted on two different substrates (carpet and vinyl) under two different ventilation conditions. Pan fires were conducted using two different fuels (heptane and alcohol), two different locations (center and corner of room), and two different ventilation conditions. Class A fuel fires were conducted for three different ignition scenarios and two different ventilation conditions. The purpose of this section is to discuss the impacts of the enclosure and the various parameters described above for each of the three fuel scenarios.

6.2.1 Spill Fires

Open burning and enclosed scenario heat release rates were compared to evaluate the impact of the enclosure on 2.0 L (0.53 gal) gasoline spill fires. Comparisons were made for spill fires on two substrates, vinyl and carpet. The spill areas for the open-air and enclosed spills were 2.0 m² (22 ft²) and 2.5 m² (27 ft²), respectively. The larger area measured in the enclosure fire scenario was due to both the non-uniformity of the enclosure floor relative to the open burning substrate and the method of release. Due to the numerous fire tests that had been conducted in the test enclosure prior to the vinyl spill fire, the sub-floor was not as level as that used in the open burning scenarios. This non-uniformity resulted in the liquid spill preferentially spreading to areas with the lowest elevation, which was not observed in the open burning scenarios. The increased area measured in the enclosed scenario could also be an artifact of the different release mechanisms used. The manual pour used in the enclosed scenario may have resulted in a preferential flow of the liquid in one direction, which could have caused a larger pattern to form. Based on these spill areas and the measured 10 second peak heat release rates, the spill fires conducted both outside and within the test enclosure had similar heat release rates per unit area (i.e., approximately 1200 kW/m²). A comparison of the heat release rates from these fires is provided in Figure 158. These heat release rates are also comparable to the data collected by Mealy et al. [2010] for gasoline spills on vinyl with 30-second ignition delay times. The growth rates of the spill fires were also consistent. They reached peak values approximately 20 seconds after ignition, also consistent with the findings of the earlier spill fire study conducted by Mealy et al. [2010].

The primary difference between the open air and enclosed tests was the burning duration. The open-air spill fire reached a peak heat release rate of approximately 2.5 MW (approximately 1200 kW/m²) twenty-two seconds after ignition and immediately transitioned to the decay phase of the fire. The enclosed spill fire grew at a similar rate to a similar peak but did not immediately transition to the decay phase. Instead, sustained burning at or near the peak value (2.5 MW) was maintained for an additional 25 seconds before beginning to decay. This sustained period of peak burning is attributed to the involvement/contribution of the vinyl flooring material and flooring adhesive present within the test enclosure. As described in Section 5.4.1, visual signs of thermal degradation of the flooring material were initially observed 10–15 seconds after ignition and the flooring material was observed to begin locally igniting in several locations 20–30 seconds after ignition. Ignition/involvement of the vinyl flooring and adhesive was not observed in any of the open-air vinyl spill fires conducted in this work or that reported in previous spill fire studies

[Mealy et al. 2010]. A comparison of the post-fire damage for open air and enclosed spill fires is presented in Figure 159. Note the substantially different level of thermal degradation of the flooring material and underlying adhesive for the enclosed scenario. For the open-burn scenario (shown on left), the primary damage is thermal discoloration of the vinyl with some surface cracking of the material. No penetration through the vinyl layer was observed. For the enclosed scenario, there were several areas where the vinyl flooring was consumed and areas where large cracks in the material were formed exposing the underlying adhesive and plywood subfloor.

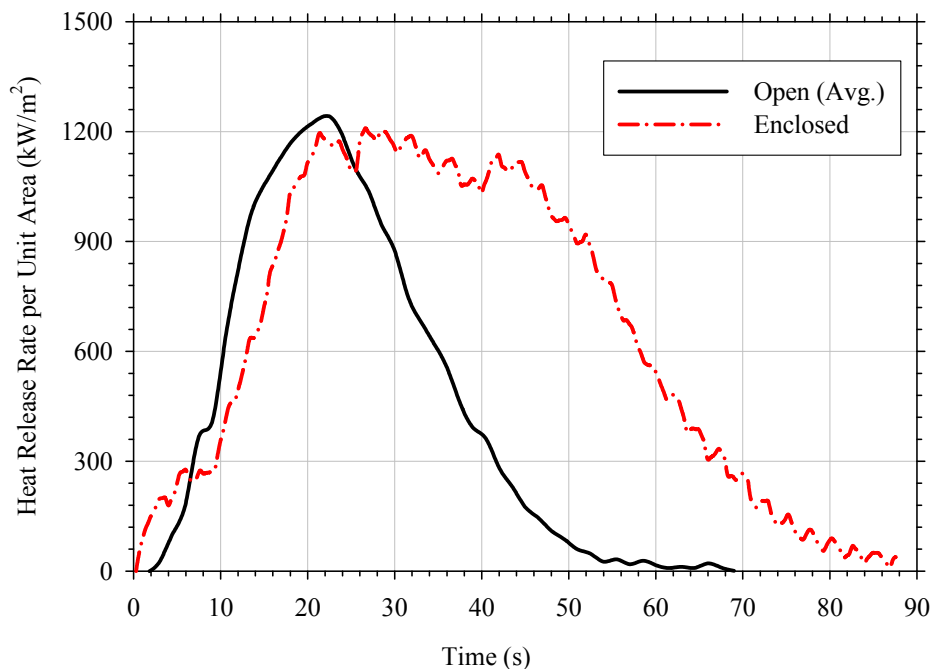


Figure 158. Comparison of gasoline spill fire heat release rate per unit area on vinyl floor between open burning and within enclosure with full-open doorway.



Figure 159. Photographs of the condition of the vinyl flooring material after open burning (left) and enclosed (right) gasoline spill fire scenarios.

In addition to the visual differences shown in Figure 159, a comparison of the total heat release measured during the open air and enclosed tests shows the additional heat contribution from the flooring material. Based on data presented in Table 4, the total heat content of a 2.0 L (0.53 gal) gasoline spill fire is 56 MJ. On average, the total heat released during the open-air spill fires was 62 MJ suggesting that a relatively small amount of heat energy (approximately 6 MJ) was contributed by the flooring material during these fires. The total heat released during the enclosed spill fire was approximately 140 MJ. Removing the heat energy associated with the gasoline spill fire (i.e., 56 MJ) leaves 84 MJ attributed to the combustion of the flooring material. Upon inspection, the localized areas of the plywood subfloor had been thermally degraded in the enclosed scenario. Based on post-test mass measurements the vinyl flooring system lost approximately 5.4 kg during this test. Using the calculated total heat released by the flooring material and the measured mass loss of the flooring system, an effective heat of combustion of 15.6 MJ/kg was calculated for the vinyl floor. This value is approximately 25 percent greater than that measured in small-scale testing (i.e., Table 8) conducted using the cone calorimeter.

The involvement of additional vinyl flooring in the enclosed scenario is attributed to both the plume bending that was observed during this test as well as the radiant heating of the flooring material by the upper layer. The tilting of the flame plume was observed soon after ignition, as was the thermal degradation of the flooring material near the vent. As stated in the results section, the upper layer in this test reached temperatures of approximately 500–600°C (932–1112°F) 20–30 seconds after ignition with heat fluxes at the floor ranging from 10–35 kW/m². This caused floor material, outside the initial spill area, to thermally degrade, off-gas, and ignite. The ignition of the flooring outside the initial spill area signified the occurrence of flashover within the enclosure, which allowed the vinyl flooring to burn for a longer duration than was measured in the open. The prolonged burning in this test was promoted by the presence of the hot upper layer providing sufficient radiant heat to allow the vinyl flooring material to burn.

On carpet, average gasoline spill areas for the open-burn and enclosed spills were 0.36 m² (3.9 ft²) and 0.2 m² (2.2 ft²), respectively. Differences in spill areas for these scenarios are attributed to the different spill mechanisms used in the tests. Open-burn spills were released from a fixed spill arm container located 0.3 m (1 ft) above the substrate with a 64 mm (2.5 in.) opening. The enclosed spills were manually poured from an elevation of 0.3 m (1 ft) above the substrate using a beaker. The larger opening on the mechanical spill arm (open burning test) resulted in a larger impact area for the gasoline on the carpet while the narrow spill stream from the beaker resulted in a smaller impact area. Even with the different spill areas, the measured 10-second peak heat release rates per unit were within eight percent of each other. A comparison of the heat release per unit area from these fires is provided in Figure 160.

The heat release rate per unit area during the initial 60–90 seconds of fuel-controlled burning was 914 kW/m² for the open scenarios and 850 kW/m² for the enclosed scenario. These heat release rates per unit area are within the range of values reported by Mealy et al. [2010] for 0.5–5.0 L (0.13–1.3 gal) gasoline spills on carpet for the initial period of burning (e.g., 284–1390 kW/m²). The range of values reported by Mealy et al. [2010] is a result of the carpet substrate and the method used to measure spill area. Despite the fact that larger quantities of liquid are poured, the porosity of the carpet prevents a larger spill area from being visually measured. Therefore, although fire size increases with increasing fuel volume, the initial spill area holds constant, which causes a range of HRRPUA values to be calculated.

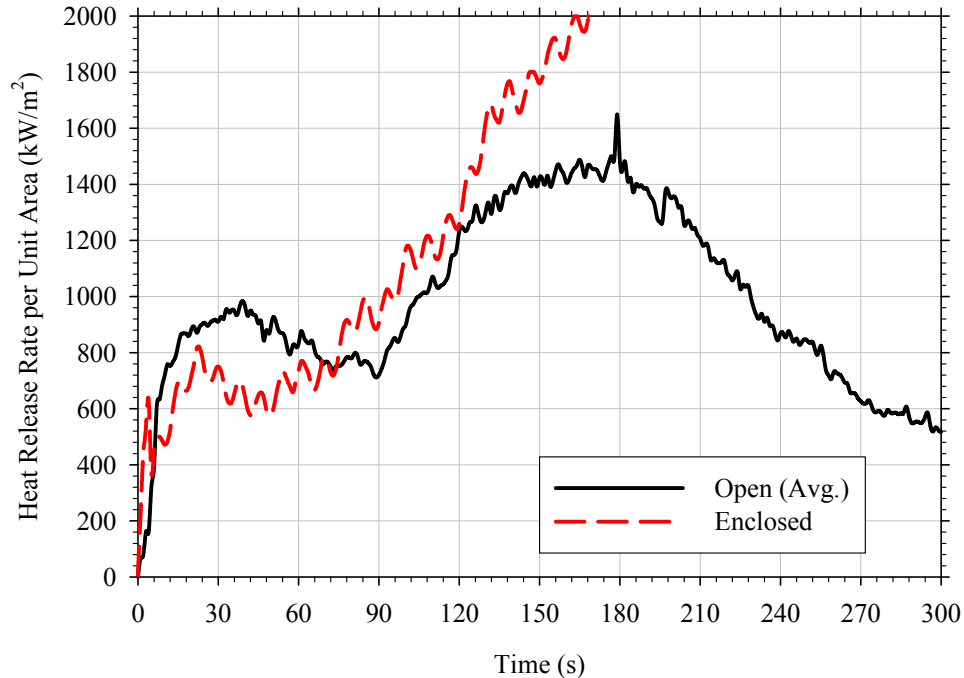


Figure 160. Comparison of average heat release rates per unit area for open burning carpet spill fire and spill fire conducted within enclosure with full-open doorway.

With respect to the growth rates measured in these fires, during the fuel-controlled (i.e., 0–90 seconds) and substrate-controlled (i.e., ~90–150 s) growth periods, the rates of growth were comparable. The primary difference between the open and enclosed tests was the duration and severity of the substrate-controlled fire and the extent of involvement of the flooring material. For open scenarios, during both fuel-controlled and substrate-controlled burning, the radiant heat feedback to the fuel surface was not sufficient to support continuous spread of the fire over the substrate. The vertical fire plume was not large enough to irradiate adjacent carpet flooring to the point of ignition. Consequently, the open burning spill fires on carpet reached a peak value 60–90 seconds after fuel-driven growth (i.e., at 150 to 180 s) and then began to decay.

This transition to a decaying fire scenario was not observed in the enclosed scenario. Instead, the fire continuously spread across the carpet, eventually involving the entire surface. The continued growth of the fire on the substrate was primarily attributed to the airflow into the compartment and the resulting flame plume bending. As shown in Figure 161, at the point in time where the open-burn and enclosed fire heat release rates diverge at 120 seconds, the upper layer has descended to approximately 0.6 m (2 ft) above the floor and has an average temperature of 235°C (455°F). The bending of the fire plume to the rear of the enclosure, due to incoming airflow, and the corresponding increased heat flux exposure to the neighboring flooring material resulted in more material becoming involved. As shown in open burning tests, in the absence of plume bending and the associated addition of incident heat flux, the carpet material does not readily become involved and spread much beyond small flamelets around the perimeter of the burning area.

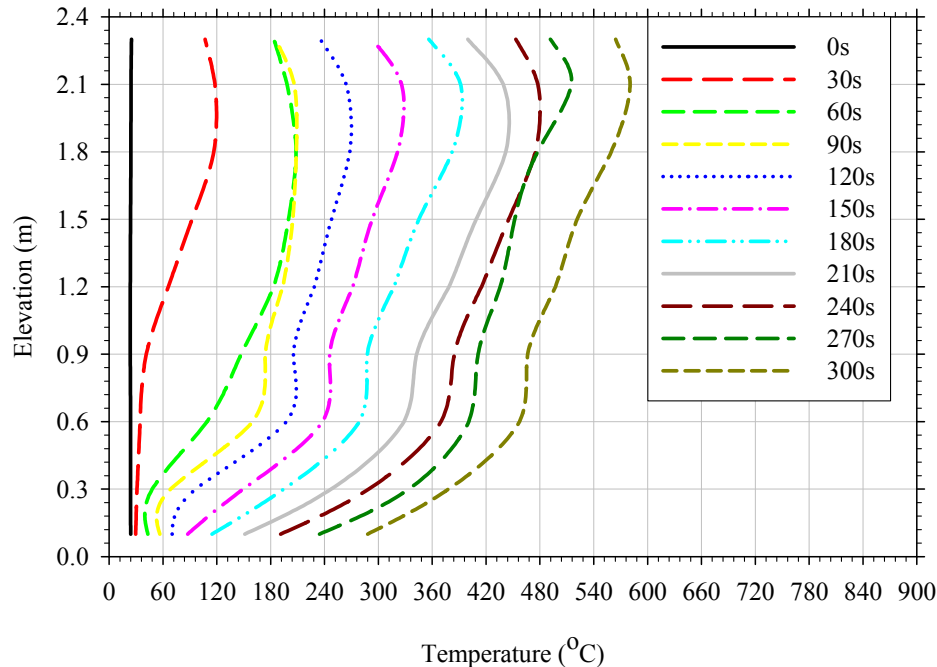


Figure 161. Thermal profile within enclosure during gasoline spill fire on carpet.

For both the vinyl and on carpet flooring, liquid fuel spill fires, the enclosure fires behaved differently than the same spill fires conducted in the open. In both cases, the primary difference was the involvement of additional combustible material (i.e., neighboring flooring material). For the vinyl substrate, the fire in the enclosure burned at the same peak value, but for an extended period of time as opposed to immediately transitioning to the decay phase as was observed in the open. Due to the involvement of additional flooring material, the carpet enclosure fire resulted in a larger fire than was observed in the open. Considering the short period of time in which the liquid fuel was the primary material burning, the enclosures did not have an effect on the spill fire, but did contribute to the fires growing larger and involving more material. There will be a certain critical room volume to fire size that will dictate whether the enclosure will lead to fires growing beyond the initial spill areas. Additional work is needed to identify this critical parameter.

6.2.2 Pan Fires

Open burning and enclosed scenario heat release rates from Test Series 2 and 5 were compared to evaluate the impact of the enclosure on the burning dynamics of heptane and denatured alcohol fuel pan fires (Figure 162). Other enclosure variables considered included the ventilation condition and the fuel location (center or corner of room). A summary of the 0.23 m² (2.5 ft²) heptane pan fire results under various enclosure conditions and the associated changes in fuel burning rates is provided in Table 23.

Heptane pan fires were evaluated in two locations, center and corner, with full door ($AH^{0.5} = 2.6$) and slit vent ($AH^{0.5} = 0.6$) conditions. During the initial 60–90 seconds of these tests, both open burning and enclosed heat release rates were generally similar. After this initial period of burning, the enclosure fires continued to grow, surpassing the steady-state value

achieved in the open. The extent of this growth was dependent upon both the pan location and ventilation condition. In three of the four scenarios, the enclosed fires eventually reached a quasi-steady-state burning rate that was on average 60 percent higher than that measured in the open. However for the majority of the time, an increase of only 15 percent over open burning conditions was measured for the slit vent corner fire scenario. For the last several minutes of this test, the heat release rose and steadied out about 800 kW, similar to the other enclosure fires.

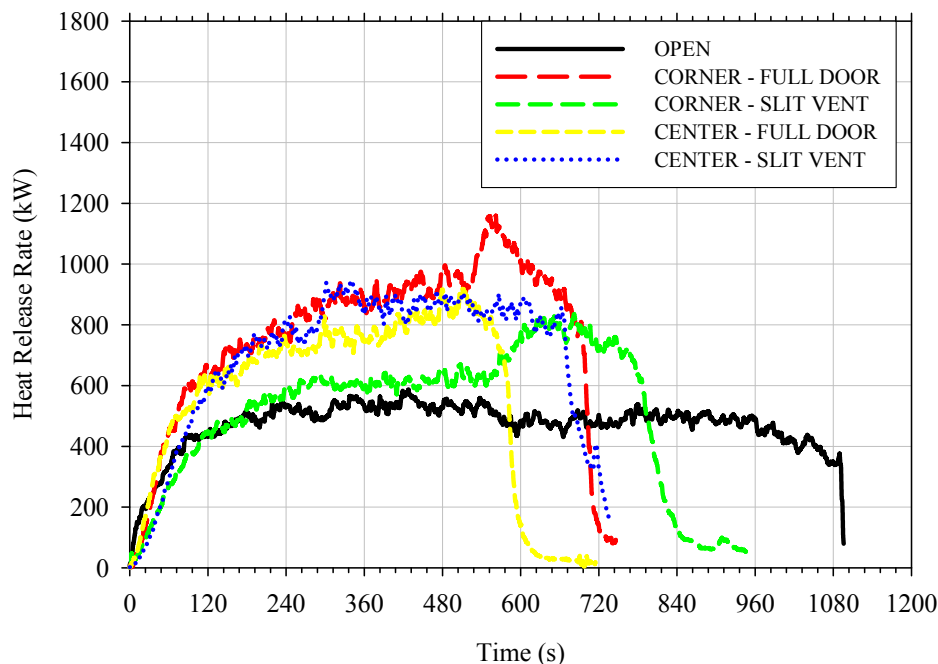


Figure 162. Heat release rates for heptane pan fires in enclosures.

Table 23. Summary of enclosure effects on 0.23 m² (2.5 ft²) heptane pan fires.

Fire Location	Ventilation Condition	Ventilation Factor	10s Avg. HRR (kW)	10s Avg. Heat Flux at Floor (kW/m ²)	Difference due to Enclosure ¹ (%)
Open	Open Burn	N/A	531	N/A	-
Corner	Full Door	2.6	899	5	69
	Slit Vent	0.6	611	2.5	15
Center	Full Door	2.6	791	7	49
	Slit Vent	0.6	857	25	61

1 – Percent difference due to enclosure, calculated by dividing the difference between each enclosure fire heat release rate and the open burning heat release rate by the open burn fire heat release rate.

Comparing similar fuel pan locations, the enhanced burning of fires in enclosures were generally higher than that reported by Parkes et al. [2009] for the larger ventilation factors and lower than that reported by Parkes et al. [2009] for the smaller ventilation factors. A comparison of the enhanced burning measured in both test programs is provided in Table 24. In the work

conducted by Parkes et al., the ventilation factor of 2.4 was created by extending a soffit down from the ventilation opening. The soffit closed off the top quarter (i.e., 0.2 m) of the front face of the enclosure. The ventilation factor of 0.4 was created using a 0.4 m (1.3 ft) wide 1.0 m (3.3 ft) high vent in the front face of the enclosure.

Table 24. Comparison of enhanced burning phenomena for heptane pan fires in enclosures.

	Fire Location	Ventilation Factor	Increase in HRR over Open burning Condition (%)
Parkes et al. [2009]	Rear Center	2.4	27
		0.4	212
	Center	2.4	8
		0.4	155
Current Work	Rear Corner	2.6	69
		0.6	15
	Center	2.6	49
		0.6	61

The differences in enhanced burning associated with the larger ventilation factors are most likely due to the different vent geometries used in the tests. The Parkes et al. ventilation factor of 2.4 was created by extending a soffit downward across the front opening of the enclosure while in this testing the ventilation factor of 2.6 was created using a full open doorway. The difference in vent geometry resulted in a deeper, hotter layer being formed within the test enclosure in the current tests. In the Parkes testing, thermal profiles show that for the ventilation factor of 2.4, upper layer temperatures never exceeded 200°C (392°F) and did not descend more than one-third the height of the enclosure. In the current study, average upper layer temperature ranged from 350–650°C (662–1202°F) and typical upper layer heights were generally half of the total height of the enclosure. The radiative heat feedback to the fuel surface was the primary factor driving the enhanced burning in these tests. The differences in layer development and proximity of the layer to the burning fuel surface are consistent with the increased burning observed in these tests.

The lower levels of enhancement compared to Parkes et al. for the tests with lower ventilation factors are again attributed to the differences in the vent geometries and the corresponding changes to layer development within the test enclosure. For this ventilation factor, Parkes et al. report substantially higher levels of enhanced burning than were measured in the current testing (a factor of about 3). This difference is due to the closer proximity of the hot upper layer to the fuel surface in the Parkes et al. testing than was observed in the current work. The Parkes et al. enclosure was only 1.2 m (4 ft) tall, resulting in upper layer temperatures between 600–700°C (1112–1292°F) with layer depths as low as 0.3 m (1 ft) above the fuel surface. While similar temperatures were observed in the current work, the upper layer was not as deep (i.e., 0.9–1.5 m (3–5 ft)), and therefore the thermal exposure to the fuel layer not as severe.

The second fuel evaluated was denatured alcohol. With the exception of the slit vent scenario with the fuel pan located in the corner, the denatured alcohol heat release rates were within three percent of the open burn fire. A plot showing this comparison is presented in Figure 163.

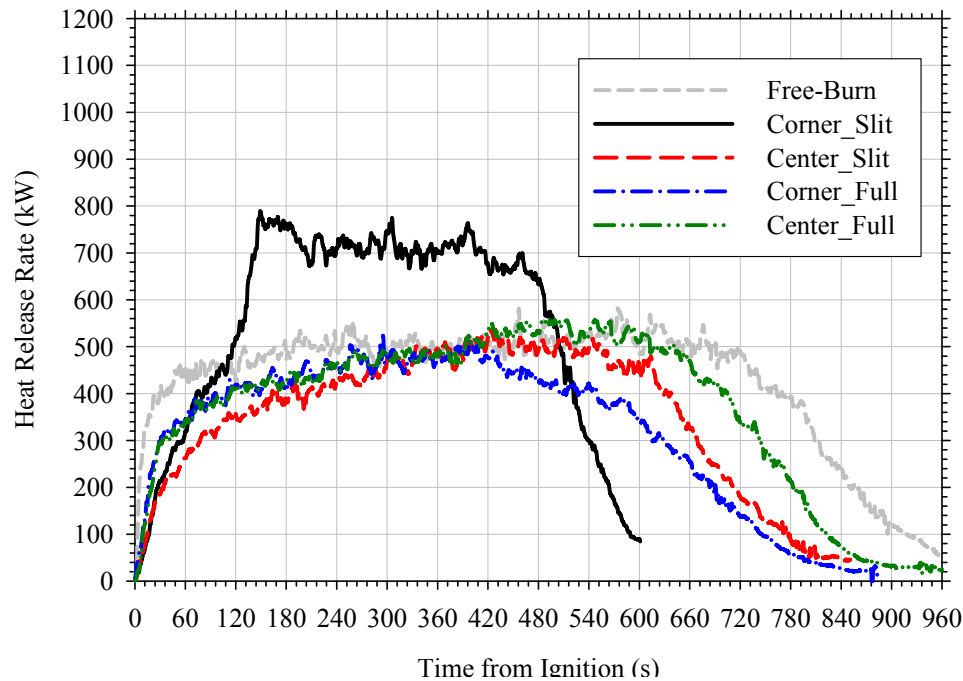


Figure 163. Heat release rates for denatured alcohol pan fires in enclosures and in the open.

As shown in Table 25, a 44 percent increase in average steady-state heat release rate was measured for the slit vent scenario with the pan in the corner of the test enclosure. The initial two minutes of growth for this scenario was comparable to all other scenarios. After 120 seconds, an increase in fire size was observed and maintained for the duration of the test. This increase was attributed to the increased radiant heat flux measured at floor level, shown in Figure 164. It was 5–6 times greater than that measured in the corner location for the full door ventilation scenario. The higher heat release for the slit vent scenario is attributed to a more radiant upper layer for this fire due to the decrease in oxygen concentration in the lower layer (i.e., vitiated air being entrained at the source). A comparison of the low-level oxygen concentration in the full door and slit vent tests is provided in Figure 165. The lower oxygen concentrations at the fire and, thus, more inefficient combustion produced a more optically thick upper layer, as shown in Figure 166, which in turn produced more severe radiant exposure at the floor of the enclosure. This enhanced radiant condition resulted in a higher burning rate as observed in the heat release rate data.

Table 25. Summary of enclosure effects on denatured alcohol pan fires.

Fire Location	Ventilation Condition	Ventilation	Avg. HRR (kW)	Difference due to Enclosure (-)
Open	Open Burn	N/A	540	-
Corner	Full Door	2.6	527	(2)
	Slit Vent	0.6	779	44
Center	Full Door	2.6	532	(1)
	Slit Vent	0.6	530	(2)

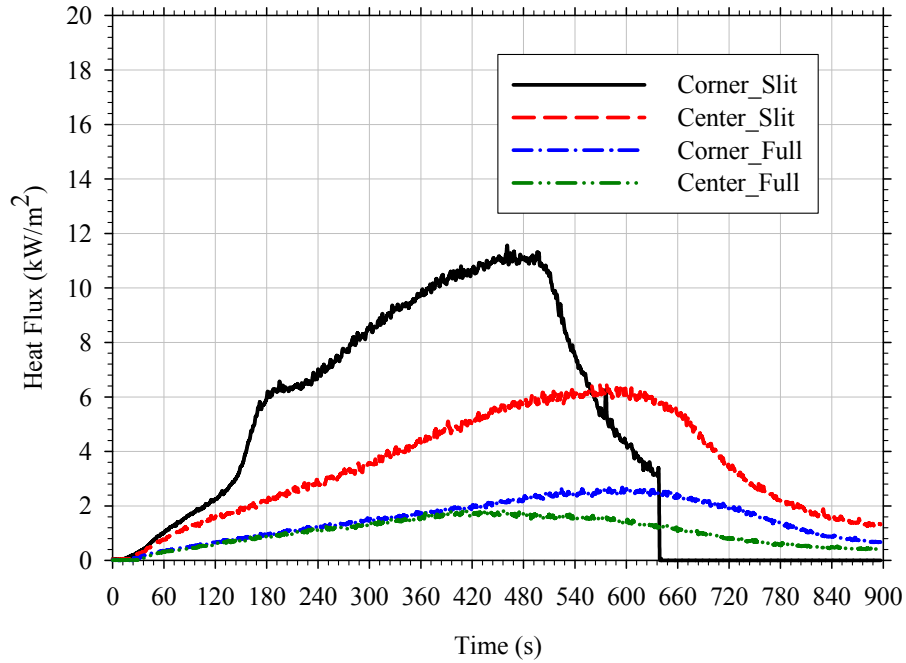


Figure 164. Comparison of floor heat fluxes for denatured alcohol pan fires in the enclosure with full door and slit vent ventilation conditions.

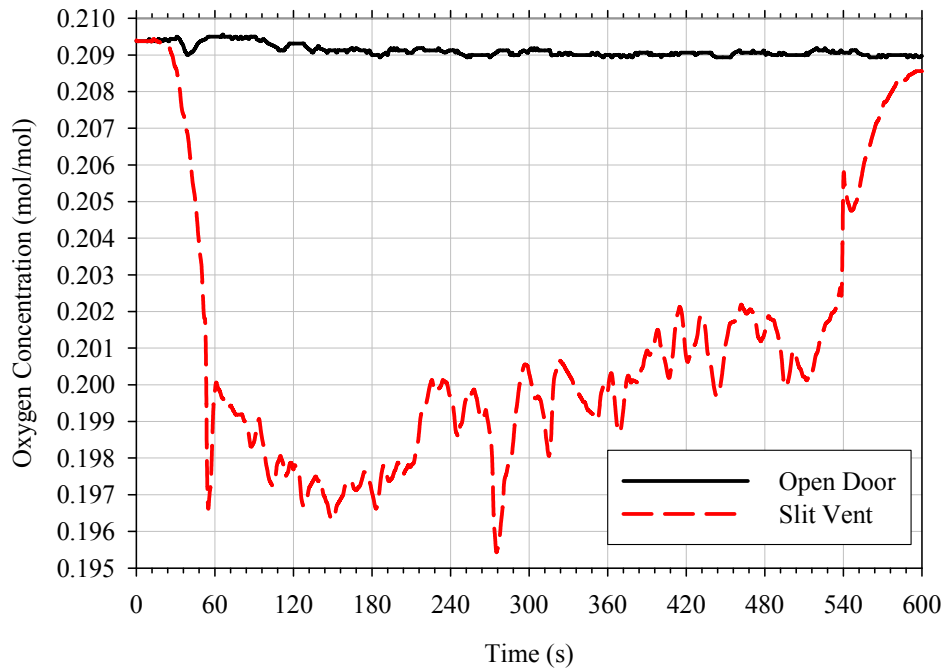


Figure 165. Comparison of low-level oxygen concentrations in denatured alcohol pan fires located in corner of enclosure.

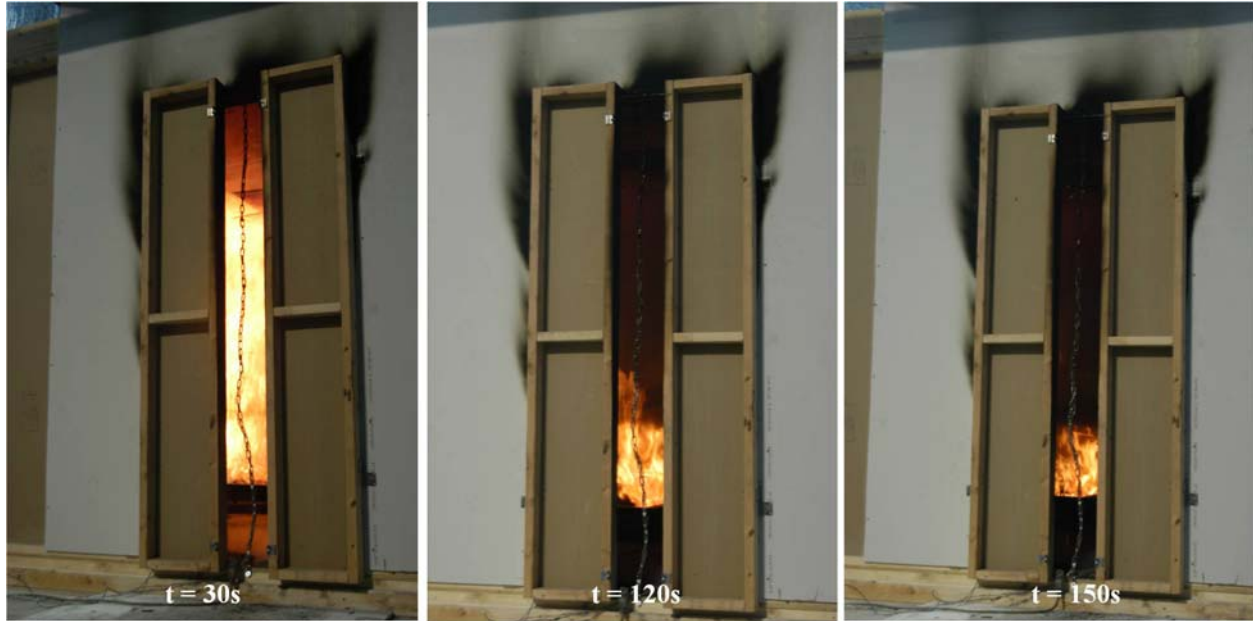


Figure 166. Comparison of upper layer development during 1.0 m² (10.8 ft²) denatured alcohol pan fire in rear corner of enclosure with slit vent condition.

In summary for the liquid fuel pan fires burning both in the open and within an enclosure, the results clearly show that enhanced burning occurs relative to open burning when a radiating upper layer is created in the compartment fire. For heptane, the presence of the enclosure enhanced the heat release rate of the fires for all scenarios, regardless of ventilation opening or location of the fire in the room. The sooty nature of heptane created a radiant upper layer that provided thermal feedback to the fuel surface. With the exception of the rear corner/slit vent scenario, the level of enhancement was similar for all scenarios, with an average enhancement of 60 percent compared to open burning fire sizes.

For the denatured alcohol fires, the presence of the enclosure had minimal impact on the heat release rate of the fuel for all scenarios except one. The denatured alcohol did not produce a sooty upper layer; therefore, the radiant heat feedback to the fuel layer was no more severe in the enclosure than it was in the open. The exceptions to this were the rear corner/slit vent and center/slit vent scenario. In this scenario, the heat flux to the floor of the enclosure was the highest measured in any denatured alcohol test. The increased heat flux was attributed to a very low, vitiated layer, which resulted in the incomplete combustion of the alcohol and the corresponding development of soot and a more radiant upper layer. These effects were demonstrated through both heat flux measurements and visual observations.

6.2.3 Class A Fuel Fires

The mass of the upholstered sofa was measured in each of the nine Class A enclosure fires conducted as well as during open burning fire testing. This data was used to compare the mass loss of the fuel as a function of different test variables (i.e., enclosure, ventilation, and first item ignited). As shown in Figure 167 for open burning, the upholstered sofa exhibited three different stages of burning. Note the mass loss data presented in Figure 167 was normalized with respect to the initial mass of the upholstered sofa (e.g., 47 kg (104 lbs)).

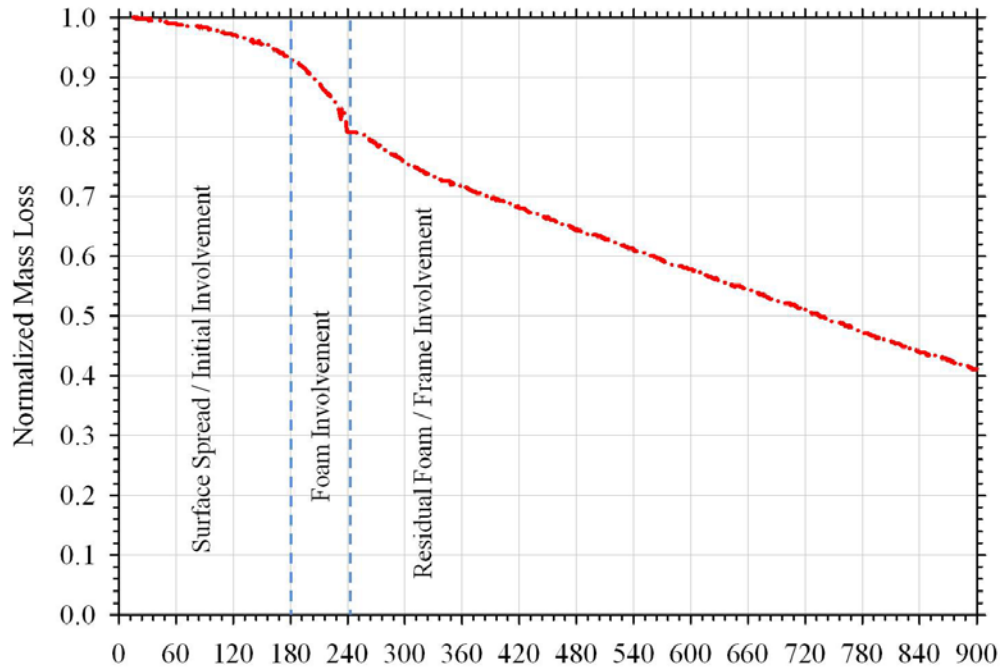


Figure 167. Normalized mass loss of the upholstered sofa burning in the open.

The initial stage consisted of the involvement and spread of flame across the surface fabric of the sofa with some involvement of the polyurethane foam. This stage is characterized by a relatively linear decrease in mass with a mass loss rate of 18 g/s. The second stage consisted of the involvement and vigorous burning of the foam cushioning (i.e., an exponential change). This stage was denoted by an average mass loss rate of 96 g/s. The final stage consisted of the combustion of the residual foam cushioning and the wood frame of the sofa, which was characterized by a linear change in mass loss with an average mass loss rate of 36 g/s. This normalized mass loss is compared to that of the upholstered sofa burning within the enclosure, shown in Figure 168. In general, enclosure fire scenarios with the full door ventilation condition produced upholstered sofa burning rates that were greater than that measured in the open. With the slit ventilation condition (Figure 169), the upholstered surface burning rates were less than that measured in the open.

The curves for the open burning fire and the baseline enclosure fire scenario (Test 6-0, sofa in an enclosure with a Class A ignition source) reached much lower mass values due to the extended burning durations permitted in these tests. The impact of the enclosure is not immediately evident when comparing the initial slopes of the open burning and enclosed fire scenarios. As shown in Table 26, in general, the enclosure does not affect the initial burning rate, but it does alter the third phase burning rate, which is visible with Test 6-0 and to some extent with 6-1 and 6-3. Once the fire transitions to the foam, it appears that there is little difference between scenarios as to how the foam burns.

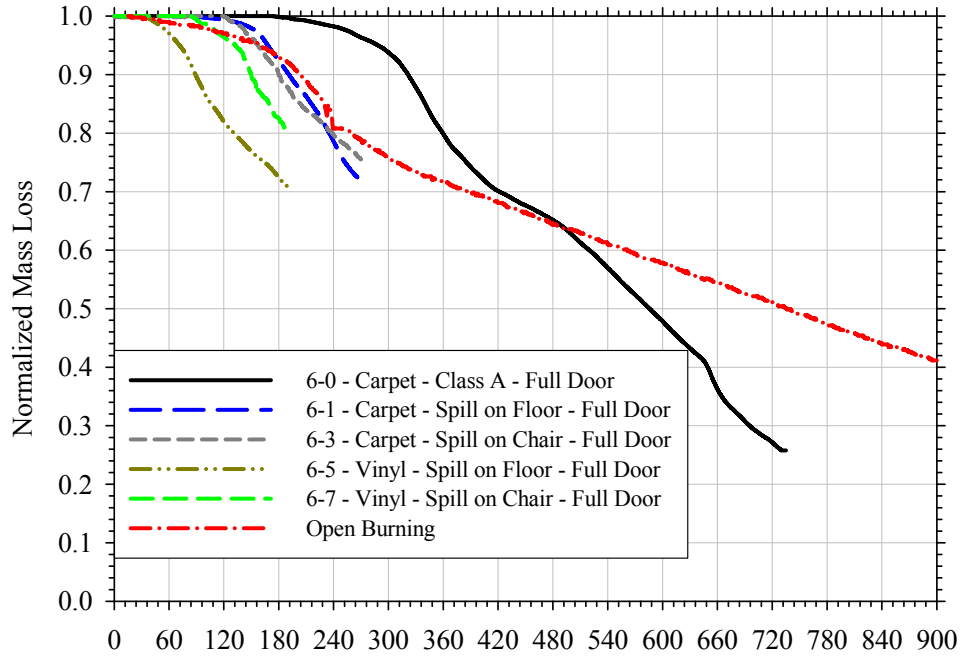


Figure 168. Comparison of normalized mass loss curves for open-burning and enclosed sofa fire scenarios with full door ventilation.

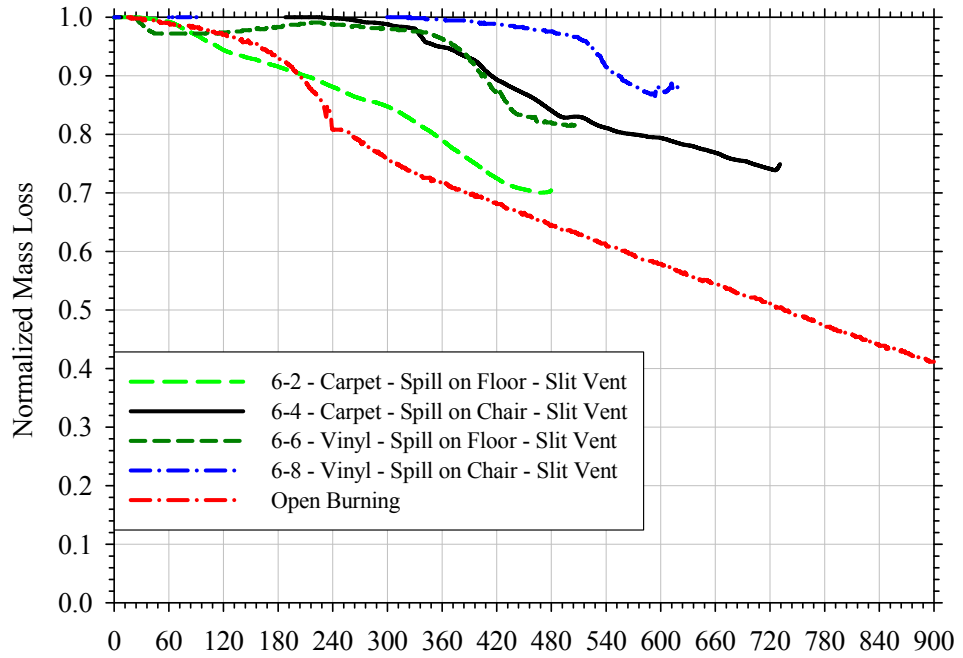


Figure 169. Comparison of normalized mass loss curves for open burning and enclosed sofa fire scenarios with slit ventilation.

The mass burning rates associated with each of the enclosure fires with full door ventilation and the use of an accelerant ignition source were generally consistent with one another. As shown in Table 26, the enhanced burning of the upholstered sofa within the enclosure was observed in all four, full door ventilation scenarios. In these scenarios, the average burning rate was 15 percent higher than that measured in the open with individual tests ranging from 15–24 percent increases. The average mass burning rate was determined using the linear best fit for the mass loss over the period of steady state burning. The highest increase in burning rate observed was for Test 6-7. In this test, the ignition scenario did not result in the direct ignition of the upholstered sofa and consequently the sofa became involved late in the fire. At the stage in which the sofa became involved, a hot upper layer had already developed and pre-heated the sofa such that once involved it rapidly transitioned to fully-involved burning.

Reduced mass loss rates compared to open air burning were measured for all slit ventilation scenarios. The extent of the reduction was found to vary depending on the ignition scenario, which is indirectly related to the type of flooring material present. As shown in Figure 169, the slope of normalized mass loss rates for tests 6-2 and 6-4 were not as steep as those measured in Tests 6-6 and 6-8. The average mass loss rates for these test pairs were 31 and 47 g/s, respectively. For the carpeted scenarios (Test 6-2 and 6-4), a reduction of 64 percent compared to open air burning was observed. These reduced mass loss rates are attributed to the limited involvement of the sofa during the initial ignition fire and the vitiation of the enclosure later in the test when the upholstered sofa became involved. The vitiated (low oxygen) environment reduced the burning rate.

6.2.4 Ventilation Effects

The impact of the ventilation in each of the tests in Test Series 6 was evident for each of the four comparative scenarios. For each ignition scenario/flooring combination, the full door ventilation conditions ($AH^{0.5} = 2.6$) resulted in the rapid development to flashover and post-flashover conditions, while the slit vent condition ($AH^{0.5} = 0.56$) resulted in less severe burning conditions with no clear flashover event occurring. A comparison of the measured heat release rates for each of these variable combinations is provided in Figure 170.

In all four full-door ventilation scenarios, flashover conditions were reached 60–120 seconds after ignition with peak fire sizes ranging from 3.7–7.2 MW. Sustained burning at the ventilation opening was observed for all full door tests. This type of burning was not observed for any of the slit vent tests, where the rate of growth and peak fire sizes achieved were substantially lower than that observed for the full door scenarios. Only Test 6-4 with a slit vent had intermittent ignition of the door plume. Full door vented fires had heat release rates approximately four times larger than the slit vent fires. In general, for the slit vent scenarios, the upper layer developed quickly and descended to the floor relatively early in the test. This vitiation over the entire height of the enclosure generally limited the involvement of the Class A materials within the enclosure, resulting in relatively steady-state conditions.

Table 26. Summary of average mass loss rate (MLR) of upholstered sofas measured during open burning and enclosed fire scenarios.

Test	Flooring Material	Ventilation Condition	Ignition Scenario	1 st Item Ignited	Mass Loss over Timeframe Considered (kg)	Timeframe Considered (s)	Avg. MLR (g/s)	% Difference from Open Burning
6-0	Carpet	Full Door	Class A	Sofa	11	300–420	90	3
6-1		Full Door	Fuel Spill on Floor	Sofa	9	150–240	105	21
6-2		Slit Vent		Sofa	11	90–420	32	-63
6-3		Full Door	Fuel Spill on Upholstered Chair	Chair	9	150–240	101	16
6-4		Slit Vent		Chair	11	360–720	31	-64
6-5	Vinyl	Full Door	Fuel Spill on Floor	Sofa	12	60–180	100	15
6-6		Slit Vent		Sofa	7	360–480	58	-33
6-7		Full Door	Fuel Spill on Upholstered Chair	Chair	8	120–195	108	24
6-8		Slit Vent		Chair	4	480–570	47	-46
Open Burning	N/A	N/A	Class A	N/A	5	180–240	87/27*	N/A

*Average mass burning rate measured during the third stage of burning.

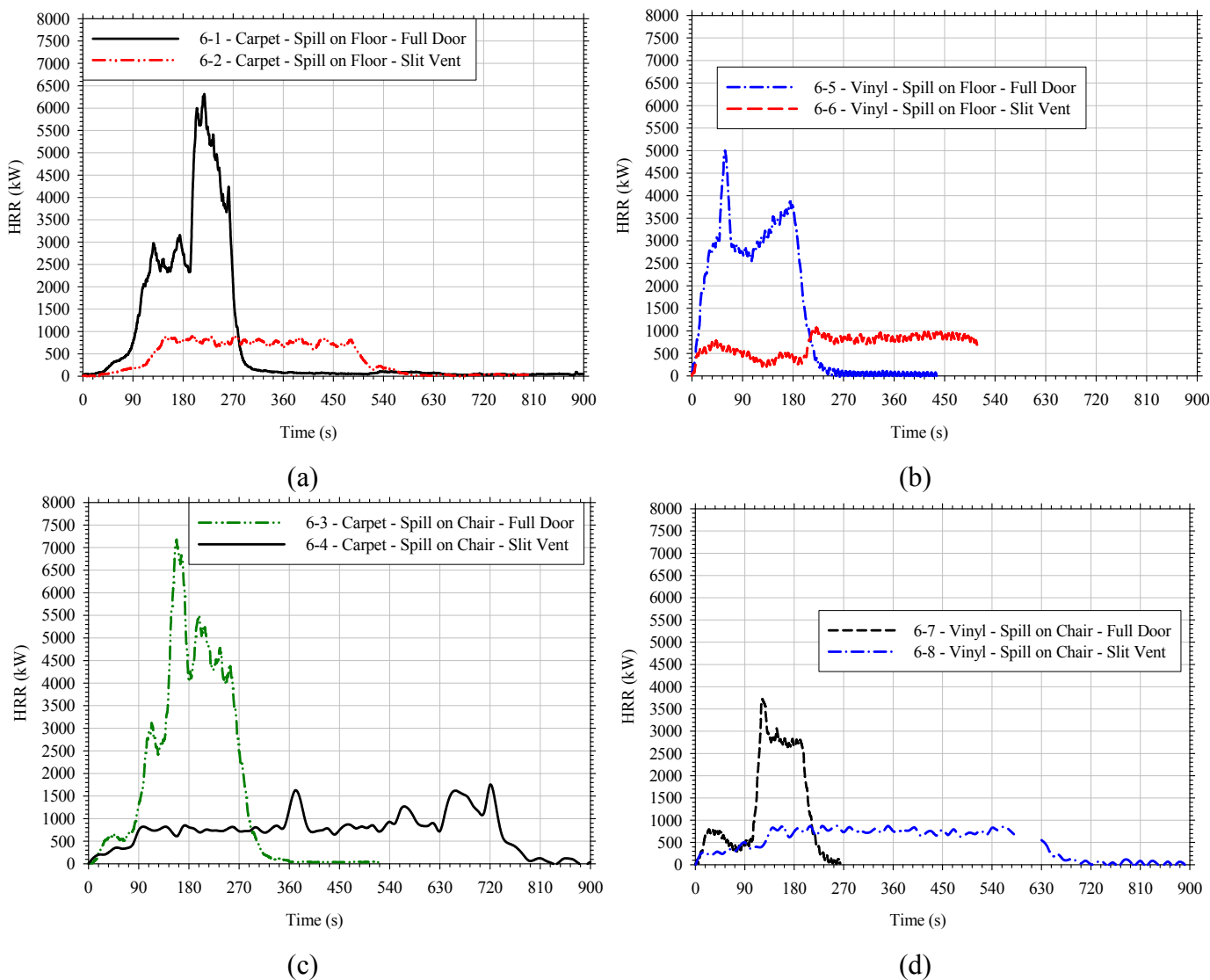


Figure 170. Comparison of enclosure fire heat release rates from open door and slit vent scenarios with (a) carpet flooring and the upholstered sofa being the first item ignited, (b) vinyl flooring and the upholstered sofa being the first item ignited, (c) carpet flooring and the upholstered chair being the first item ignited, and (d) vinyl flooring and the upholstered chair being the first item ignited.

As shown in Figure 170 for all of the full door ventilation scenarios, the fire continued to grow while in the slit vent scenarios the fires reached a quasi-steady-state condition. This divergence in fire growth within the first two minutes is attributed to the lower interface height (i.e., deeper, vitiated upper layer) in the enclosure for the slit vent tests and the corresponding thermal exposure and vitiated layer conditions. Average upper layer temperatures (Table 11) and gas species at 0.45 m (18 in.) above the floor support this divergence. Table 27 presents a summary of floor level oxygen concentrations at the time the fires first reached 500 kW, approximately the value at which the full door and slit vent fire developments diverge. This data shows that for the full door scenarios, the low-level gas concentrations are at nominally ambient conditions, and for the slit vent conditions the concentrations are at levels between 17–19 percent. These limiting oxygen values are consistent with those derived by Wolfe et al. [2009] who found limiting oxygen indices ranging from 16–20 percent for both wood and polyurethane foam materials. It should be noted that these low-level gas measurements were collected at a location 0.9 m (3 ft) from the vent opening. It is likely that low-level gas conditions further into the enclosure were lower making the burning environment even more vitiated.

Although the thermal criteria of upper layer temperature greater than 600°C and floor heat flux greater than 20 kW/m² were partially achieved, these limited ventilation compartment fires did not actually flash over. This analysis is discussed in detail in Section 6.1. As noted above, exterior flaming was only observed in one slit vent fire (Test 6-4). In this test, pulsed airflow into and out of the slit vent (i.e., puffing) was observed approximately 280 seconds after ignition. This pulsed airflow allowed the Class A materials within the enclosure to become more involved which eventually produced the largest fire size measured for the slit vent condition. Oscillating vent flow and intermittent ignition of the door plume were observed for the duration of this test.

Table 27. Summary of Oxygen Concentrations at time when fire reached 500kW.

Test ID	Ventilation Condition	Oxygen Concentration at 0.45 m (1.5 ft) above the Floor (% vol)
6-1	Full Door	20.9
6-2	Slit Vent	18.6
6-3	Full Door	20.8
6-4	Slit Vent	17.4
6-5	Full Door	20.9
6-6	Slit Vent	16.9
6-7	Full Door	21.1
6-8	Slit Vent	18.6
Full Door (Avg./Std. Dev.)		20.9/0.1
Slit Vent (Avg./Std. Dev.)		17.9/0.9

6.2.5 First Item Ignited

The impact of the first item ignited, the sofa or the chair (Table 24), was somewhat dependent on the type of flooring present during the test. For the full door, carpeted scenarios shown in Figure 171, the initial growth rates (i.e., 0–120 s) for both ignition scenarios were generally comparable, as they were dictated by the gasoline spill. Both fires temporarily leveled off between 2.5–3.0 MW. In the test where the upholstered chair was ignited first, this period of burning only lasted approximately 30 seconds. In the test in which the upholstered sofa was ignited first (i.e. spill on floor), the quasi-steady burning was observed for approximately 90 s. After burning at a quasi-steady-state, both tests quickly grew to peak burning conditions between 6.0–7.0 MW. The earlier transition out of this quasi-steady burning in Test 6-3 is attributed to the chair being initially involved due to the gasoline spilled on it compared to the sofa which was ignited by the adjacent spill fire on the carpet. This delay for the sofa fire demonstrates the difference in the accelerated effect from gasoline (as on the chair) compared to being exposed by an external fire.

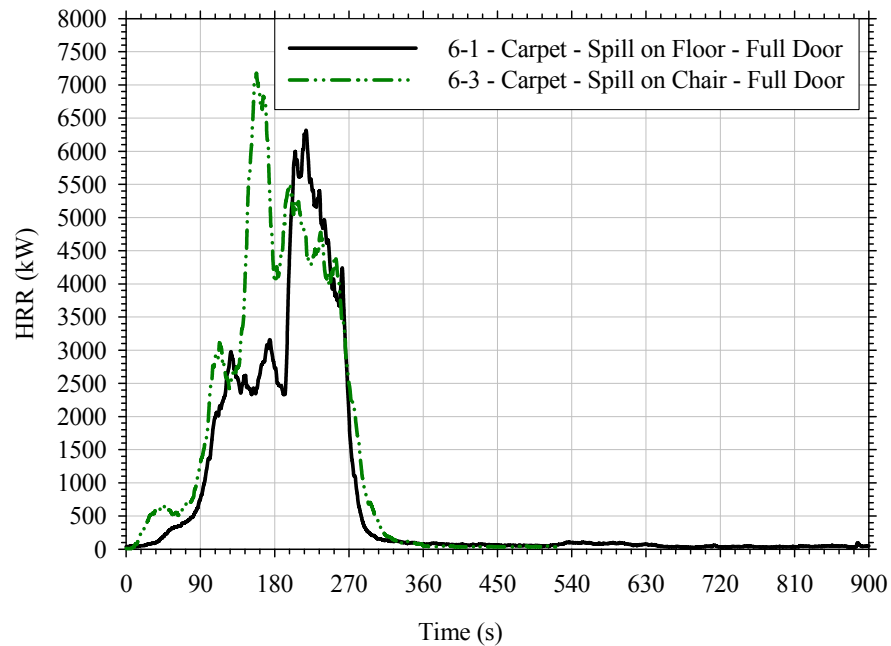


Figure 171. Comparison of enclosure fire heat release rates from full-open door testing with carpet flooring where the upholstered sofa was the first item ignited (6-1) and where the upholstered chair was the first item ignited (6-3).

As shown in Figure 172, heat release rates measured for both ignition scenarios with the slit vent and carpet flooring fires were similar with the exception of the intermittent puffing/external flaming observed toward the end of Test 6-4. It should also be noted that in Test 6-4, the temperature and heat flux thresholds associated with flashover conditions were limitedly exceeded while in Test 6-2, the conditions were not achieved. However, the fire in test 6-2 was extinguished at 480 seconds (4 minutes earlier than test 6-2). In Test 6-4, the upholstered chair was the first item ignited along with the fuel trailer leading from the vent to the chair. The upholstered sofa became involved later than the chair initiated test (i.e., 4–5 minutes after ignition).

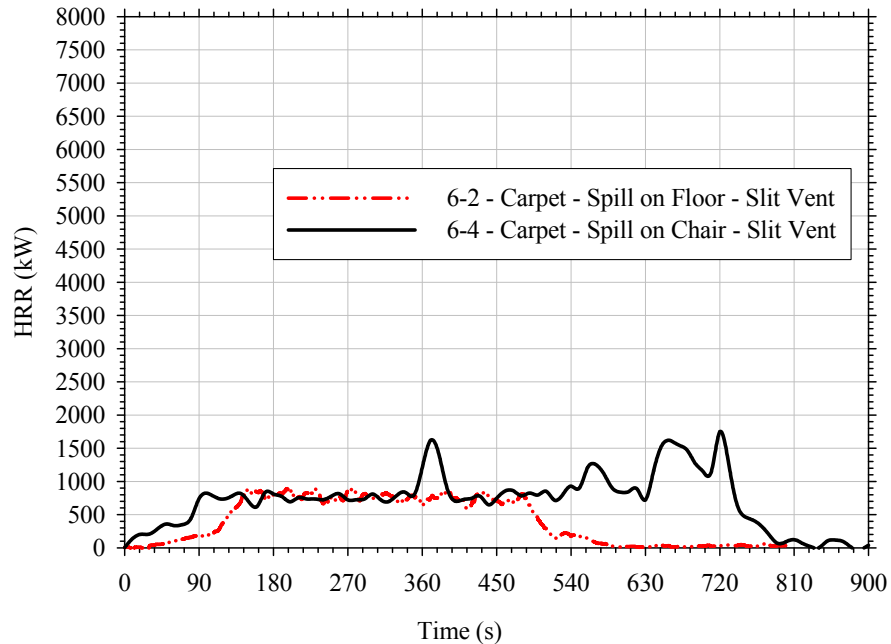


Figure 172. Comparison of enclosure fire heat release rates from slit vent testing with carpet flooring where the upholstered sofa was the first item ignited (6-2) and where the upholstered chair was the first item ignited (6-4).

For the full door, vinyl scenarios, shown in Figure 173, the initial growth rates (i.e., 0–120 s) were very different. In Test 6-5 with the fuel spill to sofa ignition, the fire rapidly grew to fully-involved conditions as a result of the large fuel spill fire centrally located within the space. This fire grew much more rapidly because the gasoline was spilled directly onto the floor and permitted to spread over a large surface area, thus involving all of the Class A materials immediately upon ignition. Due to the rapid growth to peak burning, this fire also reached steady-state burning conditions earlier as well. A similar growth and steady-state burning trend was observed in Test 6-7, however, it was delayed and not as severe. In this test, the bulk of the gasoline was poured onto the upholstered chair, thereby limiting the fuel surface area on the floor. The liquid fuel fire first involved the upholstered chair and gradually spread to neighboring combustibles via radiant ignition from both the upper layer and the chair fire plume. This gradual fire spread delayed peak burning by 60–90 seconds when compared to the fuel spill fire on the floor used in Test 6-5.

Behavior similar to the slit ventilation fires with carpet flooring (Figure 172) was also observed for the vinyl flooring, shown in Figure 174 for Test 6-6 (Spill on Floor) and Test 6-8 (Spill on Chair). With the slit vent, the growth of the gasoline spill and upholstered furniture fires was limited by the ventilation opening. Overall, the differences between ignition scenarios were quite minor as both reached their steady-state conditions within four minutes and the net heat release for both fires were about the same for the first four minutes (130 MJ and 127 MJ). The gasoline spill on the floor grew larger initially compared to the spill on the chair due to the larger spill area. However, the fire quickly started to decay (within a minute) due to a lack of oxygen in the rapidly descending layer. This decay continued until the fire gradually spread to neighboring combustibles and eventually reached a steady-state heat release rate that was comparable to that in Test 6-8 where the gasoline soaked chair was ignited first.

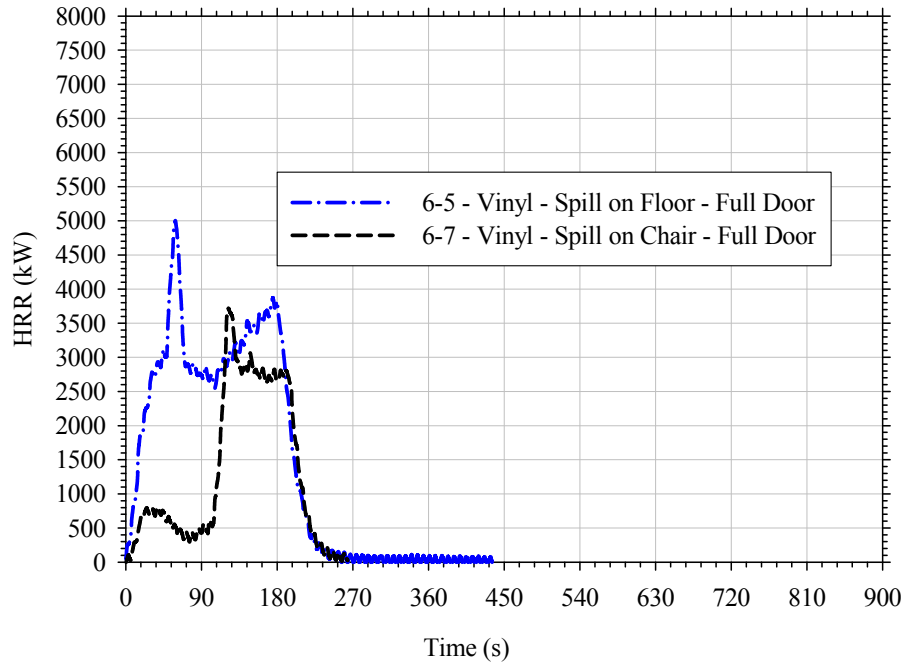


Figure 173. Comparison of enclosure fire heat release rates from full-open door testing with vinyl flooring where the gasoline spill fire involved all combustibles simultaneously (6-5) and where the upholstered chair was the first item ignited (6-7).

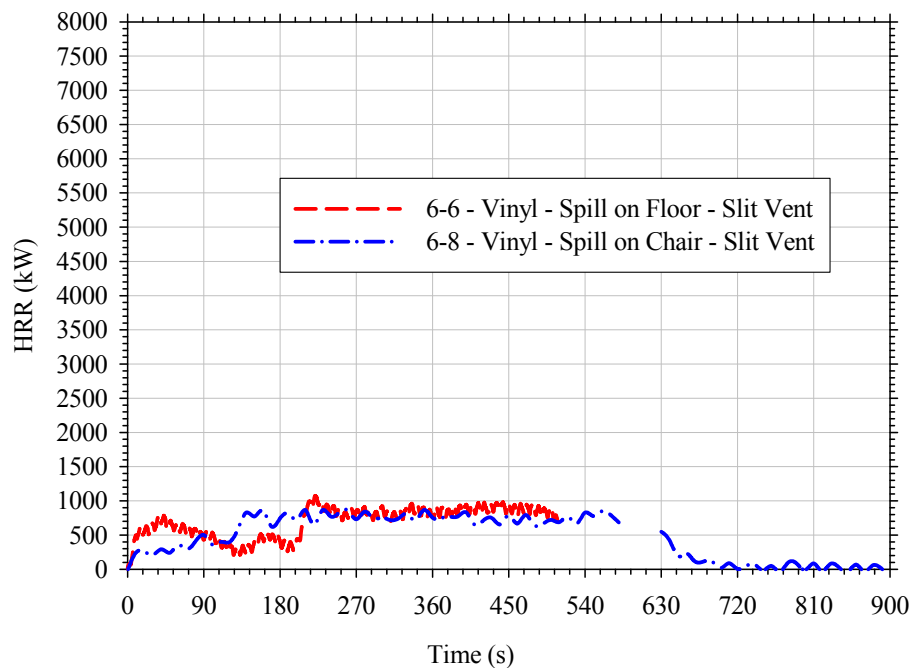


Figure 174. Comparison of enclosure fire heat release rates from slit vent testing with vinyl flooring where the gasoline spill fire involved all combustibles simultaneously (6-6) and where the upholstered chair was the first item ignited (6-8).

In summary, although there were some shifts in time of development related to the initiating fire scenarios, the overall fire growth and size were quite similar, regardless of whether the chair or sofa (or larger spill fire) was ignited first. For these 13.4 m² (144 ft²) enclosures, all these fires developed quickly within 2 to 4 minutes.

6.3 Effect of Gasoline Spill on Fire Development

Figure 175 shows a comparison of the heat release rates from the Class A ignition scenario (i.e., Test 6-0, furnished enclosure with Class A ignition on the sofa in Sec. 5.6.1) and the same carpeted, furnished scenario with a gasoline spill in front of the sofa (Test 6-1). Both scenarios had a full door vent. The primary difference between fires is the approximately 4 minute delay in fire development for the Class A ignition. Otherwise, the heat release rate curves are quite similar. The extended burning for Test 6-0 is a result of that test being allowed to burn longer, whereas Test 6-1 was manually extinguished at 260 seconds. If gasoline had been spilled on the sofa directly instead of the carpet, the compartment fire would have developed even quicker than in Test 6-1, which had exponential growth within 1.5 minutes and had reached flashover within 3 minutes. Consequently based on these tests, although spill fires can accelerate fires in time, the resulting fire size and heat output is not substantially changed for gasoline quantities up to 2 L.

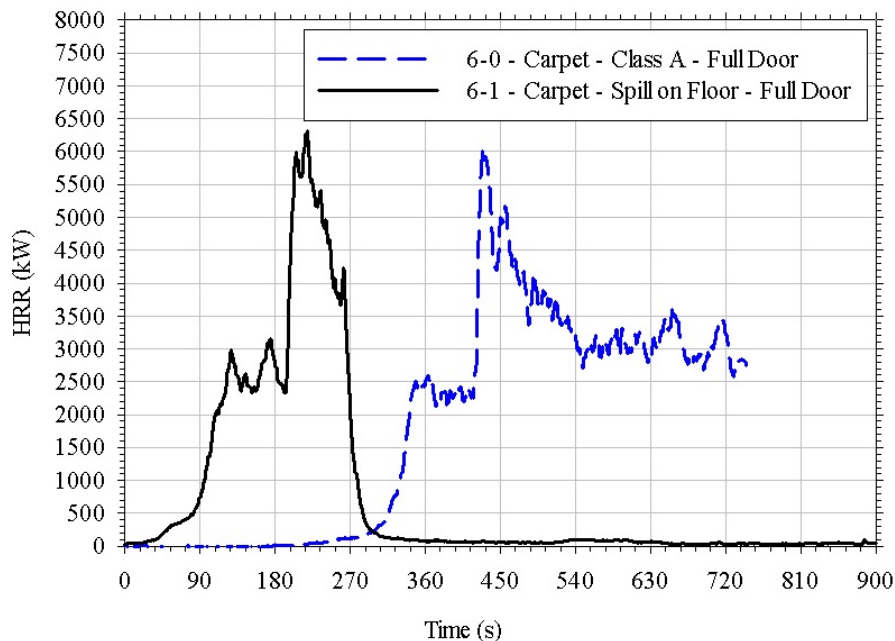


Figure 175. Comparison of enclosure heat release rates from full open door testing with Class A ignition scenario on the sofa (Test 6-0) and with a gasoline spill in front of the sofa (Test 6-1).

7.0 CONCLUSIONS

In this work, the burning dynamics of both confined and unconfined liquid fuel fires as well as Class A fuel packages were characterized. The liquid fuels used in this work were gasoline, heptane, and denatured alcohol. These fuels were selected for their prevalence in real-world forensic fire scenarios (gasoline), their historical presence in experimental fire research (heptane), and their differences in combustion chemistry (denatured alcohol). More specifically

the denatured alcohol fuel was selected because of its negligible soot yield, which differs from both gasoline and heptane. The Class A materials (furniture and flooring) used in these tests were all selected because of their relevance to residential fires and their use in previous research efforts [Wolfe et al. 2009, Mealy et al. 2010], which allows for the comparison of results to existing data sets. The enclosure used in this work was designed to be representative of typical building spaces (i.e., 13.4 m² (144 ft²) with a height to width ratio of less than one).

These tests allowed for direct comparisons between full-scale open burning and enclosure fire scenarios. This work provides an improved understanding of the impact of the enclosure on fuel burning dynamics for three different fuel scenarios and identifies some of the key factors that govern this impact.

For unconfined liquid fuel fires (i.e., a spill), the impact of the enclosure was evaluated for both vinyl and carpet flooring systems. For both open (Test Series 1) and enclosed (Test Series 4) burning conditions, a 2.0 L (0.53 gal) gasoline spill was used as the spill fire scenario. For both flooring types, the enclosure fires behaved differently than the open burning scenarios. However, the difference was not due to enhanced burning of the liquid fuel; instead, the primary difference was the involvement of additional combustible material (i.e., adjacent flooring material outside the initial spill area). For the period of time in which the liquid fuel was the primary material burning, the fires grew in a similar manner and reached peak values that were comparable. For the vinyl substrate, the fire in the enclosure burned at peak values for an extended period of time as opposed to immediately transitioning to the decay phase as was observed in the open. Due to the involvement of additional flooring material, the carpet enclosure fire resulted in a larger fire than was observed in the open. Considering the short period of time in which the liquid fuel was the primary material burning (1 to 2 minutes), the enclosures did not have an effect on the spill fire, but did contribute to the fires growing larger and involving more material. There will be a certain critical room volume to fire size that will dictate whether an enclosure will lead to fires growing beyond the initial spill areas. Additional work is needed to identify this critical parameter. The impact of an enclosure on confined area liquid fuel fires (i.e., pan fires) was determined to be dependent on fuel type, fuel location, and ventilation condition. Open (Test Series 2) and enclosed (Test Series 5) tests were conducted using 0.23 m² (2.5 ft²) and 1.0 m² (10.8 ft²) pans containing heptane and denatured alcohol, respectively. Pan fires in the enclosure were evaluated in two locations, center and corner, with full door ($AH^{0.5} = 2.6$) and slit vent ($AH^{0.5} = 0.6$) conditions. The quasi-steady-state heat release rates from these tests were compared.

In summary for the liquid fuel pan fires burning both in the open and within an enclosure (i.e., confined pool with sufficient depth to burn to steady-state), the results clearly show that enhanced burning occurs relative to open burning when a radiating upper layer is created in the compartment fire. During the initial 60–90 seconds of the heptane fire tests, both open burning and enclosed heat release rates were generally similar. After this initial period of burning, the enclosure fires continued to grow surpassing the steady-state value achieved in the open. The extent of this growth was dependent upon both the pan location and ventilation condition. In three of the four scenarios, the enclosed fires eventually reached a quasi-steady-state burning rate that was on average 60 percent higher than that measured in the open. However, an increase of only 15 percent over open burning conditions was measured for the slit vent corner fire scenario. The minimal enhancement observed in this test was attributed to the vitiation of the

combustion air being entrained into the fire plume resulting in less efficient combustion of the heptane.

The second fuel evaluated was denatured alcohol. With the exception of the slit vent scenario with the fuel pan located in the corner, the denatured alcohol fires conducted within the enclosure were within three percent of that measured during tests conducted in the open. Open burning and enclosed denatured alcohol fires were comparable with respect to both fire growth and steady-state burning conditions. The enhanced burning observed for the denatured alcohol pan fire located in the corner of the enclosure with the slit vent condition was attributed to the vitiation of the combustion air being entrained into the fire plume. However, in this case, the less efficient combustion produced a sootier, and thus a more radiative upper layer, which in turn enhanced the burning rate of the denatured alcohol. These tests illustrate the varying effect that an enclosure can have depending on the fuel that is burning within. For a non-sooting fuel (denatured alcohol), the enclosure/ventilation condition had only a minimal effect on the maximum heat release rate achieved, while for a sooty fuel (heptane) under the same conditions, the enclosure enhanced the burning of the fuel due to enhanced radiation to the floor and fuel surface.

In summary for liquid fuels in compartments:

- The fire size of a spill fire generally will not be affected by the compartment due to the relatively quick duration of the fire.
- If the fuel is contained in a pool so that it is deep enough (5 mm or more) to burn to a steady-state condition, a radiating upper smoke layer will increase the burning rate. An average 60 percent increase was observed for heptane pan fires with a full door vent. This increase can be moderated by restricted ventilation to the compartment.

For the Class A fuels, the impact of the enclosure on the burning dynamics of the fuel was evaluated based on analysis of the mass loss rates of the upholstered sofa which was the primary fuel item within the enclosure. In these tests, the Class A materials were evaluated using either a Class A ignition source or liquid fuel spill on either the floor of the enclosure or on an upholstered chair opposite the upholstered sofa. These fire scenarios were evaluated using both full door ($AH^{0.5} = 2.6$) and slit vent ($AH^{0.5} = 0.6$) ventilation conditions.

The mass burning rates associated with each of the enclosure fires with full door ventilation and the use of the liquid fuel ignition source were generally consistent with one another. The enhanced burning of the upholstered sofa within the enclosure was observed in all four, full door ventilation scenarios. In these scenarios, the average burning rate was 19 percent higher than that measured in the open with individual tests ranging from 15–24 percent increases. The greatest enhancement was observed in a test where the ignition scenario did not result in the direct ignition of the upholstered sofa and consequently the sofa became involved late in the fire. At the stage in which the sofa became involved, a hot upper layer had already developed and most likely pre-heated the sofa such that once involved it rapidly transitioned to fully-involved burning. In general, the degree of enhancement observed in these Class A fire tests was relatively minimal when compared to the values reported for the pan fire scenarios. Given the uncertainties in upholstered furniture calorimetry, the enhancement in burning for the scenarios evaluated are

minor. However, as the room size to fire size ratio decreases, the effect may increase, assuming that vitiated conditions do not suppress the fire, as seen in the limited ventilation slit vent tests.

Reduced mass loss rates compared to open air burning were measured for all slit ventilation scenarios. The extent of the reduction was found to vary depending on the ignition scenario, which is indirectly related to the type of flooring material present. For tests in which vinyl was the flooring system installed, the average mass loss rates were 36–54 percent that measured during open burning. For the carpeted scenarios, a reduction of 64 percent compared to open air burning was observed. These reduced mass loss rates were most likely due to the limited involvement of the sofa during the initial ignition fire and the vitiation of the enclosure later in the test when the upholstered sofa became involved. At this point in time in these tests, the lower level oxygen concentrations were on average 18 ± 1 percent which are considered to be in the range of the limiting oxygen index for combustion to occur.

In addition to evaluating the impact of the enclosure on the upholstered sofa burning rate, these full-scale Class A enclosure fires were also used to characterize the development of flashover conditions under varying ventilation and ignition scenarios. Flashover was evaluated relative to the ignition of paper indicators and flooring materials as well as to two established thermal criteria: the average upper layer temperature exceeding 600°C (1112°F) or the average floor level heat flux exceeding 20 kW/m^2 . In all of the full door ventilation tests conducted, the upper layer temperature threshold was reached first, followed by the floor level heat flux threshold, followed by flame extension from the vent. The occurrence of all three of these indicators typically occurred within 60 seconds. On average, the upper layer temperature threshold was reached less than ten seconds prior to the floor level flux threshold being reached. The occurrence of flashover was quite clear and indisputable for the full open door fires. Visual observations of the ignition of paper indicators and the flooring material were clearly definable. The ignition of floor level combustibles always occurred after both the 600°C (1112°F) and 20 kW/m^2 criteria were achieved, but before ignition of the door plume. The time differences between the two criteria and floor level ignition ranged from 5 to 43 seconds. In general, the layer temperature and floor heat flux criteria appear to be reasonably representative and conservative in that they predict flashover (ignition of all combustibles in the space) slightly earlier than may occur in actuality. The occurrence of external flames lagged behind the occurrence of flashover.

For the slit vent condition, the occurrence of flashover was not as clearly defined (visually) or consistent as was observed for full door ventilation. Only three of the four tests with the slit vent reached the thermal thresholds and the radiant ignition of visual indicators was only observed in one of the tests. Although the thermal criteria for flashover were achieved in these three fires, it is expected that flashover did not actually occur. In these tests, fire growth was inhibited by the limited ventilation condition. The vent condition created a vitiated upper layer that extended almost to the floor of the enclosure causing the fire to bank down and burn primarily at low levels. Over time, fire spread to adjacent combustibles and involved the whole room as evidenced post-test by fire damage across the whole space. The instantaneous involvement of all combustibles within the enclosure was not visually observed as the deep smoke layer prevented a clear view of the flooring and paper indicators. Although the average floor level heat flux reached a value of 20 kW/m^2 , this was due to a high reading above the criterion in only one of the two measurement locations. Consequently, this non-uniformity indicates that the thermal conditions throughout the space were not sufficient to cause a rapid

transition from localized burning to wide spread ignition of combustibles throughout the room. In other words, flashover did not actually occur. The upper layer temperature measurements were generally consistent with this conclusion in that upper layer values were only slightly above 600°C (1112°F) and usually for only short periods of time. Despite this assessment, to a general observer after the fire, visual observations of the damage may lead to an interpretation that the space did flashover.

This work demonstrated that ventilation conditions must be considered when evaluating the fire dynamics of a fire event relative to the post-fire damage. A limited ventilation compartment may become fully involved and result in widespread fire damage across all flooring and furniture. In addition, a generic correlation for flashover may yield a required heat release rate that is well within reason given the fuel loads in the room. For example, in the testing in this program, correlations in the literature predicted heat release rates for flashover in the slit-vent fires of approximately 400 to 600 kW. These heat release rates are in the range of the upholstered chair and coffee table, respectively. Based on this calculation and the post-fire damage, one may conclude that the fire flashed over early in the fire development and reached temperatures well in excess of 600°C (1112°F). However, similar fire damage (i.e., wide spread with all surfaces burned) can occur without flashover due to limited ventilation that can actually limit fire growth so that it progresses over a longer timeframe with temperatures below 600°C (1112°F).

8.0 REFERENCES

ASTM E603 (2007), *Standard Guide for Room Fire Experiments*, American Society of Testing and Materials.

ASTM E1354 [2010] *Standard Test Method for Heat and Visible Smoke Release Rates for Materials and Products Using an Oxygen Consumption Calorimeter*, American Society of Testing and Materials.

Babrauskas, V. (1979), "COMPF2 – A Program for Calculating Post-Flashover Fire Temperatures," Technical Note 991, National Bureau of Standards.

Babrauskas, V. (1980), "Estimating Room Flashover Potential," *Fire Technology*, **16**, pp. 94–103, 112.

Babrauskas, V. (1983), "Estimating Large Pool Fire Burning Rates," *Fire Technology*, **19**, p. 251.

Babrauskas, V., Peacock, R., Reneke, P. (2003) "Defining Flashover for Fire Hazard Calculations – Part II," *Fire Safety Journal*, **38**, pp. 613–622.

Bullen, M.L. and Thomas, P.H. (1979), "Compartment Fires with Non-Cellulosic Fuels," *17th International Symposium on Combustion*, Combustion Institute, Leeds, England.

Drysdale, D. (2011), *An Introduction to Fire Dynamics*, Wiley Interscience.

Francis, J. and Chen, A.P. (2012), "Observable characteristics of flashover," *Fire Safety Journal*, **51**, pp. 42-52.

- Fleischmann, C.M. and Parkes, A.R. (1997), "Effects of Ventilation on the Compartment Enhanced Mass Loss Rate," International Association of Fire Safety Science, Melbourne, Australia.
- Kawagoe, K. (1958), "Fire Behavior in Rooms, Report of the Building Research Institute, No. 27.
- Kawagoe, K. and Sekine, T. (1963), "Estimation of Fire Temperature-Time Curves in Rooms," Building Research Institute of Japan.
- Kung, H. C., and Stavriavidis, P. (1982), "Buoyant Plumes of Large-Scale Pool Fires," *Nineteenth Symposium (International) on Combustion*, Haffa, Israel, pp. 905–912.
- Ma, T., Olenick, S.M., Klassen, M.S., Roby, R.J., and Torero, J.L. (2004), "Burning Rate of Liquid Fuel on Carpet (Porous Media)," *Fire Technology*, **40**, pp. 227–246.
- McCaffrey, B.J. and Heskestad, G. (1976), "A Robust Bidirectional Low-Velocity Probe for Flame and Fire Application," *Combustion and Flame*, **26**, pp. 125–127.
- McCaffrey, B.J., Quintiere, J.G., and Harkleroad, M.F. (1981), "Estimating Room Fire Temperatures and the Likelihood of Flashover Using Fire Test Data Correlations," *Fire Technology*, **17** (2), pp. 98–119.
- Mealy, C.L. and Gottuk, D.T. (2006), "A Study of Unventilated Fire Scenarios for the Advancement of Forensic Investigations of Arson Crimes," 98IJCXK003, Office of Justice Programs, National Institute of Justice, Department of Justice.
- Mealy, C.L., Benfer, M., and Gottuk, D.T. (2011), "Fire Dynamics and Forensic Analysis of Liquid Fuel Fires," Grant No. 2008-DN-BX-K168, Office of Justice Programs, National Institute of Justice, Department of Justice.
- Parkes, A.R. (2009), "The Impact of Size and Location of Pool Fires on Compartment Behavior," Thesis Christchurch, University of Canterbury.
- Peacock, R., Reneke, P, Bukowski, R, Babrauskas, V. (1999) "Defining Flashover for Fire Hazard Calculations," *Fire Safety Journal*, **32**, pp. 331–345.
- Quintiere, J.G. (2006), *Fundamentals of Fire Phenomena*, Chichester, John Wiley.
- Shanley, J.H. (1997), *Report of the United States Fire Administration Program for the Study of Fire Patterns*, The USFA Fire Pattern Research Committee.
- Tarifa, C.S. (1967), "Open Fires," Instituto Nacional de Tecnica Aeroespacial Estoban Terradas, Madrid.
- Tewarson, A. (1972), "Some Observations on Experimental Fires in Enclosures, Part II – Ethyl Alcohol and Paraffin Oil," *Combustion and Flame*, **19** (3), pp. 363–371.

Thomas, P., "Testing Products for their Contribution to Flashover in Rooms," *Fire and Materials*, V5 Issue 3, pp.103-111, 1981.

Tsuchiya Y. and Sumi, K. (1971), "Computation of the Behavior of Fire in an Enclosure," *Combustion and Flame*, **16**, pp. 131–139.

Wolfe, A., Mealy, C.L., and Gottuk, D.T. (2009), "Fire Dynamics and Forensic Analysis of Limited Ventilation Compartment Fires," Grant No. 2007-DN-BX-K240, National Institute of Justice, Department of Justice.

Wolfe, A.J., Mealy, C.L., and Gottuk, D.T. (2010), "Fire Dynamics of Limited Ventilation Compartment Fires," Proceedings – *2010 International Symposium on Fire Investigation Science and Technology*, University of Maryland University College, September 28–29, 2010, pp. 603–614.

APPENDIX A – HOOD CALORIMETERS & CALIBRATION

All tests in this series were conducted in the ATF Fire Research Lab's Medium Burn Room (MBR). This room is approximately 46.2 m (151 ft) long by 24.5 m (80 ft) wide. The average height from floor to ceiling of the MBR is approximately 10.2 m (33.5 ft). The MBR contains five hood calorimeters, three of which were used in this test series and will be described. A 4 MW square shaped hood calorimeter is located in the northern side of the MBR. The southwest and southeast sides of the MBR contain a 1 MW square hood and a 1 MW round hood, respectively. In order to optimize airflow conditions in the MBR, tarps were placed from the floor to approximately 1.0 m (3 ft) from the ceiling to create separate compartments for each of the three hood calorimeters. The 1 MW (square and round) hoods are located off-center in compartments approximately 17 m (56 ft) deep by 12.2 m (40 ft) wide. The 4 MW hood area takes up the rest of the MBR and is approximately 29 m (95 ft) deep by 24.5 m (80 ft) wide. In addition to these hoods, exhaust vents are placed at the ceiling in the four corners of the MBR in the event that smoke escapes from under one of the hoods during a test.

All three hoods used in this testing were of steel construction. The 4 MW hood had a square curtain around the bottom of a conical shaped transition, leading to a circular exhaust duct. The 1 MW square hood had a square curtain and a pyramidal shaped transition leading to a circular exhaust duct. The 1 MW round hood has no curtain and only consists of a conical shaped transition leading to a circular exhaust duct.

For each of the hoods in the MBR, the exhaust duct runs vertical from the top of the hood transition through the ceiling and into the plenum space above. The ducts then make a 90 degree turn and run horizontally for a distance before entering the scrubber. For the 4 MW hood, the 90 degree turn is accomplished using an elbow connection. However, for the 1 MW square and 1 MW round hoods, the 90 degree turn is accomplished with a miter bend.

Hood calorimetry instrumentation consisted of either one (for 1 MW hoods) or two (for 4 MW hood) bi-directional velocity probes with collocated thermocouples, a set of oxygen consumption sample lines. The bi-directional velocity probes were connected to Setra Model 267 differential pressure transducers. Collocated thermocouples were Omega type-K, inconel sheathed models. Oxygen consumption sample lines run to a Servomex 4100 gas analyzer that measures O₂, CO₂, and CO concentrations. For the 1 MW round and square hoods, the velocity probes and sample lines were located in the duct at heights of 9.5 m (31 ft) and 8.5 m (28 ft) above the ground, respectively. For each individual hood, the exhaust flow rates varied from test to test as expected fire sizes changed.

Calibration Fires

Prior to testing, the hood calorimeter was calibrated using natural gas diffusion burners. A 0.3 m (1ft) square natural gas diffusion burner capable of producing 500 kW fires was used to calibrate the 1MW hood calorimeter. The larger 4MW hood calorimeter was calibrated using a natural gas tube burner. The calibrations were conducted to determine the hood correction factor (C-factor). The calibration fire used for the 1MW hood ranged from 100–500 kW in 100 kW intervals. The calibration fire used for the 4MW hood ranged in size from 0.5–4.0 MW in 1.0 MW intervals. The hoods were considered calibrated when the measured heat release rate was within ± 5 percent of the measured burner output.